FACULTY OF SCIENCE
UNIVERSITY OF COPENHAGEN

PhD thesis

Rijun Huang

Gauge and Gravity Amplitudes
from trees to loops

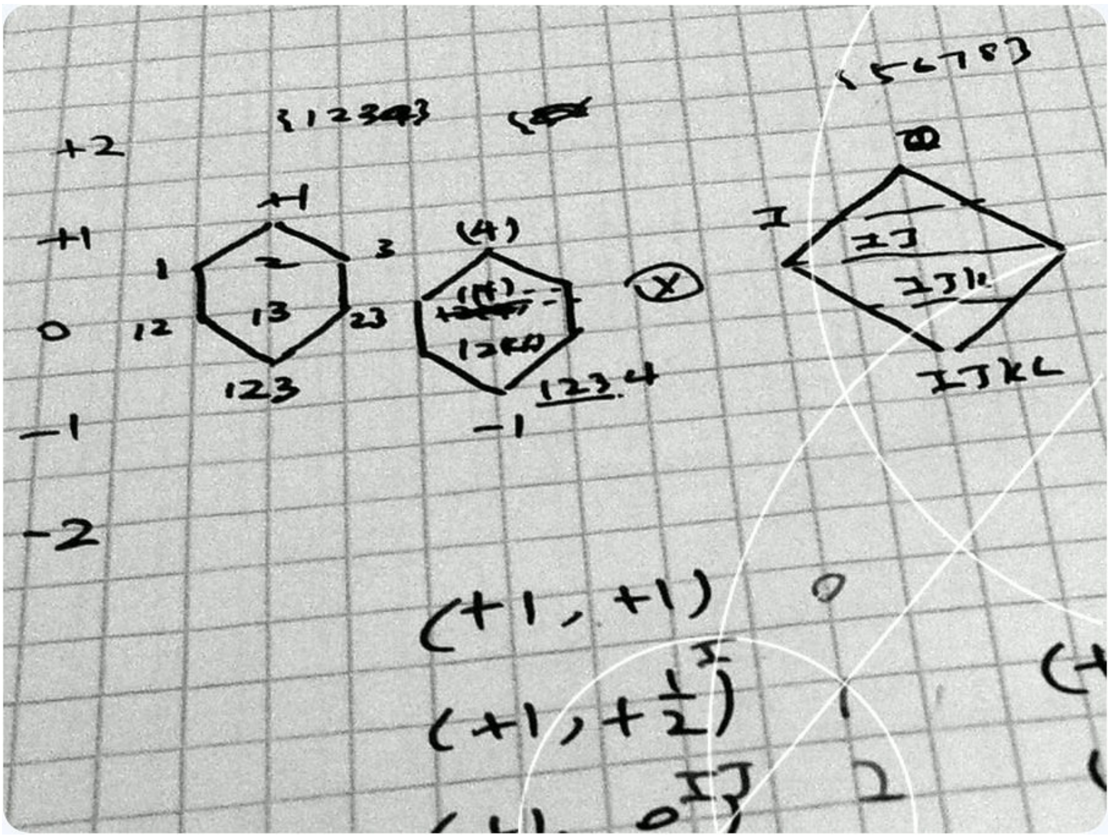

Principal Supervisor: Poul Henrik Damgaard

Submitted: November 7, 2013

University of Copenhagen

Doctoral Thesis

Gauge and Gravity Amplitudes from trees to loops

Author:
Rijun Huang

Principal Supervisor:
Poul Henrik Damgaard

A thesis submitted in fulfilment of the requirements for the degree of Doctor of Philosophy

in the Niels Bohr Institute, Faculty of Science
University of Copenhagen

December 2013

Abstract

This thesis describes two subjects that I mainly work on during my PhD study. They are both about scattering amplitudes, covering gravity and gauge theories, tree and loop level, with or without supersymmetry. The first subject is Kawai-Lewellen-Tye(KLT) relation in field theory, which mysteriously relates Yang-Mills amplitudes to gravity amplitudes. Based on many known works about KLT and super-KLT relations, we provide a complete map between super-gravity amplitudes and super-Yang-Mills amplitudes for any number of supersymmetry that allowed in 4-dimensional theory. We also provide an explanation for vanishing identities of Yang-Mills amplitudes as violation of linear symmetry groups based on KLT relation argument. The second subject is integrand reduction of multi-loop amplitude. The recent methods based on computational algebraic geometry make it possible to systematically study multi-loop amplitude with generalized unitarity cut. Using Gröbner basis and primary decomposition, we thoroughly study integrand basis and solution space of equations from maximal unitarity cut for all 4-dimensional two-loop topologies. Algorithm and examples of this computation are illustrated in this thesis. We also study a special type of two-loop and three-loop diagrams where equations of maximal unitarity cut define complex curve. Geometry genus of complex curve is a topological invariant, and characterizes the property of curve. We compute the genus of complex curve for some two-loop and three-loop diagrams from information of degree and singular points of that curve using algebraic geometry method. Information of integrand basis, structure of solution space as well as geometric genus is useful for future multi-loop amplitude computation.

Publication list

During PhD Study

1. R. Huang and Y. Zhang, **On Genera of Curves from High-loop Generalized Unitarity Cuts**, JHEP **1304**, 080 (2013), arXiv:1302.1023 [hep-ph].
2. B. Feng and R. Huang, **The classification of two-loop integrand basis in pure four-dimension**, JHEP **1302**, 117 (2013), arXiv:1209.3747 [hep-ph].
3. P. H. Damgaard, R. Huang, T. Sondergaard and Y. Zhang, **The Complete KLT-Map Between Gravity and Gauge Theories**, JHEP **1208**, 101 (2012), arXiv:1206.1577 [hep-th].

Before PhD Study

1. B. Feng, Y. Jia and R. Huang, **Relations of loop partial amplitudes in gauge theory by Unitarity cut method**, Nucl. Phys. B **854**, 243 (2012), arXiv:1105.0334 [hep-ph].
2. J. -H. Huang, R. Huang and Y. Jia, **Tree amplitudes of noncommutative U(N) Yang-Mills Theory**, J. Phys. A **44**, 425401 (2011), arXiv:1009.5073 [hep-th].
3. B. Feng, S. He, R. Huang and Y. Jia, **Note on New KLT relations**, JHEP **1010**, 109 (2010), arXiv:1008.1626 [hep-th].
4. Y. Jia, R. Huang and C. -Y. Liu, $U(1)$**-decoupling, KK and BCJ relations in** $\mathcal{N} = 4$ **SYM**, Phys. Rev. D **82**, 065001 (2010), arXiv:1005.1821 [hep-th].
5. B. Feng, R. Huang and Y. Jia, **Gauge Amplitude Identities by On-shell Recursion Relation in S-matrix Program**, Phys. Lett. B **695**, 350 (2011), arXiv:1004.3417 [hep-th].
6. B. Feng, R. Huang, Y. Jia, M. Luo and H. Wang, **Cross section evaluation by spinor integration: The massless case in D-4**, Phys. Rev. D **81**, 016003 (2010), arXiv:0905.2715 [hep-ph].

Acknowledgements

I would like to thank my PhD supervisor Poul Henrik Damgaard and co-supervisor Emil Bjerrum-Bohr, who provide me such a wonderful opportunity studying in the Niels Bohr Institute, and also for the discussions and encouragements both in academy and personal life. The Niels Bohr Institute is the best place I have ever been, and I think it would be the best for many years before I can find a better one.

I would also like to thank my master supervisor Bo Feng in Zhejiang University. His insight in life and personal style in research greatly inspire my style of doing research. I also want to thank my collaborator Yang Zhang in Niels Bohr Institute, whose hard working and knowledge of mathematics and chemistry always make me feel shame.

Grateful thanks should be given to our group secretary Helle Kiilerich. She always takes care about everything, which makes the research and life in Copenhagen very comfortable.

I would like to thank all my colleges at Niels Bohr Institute and Niels Bohr International Academy for so many interesting discussions about physics and life in coffee lounge.

Special thanks to my family and my girl friend Yazhi Qin. I could not enjoy the academy life without their supports.

Contents

Dedicated to all the people who helped and inspired me during my growing up and then disappeared in my life.

Chapter 1

Introduction

1.1 Scattering amplitude in a nutshell

Pursuit of simplicity has never been stopped for physics research, even though we are confronting more and more complicated phenomena. In the past decade, tremendous researches have been done to uncover the simplicity of scattering amplitude[1]. Many old ideas are studied again. With a modern interpretation, their hidden power has been released for amplitude computations that can not even image to do so in old days.

Traditionally, scattering amplitude is computed perturbatively by Feynman rules of Feynman diagrams. Feynman rules are derived from Lagrangian description of field theories. In the days when it is firstly proposed, it served as very efficient method for computing amplitude. However, the Feynman diagram approach suffers many disadvantages in modern amplitude computations. This is because we are already going beyond simple amplitude of few points and tree level scattering process. The complexity of computation using Feynman rules is factorial in the number of particles as well as number of loops. This leads to a bottleneck for computing complicated amplitudes. It also suffers from unphysical singularities in intermediate steps of computations, which cause unnecessary errors in numeric computations.

To bypass disadvantages of Feynman diagram approach, we have a straightforward way: throw it away. New changes for amplitude computation take place since 2003, at which time Witten showed that perturbative gauge theory can be described as string theory in twistor space[2]. The simplicity of scattering amplitudes then shows up, and hints new methods for amplitude computation. Soon after that, a method is proposed in Cachazo-Svrcek-Witten(CSW) formalism[3, 4]. By using MHV rules, it is possible to compute Maximal-Helicity-Violating(MHV) amplitude from MHV vertices through certain off-shell continuation. Then a simple and powerful recursion relation is proposed by Britto-Cachazo-Feng-Witten(BCFW)[5, 6]. The BCFW recursion relation interprets amplitude as complex function of single variable. Then complex analysis can be introduced in amplitude computation, especially Cauchy's theorem. The physical amplitude is computed from lower-point on-shell tree amplitudes. The on-shell condition excludes many Feynman diagrams, which greatly simplify the computation. Since it does not rely on any specific Lagrangian description of field theories, this motives us to re-think the S-matrix program proposed in 1960'th[7–9]. Many well known results are re-studied in the framework of S-matrix program using BCFW recursion relation, especially for tree amplitudes. On one hand, complicated tree amplitudes are being computed from three-point amplitudes without referring to the Lagrangian of field theory[10–12]. On the other hand, non-trivial relations of tree amplitudes are proved. These non-trivial relations include the $U(1)$-decoupling relation[13–15], Kleiss-Kuijf(KK) relation[16] as well as recently proposed Bern-Carrasco-Johansson(BCJ) relation[17]. They are examined from string theory approach[18, 19] and pure field theory approach[20–25].

Since so many works have been done for tree amplitudes from 2003, there are almost no simple researches left now. We are forced to study gravity amplitude and loop amplitude. This is of course lucky for physics, but somehow unlucky for students, since computation of gravity amplitude and loop amplitude is so difficult. Every small effort contributes to a little progress, which pushes the research a step forward. But we are still on the road no matter how difficult it is.

Almost no one likes gravity amplitude computation, not even drawing all contributing Feynman diagrams. Fortunately, there is an indirect way of computing gravity amplitude from Yang-Mills amplitudes via Kawai-Lewellen-Tye relation[26]. This relation is proposed in 1985 for string amplitudes, but it finds its important application in field theory amplitude computation. However, KLT relation is only valid for tree gravity and Yang-Mills amplitudes. We should go beyond tree level, since any simple and not so simple pieces of tree amplitudes have already been studied and re-studied during last decade. Shortly after the discovery of BCJ relation, a BCJ conjecture[27, 28] has been proposed. This conjecture states that, for representations of Yang-Mills amplitudes where kinematic factors of diagrams follow the same Jacobi identity of color factors from corresponding diagrams, the gravity amplitude can be straightforwardly produced by squaring kinematic factors of two Yang-Mills amplitudes in those representations. Such representation can be constructed for both tree and loop amplitudes, as far as the Feynman diagrams to be included are cubic diagrams. So the BCJ conjecture can be used to compute loop gravity amplitude from loop Yang-Mills amplitude[29–37], with the help of computer.

Computation of loop Yang-Mills amplitudes goes far beyond computation of loop gravity amplitudes. While results of loop gravity amplitudes are still restricted to some examples, the systematic computation of one-loop Yang-Mills amplitudes is already fully implemented[38]. Any one-loop integrals can be expanded to finite number of known integrals, and the expansion coefficients can be computed by unitarity cut. The computation takes advantages of spinor-helicity formalism and compact tree amplitude results produced by BCFW recursion relation. Researches on integral reduction of two-loop and three-loop amplitudes also provide very inspiring results[39–47]. For the integrand reduction approach, recent researches inspired by computational algebraic geometry method[48, 49] push one-loop integrand induction[50–55] to multi-loop integrand reduction[56–65]. This is theoretically true, but practical computation still depends on the efficiency of algorithm and ability of computer. The first step is taken by computing integrand basis of multi-loop amplitudes via Gröbner basis method and generalized unitarity cut method. It is totally translated to mathematical problem, so systematic algorithm can be implemented. Further information of the algebraic system defined by generalized unitarity cut of multi-loop amplitude is detailed explored by algebraic geometry methods such as Gröbner basis, primary decomposition of ideal, varieties and branch structures of reducible algebraic set, geometric genus of complex curve, etc. This information can be used in the further steps of multi-loop amplitude computations such as integral reduction with Integration-By-Parts(IBP) method[66–69] or fitting coefficients of master integrals.

Although theoretical tree amplitude computation is approaching the final stage, theoretical loop amplitude computation is still in its very early period. The complexity of multi-loop gravity and Yang-Mills amplitudes is really a challenge both for theoretical and practical computations. The simplicity of tree amplitude discovered in the past decade starts a revolution of tree amplitude computation, and finally makes it trivial to compute any tree amplitudes theoretically. We believe that the simplicity of multi-loop amplitude is still hidden somewhere waiting for us to pursuit. This belief will inspire further researches on the amplitude community.

1.2 Outline of the thesis

This thesis describes two subjects that I mainly work on during my PhD study[61, 70, 71]. They are presented in following chapters after a brief introduction of basic knowledge and convention that are frequently used in amplitude computations.

The whole chapter 2 is devoted to KLT and super-KLT relations in field theory. Since (super-)KLT relation has already been proven by pure field theory method, we think it is consistent within field theory and do not mention its string theory origin in this thesis. The first section describes various formulations of KLT relations and shows that they are equivalent through BCJ relation. The second section describes our work on super-KLT relation. The complete map between super-gravity amplitudes and super-Yang-Mills amplitudes for any number of supersymmetry in 4-dimensional theory is provided. The linear symmetry groups of super-gravity theories that inferred from KLT products are also illustrated, and their roles in the vanishing identities of Yang-Mills amplitudes are discussed. The main results of this section have been published in [70].

Chapter 3 describes the basics of loop amplitude computation. After introducing two major representations of loop integral, we focus on one of them where color information is separated and kinematic information defines color-ordered partial amplitude. This representation is especially useful for practical computation. Firstly we introduce the traditional integral reduction procedure, and concentrate on one-loop integral reduction. The unitarity cut and generalized unitarity cut are introduced for the reduction. Then a whole section is devoted to the introduction of algebraic geometry. With these mathematical concepts, the last section describes integrand reduction of multi-loop amplitude as a problem of algebraic geometry. Ideas and algorithms discussed in this section will be applied to detailed analysis of two-loop and three-loop diagrams in chapter 4 and chapter 5.

Chapter 4 describes integrand basis of 4-dimensional two-loop topologies. The integrand basis is obtained by computational algebraic geometry methods. Possible topologies of two-loop amplitude are discussed in the first section. The second section provides general discussion of algebraic system defined by equations of maximal unitarity cut of 4-dimensional two-loop topologies. Since complete results for all topologies are too much to present, in this thesis, we select two typical topologies and provide detailed analysis in section 3 and section 4. The complete results have been published in [61].

Chapter 5 describes a special type of multi-loop topologies where equations of maximal unitarity cut define a complex curve. For this complex curve, we compute the geometric genus. Since geometric genus is topological invariant, it characterizes properties of curve. It is also a judgement of rational solution for equations of maximal unitarity cut. The first section describes the way of birationally mapping non-plane curve to plane curve, whose genus is much easier to be computed. The second section discuss genus of curves from two-loop diagrams and the third section discuss genus of curve from three-loop diagrams. The main results of this chapter have been published in [71].

Conclusion and outlook are given in the last chapter.

1.3 Preliminary

Many concepts and notations are frequently used in amplitude computations. In this section, we introduce some basics which will be used in following chapters. They can be found in many review papers, for example [72, 73].

1.3.1 Gauge group

For convenience we can study Yang-Mills theory of $SU(N)$ group. The generators $(T^a)_i^{\ \bar{j}}$, $a = 1, 2, \ldots, N^2 - 1$, of $SU(N)$ group in fundamental representation are $N \times N$ traceless Hermitian matrices. They can be normalized as

$$\mathrm{Tr}(T^a T^b) = \delta^{ab} \quad , \quad [T^a, T^b] = i\sqrt{2} f^{abc} T^c \ , \tag{1.1}$$

where square bracket is normal commutator and f^{abc} is Lie algebra structure constant.

Gluon is in the adjoint representation of $SU(N)$ group, and it carries an adjoint color index a, $a = 1, 2, \ldots, N^2 - 1$. Quark or antiquark is in the fundamental representation, and carries an i or $\bar{j}$ index, $i, \bar{j} = 1, 2, \ldots, N$, but color free. Each gluon-quark-antiquark vertex contains a factor $(T^a)_i^{\ \bar{j}}$, each gluon three-vertex contains a structure constant f^{abc}, and each gluon four-vertex contains structure constants $f^{abe} f^{cde}$. To simplify amplitude computation, it is better to eliminate all structure constants by generators T^a before computation. This can be done by applying identity

$$i\sqrt{2} f^{abc} = \mathrm{Tr}(T^a T^b T^c) - \mathrm{Tr}(T^a T^c T^b) \ . \tag{1.2}$$

As a result, the color factors of Feynman diagram are represented by products of traces of generators as $\mathrm{Tr}(\ldots)\ldots\mathrm{Tr}(\ldots)$. If external quarks are also involved, there will be strings of generators ended by fundamental indices as $(T^{a_1} \ldots T^{a_m})_i^{\ \bar{j}}$. Then we can apply Fierz identity of $SU(N)$ group

$$\sum_a (T^a)_{i_1}^{\ \bar{j}_1} (T^a)_{i_2}^{\ \bar{j}_2} = \delta_{i_1}^{\ \bar{j}_2} \delta_{i_2}^{\ \bar{j}_1} - \frac{1}{N} \delta_{i_1}^{\ \bar{j}_1} \delta_{i_2}^{\ \bar{j}_2} \tag{1.3}$$

to reduce all color structures in terms of traces of generators.

The second term in the right hand side of (1.3) is introduced to implement the traceless condition of $SU(N)$ group. Identity (1.3) states that the $SU(N)$ generators T^a form a complete set of $N \times N$ traceless Hermitian matrices. Sometimes it is convenient to get rid of the second term $-1/N$ in (1.3) by considering $U(N) = SU(N) \times U(1)$ group. The traceless condition is then relaxed, and the additional $U(1)$ generator is proportional to identity matrix

$$(T^{a_0})_i^{\ \bar{j}} = \frac{1}{\sqrt{N}}\delta_i^{\ \bar{j}} \ . \tag{1.4}$$

This $U(1)$ gauge field is referred to as photon. The generator commutes with all generators of $SU(N)$ group with zero structure constant, so it does not couple to gluon.

From Fierz identity, it is possible to write the product of two traces as

$$\begin{aligned} \mathrm{Tr}(T^aX)\mathrm{Tr}(T^aY) &= \sum_{i,k}(T^a)_k^{\ i}X_i^{\ k}\sum_{j,m}(T^a)_m^{\ j}Y_j^{\ m} \\ &= \sum_{i,k,j,m}\delta_m^{\ i}\delta_k^{\ j}X_i^{\ k}Y_j^{\ m} - \sum_{i,k,j,m}\frac{1}{N}\delta_k^{\ i}\delta_m^{\ j}X_i^{\ k}Y_j^{\ m} \\ &= \mathrm{Tr}(XY) - \frac{1}{N}\mathrm{Tr}(X)\mathrm{Tr}(Y) \ , \end{aligned} \tag{1.5}$$

where X, Y are any sequences of generators. There are two terms in the Fierz identity. However, if we only consider contracting structure constants such as

$$f^{a_1b_1e_1}f^{e_1b_2e_2}\cdots f^{e_{k-1}b_kc_k},$$

since f^{abe} can be replaced by $\mathrm{Tr}(T^aT^bT^e)-\mathrm{Tr}(T^bT^aT^e)$, after contracting we can always get $-1/N$ terms as

$$-\frac{1}{N}\cdots(\mathrm{Tr}(T^aT^b) - \mathrm{Tr}(T^bT^a)) \ , \tag{1.6}$$

where $\cdots$ represents any products of traces from contracting other structure constants. They are all canceled out since cyclic permutation invariance of trace implies $\mathrm{Tr}(T^aT^b) = \mathrm{Tr}(T^bT^a)$. So the $-1/N$ term in (1.5) does not contribute in the color structures of gluon vertices. This is expected since photon dose not couple to gluon. So we can write products of traces of $SU(N)$ generators as

$$\sum_a \mathrm{Tr}(T^aX)\mathrm{Tr}(T^aY) = \mathrm{Tr}(XY) \ \ , \ \ \sum_a \mathrm{Tr}(T^aXT^aY) = \mathrm{Tr}(X)\mathrm{Tr}(Y) \ . \tag{1.7}$$

The second relation in (1.7) is useful when working out color structures of loop amplitude. Especially, if X is identity, we have

$$\sum_a \mathrm{Tr}(T^aT^aY) = \sum_a\sum_{i,j,k}(T^a)_j^{\ i}(T^a)_k^{\ j}Y_i^{\ k} = \sum_a\sum_{i,j,k}\delta_k^{\ i}\delta_j^{\ j}Y_i^{\ k} = N\mathrm{Tr}(Y) \ , \tag{1.8}$$

where $N = \mathrm{Tr}(I)$ is the trace of identity matrix. This is the reason why we only have single trace structure for tree amplitudes, but double, triple or N-ple trace structures for loop amplitudes.

After eliminating structure constants by traces of generators, we separate color part and kinematic part from full amplitude. The kinematic information associated with certain trace structures then can be identified as partial amplitudes, which are color-ordered and much easier to be computed than full amplitude. In fact, we can compute partial amplitudes, and assemble them into full amplitude according to the color structures.

1.3.2 Spinor-Helicity formalism

The spinor-helicity formalism is widely used in recent methods of amplitude computation, and responsible for compact and simple final results. The idea is to express the mathematical structures of amplitude with two-dimensional irreducible representation of Lorentz group, especially the Dirac spinors, polarization vectors and momenta. The representation can be chosen as Weyl spinor of massless particles. Note that Lorentz group can be expressed as $SU(2)_L \times SU(2)_R$, so we can use two independent two-dimensional representations $(1/2, 0)$ and $(0, 1/2)$ to express the finite dimensional representation of Lorentz group.

Let us start from the Weyl spinor of massless momentum, which can be found by solving massless Dirac equation

$$p_\mu \gamma^\mu u(p) = 0 \ , \tag{1.9}$$

where $u(p)$ is four-component vector, and gamma matrices satisfy anti-commutation relations

$$\{\gamma^\mu, \gamma^\nu\} = 2g^{\mu\nu} I_{4\times 4} \quad , \quad g^{\mu\nu} = \mathrm{diag}(+,-,-,-) \ . \tag{1.10}$$

In the Weyl representation, gamma matrices have explicit form as

$$\gamma^0 = \begin{pmatrix} 0 & I_{2\times 2} \\ I_{2\times 2} & 0 \end{pmatrix} \ , \quad \gamma^i = \begin{pmatrix} 0 & \sigma^i \\ -\sigma^i & 0 \end{pmatrix} \ , \tag{1.11}$$

where σ^i is 2×2 Pauli matrix. So the four-component Dirac spinor can be written as two two-component Weyl spinors

$$u(p) = \begin{pmatrix} u_\alpha(p) \\ \widetilde{u}^{\dot\alpha}(p) \end{pmatrix} \ , \tag{1.12}$$

and the Dirac equation becomes

$$p\cdot\sigma_{\beta\dot\alpha}\widetilde{u}^{\dot\alpha} = 0 \quad , \quad p\cdot\sigma^{\dot\beta\alpha}u_\alpha = 0 \ . \tag{1.13}$$

The index of Weyl spinor is raised and lowered by two-dimensional anti-symmetric Levi-Civita tensor $\epsilon_{\alpha\beta}$ or $\epsilon_{\dot{\alpha}\dot{\beta}}$. A commonly used notation of spinor is given by

$$\lambda^{\alpha}(p) = \langle p| \ \ , \ \ \lambda_{\alpha}(p) = |p\rangle \ \ , \ \ \widetilde{\lambda}_{\dot{\alpha}}(p) = [p| \ \ , \ \ \widetilde{\lambda}^{\dot{\alpha}}(p) = |p] \ . \tag{1.14}$$

With this notation, the inner product of two Weyl spinors associated to two massless momenta p_i, p_j can be expressed as

$$\langle i\ j\rangle \equiv \lambda^{\alpha}(p_i)\lambda_{\alpha}(p_j) = \epsilon^{\alpha\beta}\lambda_{\alpha}(p_i)\lambda_{\beta}(p_j) = \lambda_1(p_i)\lambda_2(p_j) - \lambda_2(p_i)\lambda_1(p_j) \ , \tag{1.15}$$

$$[i\ j] \equiv \widetilde{\lambda}_{\dot{\alpha}}(p_i)\widetilde{\lambda}^{\dot{\alpha}}(p_j) = \epsilon_{\dot{\beta}\dot{\alpha}}\widetilde{\lambda}^{\dot{\alpha}}(p_i)\widetilde{\lambda}^{\dot{\beta}}(p_j) = \widetilde{\lambda}^{\dot{1}}(p_i)\widetilde{\lambda}^{\dot{2}}(p_j) - \widetilde{\lambda}^{\dot{2}}(p_i)\widetilde{\lambda}^{\dot{1}}(p_j) \ . \tag{1.16}$$

We can decompose massless momentum as two Weyl spionrs

$$p^{\alpha\dot{\alpha}} = p^{\mu}\cdot(\sigma_{\mu})^{\alpha\dot{\alpha}} = \lambda^{\alpha}\widetilde{\lambda}^{\dot{\alpha}} = |p]\langle p| \ \ , \ \ p_{\alpha\dot{\alpha}} = p^{\mu}\cdot(\sigma_{\mu})_{\alpha\dot{\alpha}} = \lambda_{\alpha}\widetilde{\lambda}_{\dot{\alpha}} = |p\rangle[p| \ , \tag{1.17}$$

since $\det(p\cdot\sigma) = p^2 = 0$ for massless momentum. If we treat momentum as complex valued, then $\lambda, \widetilde{\lambda}$ are independent. If momentum is real in Minkowski space, we should constrain $\widetilde{\lambda} = \bar{\lambda}$, the complex conjugate of λ. The inner product of two momenta is related to the inner product of spinors as

$$\langle i\ j\rangle\,[j\ i] = \lambda^{\alpha}(p_i)\lambda_{\alpha}(p_j)\widetilde{\lambda}_{\dot{\alpha}}(p_j)\widetilde{\lambda}^{\dot{\alpha}}(p_i) = p_i^{a\dot{\alpha}}p_{j,\alpha\dot{\alpha}} = p_{i,\mu}\sigma^{\mu,\alpha\dot{\alpha}}\sigma^{\nu}_{\alpha\dot{\alpha}}p_{j,\nu} = 2p_i\cdot p_j \ . \tag{1.18}$$

We use QCD convention in above relation, while the string convention differs with a minus sign.

Many identities are quite useful for computation with spinors. They are

- $\langle i|\gamma^{\mu}|i] = 2p_i^{\mu}$, Gordon identity,
- $\langle i\ j\rangle = -\langle j\ i\rangle$, $[i\ j] = -[j\ i]$, $\langle i\ i\rangle = [i\ i] = 0$, Antisymmetry,
- $\langle i|\gamma^{\mu}|j] = \langle j|\gamma^{\mu}|i]$, Charge conjugation,
- $\langle i|\gamma^{\mu}|j]\,\langle k|\gamma^{\mu}|l] = 2\,\langle i\ k\rangle\,[j\ l]$, Fierz rearrangement,
- $\langle i\ j\rangle\,\langle k| + \langle k\ i\rangle\,\langle j| + \langle k\ i\rangle\,\langle j| = 0$, Schouten identity,
- $\sum_k \langle i\ k\rangle\,[k\ j] = 0$, Momentum conservation.

These identities are also valid when replacing $|\cdot\rangle \to |\cdot], |\cdot] \to |\cdot\rangle$.

The next object to be expressed by Weyl spionr is polarization vector. It has two states $\epsilon^{\pm}_{\mu}$ with four components $\mu = 0, 1, 2, 3$, which produce the helicity ± 1. An explicit representation for polarization vector is given by

$$\epsilon_\mu^+(p) = \frac{\langle r|\gamma_\mu|p]}{\sqrt{2}\,\langle r\ p\rangle} \quad , \quad \epsilon_\mu^- = \frac{\langle p|\gamma_\mu|r]}{\sqrt{2}\,[p\ r]} \ , \tag{1.19}$$

or in the matrix form

$$\epsilon_{\dot\alpha\alpha}^+(p) = \frac{\sqrt{2}\widetilde{\lambda}_{\dot\alpha}(p)\lambda_\alpha(r)}{\langle r\ p\rangle} = \frac{\sqrt{2}|r\rangle[p|}{\langle r\ p\rangle} \quad , \quad \epsilon_{\dot\alpha\alpha}^-(p) = \frac{\sqrt{2}\widetilde{\lambda}_{\dot\alpha}(r)\lambda_\alpha(p)}{[p\ r]} = \frac{\sqrt{2}|p\rangle[r|}{[p\ r]} \ , \tag{1.20}$$

where r is arbitrary reference momentum representing the freedom of on-shell gauge transformation, and will disappear in the final result. The polarization vectors are normalized as

$$\epsilon^+(p)\cdot\epsilon^-(p) = -1 \quad , \quad \epsilon^\pm(p)\cdot\epsilon^\pm(p) = 0 \ . \tag{1.21}$$

They are transverse to p for any reference momentum r

$$\epsilon^\pm(p)\cdot p = 0 \ , \tag{1.22}$$

and the complex conjugation reverses helicity

$$(\epsilon^+(p))^* = \epsilon^-(p) \ . \tag{1.23}$$

The completeness relation of polarization vectors with reference momentum r gives a light-like axial gauge with gauge vector r

$$\epsilon_\mu^+(p)\epsilon_\nu^-(p) + \epsilon_\mu^-(p)\epsilon_\nu^+(p) = -g_{\mu\nu} + \frac{p_\mu r_\nu + r_\mu p_\nu}{p\cdot r} \ . \tag{1.24}$$

For gravity theory, we also have graviton states with helicity ± 2. These states can be produced by 2-dimensional polarization tensor $\epsilon_{\mu\nu}^\pm$, which can be written as products of two polarization vectors as

$$\epsilon_{\mu\nu}^\pm(p) = \epsilon_\mu^\pm(p)\epsilon_\nu^\pm(p) \ . \tag{1.25}$$

1.3.3 Three-point amplitude

The three-point amplitude is the basic building block for modern methods of amplitude computation. In Yang-Mills theory, the color-ordered three-point vertex with definite helicity is produced by contracting three-vertex with corresponding polarization vectors of external states. However, it is possible to construct three-point amplitude from discussion of consistency conditions[74, 75] without specific Lagrangian description.

For massless three-point amplitude, momentum conservation $p_1 + p_2 + p_3 = 0$ and on-shell conditions $p_i^2 = 0$, $i = 1, 2, 3$ ensure that $p_i \cdot p_j = 0$ for arbitrary $i, j = 1, 2, 3$. Expressed in spinor-helicity formalism, we have

$$\langle 1\ 2\rangle\, [2\ 1] = 0 \ \ , \quad \langle 1\ 3\rangle\, [3\ 1] = 0 \ \ , \quad \langle 2\ 3\rangle\, [3\ 2] = 0 \ . \tag{1.26}$$

We want to find the non-trivial solution of above equations. If $\langle 1\ 2\rangle = 0$ and $\langle 1\ 3\rangle = 0$, both $|2\rangle$, $|3\rangle$ are proportional to $|1\rangle$. Then we can write $|2\rangle = t_1|1\rangle$, $|3\rangle = t_2|1\rangle$, and $\langle 2\ 3\rangle$ automatically vanishes. However, if momenta are real, we have $|i] \sim |i\rangle^*$. So inner products $[i\ j]$ for any $i, j = 1, 2, 3$ also vanish. In this sense, no non-trivial three-point amplitude can be constructed from inner products of spinors. Instead, we can consider all momenta as complex valued, then $|i]$ and $|i\rangle$ are independent, and each set of solutions

$$\langle 1\ 2\rangle = \langle 2\ 3\rangle = \langle 3\ 1\rangle = 0 \ \ , \quad [i\ j] \ \text{non-zero} \ , \tag{1.27}$$

$$[1\ 2] = [2\ 3] = [3\ 1] = 0 \ \ , \quad \langle i\ j\rangle \ \text{non-zero} \tag{1.28}$$

satisfies momentum conservation and on-shell conditions. So the complex three-point amplitude should be a purely holomorphic or anti-holomorphic function of spinors. By requiring consistency conditions from assumption of S-matrix that the Poincaré group acts on scattering amplitude as it acts on individual one-particle states, the three-point amplitude is forced to be

$$A_3(1^{h_1}, 2^{h_2}, 3^{h_3}) = \kappa_H \,\langle 1\ 2\rangle^{d_3} \langle 2\ 3\rangle^{d_1} \langle 3\ 1\rangle^{d_2} + \kappa_A \,[1\ 2]^{-d_3}\, [2\ 3]^{-d_1}\, [3\ 1]^{-d_2} \ \ , \tag{1.29}$$

where h_i is helicity of particle p_i, and $d_1 = h_1 - h_2 - h_3$, $d_2 = h_2 - h_3 - h_1$, $d_3 = h_3 - h_1 - h_2$. κ_H, κ_A are constants, and one of them should be zero, in order to fulfill the correct physics behavior in the limit of real momentum. Explicitly, if $d_1 + d_2 + d_3$ is positive, then κ_A should be zero in order to avoid infinity. Similarly, if $d_1 + d_2 + d_3$ is negative, then κ_H should be zero.

Let us apply above discussion in Yang-Mills theory, where the helicity could be $\pm 1, \pm 1/2$ or 0. Note that above discussion could not exclude the possibility of theories with three-point amplitude of the form $A_3(1^\pm, 2^\pm, 3^\pm)$. But such theories will contain a high power of momenta in cubic vertex. In Yang-Mills theory, we can only consider following non-trivial three-point vertices. (1) pure gluon three-vertex,

$$A_3(1^-, 2^-, 3^+) = \frac{\langle 1\ 2\rangle^3}{\langle 2\ 3\rangle\, \langle 3\ 1\rangle} \ \ , \quad A_3(1^+, 2^+, 3^-) = \frac{[1\ 2]^3}{[2\ 3]\, [3\ 1]} \ , \tag{1.30}$$

(2) gluon coupled to fermion pair three-vertex

$$A_3(1^{-\frac{1}{2}}, 2^{+\frac{1}{2}}, 3^-) = \frac{\langle 3\ 1\rangle^2}{\langle 1\ 2\rangle} \quad , \quad A_3(1^{-\frac{1}{2}}, 2^{+\frac{1}{2}}, 3^+) = \frac{[3\ 1]^2}{[1\ 2]} \ , \tag{1.31}$$

and (3) gluon coupled to scalar pair three-vertex

$$A_3(1^0, 2^0, 3^-) = \frac{\langle 2\ 3\rangle \langle 3\ 1\rangle}{\langle 1\ 2\rangle} \quad , \quad A_3(1^0, 2^0, 3^+) = \frac{[2\ 3]\,[3\ 1]}{[1\ 2]} \ . \tag{1.32}$$

All constant pre-factors have been ignored in above expressions.

1.3.4 BCFW recursion relation

Taking advantages of spinor-helicity formalism and complex momentum, the Britto-Cachazo-Feng-Witten(BCFW) recursion relation[5, 6] is a powerful tool for analyzing and computing amplitudes. This method dose not rely on Lagrangian description of field theories, but tries to extract as much information as possible from general assumptions.

The amplitude is real valued, but it has no problem to extend it to complex plane, provided that the amplitude is analytic function. One way of complexifying amplitude as function of complex variable is to deform external momentum. Suppose we have selected two massless gluons whose momenta are $p_k = \lambda_k \widetilde{\lambda}_k$ and $p_n = \lambda_n \widetilde{\lambda}_n$, then we can introduce a complex variable z, and deform them as

$$\widehat{p}_k(z) = \lambda_k(\widetilde{\lambda}_k - z\widetilde{\lambda}_n) \quad , \quad \widehat{p}_n(z) = (\lambda_n + z\lambda_k)\widetilde{\lambda}_n \ . \tag{1.33}$$

The other external momenta are kept the same. This deformation modifies the anti-holomorphic part of momentum p_k and holomorphic part of momentum p_n, while preserves two properties, (1) all momenta after deformation are still on-shell, (2) momentum conservation of all external momenta after deformation still holds. In fact, it is not necessary to use spinor-helicity formalism. We can introduce an arbitrary four-vector q, and deform two momenta as

$$\widehat{p}_k(z) = p_k - zq \quad , \quad \widehat{p}_n(z) = p_n + zq \ , \tag{1.34}$$

with $q^2 = p_k \cdot q = p_n \cdot q = 0$. But spinor-helicity formalism makes computation simple. With momenta deformation, the amplitude becomes a function of single complex variable

$$A(z) = A(p_1, \ldots, p_{k-1}, \widehat{p}_k(z), p_{k+1}, \ldots, p_{n-1}, \widehat{p}_n(z)) \ . \tag{1.35}$$

The advantage of such deformation is that, for generic external momenta, $A(z)$ is rational function of complex variable z with only simple poles. The poles come from propagators where only one $\widehat{p}_k(z)$ or $\widehat{p}_n(z)$ is included, since $\widehat{p}_k(z) + \widehat{p}_n(z) = p_k + p_n$, which is independent of z. Furthermore, if we consider following Cauchy's theorem

$$0 = \frac{1}{2\pi i}\oint_{\Gamma} dz \frac{A(z)}{z} \ , \tag{1.36}$$

where Γ is a large enough contour, and assume that $A(z)$ vanishes at infinity, then there is no boundary contribution, and above contour integration is totally given by its residues. These residues are computed at $z = 0$ and at locations of simple poles from $A(z)$. So we have

$$A_n(0) = -\sum_{i,j}\sum_{h=\pm} A_L(\ldots,\widehat{p}_k(z_{ij}),\ldots,\widehat{p}_{ij}^{h}(z_{ij}))\frac{1}{p_{ij}^2}A_R(-\widehat{p}_{ij}^{-h}(z_{ij}),\ldots,\widehat{p}_n(z_{ij}),\ldots) \ . \tag{1.37}$$

The summation is over all possible helicity configurations and diagrams of propagators with only one $\widehat{p}_k(z)$ or $\widehat{p}_n(z)$. z_{ij} is the solution of $\widehat{p}_{ij}(z)^2 = (p_{ij} + z\lambda_k\widetilde{\lambda}_n)^2 = 0$,

$$z_{ij} = \frac{p_{ij}^2}{\langle k|p_{ij}|n]} \ . \tag{1.38}$$

Since the amplitude is computed at phase space where propagators $\widehat{p}_{ij}(z)$ are on-shell, the summation only contains on-shell diagrams. $A_n(0)$ is the physical amplitude we want, and A_L, A_R are tree amplitudes that having fewer external momenta than A_n. If A_L contains n_1 external legs, then it is $(n_1 + 1)$-point tree amplitude, and A_R is $(n-n_1+1)$-point tree amplitude. n_1 ranges from 2 to $(n-2)$, so (n_1+1) and $(n-n_1+1)$ are always smaller than n. We can recursively perform similar momenta deformation (1.33) and BCFW expansion (1.37) for A_L and A_R until all of them can be constructed only from three-point amplitudes. This is fascinating, since as already mentioned, three-point amplitude can be determined by general physics considerations, while BCFW recursion relation is also based on very general assumptions about field theory and scattering amplitude. So it is possible to build up field theory based on general principles without relying on specific Lagrangian.

Attention should be paid to the boundary contribution of contour integration (1.36) when $A(z)$ does not vanish as $z \to \infty$. The large z behavior of $A(z)$ depends on the way of deforming momenta (1.33). For Yang-Mills theory, it is always possible to select two momenta p_k, p_n with helicities $(-,+)$, $(+,+)$ or $(-,-)$. $A(z)$ vanishes as $z \to \infty$ under these momenta deformations. So in order to avoid boundary contributions, we can simply select two momenta p_k, p_n which have helicities $(h_k, h_n) = (-,+)$. However, even for some bad deformations where $A(z)$ does not vanish as $z \to \infty$, we can still compute the contour integration (1.36). Besides residues in locations $z = 0, z = z_{ij}$, there are as well additional terms from boundary contribution. The physical amplitude is then given by (1.37) plus corrections from boundary contribution[76–78]. Computation of boundary contribution is not easy, but if we are carefully enough and do not make mistakes, we should get the right physical amplitude.

1.3.5 MHV amplitude

We mentioned that non-trivial gluon three-point amplitudes with helicities $(-,-,+)$ or $(+,+,-)$ have very simple form when written in spinor-helicity formalism, while amplitudes of all plus or all minus helicities vanish. This can be generalized to arbitrary point gluon amplitude by introducing Maximal-Helicity-Violating(MHV) amplitude. Consider n-point amplitude with k minus helicities. When $k = 0$ or 1, the amplitudes vanish. The first non-trivial amplitude is MHV amplitude when $k = 2$, known as the Parke-Taylor amplitude[79], and it takes a simple form as

$$A_n(1^+,\dots,i^-,\dots,j^-,\dots,n^+) = \frac{\langle i\ j\rangle^4}{\langle 1\ 2\rangle\langle 2\ 3\rangle\cdots\langle n-1,n\rangle\langle n\ 1\rangle}\ , \tag{1.39}$$

where p_i, p_j are chosen to be minus helicities. Similarly, we define anti-MHV amplitude as amplitude with two-plus helicities and others minus. It also takes a simple form as

$$A_n(1^-,\dots,i^+,\dots,j^+,\dots,n^-) = \frac{[i\ j]^4}{[1\ 2]\,[2\ 3]\cdots[n-1,n]\,[n\ 1]}\ , \tag{1.40}$$

where p_i, p_j are chosen to be plus helicities. If $j = i+1$, then the numerator will cancel one factor in denominator.

For 4-point and 5-point amplitudes, they should either be zero or MHV, anti-MHV amplitudes. Especially for 4-point amplitudes, the MHV amplitude is as well the anti-MHV amplitude. This is a consequence of 4-point kinematics. Let us take $A(1^-,2^-,3^+,4^+)$ as example. Since $s_{12} = s_{34}$, we have $\langle 1\ 2\rangle[1\ 2] = \langle 3\ 4\rangle[3\ 4]$, and

$$\begin{aligned}\frac{\langle 1\ 2\rangle^3}{\langle 2\ 3\rangle\langle 3\ 4\rangle\langle 4\ 1\rangle} &= \frac{[3\ 4]^3\langle 3\ 4\rangle^3}{[1\ 2]^3\langle 2\ 3\rangle\langle 3\ 4\rangle\langle 4\ 1\rangle} = \frac{[3\ 4]^3\langle 3\ 4\rangle^2}{[1\ 2]\,\langle 3|2|1]\,\langle 4|1|2]}\\ &= \frac{[3\ 4]^3\langle 3\ 4\rangle^2}{[1\ 2]\,\langle 3|-4|1]\,\langle 4|-3|2]} = \frac{[3\ 4]^3}{[1\ 2]\,[2\ 3]\,[4\ 1]}\ .\end{aligned} \tag{1.41}$$

For A_n with $n \geq 6$, (1.39) and (1.40) are not enough to determine amplitudes of all helicity configurations. For example, 6-point amplitude could have three-minus, three-plus helicity configuration, defined as Next-MHV(NMHV) amplitude, which is far more complicated than 6-point MHV amplitude. Amplitude with $k+2$ minus helicities is called N^{k}MHV amplitude.

We can generalize MHV amplitude beyond pure gluon amplitude. The most close generalization is to include a fermion pair in the amplitude. Amplitude of a fermion pair with all plus gluon is trivially zero, and the first non-trivial amplitude is

$$A_n(1^{-\frac{1}{2}}, 2^{+\frac{1}{2}}, 3^+, \ldots, i^-, \ldots, n^+) = \frac{\langle 1\ i\rangle^3 \langle 2\ i\rangle}{\langle 1\ 2\rangle \langle 2\ 3\rangle \cdots \langle n-1, n\rangle \langle n\ 1\rangle} \ . \tag{1.42}$$

Similarly the anti-MHV amplitude is defined as

$$A_n(1^{-\frac{1}{2}}, 2^{+\frac{1}{2}}, 3^-, \ldots, i^+, \ldots, n^-) = \frac{[2\ i]^3 [1\ i]}{[1\ 2] [2\ 3] \cdots [n-1, n] [n\ 1]} \ . \tag{1.43}$$

They are also generalization of corresponding three-vertex amplitudes.

The MHV gravity amplitude also exists[80–85]. But compared to the simple formulation of MHV Yang-Mills amplitude, it is extremely complicated. A better understanding of gravity theory might be needed in order to construct a possibly simple formulation for MHV gravity amplitude.

1.3.6 Supersymmetry

Tree amplitude in Yang-Mills theory has apparent sypersymmetry[86, 87]. Supersymmetry is an idea of relating fermion and boson states, and treating them in an equivalent way. It is an extension of Poincaré algebra, by including additional anti-commutating spin half supercharge operators Q. Since this operator is fermionic, it will change spin states by half when acting on them.

Expressed in terms of Weyl spionr, the supercharge operators $Q \equiv (Q^a_\alpha, \widetilde{Q}^a_{\dot{\alpha}})$ have spinor indices $\alpha, \dot{\alpha} = 1, 2$, and also index $a = 1, 2, \ldots, \mathcal{N}$, where $\mathcal{N}$ is the number of supercharges. Q^a_α can be used to lower spin by half while $\widetilde{Q}^a_{\dot{\alpha}}$ can raise spin by half. The supercharges can be realized by Grassmann variables η through

$$\widetilde{Q}_a = \sum_{i=1}^{n} |i\rangle \eta_a \quad , \quad Q^a = \sum_{i=1}^{n} |i] \frac{\partial}{\partial \eta_a} \ . \tag{1.44}$$

η_a are numbers satisfying anti-commutating relations $\{\eta_a, \eta_b\} = 0$, but commute with normal numbers. It is easy to infer that $\eta_a^2 = 0$. The integration of Grassmann variables is defined as

$$\int d\eta = 0 \quad , \quad \int \eta d\eta = 1 \ , \tag{1.45}$$

and the differentiation of Grassmann number is identical to integration. It is also interesting to see that delta function of Grassmann number $\delta(\eta)$ is identical to η, follows directly from the definition of delta function and integration of Grassmann number. Fields in supersymmetric theories are then associated to Grassmann variables. For example, if $\mathcal{N}=1$, we have gluon g and gluino Λ fields. Using Grassmann variable η, they can be packed into a super-field

$$\Phi = g^{+} + \eta\Lambda^{+} \quad , \quad \Psi = \eta\Lambda^{-} + g^{-} \ . \tag{1.46}$$

Acting $\widetilde{Q}, Q$ on Φ, Ψ super-fields, we get

$$\widetilde{Q}\Phi = \eta g^{+} + 0 \quad , \quad \widetilde{Q}\Psi = 0 + \eta g^{-} \quad , \quad Q\Phi = 0 + \Lambda^{+} \quad , \quad Q\Psi = \Lambda^{-} + 0 \ . \tag{1.47}$$

Comparing with Φ, Ψ super-fields, it is easy to see that it gives the correct state transformation

$$\widetilde{Q} : (g^{+}, \Lambda^{+}, \Lambda^{-}, g^{-}) \to (0, g^{+}, 0, \Lambda^{-}) \quad , \quad Q : (g^{+}, \Lambda^{+}, \Lambda^{-}, g^{-}) \to (\Lambda^{+}, 0, g^{-}, 0) \ . \tag{1.48}$$

For 4-dimensional Yang-Mills theory, we have $\mathcal{N} = 1, 2, 4$. $\mathcal{N} = 3$ super-Yang-Mills theory describes the same theory as maximal $\mathcal{N} = 4$ super-Yang-Mills theory. For 4-dimensional gravity theory, $\mathcal{N}$ could be 1,2,4,6 or 8. $\mathcal{N} = 7, 5, 3$ super-gravity theories have their equivalent $\mathcal{N} = 8, 6, 4$ super-gravity theories. Generalization of supercharge operators and super-fields to $\mathcal{N}$ supersymmetric theories is straightforward, and we will discuss the details later.

Chapter 2

KLT relations

This chapter describes KLT relation[26] and its extension to supersymmetric theories[88]. The KLT relation is originally discovered almost thirty years ago when Kawai, Lewellen and Tye explored some mysterious relation between bosonic closed and open strings. By carefully defining the integral, they found that scattering amplitude of closed string can be factorized into product of two open string amplitudes. Since closed string contains spin-2 particle while open string contains spin-1 particle, they can be naturally identified as graviton and gluon. In the field theory limit, bosonic closed string provides a description of Einstein gravity theory, and open string provides a description of Yang-Mills theory. So KLT relation of string amplitudes also encodes mysterious connection between gravity amplitude and Yang-Mills amplitude. In bosonic case, it is the relation that relates pure graviton amplitude to pure gluon amplitude. This is already very surprising since such relation is totally obscure in the Lagrangian descriptions of these two theories. In heterotic string case, it is possible to go beyond pure gravity and Yang-Mills theories, but include fermion and scalar fields as well as spin $3/2$ fields into the relation. In fact, since every supersymmetric gravity and Yang-Mills theory with $\mathcal{N}$ supercharges can be reduced from certain string theory by taking string tension to the limit of infinity, it could be expected that a complete set of KLT map between all possible super-gravity theories and super-Yang-Mills theories exists, even though it might be hard to work out every corresponding string amplitude factorization. Since (super-)KLT relation has already been proven by pure field theory method[89, 90], it is therefore safe to ignore its string theory origin, and concentrate the study only on the consequences of field theories. In the gravity theory part, these consequences include constructing various super-gravity theories, and also computation of tree-level gravity amplitude[91], especially the full expression of tree-level MHV gravity amplitude[80–85]. In the Yang-Mills theory part, some interesting vanishing identities among Yang-Mills amplitudes[92, 93] are found as a result of symmetry violation.

In the following sections, we will briefly present various expressions of field theory KLT relations and their application to gravity amplitude computation. The remaining context is mainly dedicated to super-KLT relation which we have studied. After generalizing normal KLT relation to supersymmetric gravity and Yang-Mills theories, we will work out the complete KLT map between all possible 4-dimensional supersymmetric theories, and illustrate the violation of symmetry that leads to vanishing identities of Yang-Mills amplitudes.

2.1 KLT relation in field theory

2.1.1 General formula and properties of S-kernel

It only requires one sentence to describe KLT relation: gravity amplitude is a summation of products of two Yang-Mills amplitudes. Yet it is not quite easy to really work it out mathematically, since terms to be summed over is of factorial order, and the products are also dressed with complicated kinematic factors.

The expression could have many different forms[94], and one general form for n-point gravity is

$$\begin{aligned} M_n =&(-1)^{n+1} \sum_{\sigma\in S_{n-3}} \sum_{\alpha\in S_{j-1}} \sum_{\beta\in S_{n-2-j}} A_n(1,\sigma_{2,j},\sigma_{j+1,n-2},n-1,n)\mathcal{S}[\alpha_{\sigma(2),\sigma(j)}|\sigma_{2,j}]_{p_1} \\ &\times \widetilde{\mathcal{S}}[\sigma_{j+1,n-2}|\beta_{\sigma(j+1),\sigma(n-2)}]_{p_{n-1}}\widetilde{A}_n(\alpha_{\sigma(2),\sigma(j)},1,n-1,\beta_{\sigma(j+1),\sigma(n-2)},n)\ , \end{aligned} \tag{2.1}$$

where j is a fixed number taking value of $(1,2,\ldots,n-2)$. S_n is the set of permutation of n legs, and $\sigma_{i,j}$ is a permutation of indices $(i,i+1,\ldots,j)$. Coupling constants of gravity and Yang-Mills theories have been ignored here. $A_n,\widetilde{A}_n$ are two n-point Yang-Mills amplitudes, and they are not necessary to be amplitudes of the same theory. In this expression, three external legs of Yang-Mills amplitudes have been fixed, and permutation is operate on remaining $(n-3)$ external legs. This is easy to understand in string theory, since three points are fixed because of conformal invariance. The kinematic factor, also called momentum kernel or $\mathcal{S}$-kernel, is defined as

$$\mathcal{S}[i_1,\ldots,i_k|j_1,\ldots,j_k]_{p_1} \;=\; \prod_{t=1}^{k}\left(s_{i_t1}+\sum_{q>t}^{k}\theta(i_t,i_q)s_{i_ti_q}\right)\ , \tag{2.2}$$

where $\theta(i_t,i_q)$ is zero when legs (i_t,i_q) has same ordering at both sets $\mathcal{I}\equiv\{i_1,\ldots,i_k\}$ and $\mathcal{J}\equiv\{j_1,\ldots,j_k\}$, and unity for all other cases. $s_{i,\ldots,j}$ is simply Lorentz invariant scalar product $(p_i+\cdots+p_j)^2$. The dual form of $\mathcal{S}$-kernel, i.e., the $\widetilde{\mathcal{S}}$-kernel, is defined as

$$\widetilde{\mathcal{S}}[i_1,\ldots,i_k|j_1,\ldots,j_k]_{p_n} \equiv \prod_{t=1}^{k}\left(s_{j_t n}+\sum_{q<t}\theta(j_q,j_t)s_{j_t j_q}\right)\ . \tag{2.3}$$

It is helpful to mention some properties of $\mathcal{S},\widetilde{\mathcal{S}}$-kernels, which can be directly applied to the rephrasing of KLT-relation expression. One important property is the reflection symmetry

$$\mathcal{S}[i_1,\ldots,i_k|j_1,\ldots,j_k]_{p_1} = \mathcal{S}[j_k,\ldots,j_1|i_k,\ldots,i_1]_{p_1}\ , \tag{2.4}$$

$$\widetilde{\mathcal{S}}[i_1,\ldots,i_k|j_1,\ldots,j_k]_{p_n} = \widetilde{\mathcal{S}}[j_k,\ldots,j_1|i_k,\ldots,i_1]_{p_n}\ , \tag{2.5}$$

where sets $\mathcal{I}$ and $\mathcal{J}$ have been switched, as well as the ordering in each set has been reversed. Another useful property is about permutation on $\mathcal{S},\widetilde{\mathcal{S}}$-kernels. Since

$$\mathcal{P}_{ij}(\mathcal{S}[\beta|\alpha]_{p_1}) = \mathcal{S}[\mathcal{P}_{ij}(\beta)|\mathcal{P}_{ij}(\alpha)]_{p_1}\ , \tag{2.6}$$

where $\mathcal{P}_{ij}$ is the exchanging of legs i and j, we can generalize it to

$$\sum_{\beta}\mathcal{S}[\beta|\mathcal{P}_{ij}(\alpha)] = \sum_{\beta}\mathcal{P}_{ij}(\mathcal{S}[\mathcal{P}_{ij}(\beta)|\alpha]) = \mathcal{P}_{ij}(\sum_{\beta}\mathcal{S}[\mathcal{P}_{ij}(\beta)|\alpha]) = \mathcal{P}_{ij}(\sum_{\beta}\mathcal{S}[\beta|\alpha])\ , \tag{2.7}$$

where at the third step we used the fact that summing over all permutations $\sum_\beta$ commutes with permutation $\mathcal{P}_{ij}$. More generally, we have

$$\sum_{\alpha\beta}F(\beta)S[\beta|\alpha]G(\alpha) = \sum_{\mathcal{P}\{2,\ldots,n-2\}}(\sum_{\beta}F(\beta)S[\beta|2,\ldots,n-2]G(\{2,3,...,n-2\}))\ , \tag{2.8}$$

where $G(\alpha)$ is a general function. This shows that we can divide all permutations into groups of certain particular permutation $\mathcal{P}\{2,3,\ldots,n-2\}$. While the left and right hand sides are different term by term, they are equivalent after summation.

Also we have a special identity considering the combination of $\mathcal{S}$-kernel with Yang-Mills amplitudes in the following way

$$\sum_{\alpha\in S_{n-2}}\mathcal{S}[\alpha_{2,\ldots,n-1}|j_2,\ldots,j_{n-1}]_{p_1}A_n(n,\alpha_{2,\ldots,n-1},1) = 0\ . \tag{2.9}$$

Surprisingly, this is just a rewriting of BCJ relation. For example, if $n=5$, (j_2,j_3,j_4) could be any ordering of $\{2,3,4\}$ and each ordering leads to an identity, though they might not be all independent. Let us consider one specific ordering $(j_2,j_3,j_4)=(2,3,4)$. The set α has $(5-2)!=6$ elements, and we can divide it into two parts. One part keeps ordering $(2,3)$ while 4 is inserted into all possible positions of $(2,3)$, and the other keeps ordering $(3,2)$ with 4 being inserted into all possible positions of $(3,2)$. Then we get

$$\begin{aligned}
0 &= \mathcal{S}[2,3,4|2,3,4]A(5,2,3,4,1) + \mathcal{S}[2,4,3|2,3,4]A(5,2,4,3,1) \\
&\quad + \mathcal{S}[4,2,3|2,3,4]A(5,4,2,3,1) + \mathcal{S}[3,2,4|2,3,4]A(5,3,2,4,1) \\
&\quad + \mathcal{S}[3,4,2|2,3,4]A(5,3,4,2,1) + \mathcal{S}[4,3,2|2,3,4]A(5,4,3,2,1) \\
&\quad = s_{12}s_{13}\Big[s_{14}A(5,2,3,4,1) + (s_{41}+s_{43})A(5,2,4,3,1) \\
&\quad + (s_{41}+s_{42}+s_{43})A(5,4,2,3,1)\Big] + s_{12}(s_{31}+s_{32})\Big[s_{41}A(5,3,2,4,1) \\
&\quad + (s_{41}+s_{42})A(5,3,4,2,1) + (s_{41}+s_{42}+s_{43})A(5,4,3,2,1)\Big] \ . \qquad (2.10)
\end{aligned}$$

Each copy in square brackets is a fundamental BCJ relation

$$\sum_{\sigma\in\mathcal{OP}\{2,3,\ldots,n-2\}\bigcup\{n-1\}} \mathcal{S}[\sigma_{2,\ldots,n-1}|2,3,\ldots,n-1]A(1,\sigma_{2,\ldots,n-1},n) = 0 \ , \qquad (2.11)$$

where the ordered permutation $\mathcal{OP}\{\alpha\}\bigcup\{\beta\}$ is the set of permutations between sets α and β while preserving the ordering of elements inside each set. When $\{\beta\}=\{n-1\}$, which has only one element, it has a simple structure that with $(n-1)$ legs fixed ordering and bypassing one leg from left to right in each term between the first and last leg. This gives a relation among $(n-2)$ amplitudes. So we can see that (2.9) is a combination of many copies of BCJ relations. A similar relation for dual $\widetilde{\mathcal{S}}$-kernel is given by

$$\sum_{\gamma\in S_{n-2}} \widetilde{\mathcal{S}}[i_2,\ldots,i_{n-1}|\gamma_{2,n-1}]_{p_n}\widetilde{A}_n(n,\gamma_{2,n-1},1) = 0 \ . \qquad (2.12)$$

Let us go back to the general form of KLT relation (2.1). It contains a summation over

$$(n-3)!\times(j-1)!\times(n-j-2)!$$

terms. For each j, it is reduced to a specific expression of KLT relation. All of them are related by BCJ relations, thus equivalent to each other. The equivalence can be proved by shifting j repeatingly using BCJ relations and momentum conservation[89]. The main formula for shifting j is

$$\begin{aligned}
&\sum_{\alpha,\beta}\mathcal{S}[\alpha_{i_2,i_j}|i_2,\ldots,i_j]_{p_1}\widetilde{\mathcal{S}}[i_{j+1},\ldots,i_{n-2}|\beta_{i_{j+1},i_{n-2}}]_{p_{n-1}}\widetilde{A}_n(\alpha_{i_2,i_j},1,n-1,\beta_{i_{j+1},i_{n-2}},n) \\
&= \sum_{\alpha',\beta'}\mathcal{S}[\alpha'_{i_2,i_{j-1}}|i_2,\ldots,i_{j-1}]_{p_1}\widetilde{\mathcal{S}}[i_j,i_{j+1},\ldots,i_{n-2}|\beta'_{i_j,i_{n-2}}]_{p_{n-1}}\widetilde{A}_n(\alpha'_{i_2,i_{j-1}},1,n-1,\beta'_{i_j,i_{n-2}},n) \ ,
\end{aligned} \qquad (2.13)$$

where number of elements in $\mathcal{S}$ decreases from $(j-1)$ to $(j-2)$ and that in $\widetilde{\mathcal{S}}$ increases from $(n-j-2)$ to $(n-j-1)$. Then the equivalence of all KLT relations by specifying different j in general KLT formula (2.1) can be guaranteed.

2.1.2 Modified formulae and their applications in gravity amplitude computation

KLT relations of some special j of (2.1) are important in literatures. If $j=[n/2]$, it defines n-point KLT relation conjectured in [95]. This gives a summation over

$$(n-3)!\times([\frac{n}{2}]-1)!\times([\frac{n}{2}]-2)!$$

terms. A simplified expression can be obtained by assuming $j=1$,

$$M_n =(-1)^{n+1}\sum_{\sigma,\widetilde{\sigma}\in S_{n-3}} A_n(1,\sigma_{2,n-2},n-1,n)\widetilde{\mathcal{S}}[\sigma_{2,n-2}|\widetilde{\sigma}_{2,n-2}]_{p_{n-1}}\widetilde{A}_n(1,n-1,\widetilde{\sigma}_{2,n-2},n)\ , \tag{2.14}$$

and also the dual form by assuming $j=n-2$,

$$M_n =(-1)^{n+1}\sum_{\sigma,\widetilde{\sigma}\in S_{n-3}} \widetilde{A}_n(\widetilde{\sigma}_{2,n-2},1,n-1,n)\mathcal{S}[\widetilde{\sigma}_{2,n-2}|\sigma_{2,n-2}]_{p_1}A_n(1,\sigma_{2,n-2},n-1,n)\ . \tag{2.15}$$

The summation is over $(n-3)!\times(n-3)!$ terms from two independent permutation sets $\sigma,\widetilde{\sigma}$, and kinematic factors contain only one $\mathcal{S},\widetilde{\mathcal{S}}$-kernel.

Using these KLT relations, some simple gravity amplitudes are just in hand to write down explicitly. A naive example is three-point gravity amplitude, which has only one term without any kinematic factor, given by

$$M_3(1,2,3)=A_3(1,2,3)\widetilde{A}_3(1,2,3)=(A_3(1,2,3))^2\ . \tag{2.16}$$

The last step holds if we take the same Yang-Mills theory for both A and $\widetilde{A}$. Gravity amplitude is totally symmetric in the external legs, while Yang-Mills amplitudes are color-ordered. The colorless property of gravity amplitude even at three-point level is not obvious from Yang-Mills part, but it can be seen by using many non-trivial relations of Yang-Mills amplitudes. In fact, there are $3!=6$ different color-ordered three-point Yang-Mills amplitudes, while accounting cyclic relation we can fix one leg, thus remain $2!=2$ independent amplitudes, say $A_3(1,2,3)$ and $A_3(1,3,2)$. Furthermore, reflection relation $A(1,2,3)=-A(3,2,1)=-A(1,3,2)$ ensures that there is only one independent amplitude. Any three-point amplitudes can be related to $A_3(1,2,3)$ or $-A_3(1,2,3)$, and the square of Yang-Mills amplitudes ensures that we always get a plus sign for gravity amplitude. In this way we recover the colorless property of gravity amplitude from color-ordered Yang-Mills amplitudes. The illustration is simple for three-point amplitude, but for higher point amplitudes it remains a hard task. Let us further consider four-point gravity amplitude. It also contains one term, and the kinematic factor, if using expression (2.15), is $\mathcal{S}[2|2]_{p_1} = s_{12}$. Thus

$$M_4(1,2,3,4) = -s_{12}A_4(1,2,3,4)\widetilde{A}_4(2,1,3,4)\ . \tag{2.17}$$

Note that both Yang-Mills amplitudes $A, \widetilde{A}$ have s_{12} pole(or s_{34} pole, but $s_{34} = s_{12}$ from 4-point kinematics), the kinematic factor s_{12} will cancel one of them to make correct pole structure for gravity amplitude. s_{12} of course does not have crossing symmetry when relabeling all four external legs. This requires us to use BCJ relations to show crossing symmetry of gravity amplitude. If we consider an arbitrary ordering $M_4(\sigma_1,\sigma_2,\sigma_3,\sigma_4)$, the Yang-Mills part is $-s_{\sigma_1\sigma_2}A_4(\sigma_1,\sigma_2,\sigma_3,\sigma_4)\widetilde{A}_4(\sigma_1,\sigma_3,\sigma_4,\sigma_2)$. Because of cyclic symmetry of Yang-Mills amplitude, we can fix leg 1 in the first position. One of σ_i would be leg 1. If σ_1 or σ_2 is leg 1, we simply have $s_{1\sigma_k}$. If σ_3 or σ_4 is leg 1, we also have $s_{\sigma_1\sigma_2} = s_{\sigma_3\sigma_4} = s_{1\sigma_i}$. So formally the Yang-Mills part can be fixed to

$$-s_{1,\sigma_2'}A_4(1,\sigma_2',\sigma_3',\sigma_4')\widetilde{A}_4(1,\sigma_3',\sigma_4',\sigma_2')\ . \tag{2.18}$$

Using KK-relation and fundamental BCJ relation, we get three equivalent expressions

$$\begin{aligned} & s_{1,\sigma_2'}A_4(1,\sigma_2',\sigma_3',\sigma_4')\widetilde{A}_4(1,\sigma_3',\sigma_2',\sigma_4') + s_{1,\sigma_3'}A_4(1,\sigma_2',\sigma_3',\sigma_4')\widetilde{A}_4(1,\sigma_3',\sigma_2',\sigma_4') \\ = \ & -s_{1,\sigma_2'}A_4(1,\sigma_4',\sigma_3',\sigma_2')\widetilde{A}_4(1,\sigma_3',\sigma_4',\sigma_2') \\ = \ & s_{1,\sigma_4'}A_4(1,\sigma_4',\sigma_2',\sigma_3')\widetilde{A}_4(1,\sigma_2',\sigma_4',\sigma_3') + s_{1,\sigma_2'}A_4(1,\sigma_4',\sigma_2',\sigma_3')\widetilde{A}_4(1,\sigma_2',\sigma_4',\sigma_3')\ . \end{aligned}$$

Symmetry of relabeling $(2,3), (3,4)$ or $(2,4)$ can be seen in above three expressions respectively. So the total crossing symmetry of four-point gravity amplitude from color-ordered four-point Yang-Mills amplitudes is recovered. If $n = 5$, j could be $1,2,3$. Gravity amplitude contains two terms when $j = 2$, which is given directly by (2.1) as

$$\begin{aligned} M_5(1,2,3,4,5) \ = \ & s_{12}s_{34}A_5(1,2,3,4,5)\widetilde{A}_5(2,1,4,3,5) \\ & + s_{13}s_{24}A_5(1,3,2,4,5)\widetilde{A}_5(3,1,4,2,5)\ . \end{aligned} \tag{2.19}$$

Again kinematic factors are responsible to cancel double poles from product of two Yang-Mills amplitudes, which is easy to see since the first term has double s_{12}, s_{34} poles while the second term has double s_{13}, s_{24} poles. While $j = 1$ or $j = 3$, the gravity amplitude contains 4 terms. Taking expression (2.15) we have

$$\begin{aligned}
& M_5(1,2,3,4,5) \\
= \; & s_{12}s_{13}A_5(1,2,3,4,5)\widetilde{A}_5(1,4,5,2,3)+(s_{13}+s_{23})s_{12}A_5(1,2,3,4,5)\widetilde{A}_5(1,4,5,3,2) \\
& +(s_{12}+s_{23})s_{13}A_5(1,3,2,4,5)\widetilde{A}_5(1,4,5,2,3)+s_{13}s_{12}A_5(1,3,2,4,5)\widetilde{A}_5(1,4,5,3,2) \\
= \; & s_{12}A_5(1,2,3,4,5)\Big[s_{13}\widetilde{A}_5(1,4,5,2,3)+(s_{13}+s_{23})\widetilde{A}_5(1,4,5,3,2)\Big] \\
& +s_{13}A_5(1,3,2,4,5)\Big[(s_{12}+s_{23})\widetilde{A}_5(1,4,5,2,3)+s_{12}\widetilde{A}_5(1,4,5,3,2)\Big]\;. \qquad (2.20)
\end{aligned}$$

After using BCJ relation and momentum conservation for expressions in square brackets, above result returns to the one given by $j=2$. This explicitly shows the equivalence among different KLT relations. The pole structure becomes difficult to see, as well as the crossing symmetry of gravity amplitude.

As the number of external legs keeping growing, the computation difficulty increases so fast that it is even impossible to get any realistic results. However, tree-level MHV gravity amplitude is a successful example of applying KLT relations, and compact formulae are derived. There is also schematic result of all $\mathcal{N}=8$ tree-level super-gravity amplitude[91]. But it is so complicated that not even possible to really write down the result. The MHV amplitude for Yang-Mills theory is surprisingly simple, as shown in (1.39). So it should not be a difficult task to compute MHV gravity amplitude by KLT relation. There are many MHV gravity amplitude results calculated from many different methods. The original one is BGK conjectured result[80], and proved by Mason and Skinner[84] in the form

$$\mathcal{M}_{MS}^{MHV}=(-)^{n-3}\sum_{\mathcal{P}(2,\ldots,n-2)}\frac{A^{MHV}(1,2,\ldots,n)}{\langle 1|n-1\rangle\langle n-1|n\rangle\langle n|1\rangle}\prod_{k=2}^{n-2}\frac{[k|p_{k+1}+\cdots+p_{n-1}|n\rangle}{\langle k|n\rangle}\;, \qquad (2.21)$$

where the sum is over all S_{n-3} permutation of legs $(2,...,n-2)$. The equivalence of all KLT relations indicates that we should able to reach this form from general KLT relation (2.1). To show the equivalence, we can of course start from the simplified formula (2.14). Using property of $\mathcal{S}$-kernel (2.8) for formula (2.14), we get

$$\begin{aligned}
M_n^{KLT-MHV}=(-)^{n+1}&\sum_{\mathcal{P}(2,\ldots,n-2)}A^{MHV}(1,2,\ldots,n-1,n) \\
&\times\sum_{\beta}S[\beta|2,\ldots,n-2]_{p_1}\widetilde{A}^{MHV}(n,\beta,1,n-1)\;. \qquad (2.22)
\end{aligned}$$

Then the remaining task is to show the equivalence

$$\begin{aligned}
& \frac{1}{\langle 1|n-1\rangle \langle n-1|n\rangle \langle n|1\rangle}\prod_{k=2}^{n-2}\frac{[k|p_{k+1}+\cdots+p_{n-1}|n\rangle}{\langle k|n\rangle} \\
= & \sum_{\beta}\mathcal{S}[\beta|2,3,\ldots,n-2]\tilde{A}^{MHV}(n,\beta,1,n-1)\ . \qquad (2.23)
\end{aligned}$$

Using BCJ relation and properties of permutation group, we get

$$\begin{aligned}
& \sum_{\beta}\mathcal{S}[\beta|2,3,\ldots,n-2]_{p_1}A(n,\beta,1,n-1) \\
& = s_{n-2,n-1}\sum_{\gamma}\mathcal{S}[\gamma|2,\ldots,n-3]_{p_1}A(n-2,n,\gamma,1,n-1)\ . \qquad (2.24)
\end{aligned}$$

The summation over $\beta \in \mathcal{P}\{2,\ldots,n-2\}$ has been reduced to summation over $\gamma \in \mathcal{P}\{2,\ldots,n-3\}$. While dealing with MHV amplitude, we can further use inverse soft factor which relates $(n-1)$-point MHV amplitude to n-point MHV amplitude as

$$A^{MHV}(n-1,n-2,n,\gamma,1) = \frac{\langle n-1|n\rangle}{\langle n-1|n-2\rangle \langle n-2|n\rangle}A^{MHV}(\widetilde{n-1},\tilde{n},\gamma,1,)\ , \qquad (2.25)$$

with modified spinor components

$$\begin{aligned}
|\widetilde{n-1}] &= \frac{|p_{n-2}+p_{n-1}|n\rangle}{\langle n-1|n\rangle}\ , \qquad |\widetilde{n-1}\rangle = |n-1\rangle\ , \\
|\tilde{n}] &= \frac{|p_{n-2}+p_n|n-1\rangle}{\langle n|n-1\rangle}\ , \qquad |\tilde{n}\rangle = |n\rangle \qquad (2.26)
\end{aligned}$$

to assure momentum conservation. For (2.25) to be true we assume that helicity of leg $(n-2)$ is positive, which can always be done for MHV amplitude since we can fix leg 1 and n to be negative helicities. Applying (2.25) to (2.24) we get

$$\begin{aligned}
& \sum_{\beta\in S_{n-3}}\mathcal{S}[\beta|2,3,\ldots,n-2]_{p_1}A_n^{MHV}(n,\beta,1,n-1) \qquad (2.27) \\
= \ & s_{n-2,n-1}\frac{\langle n-1|n\rangle}{\langle n-1|n-2\rangle \langle n-2|n\rangle}\sum_{\gamma\in S_{n-4}}\mathcal{S}[\gamma|2,\ldots,n-3]_{p_1}A_{n-1}^{MHV}(\tilde{n},\gamma,1,\widetilde{n-1})\ .
\end{aligned}$$

Repeatingly doing so we finally end up with

$$\mathcal{S}[2|2]_{p_1}A^{MHV}(\tilde{n}^{(n-4)},2,1,\widetilde{n-1}^{(n-4)})\prod_{k=3}^{n-2}s_{k,\widetilde{n-1}^{(n-2-k)}}\frac{\langle n-1|n\rangle}{\langle n-1|k\rangle \langle k|n\rangle}\ , \qquad (2.28)$$

where $\tilde{n}^{(i)}$ denotes the i-th modification of momentum p_n, given by

$$|\widetilde{n-1}^{(i)}] = \frac{|p_{n-1-i}+p_{n-i}+\cdots+p_{n-2}+p_{n-1}|n\rangle}{\langle n-1|n\rangle}\ . \qquad (2.29)$$

Using explicit result of four-point MHV Yang-Mills amplitude with modified spinor (2.29) in (2.28), the equivalence (2.23) automatically becomes true. This finishes the proof[96].

So far the KLT relations discussed all contain Yang-Mills amplitude with three legs fixed, which has a clear explanation in string amplitude. There exists another regularized KLT relation where Yang-Mills amplitudes have two legs fixed. If we choose two legs p_1, p_n, and deform them as

$$p_1 \to p_1' = p_1 - xq \quad , \quad p_n \to p_n' = p_n + xq \ , \tag{2.30}$$

where x is an arbitrary non-zero parameter and q is an auxiliary momentum satisfying $q^2 = p_1 q = 0$. This means that momentum conservation of deformed momenta is still valid. The deformed p_1' is on-shell but the deformed $(p_n')^2 = xp_n q$ is a function of x, which is off-shell. In the $x \to 0$ limit, p_1', p_n' go back to the original momenta. The regularized KLT relation can be expressed as on-shell limit of following expression[94]

$$M_n = (-1)^n \sum_{\gamma,\beta} \frac{\widetilde{A}_n(n, \gamma_{2,n-1}, 1)\mathcal{S}[\gamma_{2,n-1}|\beta_{2,n-1}]_{p_1} A_n(1, \beta_{2,n-1}, n)}{s_{12\ldots(n-1)}} \ . \tag{2.31}$$

When $x \to 0$, the denominator $s_{12\ldots(n-1)} \sim xp_n q$ approaches to zero, while the numerator becomes a rewriting of BCJ relation (2.9) and also goes to zero. The limit however is finite, and gives correct KLT relation.

The regularized KLT relation contains a summation over $(n-2)! \times (n-2)!$ terms, and $x \to 0$ limit is usually quite difficult to calculate. So it helps little to practical computation of gravity amplitude. Yet the Yang-Mills amplitudes have two legs fixed, which is more convenient to implement BCFW recursion relation. So the field theory proof of KLT relation, which takes advantages of BCFW recursion relation, is more natural with this form. We mention that the field theory proof of KLT relation can be finished by BCFW recursion relation no matter in the form (2.1) or (2.31). Since the proof is out of the scope of this thesis, it will not be described here.

2.2 Super-KLT relation in field theory

The KLT relation discussed in previous section is about pure graviton and gluon amplitudes. It is natural to ask the question if other particle states can be included or not. A way of creating other particle states is to use supersymmetry. In fact, a generalization of KLT relation to super-KLT relation with maximal $\mathcal{N} = 8$ super-gravity theory and maximal $\mathcal{N} = 4$ super-Yang-Mills theory has been proposed[88], and already been proven by BCFW recursion relation method[90]. Super-KLT relations of non-maximal super-gravity and super-Yang-Mills theories are not hard to be truncated from maximal super-KLT relation. The generalization and truncation are quite intuitive with help of super-field formalism. Instead of using graviton and gluon fields in pure gravity and Yang-Mills amplitudes, we should introduce super-fields. All particle states, with spin $(0, \pm 1/2, \pm 1, \pm 3/2, \pm 2)$ for gravity and $(0, \pm 1/2, \pm 1)$ for Yang-Mills fields, can be packed into single super-field. With this formalism, expression become very compact, yet it is easy to restore results for specific particle state by super-field expansion.

2.2.1 Super-field representation and truncation of component fields

With help of Grassmann variables, we can write the super-field for $\mathcal{N} = 4$ super-Yang-Mills theory as

$$\Phi^{\mathcal{N}=4} = g_+ + \eta_a f_+^a + \frac{1}{2!}\eta_a\eta_b s^{ab} + \frac{1}{3!}\eta_a\eta_b\eta_c f_-^{abc} + \eta_1\eta_2\eta_3\eta_4 g_-^{1234} \ . \tag{2.32}$$

It contains all component fields in $\mathcal{N} = 4$ super-Yang-Mills theory, which are tracked by appropriate coefficients of Grassmann variables. The Grassmann variable $\eta_{i,a}$ carries a $SU(4)_R$ symmetry index $a = 1, 2, 3, 4$, and subscript i distinguishes different particles. They follow the anti-commutative relation

$$\{\eta_{i,a}, \eta_{j,b}\} = 0 \ . \tag{2.33}$$

So it is easy to infer that in monomial of Grassmann variables, $\eta_{i,a}$ of a given i and $SU(4)_R$ index a at most has rank 1, otherwise we will always end up with a factor $(\eta_{i,a})^2$, which is zero by definition. The component fields also carry $SU(4)_R$ symmetry index, so they are restricted by $SU(4)_R$ symmetry as well as anti-commutative of Grassmann variables. For a super-field, there are two gluon states g_+, g_-^{1234}, four positive fermion states f_+^a with index $a = 1$ to 4, and four negative fermion states f_-^{abc} with index from selecting any three indices out of $(1, 2, 3, 4)$, normalized by increasing ordering, as well as six scalars s^{ab} satisfying reality condition $s^{ab} = \epsilon^{abcd}s_{cd}/2$, where $s^{ab} \equiv s_{ab}^\dagger$, with index from selecting any two indices out of $(1, 2, 3, 4)$ and normalized. These 16 states transform as anti-symmetric products in the fundamental representation of $SU(4)_R$ group.

With super-field formalism, we can simply generalize amplitude to super-amplitude by replacing normal fields with super-fields as

$$\mathcal{A}_n^{\mathcal{N}=4}(\Phi_1, \Phi_2, \ldots, \Phi_n) \ . \tag{2.34}$$

The super-states Φ_i encodes all information of helicity assignment and external states. In fact, it can be expanded as a sum of normal amplitudes with coefficients of Grassmann variable monomials identifying field contents of corresponding amplitudes. The $SU(4)_R$ symmetry constraints the rank of Grassmann variable monomials to be $(\eta)^{4k}$. Of course all Grassmann variables should be different in one monomial. Schematically, we can expand super-amplitude according to helicity information as

$$\mathcal{A}_n^{\mathcal{N}=4} = \sum A_n^{MHV}(\eta)^8 + \sum A_n^{NMHV}(\eta)^{12} + \ldots + \sum A_n^{\overline{MHV}}(\eta)^{4n-8} , \tag{2.35}$$

where summation starts from MHV amplitude and ends with anti-MHV amplitude, since amplitudes with all plus(or minus) or with one plus(or minus) vanish. The $SU(4)_R$ symmetry index a appears the same number of times in each monomial of $\eta_{i,a}$. The amplitude $A_n^{N^kMHV}$ is still a summation of N^{k}MHV component amplitudes. For example, pure gluon MHV amplitude $A_4(g_1^+, g_2^+, g_3^-, g_4^-)$, identified by Grassmann variable monomial $\eta_{3,1}\eta_{3,2}\eta_{3,3}\eta_{3,4}\eta_{4,1}\eta_{4,2}\eta_{4,3}\eta_{4,4}$(the first index is particle label and the second $SU(4)_R$ index), is one term in A_4^{MHV}, while amplitude of gluon coupled to a pair of fermion $A_4(g_1^+, g_2^-, f_3^+, f_4^-)$, identified by Grassmann variable monomial $\eta_{2,1}\eta_{2,2}\eta_{2,3}\eta_{2,4}\eta_{3,1}\eta_{4,2}\eta_{4,3}\eta_{4,4}$, is also a term in A_4^{MHV}. Notice that there are more than one fermion and scalar states, we could have different Grassmann variable monomials representing component amplitudes with the same field contents. For example, both Grassmann variable monomials

$$\eta_{2,1}\eta_{2,2}\eta_{2,3}\eta_{2,4}\eta_{3,1}\eta_{4,2}\eta_{4,3}\eta_{4,4} \text{ and } \eta_{2,1}\eta_{2,2}\eta_{2,3}\eta_{2,4}\eta_{3,3}\eta_{4,1}\eta_{4,2}\eta_{4,4}$$

identify amplitude $A_4(g_1^+, g_2^-, f_3^+, f_4^-)$, while monomial

$$\eta_{2,1}\eta_{2,2}\eta_{2,3}\eta_{2,4}\eta_{3,1}\eta_{4,1}\eta_{4,2}\eta_{4,4}$$

identifies nothing since $SU(4)_R$ index do not appear the same number of times.

In spinor-helicity formalism, MHV super-amplitude also takes a simple form as

$$A_n^{MHV} = \frac{\delta^{4\times2}(\sum_{i=1}^n \eta_{i,a}\lambda_i^\alpha)}{\langle 1,2\rangle\langle 2,3\rangle\cdots\langle n-1,n\rangle\langle n,1\rangle} , \tag{2.36}$$

with delta function $\delta^{4\times2}(\sum_{i=1}^n \eta_{i,a}\lambda_i^\alpha)$ representing super-momentum conservation. The $SU(4)_R$ index $a = 1, 2, 3, 4$, while spinor index $\alpha = 1, 2$. The eight-fold delta function is in fact delta function of Grassmann variables, so we can also treat them directly as products of eight factors. Expanding them we get a mount of terms identified by Grassmann variable monomials, and kinematic factor of each Grassmann variable monomial is a component MHV amplitude. As an illustration, let us truncate gluon MHV amplitude

$A_n(1^+,\cdots,i^-,\cdots,j^-,\cdots,n^+)$. From the field contents, we know that it follows from Grassmann variable monomial $\eta_{i,1}\eta_{i,2}\eta_{i,3}\eta_{i,4}\eta_{j,1}\eta_{j,2}\eta_{j,3}\eta_{j,4}$. So we can concentrate on the i-th and j-th particles in delta function

$$\begin{aligned}
\delta^{4\times 2}(\eta_{i,a}\lambda_i^{\alpha}+\eta_{j,a}\lambda_j^{\alpha}) &= \prod_{a=1,2,3,4}(\eta_{i,a}\lambda_i^1+\eta_{j,a}\lambda_j^1)(\eta_{i,a}\lambda_i^2+\eta_{j,a}\lambda_j^2)\\
&= \prod_{a=1,2,3,4}(\eta_{i,a}^2\lambda_i^1\lambda_i^2+\eta_{j,a}\eta_{i,a}\lambda_j^1\lambda_i^2+\eta_{i,a}\eta_{j,a}\lambda_i^1\lambda_j^2+\eta_{j,a}^2\lambda_j^1\lambda_j^2)\\
&= \prod_{a=1,2,3,4}\eta_{i,a}\eta_{j,a}(\lambda_i^1\lambda_j^2-\lambda_i^2\lambda_j^1)=\eta_{i,1}\eta_{j,1}\eta_{i,2}\eta_{j,2}\eta_{i,3}\eta_{j,3}\eta_{i,4}\eta_{j,4}\left\langle i\ j\right\rangle^4 \ . \qquad (2.37)
\end{aligned}$$

This is in accordance with gluon MHV amplitude, with correct numerator factor $\langle i\ j\rangle^4$. The other component MHV amplitudes can be obtained similarly.

The super-field formalism for $\mathcal{N}=8$ super-gravity theory can be treated in the same way. We use eight Grassmann variables to encode all states as

$$\begin{aligned}
\Phi^{\mathcal{N}_G=8} = \quad & h_+ + \eta_A\psi_+^A + \tfrac{1}{2!}\eta_A\eta_B v_+^{AB} + \tfrac{1}{3!}\eta_A\eta_B\eta_C\chi_+^{ABC} + \tfrac{1}{4!}\eta_A\eta_B\eta_C\eta_D\phi^{ABCD}\\
& + \tfrac{1}{5!}\eta_A\eta_B\eta_C\eta_D\eta_E\chi_-^{ABCDE} + \tfrac{1}{6!}\eta_A\eta_B\eta_C\eta_D\eta_E\eta_F v_-^{ABCDEF}\\
& + \tfrac{1}{7!}\eta_A\eta_B\eta_C\eta_D\eta_E\eta_F\eta_G\psi_-^{ABCDEFG} + \eta_1\eta_2\eta_3\eta_4\eta_5\eta_6\eta_7\eta_8 h_-^{12345678}\ ,
\end{aligned}$$

where $SU(8)_R$ index A takes value from 1 to 8. It is easy to count the particle states. There are two graviton states $h_+, h_-^{12345678}$ with spin ± 2, $\binom{8}{1}=8$ positive gravitino states ψ_+^A with spin $+\frac{3}{2}$, $\binom{8}{7}=8$ negative gravitino states $\psi_-^{ABCDEFG}$ with spin $-\frac{3}{2}$, $\binom{8}{2}=28$ positive graviphoton states v_+^{AB} with spin $+1$, $\binom{8}{6}=28$ negative graviphoton states v_-^{ABCDEF} with spin -1, $\binom{8}{3}=56$ positive garviphotino states χ_+^{ABC} with spin $+\frac{1}{2}$, $\binom{8}{5}=56$ negative graviphotino states χ_-^{ABCDE} with spin $-\frac{1}{2}$, and finally $\binom{8}{4}=70$ real scalars ϕ^{ABCD} with spin 0. These 256 states transform as anti-commutative products in fundamental representation of $SU(8)_R$ group.

The gravity super-amplitude is then simply generalized by replacing normal fields as super-fields

$$\mathcal{M}_n^{\mathcal{N}_G=8}(\Phi_1,\Phi_2,\ldots,\Phi_n)\ . \qquad (2.38)$$

Analogously, we can treat it as a sum of all component amplitudes with coefficients of Grassmann variable monomials. The $SU(8)_R$ symmetry invariance restricts these monomials to be η^{8k}, and each index A appears the same number of times in monomials. Otherwise it should vanish and corresponding amplitude disappears in super-field expansion.

When talking about theories with less supersymmetry, we can not pack all states into only one super-field. For example, $\mathcal{N}=3$ super-Yang-Mills theory can at most have three Grassmann variables $\eta_a, a=1,2,3$, so we can only expand super-field as

$$\Phi^{\mathcal{N}=3} = g_+ + \eta_a f_+^a + \frac{1}{2!}\eta_a\eta_b s^{ab} + \eta_1\eta_2\eta_3 f_-^{123} \ , \tag{2.39}$$

and the negative gluon state is missing. In order to recover the full set of states, we need to introduce another super-field

$$\Psi^{\mathcal{N}=3} = f_+ - \eta_a s^a + \frac{1}{2!}\eta_a\eta_b f_-^{ab} - \eta_1\eta_2\eta_3 g_-^{123} \ , \tag{2.40}$$

where $a=1,2,3$. The (Φ,Ψ)-super-field gives all states for $\mathcal{N}=3$ super-Yang-Mills theory. The Φ-field has one positive gluon state g_+, three positive fermion state f_+^a, three real scalar states s^{ab}, one negative fermion state f_-^{123}, while the Ψ-field has one positive fermion state f_+, three real scalar s^a, three negative fermion states f_-^{ab}, and one negative gluon state g_-^{123}. In total it has the same number and types of states as $\mathcal{N}=4$ super-Yang-Mills theory in coincidence, which hints that $\mathcal{N}=3$ super-Yang-Mills is equivalent to $\mathcal{N}=4$ super-Yang-Mills theory.

There is a systematic way of producing (Φ,Ψ)-super-field for non-maximal supersymmetric theories from maximal supersymmetric theory[97]. The Φ-super-field can be obtained by setting unwanted Grassmann variables to zero in the maximal super-field, and the Ψ-super-field can be obtained by integrating out unwanted Grassmann variables in the maximal super-field. For super-Yang-Mills theory, we have

$$\Phi^{\mathcal{N}<4} = \Phi^{\mathcal{N}=4}|_{\eta_{\mathcal{N}+1},\ldots,\eta_4\to 0} \ . \tag{2.41}$$

$$\Psi^{\mathcal{N}<4} = \int \prod_{a=\mathcal{N}+1}^{4} d\eta_a \Phi^{\mathcal{N}=4} \ . \tag{2.42}$$

Then for $\mathcal{N}=3$ theory, the Φ-super-field by setting $\eta_4=0$ is just the one shown in (2.39), while Ψ-super-field by integrating out η_4 can be written as

$$\Psi^{\mathcal{N}=3} = f_+^{(4)} - \eta_a s^{a(4)} + \frac{1}{2!}\eta_a\eta_b f_-^{ab(4)} - \eta_1\eta_2\eta_3 g_-^{123(4)} \ . \tag{2.43}$$

The difference of this expression from (2.40) is that we keep track of index 4 in component fields, although η_4 has already been integrated out. For $\mathcal{N}=3$ super-Yang-Mills theory, it is a hidden index and has nothing to do with $SU(3)_R$ symmetry. But we will show that it is necessary for assigning correct charge to particle states in the next section.

Setting η_3, η_4 to zero we get $\Phi^{\mathcal{N}=2}$-super-field, and integrating out η_3, η_4 we get $\Psi^{\mathcal{N}=2}$-super-field. They are given by

$$\Phi^{\mathcal{N}=2} = g_+ + \eta_a f_+^a + \eta_1\eta_2 s^{12} \ , \tag{2.44}$$

$$\Psi^{\mathcal{N}=2} = -s^{(34)} - \eta_a f_-^{a(34)} - \eta_1\eta_2 g_-^{12(34)} \ . \tag{2.45}$$

We keep hidden indices (34) in parenthesis, and $a = 1, 2$. This (Φ, Ψ)-super-field has two gluon states g_+, $g_-^{12(34)}$, four fermion states f_+^a, $f_-^{a(34)}$ and two scalars $s^{12}, s^{(34)}$. Setting η_2, η_3, η_4 to zero we get $\Phi^{\mathcal{N}=1}$-super-field, and integrating out η_2, η_3, η_4 we get $\Psi^{\mathcal{N}=1}$-super-field. They are given by

$$\Phi^{\mathcal{N}=1} = g_+ + \eta_1 f_+^1 \ , \tag{2.46}$$

$$\Psi^{\mathcal{N}=1} = -f_-^{(234)} + \eta_1 g_-^{1(234)} \ . \tag{2.47}$$

This (Φ, Ψ)-super-field has two gluon states $g_+, g_-^{1(234)}$, and two fermion states $f_+^1, f_-^{(234)}$. Setting all four Grassmann variables to zero, we get a positive gluon state g_+, and integrating out all four Grassmann variables we get a negative gluon state g_-. So it indeed describes the states of pure Yang-Mills theory.

Super-amplitude of non-maximal supersymmetric theories is now a function of Φ, Ψ-super-fields. It can be truncated from maximal super-amplitude in the same way as Φ, Ψ-super-fields. For n-point super-amplitude, if assuming $i_1 < i_2 < \ldots < i_m$ external legs are Ψ-super-fields, while $j_1 < j_2 < \ldots < j_l$ external legs are Φ-super-fields, with $m + l = n$, then $\mathcal{N} < 4$ super-Yang-Mills amplitude takes the form

$$\mathcal{A}_{n,i_1\cdots i_m}^{\mathcal{N}<4} = \left[\int \prod_{a_1=\mathcal{N}+1}^{4} d\eta_{i_1,a_1} \cdots \prod_{a_m=\mathcal{N}+1}^{4} d\eta_{i_m,a_m} \mathcal{A}_n^{\mathcal{N}=4}(\Phi_1, \Phi_2, \ldots, \Phi_n) \right]_{\eta_{\mathcal{N}+1},\cdots,\eta_4 \to 0} . \tag{2.48}$$

A transparent way of representing super-field with its component fields is the diamond diagram as shown in Figure (2.1). These diagrams contain information of helicities, R-symmetry charges, hidden indices as well as the number of each states. For non-maximal super-Yang-Mills theories, we have two diamonds. The top one represents Φ-super-field while the bottom one represents Ψ-super-field. Combining both of them we get single (Φ, Ψ)-super-field. For $\mathcal{N} = 4$ theory, every component field can find its CPT conjugate field inside one diamond, so it is enough to represent single $\Phi^{\mathcal{N}=4}$-super-field with only one diamond. This diagram can be better understood using supercharge operators $\widetilde{Q}_a$,

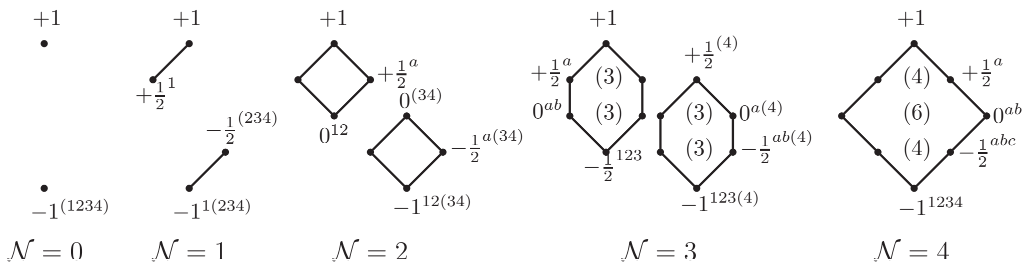

FIGURE 2.1: Diamond diagrams for super-fields of $\mathcal{N}=1,2,3,4$ super Yang-Mills theories. The $SU(\mathcal{N})_R$ indices a,b,c are labeled as superscripts. The hidden indices are indicated in parentheses. The numbers inside diamonds states the number of corresponding states.

Q_a defined in (1.44). For example, if acting $\widetilde{Q}_1$ on $\Phi^{\mathcal{N}=3}$ we get

$$\begin{aligned}\widetilde{Q}_1\Phi^{\mathcal{N}=3} &= \sum_{i=1}^{n}|i\rangle\eta_1(\Phi^{\mathcal{N}=3}=g_+ + \eta_a f_+^a + \frac{1}{2!}\eta_a\eta_b s^{ab} + \eta_1\eta_2\eta_3 f_-^{123}) \\ &= \sum_{i=1}^{n}|i\rangle(\eta_1 g_+ + \eta_1\eta_a f_+^a + \frac{1}{2!}\eta_1\eta_a\eta_b s^{ab} + \eta_1\eta_1\eta_2\eta_3 f_-^{123})\ .\end{aligned} \tag{2.49}$$

The last term vanishes because $(\eta_1)^2=0$. The transformation of each component field can be easily identified by comparing terms with η-expansion. We have

$$g_+\to 0\ ,\ f_+^a\to|p\rangle\delta_1^a g_+\ ,\ s^{ab}\to|p\rangle 2!(\delta_1^a f_+^b-\delta_1^b f_+^a)\ ,\ f_-^{123}\to|p\rangle\frac{1}{2!}s^{23}\ , \tag{2.50}$$

where we denote $\sum_{i=1}^{n}|i\rangle=|p\rangle$ for simplicity. This transformation means that each component field inside one diamond is connected by supercharges Q, and no other states can be further included. So in diamond diagrams (2.1), component fields inside one diamond are all related by supercharge operators, and each one can be transformed to another one inside the same diamond after acting certain times of supercharge operators. While between different diamonds, the particle states are unrelated. The $SU(\mathcal{N})_R$ invariance is realized in each diamond for $SU(\mathcal{N})_R$-indices, but not hidden indices inside parentheses.

The same diamond diagram can be adapted for super-gravity theories. For $\mathcal{N}=8$ maximal super-gravity, we only need one diamond to represent super-field $\Phi^{\mathcal{N}=8}$, while for non-maximal super-gravities, more than one diamonds should be used. Since we are constructing super-gravity amplitudes from super-Yang-Mills amplitudes with super-KLT relations, the particle states of super-gravities can also be constructed by tensor products of particle states of two super-Yang-Mills theories. The mapping of particle states between super-gravity and super-Yang-Mills theories will be discussed later, after introducing complete super-KLT relation family.

2.2.2 Super-KLT relations from $\mathcal{N}=8$ to $\mathcal{N}=0$

With all above knowledge, it is almost trivial to generalize KLT relation to maximal supersymmetric theory. We replace every graviton and gluon field with corresponding $\Phi^{\mathcal{N}=8}$, $\Phi^{\mathcal{N}=4}$, $\widetilde{\Phi}^{\mathcal{N}=4}$-super-fields, and pure gravity and Yang-Mills amplitudes with super-amplitudes, without changing anything else. Explicitly, following the expression (2.15), we have

$$\mathcal{M}_n^{\mathcal{N}_G=8} = (-)^{n-1} \sum_{\gamma,\beta\in S_{n-3}} \widetilde{\mathcal{A}}_n^{\widetilde{\mathcal{N}}=4}(n-1,n,\gamma,1)\mathcal{S}[\gamma|\beta]_{p_1}\mathcal{A}_n^{\mathcal{N}=4}(1,\beta,n-1,n) \ . \qquad (2.51)$$

The summation is over permutation of $\gamma,\beta\in\mathcal{P}\{2,3,\ldots,n-2\}$, and $\mathcal{S}$-kernel is the same as normal KLT relation, defined in (2.2). We use $SU(8)_R$ index 1 to 8 for super-gravity theory, $SU(4)_R$ index 1 to 4 for one super-Yang-Mills theory and 5 to 8 for the other Yang-Mills theory.

The super-KLT relation unifies all KLT relations for amplitudes of component fields. After super-field expansion in both sides of (2.51), we can automatically get all relations identified by Grassmann variable monomials. Especially, the pure gravity and Yang-Mills KLT relation (2.15) can be obtained by taking gravity amplitudes identified by Grassmann variable monomials $\prod_{i=1}^n(\eta_{i,1}\eta_{i,2}\eta_{i,3}\eta_{i,4}\eta_{i,5}\eta_{i,6}\eta_{i,7}\eta_{i,8})^{k_i}$(where k_i is zero if positive graviton and 1 if negative graviton for particle i) in the left hand side, and Yang-Mills amplitudes identified by Grassmann variable monomials $\prod_{i=1}^n(\eta_{i,1}\eta_{i,2}\eta_{i,3}\eta_{i,4}\widetilde{\eta}_{i,5}\widetilde{\eta}_{i,6}\widetilde{\eta}_{i,7}\widetilde{\eta}_{i,8})^{k_i}$ in the right hand side.

The super-KLT relations for non-maximal supersymmetric theories are almost the same. But since there are two super-fields (Φ,Ψ) instead of one, we can not trivially write it down as an one-line expression. The idea is still replacing all pure graviton and gluon fields with corresponding (Φ,Ψ), $(\widetilde{\Phi},\widetilde{\Psi})$-super-fields, and pure gravity and Yang-Mills amplitudes with super-amplitudes. According to the $\Phi,\widetilde{\Phi}$ or $\Psi,\widetilde{\Psi}$-superfields of super-Yang-Mills theory for particle i, we can get four different super-fields of super-gravity theory for particle i, i.e., $(\widetilde{\Phi},\Phi)$, $(\widetilde{\Psi},\Phi)$, $(\widetilde{\Phi},\Psi)$, $(\widetilde{\Psi},\Psi)$. More explicitly, KLT-product of two arbitrary super-Yang-Mills amplitudes produces

$$\begin{aligned}
&\sum_{\gamma,\beta\in S_{n-3}} \widetilde{\mathcal{A}}^{\widetilde{\mathcal{N}}\leq 4}_{n,\tilde{i}_1,\ldots\tilde{i}_{\widetilde{m}}}(n-1,n,\gamma,1)\mathcal{S}[\gamma|\beta]_{p_1}\mathcal{A}^{\mathcal{N}\leq 4}_{n,i_1\ldots i_m}(1,\beta,n-1,n) \\
&= \sum_{\gamma,\beta\in S_{n-3}}\left[\int\prod_{\tilde{a}_1=\widetilde{\mathcal{N}}+1}^{4} d\eta_{\tilde{i}_1,\tilde{a}_1}\cdots\prod_{\tilde{a}_{\widetilde{m}}=\widetilde{\mathcal{N}}+1}^{4} d\eta_{\tilde{i}_{\widetilde{m}},\tilde{a}_{\widetilde{m}}}\widetilde{\mathcal{A}}^{\widetilde{\mathcal{N}}=4}_n(n-1,n,\gamma,1)\right]_{\eta_{\widetilde{\mathcal{N}}+1},\ldots,\eta_4\to 0} \\
&\qquad \times\mathcal{S}[\gamma|\beta]_{p_1}\times\left[\int\prod_{a_1=\mathcal{N}+5}^{8} d\eta_{i_1,a_1}\cdots\prod_{a_m=\mathcal{N}+5}^{8} d\eta_{i_m,a_m}\mathcal{A}^{\mathcal{N}=4}_n(1,\beta,n-1,n)\right]_{\eta_{\mathcal{N}+5},\ldots,\eta_8\to 0} \\
&= \Bigg[\int\prod_{\tilde{a}_1=\widetilde{\mathcal{N}}+1}^{4} d\eta_{\tilde{i}_1,\tilde{a}_1}\cdots\prod_{\tilde{a}_{\widetilde{m}}=\widetilde{\mathcal{N}}+1}^{4} d\eta_{\tilde{i}_{\widetilde{m}},\tilde{a}_{\widetilde{m}}}\prod_{a_1=\mathcal{N}+5}^{8} d\eta_{i_1,a_1}\cdots\prod_{a_m=\mathcal{N}+5}^{8} d\eta_{i_m,a_m} \\
&\qquad \times\sum_{\gamma,\beta\in S_{n-3}}\widetilde{\mathcal{A}}^{\widetilde{\mathcal{N}}=4}_n(n-1,n,\gamma,1)\mathcal{S}[\gamma|\beta]_{p_1}\mathcal{A}^{\mathcal{N}=4}_n(1,\beta,n-1,n)\Bigg]_{\substack{\eta_{\widetilde{\mathcal{N}}+1},\ldots,\eta_4\to 0\\ \eta_{\mathcal{N}+5},\ldots,\eta_8\to 0}} \\
&= \Bigg[\int\prod_{\tilde{a}_1=\widetilde{\mathcal{N}}+1}^{4} d\eta_{\tilde{i}_1,\tilde{a}_1}\cdots\prod_{\tilde{a}_{\widetilde{m}}=\widetilde{\mathcal{N}}+1}^{4} d\eta_{\tilde{i}_{\widetilde{m}},\tilde{a}_{\widetilde{m}}} \\
&\qquad \times\prod_{a_1=\mathcal{N}+5}^{8} d\eta_{i_1,a_1}\cdots\prod_{a_m=\mathcal{N}+5}^{8} d\eta_{i_m,a_m}\mathcal{M}^{\mathcal{N}_G=8}_n(\Phi_1,\Phi_2,\ldots,\Phi_n)\Bigg]_{\substack{\eta_{\widetilde{\mathcal{N}}+1},\ldots,\eta_4\to 0\\ \eta_{\mathcal{N}+5},\ldots,\eta_8\to 0}} \\
&\equiv \mathcal{M}^{\mathcal{N}_G\leq 8}_{n,(\tilde{i}_1,\ldots,\tilde{i}_{\widetilde{m}});(i_1,\ldots,i_m)}\,, \qquad (2.52)
\end{aligned}$$

where we use labels $(\tilde{i}_1,\ldots,\tilde{i}_{\widetilde{m}})$ and $(i_1,\ldots,i_m)$ to denote $\widetilde{\Psi}$ and Ψ-super-fields respectively, and others $\widetilde{\Phi},\Phi$-super-fields. In above derivation, firstly we write $\widetilde{\mathcal{A}}^{\widetilde{N}\leq 4},\mathcal{A}^{N\leq 4}$ as truncation of maximal super-Yang-Mills amplitudes, and before taking corresponding η variables to zero or integrating them out, we use KLT relation for maximal supersymmetry (2.51) to rewrite the product of two maximal super-Yang-Mills amplitudes as maximal super-gravity amplitude. Finally we get super-gravity amplitude $\mathcal{M}^{\mathcal{N}_G\leq 8}_n$ as truncation from maximal super-gravity amplitude.

To complete the formulation of super-KLT relations for arbitrary $\mathcal{N}$, we need to work out explicitly the four types of super-fields for super-gravity amplitude. They can be truncated from maximal $\mathcal{N}=8$ super-gravity amplitude according to

- $(\widetilde{\Phi},\Phi)$: if $k\notin(\tilde{i}_1,\ldots,\tilde{i}_{\widetilde{m}})$ and $k\notin(i_1,\ldots,i_m)$, we get $\Phi_k^{\mathcal{N}_G=\widetilde{\mathcal{N}}+\mathcal{N}}$ super-field

$$\Phi_k^{\mathcal{N}_G=\widetilde{\mathcal{N}}+\mathcal{N}} = \Phi_k^{\mathcal{N}_G=8}|_{\eta_{k,\widetilde{\mathcal{N}}+1},\ldots,\eta_{k,4};\eta_{k,\mathcal{N}+5},\ldots,\eta_{k,8}\to 0}\;. \qquad (2.53)$$

- $(\widetilde{\Psi},\Psi)$: if $k\in(\tilde{i}_1,\ldots,\tilde{i}_{\widetilde{m}})$ and $k\in(i_1,\ldots,i_m)$, we get $\Psi_k^{\mathcal{N}_G=\widetilde{\mathcal{N}}+\mathcal{N}}$ super-field

$$\Psi_k^{\mathcal{N}_G=\widetilde{\mathcal{N}}+\mathcal{N}}=\int\prod_{a=\widetilde{\mathcal{N}}+1}^{4}d\eta_{k,a}\prod_{b=\mathcal{N}+5}^{8}d\eta_{k,b}\Phi_k^{\mathcal{N}_G=8}\ . \tag{2.54}$$

$(\Phi_k^{\mathcal{N}_G=\widetilde{\mathcal{N}}+\mathcal{N}},\Psi_k^{\mathcal{N}_G=\widetilde{\mathcal{N}}+\mathcal{N}})$ is a complete $SU(\mathcal{N}_G)$ super-gravity multiplet.

- $(\widetilde{\Psi},\Phi)$: if $k\in(\tilde{i}_1,\ldots,\tilde{i}_{\widetilde{m}})$ and $k\notin(i_1,\ldots,i_m)$, we get $\Theta_k^{\mathcal{N}_G=\widetilde{\mathcal{N}}+\mathcal{N}}$ super-field

$$\Theta_k^{\mathcal{N}_G=\widetilde{\mathcal{N}}+\mathcal{N}}=\int\prod_{a=\widetilde{\mathcal{N}}+1}^{4}d\eta_{k,a}\Phi_k^{\mathcal{N}_G=8}|_{\eta_{k,\mathcal{N}+5},\ldots,\eta_{k,8}\to 0}\ . \tag{2.55}$$

- $(\widetilde{\Phi},\Psi)$: $k\notin(\tilde{i}_1,\ldots,\tilde{i}_{\widetilde{m}})$ and $k\in(i_1,\ldots,i_m)$, we get $\Gamma_k^{\mathcal{N}_G=\widetilde{\mathcal{N}}+\mathcal{N}}$ super-field

$$\Gamma_k^{\mathcal{N}_G=\widetilde{\mathcal{N}}+\mathcal{N}}=\int\prod_{b=\mathcal{N}+5}^{8}d\eta_{k,b}\Phi_k^{\mathcal{N}_G=8}|_{\eta_{k,\widetilde{\mathcal{N}}+1},\ldots,\eta_{k,4}\to 0}\ . \tag{2.56}$$

$(\Theta_k^{\mathcal{N}_G=\widetilde{\mathcal{N}}+\mathcal{N}},\Gamma_k^{\mathcal{N}_G=\widetilde{\mathcal{N}}+\mathcal{N}})$ is a complete $SU(\mathcal{N}_G)$ matter super-multiplet.

Thus $\mathcal{M}^{\mathcal{N}_G\leq 8}_{n,(\tilde{i}_1,\ldots,\tilde{i}_{\widetilde{m}});(i_1,\ldots,i_m)}$ is a function of super-fields $\Phi^{\mathcal{N}_G},\Psi^{\mathcal{N}_G},\Theta^{\mathcal{N}_G}$ and $\Gamma^{\mathcal{N}_G}$.

Now we are going to work out the particle states with help of diamond diagram. The particle states of super-gravity field can be constructed from tensor products of particle states of two super-Yang-Mills fields. For maximal theory, we already know that super-Yang-Mills theory has 16 states. The product of two super-Yang-Mills theories will give $16\times 16=256$ states, which is exactly the number of states that maximal super-gravity theory has. In fact there is one to one correspondence between super-gravity states and tensor products of two super-Yang-Mills states. All states of $\mathcal{N}=4$ super-Yang-Mills field are $(+1,+\frac{1}{2}^4,0^6,-\frac{1}{2}^4,-1)$, where superscript denotes the degeneracy of specific state. Taking tensor product, we immediately get two graviton states

$$(+1)\otimes(+1)\ \ \text{and}\ \ (-1)\otimes(-1)\ ,$$

16 gravitino states $\psi^{\pm}$

$$(+1/2)^4\otimes(+1)\ ,\ (+1)\otimes(+1/2)^4\ \ \text{and}\ \ (-1/2)^4\otimes(-1)\ ,\ (-1)\otimes(-1/2)^4,$$

56 graviphoton states $v^{\pm}$

$$(0)^6\otimes(+1)\ ,\ (+1/2)^4\otimes(+1/2)^4\ ,\ (+1)\otimes(0)^6\ \ \text{and}\ \ (0)^6\otimes(-1)\ ,\ (-1/2)^4\otimes(-1/2)^4\ ,\ (-1)\otimes(0)^6\ ,$$

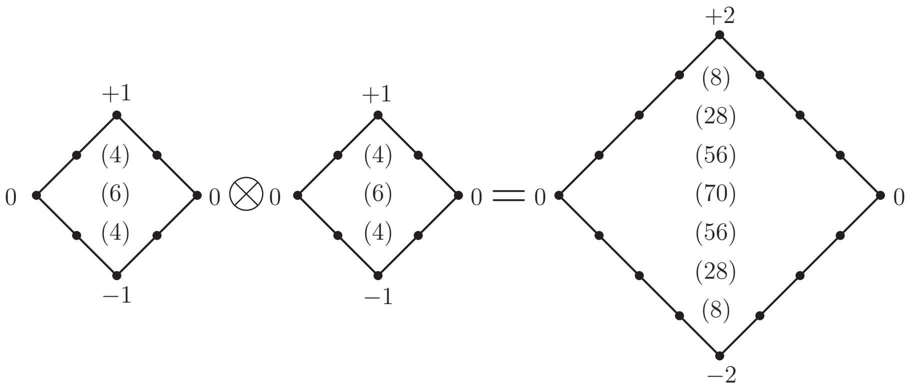

FIGURE 2.2: Matching of particle states for KLT relation of (supergravity)$_{\mathcal{N}_G=8}$ = (super Yang-Mills)$_{\widetilde{\mathcal{N}}=4}\otimes$ (super Yang-Mills)$_{\mathcal{N}=4}$.

112 spin-1/2 graviphotino states $\chi^{\pm}$

$$(-1/2)^4\otimes(+1)\ ,\ (0)^6\otimes(+1/2)^4\ ,\ (+1/2)^4\otimes(0)^6\ ,\ (+1)\otimes(-1/2)^4\ ,$$

$$(+1/2)^4\otimes(-1)\ ,\ (0)^6\otimes(-1/2)^4\ ,\ (-1/2)^4\otimes(0)^6\ ,\ (-1)\otimes(+1/2)^4\ ,$$

and 70 scalars

$$(-1)\otimes(+1)\ ,\ (-1/2)^4\otimes(+1/2)^4\ ,\ (0)^4\otimes(0)^4\ ,\ (+1/2)^4\otimes(-1/2)^4\ ,\ (+1)\otimes(-1)\ .$$

Again if denoting R-indices as $1,2,3,4$ for one super-Yang-Mills theory, and $5,6,7,8$ for the other super-Yang-Mills theory, we recover R-indices of $SU(8)_R$ super-gravity by just combining indices together from two super-Yang-Mills theories. The diagrammatic representation is shown in Figure (2.2).

The discussion applies similarly to non-maximal supersymmetric theories. The only difference is that since we are using (Φ,Ψ)-super-field, there are two diamonds for each super-Yang-Mills field, and the tensor product should be worked out separately for each diamond. For example, $\mathcal{N}=2$ super-Yang-Mills theory has two super-fields. The $\Phi^{\mathcal{N}=2}$-super-field contains states $(+1,+\frac{1}{2}^2,0)$ and the $\Psi^{\mathcal{N}=2}$-super-field contains states $(0,-\frac{1}{2}^2,-1)$. Tensor product of $(\Phi^{\mathcal{N}=2},\widetilde{\Phi}^{\mathcal{N}=2})$ gives a super-gravity multiplet $\Phi^{\mathcal{N}_G=2+2}$ with states $(+2,+(3/2)^4,+1^6,+(1/2)^4,0)$, tensor product of $(\Psi^{\mathcal{N}=2},\widetilde{\Psi}^{\mathcal{N}=2})$ gives $\Psi^{\mathcal{N}_G=2+2}$ with states $(0,-(1/2)^4,-1^6,-(3/2)^4,-2)$, which is the CPT conjugate of $\Phi^{\mathcal{N}_G=2+2}$. The tensor product of $(\Phi^{\mathcal{N}=2},\widetilde{\Psi}^{\mathcal{N}=2})$ gives a vector super-multiplet $\Theta^{\mathcal{N}_G=2+2}_{vector}$ with states $(+1,+(1/2)^4,0^6,-(1/2)^4,-1)$, and finally tensor product of $(\Psi^{\mathcal{N}=2},\widetilde{\Phi}^{\mathcal{N}=2})$ gives another vector super-multiplet $\Gamma^{\mathcal{N}_G=2+2}_{vector}$. Θ,Γ are CPT self-conjugate vector super-multiplets, but having different R-indices for component fields.

By working out all tensor products of two arbitrary super-Yang-Mills theories, we get

$\mathcal{N}_G$	$\widetilde{\mathcal{N}} \otimes \mathcal{N}$	Description
8	$4 \otimes 4$	Maximal $\mathcal{N}_G = 8$ Supergravity
7	$4 \otimes 3$	Maximal $\mathcal{N}_G = 8$ Supergravity
6	$4 \otimes 2$	Minimal $\mathcal{N}_G = 6$ Supergravity with $SU(6)$ supergravity multiplet
6	$3 \otimes 3$	Maximal $\mathcal{N}_G = 8$ Supergravity
5	$4 \otimes 1$	Minimal $\mathcal{N}_G = 5$ Supergravity with $SU(5)$ supergravity multiplet
5	$3 \otimes 2$	Minimal $\mathcal{N}_G = 6$ Supergravity with $SU(6)$ supergravity multiplet
4	$4 \otimes 0$	Minimal $\mathcal{N}_G = 4$ Supergravity with $SU(4)$ supergravity multiplet
4	$3 \otimes 1$	Minimal $\mathcal{N}_G = 5$ Supergravity with $SU(5)$ supergravity multiplet
4	$2 \otimes 2$	$\mathcal{N}_G = 4$ Supergravity multiplet coupled to vector multiplet
3	$3 \otimes 0$	Minimal $\mathcal{N}_G = 4$ Supergravity with $SU(4)$ supergravity multiplet
3	$2 \otimes 1$	$\mathcal{N}_G = 3$ Supergravity multiplet coupled to vector multiplet
2	$2 \otimes 0$	$\mathcal{N}_G = 2$ Supergravity multiplet coupled to vector multiplet
2	$1 \otimes 1$	$\mathcal{N}_G = 2$ Supergravity multiplet coupled to hypermultiplet
1	$1 \otimes 0$	$\mathcal{N}_G = 1$ Supergravity multiplet coupled to chiral multiplet
0	$0 \otimes 0$	Einstein gravity coupled to two scalars

TABLE 2.1: List of all possible super-gravity theories that are allowed by super-KLT-relations.

the complete set of super-gravity theories that are allowed by super-KLT relations. The results are summarized in Table (2.1).

According to the types of super-gravity fields obtained, we can classify all super-gravity theories into three categories. In category I, we only need a single super-filed Φ to encode all particles states. This category consists of maximal $\mathcal{N}_G = 8$ super-gravity theory, the equivalent $\mathcal{N}_G = 7$ super-gravity theory, and the $(\widetilde{\mathcal{N}} = 3) \otimes (\mathcal{N} = 3)$ theory. In fact, they are the same theory but with super-fields written in different ways. For $\mathcal{N}_G = 8$ super-gravity theory we need $\Phi^{\mathcal{N}_G=8}$-super-field, while expanding $\Phi^{\mathcal{N}_G=8} = \Phi^{\mathcal{N}_G=7} + \eta_8 \Psi^{\mathcal{N}_G=7}$ we get $\mathcal{N}_G = 7$ super-gravity theory, and expanding

$$\Phi^{\mathcal{N}_G=8} = \Phi^{\mathcal{N}_G=6} + \eta_4 \Theta^{\mathcal{N}_G=6} + \eta_8 \Gamma^{\mathcal{N}_G=6} + \eta_4\eta_8 \Psi^{\mathcal{N}_G=6}$$

we get $(\widetilde{\mathcal{N}} = 3) \otimes (\mathcal{N} = 3)$ theory. The super KLT-relations for these theories are equivalent to (2.51).

Theories in category II requires two super-fields (Φ, Ψ)(thus two diamonds) to encode all particle states. These are all minimal super-gravity theories with $4 \leq \mathcal{N}_G < 8$. They arise from KLT product $(\widetilde{\mathcal{N}} = 4) \otimes (\mathcal{N} \leq 2)$ (or $(\widetilde{\mathcal{N}} = 3) \otimes (\mathcal{N} \leq 2)$ due to the equivalence between $\widetilde{\mathcal{N}} = 3$ and $\widetilde{\mathcal{N}} = 4$). Super KLT-relations for them can be written as

$$\begin{aligned} &\mathcal{M}_n^{\mathcal{N}_G=4+\mathcal{N}}(\Phi^{\mathcal{N}_G}_{i_1,\ldots,i_{m_1}}, \Psi^{\mathcal{N}_G}_{j_1,\ldots,j_{m_2}}) = \\ &\sum_{\gamma,\beta\in S_{n-3}} \widetilde{\mathcal{A}}_n^{\widetilde{\mathcal{N}}=4}(\Phi^{\widetilde{\mathcal{N}}=4}_{1,\ldots,n}) \times \mathcal{S}[\gamma|\beta]_{p_1} \times \mathcal{A}_n^{\mathcal{N}\leq 2}(\Phi^{\mathcal{N}\leq 2}_{i_1,\ldots,i_{m_1}}, \Psi^{\mathcal{N}\leq 2}_{j_1,\ldots,j_{m_2}}) \ , \end{aligned} \tag{2.57}$$

where indices $(i_1,\ldots,i_{m_1})$ and $(j_1,\ldots,j_{m_2})$ denote legs of corresponding super-fields and $m_1+m_2=n$.

All remaining theories require four super-fields $(\Phi,\Theta,\Gamma,\Psi)$(thus four diamonds) to encode all particle states. They describe minimal super-gravity coupled to a variety of matter multiplets. The super KLT-relations for them can be compactly expressed as

$$\begin{aligned}\mathcal{M}_n^{\mathcal{N}_G=\widetilde{\mathcal{N}}+\mathcal{N}}(\Phi^{\mathcal{N}_G}_{i_1,\ldots,i_{m_1}},\Psi^{\mathcal{N}_G}_{j_1,\ldots,j_{m_2}},\Theta^{\mathcal{N}_G}_{k_1,\ldots,k_{m_3}},\Gamma^{\mathcal{N}_G}_{l_1,\ldots,l_{m_3}}) = \\ \sum_{\gamma,\beta\in S_{n-3}}\widetilde{\mathcal{A}}_n^{\widetilde{\mathcal{N}}\leq 2}(\Phi^{\widetilde{\mathcal{N}}\leq 2}_{i_1,\ldots,i_{m_1},l_1,\ldots,l_{m_3}},\Psi^{\widetilde{\mathcal{N}}\leq 2}_{j_1,\ldots,j_{m_2},k_1,\ldots,k_{m_3}}) \\ \times\mathcal{S}[\gamma|\beta]_{p_1}\times\mathcal{A}_n^{\mathcal{N}\leq 2}(\Phi^{\mathcal{N}\leq 2}_{i_1,\ldots,i_{m_1},k_1,\ldots,k_{m_3}},\Psi^{\mathcal{N}\leq 2}_{j_1,\ldots,j_{m_2},l_1,\ldots,l_{m_3}})\ ,\end{aligned} \tag{2.58}$$

where again $(i_1,\ldots,i_{m_1}),(j_1,\ldots,j_{m_2}),(k_1,\ldots,k_{m_3})$ and $(l_1,\ldots,l_{m_3})$ denote corresponding super-fields and $m_1+m_2+2m_3=n$. The $SU(\mathcal{N}_G)_R$ invariance requires that (Θ,Γ)-super-fields should come in pair.

A complete set of diamond diagrams and explicit expression of various super-fields can be found in [70].

When writing down maximal supersymmetric KLT relation, we mentioned that all KLT relations for component amplitude can be obtained from η-expansion of super-gravity and super-Yang-Mills amplitudes in left and right hand sides of (2.51). The physical KLT relations for component amplitudes come from Grassmann variable monomials $\prod_i\eta_i$ that preserving $SU(8)_R$ invariance of super-gravity amplitude and $SU(4)_R$ invariance of each super-Yang-Mills amplitude. However, terms of η-monomials that violating $SU(\mathcal{N})_R$ symmetry do exist. For example, 5-point gluon MHV amplitudes

$$A_5(g_1^+,g_2^+,g_3^+,g_4^-,g_5^-)\widetilde{A}_5(g_1^-,g_2^+,g_3^+,g_4^-,g_5^-)\ ,$$

which follows from Grassmann variable monomials

$$\eta_{4,1}\eta_{4,2}\eta_{4,3}\eta_{4,4}\eta_{5,1}\eta_{5,2}\eta_{5,3}\eta_{5,4}\widetilde{\eta}_{1,5}\widetilde{\eta}_{1,6}\widetilde{\eta}_{1,7}\widetilde{\eta}_{1,8}\widetilde{\eta}_{4,5}\widetilde{\eta}_{4,6}\widetilde{\eta}_{4,7}\widetilde{\eta}_{4,8}\widetilde{\eta}_{5,5}\widetilde{\eta}_{5,6}\widetilde{\eta}_{5,7}\widetilde{\eta}_{5,8}\ ,$$

are non-zero, and each $SU(4)_R$ invariance is preserved. The component gravity amplitude, identified by monomial

$$\eta_{1,5}\eta_{1,6}\eta_{1,7}\eta_{1,8}\eta_{4,1}\eta_{4,2}\eta_{4,3}\eta_{4,4}\eta_{4,5}\eta_{4,6}\eta_{4,7}\eta_{4,8}\eta_{5,1}\eta_{5,2}\eta_{5,3}\eta_{5,4}\eta_{5,5}\eta_{5,6}\eta_{5,7}\eta_{5,8}\ ,$$

violates $SU(8)_R$ symmetry, and corresponding gravity amplitude $M_5(s,h^+,h^+,h^-,h^-)$ vanishes. Thus we have a vanishing identity, i.e., KLT product of pure gluon amplitudes with specific helicity configurations $(1^+,2^+,3^+,4^-,5^-)$ and $(1^-,2^+,3^+,4^-,5^-)$ vanishes, although individually each gluon amplitude does not vanish.

More generally, we have vanishing identity[93]

$$0 = \sum_{\sigma\in S_{n-3}}\sum_{\alpha\in S_{j-1}}\sum_{\beta\in S_{n-2-j}} A_n^{N^k MHV}(1,\sigma_{2,j},\sigma_{j+1,n-2},n-1,n)\mathcal{S}[\alpha_{\sigma(2),\sigma(j)}|\sigma_{2,j}]_{p_1}$$
$$\times\, \widetilde{\mathcal{S}}[\sigma_{j+1,n-2}|\beta_{\sigma(j+1),\sigma(n-2)}]_{p_{n-1}}\widetilde{A}_n^{N^{k'} MHV}(\alpha_{\sigma(2),\sigma(j)},1,n-1,\beta_{\sigma(j+1),\sigma(n-2)},n)\ , \tag{2.59}$$

when $k \neq k'$. A systematic way of understanding the family of vanishing identities is to study the symmetry group of various super-gravity theories from super-KLT relations, and interpret the vanishing identities as consequence of symmetry violation.

2.2.3 Linear symmetry group for super-gravity theories

Generally, for supersymmetric theory with $\mathcal{N}$ supercharges $Q_A, \widetilde{Q}^A, A = 1, 2, \ldots, \mathcal{N}$, we have $U(\mathcal{N})_R$ invariant group of rotating $Q_A, \widetilde{Q}^A$. However, the supersymmetric theory could also possess some invariant groups which are subgroups of $U(\mathcal{N})_R$. One typical subgroup is $SU(\mathcal{N})_R$ group, which mentioned several times in previous sections that constraining Grassmann variable monomials. This subgroup comes out naturally from decomposition of $U(\mathcal{N})_R = SU(\mathcal{N})_R \otimes U(1)_R$. While $SU(\mathcal{N})_R$ is an invariant subgroup, what is the role of $U(1)_R$ group in these various theories? Besides these two subgroups, is there any other invariant subgroup?

Based on the super-KLT relations, it is possible to argue that

- For maximal supersymmetric theory, the invariant symmetry group is $SU(\mathcal{N})_R$. There is a $SU(\mathcal{N})_R$ charge assigned to component fields in super-gravity multiplet.
- For $4 < \mathcal{N}_G < 8$ minimal super-gravity theories, the invariant symmetry group is $SU(\mathcal{N})_R \otimes U(1)_R$. Besides $SU(\mathcal{N})_R$ charge, there is also a $U(1)_R$ charge distinguishing Φ, Ψ-super-fields of super-gravity multiplet.
- For $0 < \mathcal{N}_G < 4$ minimal super-gravity theories coupled to matter multiplet, the symmetry group is $SU(\mathcal{N})_R \otimes U(1)_R \otimes U(1)$. The extra $U(1)$ invariant group comes from the freedom of assigning a charge to component fields in matter multiplet.

Let us discuss them in detail. The maximal super-gravity theory only contains one super-field, and all particle states can find their CPT conjugate partners inside the super-field. If non-trivial $U(1)_R$ group exists, then some of the component fields should carry non-vanishing $U(1)_R$ charge. (1) Suppose there is $U(1)_R$ charge β for graviton. Consider MHV gravity amplitude $M_n(h^-, h^-, h^+, \ldots, h^+)$, which has a total $U(1)_R$ charge of $-2\beta + (n-2)\beta = (n-4)\beta$. The non-vanishing of this amplitude indicates that $(n-4)\beta$

should be zero to ensure charge conservation. Since n is arbitrary, we should take $\beta = 0$. So graviton can not carry non-zero $U(1)_R$ charge. (2) Suppose scalar has non-vanishing $U(1)_R$ charge. If we assign $+\beta$ to s^{1234}, then the complex conjugate scalar s^{5678} has charge $-\beta$. Since they are inside one super-field, they must carry the same charge, thus $\beta = -\beta \to \beta = 0$. (3) Suppose graviphoton v, with helicity ± 1, has $U(1)_R$ charge $\pm\beta$. If we consider the non-vanishing three-vertex amplitude

$$\mathcal{M}(\phi, v^-, v^-) = \frac{\langle 12\rangle^2\langle 13\rangle^2\langle 23\rangle^4}{\langle 12\rangle^2\langle 23\rangle^2\langle 31\rangle^2} = \langle 23\rangle^2 \ , \tag{2.60}$$

then conservation of total charge $0 - \beta - \beta = 0$ implies $\beta = 0$. (4) Suppose graviphotino χ, with helicity $\pm 1/2$, has $U(1)_R$ charge $\pm\beta$. Since we have non-vanishing three-vertex amplitude

$$\mathcal{M}(v^-, \chi^-, \chi^-) = \frac{\langle 12\rangle^3\langle 13\rangle^3\langle 23\rangle^2}{\langle 12\rangle^2\langle 23\rangle^2\langle 31\rangle^2} = \langle 12\rangle\langle 13\rangle \ , \tag{2.61}$$

and also $U(1)_R$ charge for v^- is 0, so total $U(1)_R$ charge from χ^- should be zero and we have $\beta = 0$. (5) Finally, suppose gravitino ψ with helicity $\pm 3/2$ has non-zero charge $\pm\beta$. We can consider non-vanishing three-vertex amplitude

$$\mathcal{M}(\phi, \chi^-, \psi^-) = \frac{\langle 12\rangle\langle 13\rangle^3\langle 23\rangle^4}{\langle 12\rangle^2\langle 23\rangle^2\langle 31\rangle^2} = \frac{\langle 13\rangle\langle 23\rangle^2}{\langle 12\rangle} \ . \tag{2.62}$$

Since we already argued that ϕ, χ has zero $U(1)_R$ charge, it follows immediately that ψ also has zero $U(1)_R$ charge. In summary, even if there is $U(1)_R$ symmetry group, the $U(1)_R$ charge for each component field is zero, which has no effect at all for the theory. So the linear symmetric group for $\mathcal{N}_G = 8$ super-gravity is $SU(8)_R$. Similarly, the linear symmetric group for $\mathcal{N} = 4$ super-Yang-Mills theory is $SU(4)_R$.

Above argument is not valid for non-maximal supersymmetric theories, since more than one super-fields are presented in those theories, and no confliction can be found for assignment of $U(1)_R$ charge to component fields. In order to assign charge to component fields of $\mathcal{N}_G < 8$ super-gravity theories, we can start from studying certain $k \times k$ matrix B_{x_i,x_j} acting on indices $(x_1, x_2, \ldots, x_k)$ of Grassmann variables η. The anti-commutative of η leads us to consider matrix B_{x_i,x_j} acting on wedge product of $\eta_{x_1} \wedge \eta_{x_2} \wedge \cdots \wedge \eta_{x_k}$, where Grassmann variables η span a super-space with each η_{x_i} a basis vector $\eta_{x_i} =$

$(0,\ldots,1_{i-th},\ldots,0)^T$. When B_{x_i,x_j} acts on the basis vector η_{x_i}, we have

$$\begin{pmatrix} B_{11} & \cdots & \cdots & \cdots & B_{1k} \\ \vdots & \ddots & & & \vdots \\ \vdots & & \ddots & & \vdots \\ \vdots & & & \ddots & \vdots \\ B_{k1} & \cdots & \cdots & \cdots & B_{kk} \end{pmatrix}_{k\times k} \begin{pmatrix} 0 \\ \vdots \\ 1 \\ \vdots \\ 0 \end{pmatrix} = \begin{pmatrix} B_{1i} \\ B_{2i} \\ \vdots \\ \vdots \\ B_{ki} \end{pmatrix} = \sum_{j=1}^{k} B_{ji}\eta_{x_j} \ , \tag{2.63}$$

Then the matrix acts on wedge product of all basis vectors implies that

$$B(\eta_{x_1}\wedge\eta_{x_2}\wedge\cdots\wedge\eta_{x_k}) \ = \ (\sum_{i=1}^{k} B_{ii})(\eta_{x_1}\wedge\eta_{x_2}\wedge\cdots\wedge\eta_{x_k}) \ .$$

So only trace of matrix B plays a role. This trace is responsible for assigning charge to states.

The maximal $\mathcal{N}_G = 8$ super-gravity theory has traceless 8×8 Hermitian matrix, which acts on the vector space spanned by 8 Grassmann variables η_A. Since non-maximal supersymmetric theories can be truncated or integrated out from maximal theory, the $\mathcal{N}_G$ Grassmann variables are then a subset of eight η_A. The $\mathcal{N}_G\times\mathcal{N}_G$ matrix acting on vector space spanned by $\mathcal{N}_G$ Grassmann variables and also the $(8-\mathcal{N}_G)\times(8-\mathcal{N}_G)$ matrix acting on vector space spanned by $(8-\mathcal{N}_G)$ hidden Grassmann variables are all embedded in the traceless (8×8) Hermitian matrix.

The $4 < \mathcal{N}_G < 8$ minimal super-gravity theories come from KLT product of maximal super-Yang-Mills amplitude with another $\widetilde{\mathcal{N}} < 4$ super-Yang-Mills amplitude. So there is only one group of hidden indices. The matrix can be expressed as

$$\begin{pmatrix} T_{\mathcal{N}_G\times\mathcal{N}_G} & \\ & B_{(8-\mathcal{N}_G)\times(8-\mathcal{N}_G)} \end{pmatrix}_{8\times 8} \ . \tag{2.64}$$

Matrix T acts on indices 1 to $\mathcal{N}_G$ while matrix B acts on hidden indices $\mathcal{N}_G+1$ to 8. Since we want to discuss the role of $U(1)_R$ symmetry, we can take matrix T to commute with all $SU(\mathcal{N}_G)_R$ generators, thus T must be diagonal matrix proportional to identity $T = \alpha I_{\mathcal{N}_G\times\mathcal{N}_G}$. Then we can assign a charge α for each index from 1 to $\mathcal{N}_G$. The B matrix, acting on hidden indices, satisfies two conditions. Firstly only the trace of B contributes to the charge when acting on hidden indices. Secondly, the trace of B should be taken so that the whole 8×8 matrix should still be traceless. In these cases, we can assign a charge $\beta\equiv \mathrm{Tr}(B)$ for all hidden indices $(\mathcal{N}_G+1,\ldots,8)$ with condition $\beta+\mathcal{N}_G\alpha = 0$. Since hidden indices always appear together, there is no trouble that we can not assign charge for each hidden index. The total charge of particle state can be obtained by adding all corresponding charges of indices that specifying the state. Taking $\mathcal{N}_G = 6$ for example, the graviton state h_+ has no R-indices, so we can assign 0 to it, while the $h_-^{123456(78)}$ state has 6 $SU(6)_R$ indices and 2 hidden indices, so the total charge is $6\alpha+\beta = 0$. The graviphoton state v_+^{12} in Φ-super-field has total charge of $+2\alpha$, while $v_-^{1256(78)}$ has total charge of $4\alpha+\beta = -2\alpha$. This could be expected since v_- is the complex conjugate state of v_+, thus has the opposite charge. From above discussion, we see that for $4 < \mathcal{N}_G < 8$ minimal super-gravity theories, the linear symmetric group is $SU(\mathcal{N}_G)_R \times U(1)_R$. Amplitudes that violating either $SU(\mathcal{N}_G)_R$ or $U(1)_R$ symmetry should vanish.

The $0 < \mathcal{N}_G < 4$ super-gravity theories come from KLT product of $\mathcal{N} < 4$ super-Yang-Mills amplitude and another $\widetilde{\mathcal{N}}_G < 4$ super-Yang-Mills amplitude. So we have two groups of hidden indices. They are unrelated because of coming from integrating out η variables in different super-Yang-Mills theories. So we can express the matrix as

$$\begin{pmatrix} T^{(1)}_{\mathcal{N}\times\mathcal{N}} & & T^{(2)}_{\mathcal{N}\times\widetilde{\mathcal{N}}} & \\ & B_{(4-\mathcal{N})\times(4-\mathcal{N})} & & \\ T^{(3)}_{\widetilde{\mathcal{N}}\times\mathcal{N}} & & T^{(4)}_{\widetilde{\mathcal{N}}\times\widetilde{\mathcal{N}}} & \\ & & & C_{(4-\widetilde{\mathcal{N}})\times(4-\widetilde{\mathcal{N}})} \end{pmatrix}_{8\times 8} . \tag{2.65}$$

The $(\mathcal{N}+\widetilde{\mathcal{N}}) \times (\mathcal{N}+\widetilde{\mathcal{N}})$ matrix T

$$\begin{pmatrix} T^{(1)}_{\mathcal{N}\times\mathcal{N}} & T^{(2)}_{\mathcal{N}\times\widetilde{\mathcal{N}}} \\ T^{(3)}_{\widetilde{\mathcal{N}}\times\mathcal{N}} & T^{(4)}_{\widetilde{\mathcal{N}}\times\widetilde{\mathcal{N}}} \end{pmatrix}_{(\mathcal{N}+\widetilde{\mathcal{N}})\times(\mathcal{N}+\widetilde{\mathcal{N}})} \tag{2.66}$$

acts on $SU(\mathcal{N}+\widetilde{\mathcal{N}})_R$ indices of super-gravity theory, while B matrix acts on hidden indices $(\mathcal{N}+1,\ldots,4)$ and C matrix acts on hidden indices $(\widetilde{\mathcal{N}}+5,\ldots,8)$. Again since we want to study the effect of $U(1)$ subgroup, we can take T matrix to commute with all $SU(\mathcal{N}+\widetilde{\mathcal{N}})_R$ generators. So it should be proportional to identity, i.e., $T^{(1)} = \alpha I_{\mathcal{N}\times\mathcal{N}}$, $T^{(2)} = 0_{\mathcal{N}\times\widetilde{\mathcal{N}}}$, $T^{(3)} = 0_{\widetilde{\mathcal{N}}\times\mathcal{N}}$ and $T^{(4)} = \alpha I_{\widetilde{\mathcal{N}}\times\widetilde{\mathcal{N}}}$. Similarly, two conditions should be satisfied by matrices T, B, C. Firstly, only trace of B, C contribute to charge when acting on their corresponding hidden indices. Secondly, trace of B and C should be taken so that the whole 8×8 matrix is still traceless. Therefore we can assign a charge α for each index of $SU(\mathcal{N}+\widetilde{\mathcal{N}})_R$ symmetry, $\beta \equiv \mathrm{Tr}(B)$ for hidden indices $(\mathcal{N}+1,\ldots,4)$ and $\gamma \equiv \mathrm{Tr}(C)$ for hidden indices $(\widetilde{\mathcal{N}}+5,\ldots,8)$, with the constraint $(\mathcal{N}+\widetilde{\mathcal{N}})\alpha+\beta+\gamma = 0$. The total charge of particle state can be obtained by adding all corresponding charges of indices that specifying the state.

In order to illustrate it transparently, let us take $\mathcal{N}_G = 4$ super-gravity theory from KLT product of two $\mathcal{N} = 2$ super-Yang-Mills theories as example. The charge for each state is listed below.

For Φ-super-field, R-index $a_i = 1, 2$ and $b_i = 5, 6$. We have

Helicity	KLT Product	Charge
$+2$	$(+1) \otimes (+1)$	0
$+\frac{3}{2}$	$(+\frac{1}{2}^{a_1}) \otimes (+1)$, $(+1) \otimes (+\frac{1}{2}^{b_1})$	α
$+1$	$(0^{12}) \otimes (+1)$, $(+\frac{1}{2}^{a_1}) \otimes (+\frac{1}{2}^{b_1})$, $(+1) \otimes (0^{56})$	2α
$+\frac{1}{2}$	$(0^{12}) \otimes (+\frac{1}{2}^{b_1})$, $(+\frac{1}{2}^{a_1}) \otimes (0^{56})$	3α
0	$(0^{12}) \otimes (0^{56})$	4α

For Θ-super-field, we have

Helicity	KLT Product	Charge
$+1$	$(0^{(34)}) \otimes (+1)$	$0 + \beta$
$+\frac{1}{2}$	$(0^{(34)}) \otimes (+\frac{1}{2}^{b_1})$, $(-\frac{1}{2}^{a_1(34)}) \otimes (+1)$	$\alpha + \beta$
0	$(0^{(34)}) \otimes (0^{56})$, $(-\frac{1}{2}^{a_1(34)}) \otimes (+\frac{1}{2}^{b_1})$, $(-1^{12(34)}) \otimes (+1)$	$2\alpha + \beta$
$-\frac{1}{2}$	$(-\frac{1}{2}^{a_1(34)}) \otimes (0^{56})$, $(-1^{12(34)}) \otimes (+\frac{1}{2}^{b_1})$	$3\alpha + \beta$
-1	$(-1^{12(34)}) \otimes (0^{56})$	$4\alpha + \beta$

For Γ-super-field, we have

Helicity	KLT Product	Charge
$+1$	$(+1) \otimes (0^{(78)})$	$-4\alpha - \beta$
$+\frac{1}{2}$	$(+1) \otimes (-\frac{1}{2}^{b_1(78)})$, $(+\frac{1}{2}^{a_1}) \otimes (0^{(78)})$	$-3\alpha - \beta$
0	$(0^{12}) \otimes (0^{(78)})$, $(+\frac{1}{2}^{a_1}) \otimes (-\frac{1}{2}^{b_1(78)})$, $(+1) \otimes (-1^{56(78)})$	$-2\alpha - \beta$
$-\frac{1}{2}$	$(0^{12}) \otimes (-\frac{1}{2}^{b_1(78)})$, $(+\frac{1}{2}^{a_1}) \otimes (-1^{56(78)})$	$-\alpha - \beta$
-1	$(0^{12}) \otimes (-1^{56(78)})$	$0 - \beta$

For Ψ-super-field, we have

Helicity	KLT Product	Charge
0	$(0^{(34)}) \otimes (0^{(78)})$	-4α
$-\frac{1}{2}$	$(0^{(34)}) \otimes (-\frac{1}{2}^{b_1(78)})$, $(-\frac{1}{2}^{a_1(34)}) \otimes (0^{(78)})$	-3α
-1	$(0^{(34)}) \otimes (-1^{56(78)})$, $(-\frac{1}{2}^{a_1(34)}) \otimes (-\frac{1}{2}^{b_1(78)})$, $(-1^{12(34)}) \otimes (0^{(78)})$	-2α
$-\frac{3}{2}$	$(-\frac{1}{2}^{a_1(34)}) \otimes (-1^{56(78)})$, $(-1^{12(34)}) \otimes (-\frac{1}{2}^{b_1(78)})$	$-\alpha$
-2	$(-1^{12(34)}) \otimes (-1^{56(78)})$	0

Component fields of super-gravity multiplet Φ, Ψ are assigned with charge α from $U(1)_R$ symmetry. Component fields of matter super-multiplet Θ, Γ are assigned with additional charge β from an extra $U(1)$ symmetry group. This $U(1)$ generator commutes with all supercharges $Q_A, \widetilde{Q}^A$. So linear symmetry group for this $\mathcal{N}_G = 4$ super-gravity theory is $SU(4)_R \otimes U(1)_R \otimes U(1)$.

Generally, the linear symmetry group for $0 < \mathcal{N}_G < 4$ super-gravity theories that coupled to matter super-multiplet is $SU(\mathcal{N}_G)_R \otimes U(1)_R \otimes U(1)$. The total charge of particle state can be obtained by adding all α, β, γ charges corresponding to $SU(\mathcal{N}_G)_R$ indices and hidden indices that specifying the state. The total charge of amplitude should be conserved, and if it is non-zero, the amplitude will vanish. So non-vanishing amplitudes should not violate $SU(\mathcal{N}_G)_R$ symmetry, as well as preserving $U(1)_R \otimes U(1)$ charge. Invariance of $SU(\mathcal{N}_G)$ symmetry requires each $SU(\mathcal{N}_G)_R$ index appear the same number of times, and invariance of $U(1)_R \otimes U(1)$ constrains the amplitude in the hidden indices, which originate from $SU(8)_R$ indices.

We will show some examples to illustrate the violation of symmetry groups by considering component super-gravity amplitudes of $(\mathcal{N}_G = 4) = (\mathcal{N} = 2) \times (\widetilde{\mathcal{N}} = 2)$. Firstly consider amplitude of graviton coupled to two scalars, where the scalars are taken from $\Theta^{\mathcal{N}_G=4}_{vector}$ and $\Gamma^{\mathcal{N}_G=4}_{vector}$ super-fields. They are denoted by ϕ_1 of charge 2α and R-index (34)56, ϕ_2 of charge β and R-index 12(34), ϕ_3 of charge -2α and R-index 12(78), ϕ_4 of charge $-\beta$ and R-index 56(78). The MHV gravity amplitude

$$M_n^{\mathcal{N}_G=2}(\phi_i, \phi_j, h^-, h^+, \ldots, h^+) \tag{2.67}$$

can be computed from KLT relations. The non-vanishing amplitudes

$$M_n^{\mathcal{N}_G=4}(\phi_1, \phi_3, h^-, h^+, \ldots, h^+)\ , \quad M_n^{\mathcal{N}_G=4}(\phi_2, \phi_4, h^-, h^+, \ldots, h^+) \tag{2.68}$$

can be explained as preservation of $SU(4)_R$ symmetry since Grassmann variable monomial associated to these amplitudes

$$\eta_{1,1}\eta_{1,2}\eta_{2,5}\eta_{2,6}\eta_{3,1}\eta_{3,2}\eta_{3,5}\eta_{3,6}$$

do have the same number of each index, as well as preservation of $U(1)_R \times U(1)$ symmetry since charge is zero.

Vanishing amplitudes

$$\begin{aligned} &M_n^{\mathcal{N}_G=4}(\phi_1, \phi_1, h^-, h^+, \ldots, h^+)\ , \quad M_n^{\mathcal{N}_G=4}(\phi_2, \phi_2, h^-, h^+, \ldots, h^+)\ , \\ &M_n^{\mathcal{N}_G=4}(\phi_3, \phi_3, h^-, h^+, \ldots, h^+)\ , \quad M_n^{\mathcal{N}_G=4}(\phi_4, \phi_4, h^-, h^+, \ldots, h^+) \end{aligned} \tag{2.69}$$

$\mathcal{N}_G$	$\widetilde{\mathcal{N}} \otimes \mathcal{N}$	Number of states for component fields					Linear symmetry group from KLT product
		2	3/2	1	1/2	0	
8	$4 \otimes 4$	1	8	28	56	70	$SU(8)_R$
7	$4 \otimes 3$	1	7+1	21+7	35+21	35+35	$SU(8)_R$
6	$3 \otimes 3$	1	6+1+1	15+6+6+1	20+15+15+6	15+20+20+15	$SU(8)_R$
6	$4 \otimes 2$	1	6	15+1	20+6	15+15	$U(6)_R$
5	$3 \otimes 2$	1	5+1	10+5+1	10+10+5+1	5+10+10+5	$U(6)_R$
5	$4 \otimes 1$	1	5	10	10+1	5+5	$U(5)_R$
4	$3 \otimes 1$	1	4+1	6+4	4+6+1	1+4+4+1	$U(5)_R$
4	$4 \otimes 0$	1	4	6	4	1+1	$U(4)_R$
3	$3 \otimes 0$	1	3+1	3+3	1+3	1+1	$U(4)_R$
4	$2 \otimes 2$	1	4	6+1+1	4+4+4	1+6+6+1	$U(4)_R \otimes U(1)$
3	$2 \otimes 1$	1	3	3+1	1+3+1	3+3	$U(3)_R \otimes U(1)$
2	$2 \otimes 0$	1	2	1+1	2	1+1	$U(2)_R \otimes U(1)$
2	$1 \otimes 1$	1	2	1	1+1	2+2	$U(2)_R \otimes U(1)$
1	$1 \otimes 0$	1	1	0	1	1+1	$U(1)_R \otimes U(1)$
0	$0 \otimes 0$	1	0	0	0	1+1	$U(1)$

Table 2.2: Field contents of super-gravity theories that are allowed by super-KLT-relations, and their invariant linear symmetry groups. They are also listed in [98].

can be explained as violation of $SU(4)_R$ symmetry as well as $U(1)_R \otimes U(1)$ symmetry. Vanishing amplitudes

$$M_n^{\mathcal{N}_G=4}(\phi_1, \phi_2, h^-, h^+, \dots, h^+) \ , \quad M_n^{\mathcal{N}_G=4}(\phi_3, \phi_4, h^-, h^+, \dots, h^+) \ , \tag{2.70}$$

can be explained as violation of $U(1)_R \otimes U(1)$ symmetry, although $SU(4)_R$ symmetry is preserved. Vanishing amplitudes

$$M_n^{\mathcal{N}_G=4}(\phi_1, \phi_4, h^-, h^+, \dots, h^+) \ , \quad M_n^{\mathcal{N}_G=4}(\phi_2, \phi_3, h^-, h^+, \dots, h^+) \tag{2.71}$$

can be explained as violation of $SU(4)_R$ symmetry, although $U(1)_R \otimes U(1)$ symmetry is preserved.

$U(1)_R$ symmetry and $U(1)$ symmetry can also be violated individually. This can be shown by considering amplitudes of graviton coupled to two graviphoton. We have v_2^- with charge $(4\alpha + \beta)$ and v_1^- with charge $(0 - \beta)$. The amplitude

$$M_n^{\mathcal{N}_G=4}(v_1^-, v_1^-, h^-, h^+, \dots, h^+) \tag{2.72}$$

does not violate $SU(4)_R$ symmetry, and also preserves $U(1)_R$ symmetry. However, $U(1)$ charge is $-2\beta \neq 0$. So it vanishes by violating $U(1)$ symmetry. Also amplitude

$$M_n^{\mathcal{N}_G=4}(v_1^-, v_2^-, h^-, h^+, \dots, h^+) \tag{2.73}$$

does not violate $SU(4)_R$ symmetry and preserves $U(1)$ symmetry. However, $U(1)_R$ charge is $4\alpha \neq 0$. So it vanishes by violating $U(1)_R$ symmetry.

When $\mathcal{N}_G = 1$, the invariant linear symmetry group $SU(\mathcal{N}_G)_R \otimes U(1)_R \otimes U(1)$ reduces to $U(1)_R \otimes U(1)$, since $SU(1)$ is just an identity. When $\mathcal{N}_G = 0$, there is no rotation invariance for η, so the linear symmetry group further reduces to $U(1)$.

The field contents, particle states and linear symmetry groups for all super-gravity theories that constructed from KLT products are summarized in Table (2.2).

Chapter 3

Loop amplitude computation and Algebraic geometry method

This chapter describes general knowledge for multi-loop amplitude computation. It includes traditional methods for 1-loop amplitude computation as well as very recent methods for amplitude computation beyond 1-loop. Properties and relations of tree amplitudes, traditional reduction procedure and (generalized) unitarity cut methods are briefly introduced. Computational algebraic geometry is intensively used in integrand reduction of recent multi-loop amplitude computation, so we devote one section on the basics of algebraic geometry. In the language of algebraic geometry, we introduce systematic algorithms for integrand reduction. Details of these algorithms will be implemented in next two chapters, where algebraic systems from some multi-loop amplitudes are studied.

3.1 Integral and integrand of loop amplitude

3.1.1 Integral representations

The integral of loop amplitude is an integration over phase-space of loop momenta, with integrand coming from terms of local interactions N_{local} and non-local propagators $1/q^2$. Terms of local interactions can be generated naively from Feynman diagrams, and they include all information of color structure, kinematics and particle states, etc. The behavior of Feynman diagram, explicitly expressed in integral representations, is fully encoded in the mathematical structure of integrals. Generally, n-point L-loop amplitude in d-dimension can be expressed as an integration over L independent d-dimensional loop momenta ℓ^μ, thus degrees of freedom to be integrated out are Ld. To get the full amplitude, we need to sum over all L-loop Feynman graphs(FGs) with n external legs. For each graph, the denominator of integrand is products of propagators coming from all internal lines. The propagators $D_i \equiv q_i^2$ are functions of independent loop momenta ℓ and external momenta p, in the form

$$D_i = (\sum_{k=1}^{L} a_{i,k}\ell_k + \sum_{k'=1}^{n} b_{i,k'}p_{k'})^2 \ .$$

The coefficients $a_{i,k}, b_{i,k'}$ could be $+1, -1$ or 0 depending on the way these momenta appearing in propagators. However, the rank of loop momenta in one propagator is no higher than 2, thus we have three types of terms $\ell_i \cdot \ell_j$, $\ell_i \cdot p_j$ and $p_i \cdot p_j$ in D_i. In the Feynman diagram approach, we use off-shell Feynman rules to build all terms in the integral. It is worth to mention that the local numerators N_{local} of integrand can be obtained from on-shell method without touching off-shell information. The on-shell information generated from (generalized) unitarity cuts then provides an efficient resource for constructing integrand and kinematic factors.

The set of all L-loop Feynman diagrams with n-external legs is somehow a very ambiguous terminology. For example, we can always input an identity q^2/q^2 in the integrand. While the numerator q^2 can be included in N_{local} without changing locality, the denominator q^2 provides an extra propagator for the graph. Reversely, terms of $\ell \cdot p$ in local numerator can be expressed as function of propagators, which will cancel the corresponding propagator. So in order to uniquely define a representation for integral, we should specify the way of determining graphs that to be included in the summation. Two integral representations are frequently used. One representation insists to use graphs F_3 that containing only cubic vertex. The loop amplitude

$$A_n^{(L)} = \sum_{k \in F_3} \int \frac{\prod_{i=1}^{L} d^d\ell_i}{(2\pi)^{Ld}} \frac{C_k N_k}{D_{k_1} D_{k_2} \cdots D_{k_{n+3L-3}}} \tag{3.1}$$

has maximal number of propagators $(n+3L-3)$ for all graphs. In this way graphs can be drawn without ambiguity. The local numerator N_{local} can be sorted into two parts. The kinematic part N_k contains kinematic information and the color part C_k packs all color information. It is always possible to do so if particles are in the adjoint representation of gauge group. The color structure of cubic vertex is the structure constant f^{abc}, and by addressing color structures from all cubic vertices we define the unique color factor C_i for the graph. The quartic vertex that usually appears in gauge theory is associated with color structures $f^{abe}f^{ecd}$. However we can add it to corresponding cubic graph of $q^2 = (p_i^a + p_j^b)^2$ channel by rewriting it as $f^{abe}f^{ecd}q^2/q^2$. The color factor for k-th graph is then given by

$$C_k = \prod_{j \in V_k} f^{a_{j_1} a_{j_2} a_{j_3}} \ , \tag{3.2}$$

where V_k is the set of all cubic vertices in k-th graph. The kinematic part N_k is a function of external and internal momenta, and depends on details of external states, such as polarizations, helicities, spinor, ect. When treating it as polynomial function of loop momenta ℓ, the renormalization requirement will constrain the highest degree of ℓ in the polynomial, i.e., the degree of loop momenta in numerator should less than the degree of loop momenta in denominator of integrand. In above integral representation, the number of propagators for each graph is too large, so that constraints from renormalization requirement is quite over-estimated. We can also constrain N_k by dimensional analysis. Assuming each momentum has dimension 1, then the dimension of n-point 4-dimensional gauge theory amplitude is $4-n$. In the right hand side of expression (3.1), we see that the integral measure has dimension $4L$, while the denominator of integrand has dimension $2(n+3L-3)$, then dimension $dim[N_k]$ of N_k should satisfy

$$4-n = 4L + dim[N_k] - 2(n+3L-3) \ .$$

Thus we have $dim[N_k] = n+2L-2$. N_k is polynomial function of Lorentz invariant scalar products with monomial of the form $(\ell^2)(\ell\cdot p)\cdots$. $dim(N_i)$ should be distributed between external and internal momenta, so the highest degree for loop momenta is $n+2L-2$. Then kinematic part of numerator can be expanded as polynomial with finite terms as

$$N_k = \sum_{i=0}^{n+2L-2} f_i(\ell^i) \ . \tag{3.3}$$

Note that N_k can also be treated as polynomials or rational functions of external kinematic variables if necessary. Since loop momenta in integrand will disappear after loop integration, sometimes it is more convenient to take N_k as function of external kinematic variables, so that treatments on N_k will not depend on the integration.

There also exists another more traditional integral representation. Different from previous integral representation that factorizes color and kinematic information in each graph, this representation separates the color part totally from integral based on trace structures of group generators. It can be expressed as

$$A_n^{(L)} = \sum_J G_J \sum_{k \in FG} R_{k,J} \int \frac{\prod_{i=1}^L d^d\ell_i}{(2\pi)^{Ld}} \frac{N_{k,J}}{D_{k_1} D_{k_2} \cdots D_{k_m}} \ . \tag{3.4}$$

G_J is the color factor that packing all color information. The summation of J is over all possible trace structures of gauge group. So it is an expansion of full amplitude into partial amplitudes based on trace structures. Since trace structure of gauge group generators determines the color-ordering, the integral inside the second summation of (3.4) can be identified as color-ordered partial amplitude. The second summation includes all n-point L-loop Feynman graphs with color-ordering striped, and $R_{k,J}$ are rational functions of external momenta, $N_{k,J}$ are polynomials of independent loop momenta. The set FG is still not uniquely defined here, but since there is no color information contained in the second summation, we can freely rewrite the numerator when and cancel propagators in denominator as much as possible. Systematic reduction methods have been developed, and we can reduce the number of propagator to no more than Ld. For example 1-loop 4-dimensional gauge theory can at most have 4 propagators, which correspond to bubble, triangle and box integral respectively. We will explain the color part and color-striped part of (3.4) in detail in following section, since it is an important integral representation for practical computation.

3.1.2 The color-ordered amplitudes and non-trivial relations

To illustrate trace structures of full amplitude, it is better to start with some examples. It is well know that tree-level n-point gluon amplitude can be expanded according to single trace structures[13, 99, 100] as

$$A_n^{tree-full}(\{k_i,\lambda_i,a_i\}) = g^{n-2}\sum_{\sigma\in S_n/Z_n}\mathrm{Tr}(T^{a_{\sigma_1}}\cdots T^{a_{\sigma_n}})A_n(k_{\sigma_1}^{\lambda_{\sigma_1}},\ldots,k_{\sigma_n}^{\lambda_{\sigma_n}})\ , \tag{3.5}$$

where k_i,λ_i,a_i are respectively momentum, helicity and color index of i-th external gluon. We will abbreviate $k_i^{\lambda_i}$ as i for simplicity. S_n/Z_n is the set of permutation S_n of n points subtracting cyclic permutation Z_n of n points, which represents cyclic permutation invariance of n particles. The partial amplitudes A_n are color-ordered. There are many non-trivial relations that relating different partial amplitudes, so that the independent amplitudes can be reduced significantly. The cyclic permutation invariance S_n/Z_n reduces the number of independent amplitudes to $(n-1)!$. Explicitly, from group structures, there is reflection relation(also called color-reversed relation since it reverses color ordering)

$$A_n(1,2,\ldots,n) = (-1)^n A_n(n,\ldots,2,1)\ , \tag{3.6}$$

cyclic relation

$$A_n = (1,2,\ldots,n) = A_n(2,3,\ldots,n,1)\ , \tag{3.7}$$

and KK-relation[16]

$$A_n(1,\alpha,n,\beta) = (-)^{n_\beta} \sum_{\sigma\in\mathcal{OP}\{\alpha\}\cup\{\beta^T\}} A_n(1,\sigma,n) \ , \tag{3.8}$$

where n_β is the number of β-set and ordered permutation $\mathcal{OP}$ is the set of all permutations on set $\alpha \bigcup \beta^T$ while preserving relative ordering in each set α and β^T. The KK-relation reduces the number of independent partial amplitudes to $(n-2)!$. A special case of KK-relation is the $U(1)$ decoupling relation. When set β only contains one element, we can get

$$\sum_{\sigma\in\mathcal{OP}\{2,3,\ldots,n-1\}\cup\{n\}} A_n(1,\sigma) = 0 \ . \tag{3.9}$$

This is an identity among $(n-1)$ partial amplitudes.

For loop amplitude, trace structures are more complicated. For example, n-point 1-loop amplitude can be expanded as[101]

$$\begin{aligned} &A_n^{1-loop-full}(\{k_i,\lambda_i,a_i\}) = \\ &\sum_J n_J \sum_{m=0}^{\lfloor n/2 \rfloor} \sum_{\sigma\in S_n/S_{n;m}} \mathrm{Gr}_{n-m,m}(\sigma)\ A^{[J]}_{n-m,m}(\sigma_1,\sigma_2,\ldots,\sigma_{n-m};\sigma_{n-m+1},\ldots,\sigma_n) \ , \end{aligned} \tag{3.10}$$

where we have taken gauge group as $U(N_c)$. If gauge group is $SU(N_c)$, terms of traces that containing single generator will disappear in the expansion. $\lfloor x \rfloor$ is the largest integer less than or equal to x, and n_J is the number of particles of spin J. The color factor G_J in (3.4) is denoted as $\mathrm{Gr}_{m_1,m_2}, m_1+m_2=n$, with two subscripts since there are double trace structures. All kinematic information in (3.4) is packed into color-ordered partial amplitude $A_{m_1,m_2}, m_1+m_2=n$, where m_1, m_2 are numbers of legs that associated with corresponding generators in each trace respectively. $S_{n,m}$ is a subset of permutation S_n that keeping $\mathrm{Gr}_{n-m,m}$ invariant. Explicitly, $\mathrm{Gr}_{n-m,m}$ can be written as(we abbreviate generator T^a as a)

$$\mathrm{Gr}_{n-m,m} = \mathrm{Tr}\left(a_1,\cdots,a_{n-m}\right)\, \mathrm{Tr}\left(a_{n-m+1},\cdots,a_n\right) \ .$$

If $m=0$, there is only single trace structure

$$\mathrm{Gr}_{n,0} = N_c \mathrm{Tr}\left(a_1,\cdots,a_n\right) \ ,$$

and the kinematic coefficients associated to these single trace structures are primitive partial amplitudes $A_{n,0}$. For $m\neq 0$, there is double trace structure, and partial amplitudes $A_{n-m,m}, m\neq 0$ are more difficult to evaluate. However, there are non-trivial relations that relating all partial amplitudes to primitive partial amplitudes. They can be expressed as

$$A_{n-m,m}(\alpha_1,\alpha_2,\ldots,\alpha_{n-m};\beta_1,\ldots,\beta_m) \;=\; (-1)^m \sum_{\sigma\in\mathcal{COP}\{\alpha\}\bigcup\{\beta^T\}} A_{n,0}(\sigma)\;, \tag{3.11}$$

where $\mathcal{COP}\{\alpha\}\bigcup\{\beta^T\}$ is subset of permutations S_n on $\{\alpha,\beta^T\}$ while preserving cyclic ordering of each set α or β^T. Thus 1-loop primitive partial amplitudes are enough to produce full 1-loop amplitudes. Relation (3.11) is similar to KK-relation of tree amplitudes. Similar reflection relation and cyclic relation also exist for 1-loop partial amplitudes. The reflection relation is given by

$$A_{n-m,m}(1,\ldots,m;m+1,\ldots,n) = (-1)^n A_{n-m,m}(m,\ldots,1;n,\ldots,m+1)\;, \tag{3.12}$$

and cyclic relation is given by

$$A_{n-m,m}(1,\ldots,m;m+1,\ldots,n) = A_{n-m,m}(\sigma(1,\ldots,m);\sigma(m+1,\ldots,n))\;, \tag{3.13}$$

where $\sigma(\alpha)$ is cyclic permutation of set α. The number of independent primitive partial amplitudes will be reduced when applying these non-trivial relations.

Expansion of 2-loop full amplitude based on trace structures can be written as

$$\begin{aligned} &A_n^{2-loop-full} = \\ &\sum_{\sigma\in S_n/Z_n} N_c^2\mathrm{Tr}(\sigma_1,\ldots,\sigma_n)\left(A^{LC}_{n,0,0}(\sigma_1,\ldots,\sigma_n)+\frac{1}{N_c^2}A^{SC}_{n,0,0}(\sigma_1,\ldots,\sigma_n)\right)\\ &+\sum_{m=1}^{\lfloor n/2\rfloor}\sum_{\sigma\in S_n/S_{n-m,m}} N_c\mathrm{Tr}(\sigma_1,\ldots,\sigma_m)\mathrm{Tr}(\sigma_{m+1},\ldots,\sigma_n)A_{n-m,m,0}(\sigma_1,\ldots,\sigma_m;\sigma_{m+1},\ldots,\sigma_n)\\ &+\sum_{a=1}^{\lfloor n/3\rfloor}\sum_{(b-a)=a}^{\lfloor (n-a)/2\rfloor}\sum_{\sigma\in S_n/S_{a,b-a,n-b}} \mathrm{Tr}(\alpha)\mathrm{Tr}(\beta)\mathrm{Tr}(\gamma)A_{a,b-a,n-b}(\alpha;\beta;\gamma)\;, \end{aligned} \tag{3.14}$$

where again gauge group is taken to be $U(N_c)$. Sets $\alpha=\{\sigma_1,\ldots,\sigma_a\}$, $\beta=\{\sigma_{a+1},\ldots,\sigma_b\}$ and $\gamma=\{\sigma_{b+1},\ldots,\sigma_n\}$. $S_{n-m,n}$ and $S_{n-b,b-a,a}$ are subsets of permutation S_n while keeping double trace and triple trace invariant respectively. We have four types of trace structures, the triple trace structure $\mathrm{Tr}(\alpha)\mathrm{Tr}(\beta)\mathrm{Tr}(\gamma)$, the double trace structure $N_c\mathrm{Tr}(\alpha)\mathrm{Tr}(\beta)$, and two single trace structures $N_c^2\mathrm{Tr}(\alpha)$, $\mathrm{Tr}(\alpha)$. The new single trace structure $\mathrm{Tr}(\alpha)$ does not contain N_c factor, and this is a consequence of non-planar graphs for 2-loop amplitude. Not much non-trivial relations for 2-loop partial amplitudes $A_{a,b-a,n-b}$ are known as tree and 1-loop partial amplitudes. Of course we still have reflection relation

$$\begin{aligned} &A_{a,b-a,n-b}(1,\ldots,a;a+1,\ldots,b;b+1,\ldots,n) \\ &\qquad = (-)^n A_{a,b-a,n-b}(a,\ldots,1;b,\ldots,a+1,n,\ldots,b+1) \ , \end{aligned} \tag{3.15}$$

and cyclic relation

$$\begin{aligned} &A_{a,b-a,n-b}(1,\ldots,a;a+1,\ldots,b;b+1,\ldots,n) \\ &\qquad = A_{a,b-a,n-b}(\sigma(1,\ldots,a);\sigma(a+1,\ldots,b);\sigma(b+1,\ldots,n)) \ . \end{aligned} \tag{3.16}$$

More non-trivial relations are explored, but restrict to some examples. For example, 4-point 2-loop partial amplitudes, except $A^{SC}_{n,0,0}$, can be expanded as linear combination of $A^{LC}_{n,0,0}$ and other two double trace partial amplitudes. For 2-loop A^{SC}_{n} partial amplitudes, the same KK-relation as tree amplitudes is valid up to $n = 7$ points[102]. More studies could be done on relations of loop partial amplitudes.

This full amplitude expansion based on trace structures can be systematically generalized to L loop, while $(L+1)$-fold trace structure will appear. The explicit expression is very tedious, and various trace structures could exist, corresponding to planar and non-planar graphs. Theoretically, we can explore non-trivial relations from group constraints. Relations of all loop $4, 5$ and 6-point partial amplitudes of $SU(N)_c$ gauge group have been written down, and we are still waiting for relations of general n-point L-loop partial amplitudes from solving group constraints[103–105].

We described two integral representations. They are mainly used in different situations. Representation (3.1) is ideal for BCJ conjecture[27, 28] of constructing gravity amplitude. For an integral representation where Yang-Mills amplitude can be expanded into graphs with only cubic vertex, if numerator factor N_k of each graph follows the same Jacobi identity as color factor C_k, then gravity amplitude can be obtained as square of two Yang-Mills amplitudes using numerator $N_k, \widetilde{N}_k$ as

$$M_n^{(L)} = \sum_{k\in F_3} \int \frac{\prod_{i=1}^L d^d\ell_i}{(2\pi)^{Ld}} \frac{N_k \widetilde{N}_k}{D_{k_1} D_{k_2} \cdots D_{k_{n+3L-3}}} \ , \tag{3.17}$$

where $N_k, \widetilde{N}_k$ are kinematic factors of two Yang-Mills amplitudes that satisfying

$$N_{k_1} + N_{k_2} = N_{k_3}, \widetilde{N}_{k_1} + \widetilde{N}_{k_2} = \widetilde{N}_{k_3}$$

if

$$C_{k_1} + C_{k_2} = C_{k_3}, \widetilde{C}_{k_1} + \widetilde{C}_{k_2} = \widetilde{C}_{k_3} \ .$$

This conjecture is extremely useful for calculating loop-level gravity amplitude, different from KLT relation that is only valid for tree amplitude. Representation (3.4), instead, is an ideal tool to evaluate Yang-Mills multi-loop amplitude. Since color structures have already been separated, we can focus on kinematic part. After computing color-ordered partial amplitudes, we can assemble them into full amplitude with help of trace information. Thanks to the non-trivial relations and many other methods, the independent amplitudes that need to be computed are not as much as naive counting. In following chapters, we will discuss the computation of multi-loop Yang-Mills amplitudes. So we will take this integral representation of Feynman diagrams.

3.2 Integral reduction of loop amplitude

3.2.1 The traditional reduction procedure

Let us return to integral representation (3.4). What we are really interested in is the kinematic part, given by the integral

$$\int \frac{\prod_{i=1}^{L} d^d\ell_i}{(2\pi)^{Ld}} \frac{N}{D_1 D_2 \cdots D_m} , \tag{3.18}$$

where we have chosen integral of one graph. Remind that the loop momentum dependence in numerator N takes the form $\ell^2, \ell_i \cdot \ell_j$ and $\ell \cdot p$. There are also tensor structures ℓ^μ, $\ell^\mu \ell^\nu$ and so on. The number of propagators in denominator depends on the graph considered. However, before performing integration, simplification can be taken with above integrand. This simplification can reduce the number of propagators.

Let us take 1-loop amplitude as example. The integral we want to reduce is

$$\int \frac{d^d\ell}{(2\pi)^d} \frac{N}{D_0 D_1 \cdots D_{m-1}} , \tag{3.19}$$

where we redefined propagator indices for convenience. The traditional reduction procedure, such as Passarino-Veltman reduction[106], can reduce the integral to master integrals with rational coefficients. The master integrals are independent integrals that used to expand any other integrals. In one-loop case, they are defined from scalar integrals. The n-point scalar integral is defined as

$$I_n^{scalar}[1] \equiv \int \frac{d^d\ell}{(2\pi)^d} \frac{1}{(\ell^2 - M_0^2)((\ell - p_1)^2 - M_1^2) \cdots ((\ell - p_1 - \cdots - p_{n-1})^2 - M_{n-1}^2)} ,$$

where M_i is the mass of corresponding loop momentum, p_i is external momentum.

The reduction procedure intends to eliminate loop momentum dependence in numerator N step by step, and finally ends up with minimal number of scalar integrals. The first step is to reduce integral of arbitrary N and $m \geq 5$ propagators. Among these propagators, we can select one propagator $D_0 = \ell^2 - M_0^2$ and other four $D_i = (\ell^2 - P_i)^2 - M_i^2$ from remaining propagators. P_i is the corresponding external momenta in propagator D_i, and we can rename the four selected ones as $P_i, i = 1,2,3,4$. Then each ℓ^2 in N can be replaced by $D_0 + M_0^2$. D_0 cancels a propagator, while M_0^2 goes to the scalar part. Since external momenta are 4-dimensional, they can be expanded by $P_i, i = 1,2,3,4$ using Gram determinant defined as

$$G\begin{pmatrix} p_1,\ldots,p_l \\ p'_1,\ldots,p'_l \end{pmatrix} \equiv \det(\Delta^{ij}) \ , \tag{3.20}$$

$$G(p_1,\ldots,p_l) \equiv G\begin{pmatrix} p_1,\ldots,p_l \\ p_1,\ldots,p_l \end{pmatrix} \ , \tag{3.21}$$

where Gram matrix Δ^{ij} is $l \times l$ matrix with element $\Delta^{ij} = 2p_i \cdot p'_j$ in (i,j)-th position. So Gram determinant is a function of Lorentz invariant scalar products. If either $(p_1,\ldots,p_l)$ or $(p'_1,\ldots,p'_l)$ is linearly dependent, it vanishes. Then any 4-dimensional momentum P_k can be expanded as

$$\begin{aligned} P_k^\mu \;=\; & \frac{1}{G(P_1,P_2,P_3,P_4)}\Big[G\begin{pmatrix} P_k,P_2,P_3,P_4 \\ P_1,P_2,P_3,P_4 \end{pmatrix} P_1^\mu + G\begin{pmatrix} P_1,P_k,P_3,P_4 \\ P_1,P_2,P_3,P_4 \end{pmatrix} P_2^\mu \\ & + G\begin{pmatrix} P_1,P_2,P_k,P_4 \\ P_1,P_2,P_3,P_4 \end{pmatrix} P_2^\mu + G\begin{pmatrix} P_1,P_2,P_3,P_k \\ P_1,P_2,P_3,P_4 \end{pmatrix} P_4^\mu\Big] \ . \end{aligned} \tag{3.22}$$

In this way, all scalar products of the form $\ell \cdot P_k$ in N can be expanded as $\ell \cdot P_i, i = 1,2,3,4$. Then we can use

$$D_i - D_0 = -2\ell \cdot P_i + P_i^2 + M_0^2 - M_i^2 \tag{3.23}$$

to replace $\ell \cdot P_i$. Again D_0, D_i cancel corresponding propagators in denominator, and remaining terms P_i^2, M_0^2, M_i^2 go to scalar part. Repeatingly doing so, we reduce the integral to two types. One type is scalar integral with arbitrary number of propagators, and the other type is integral with $m \leq 4$ propagators, but still contains loop momentum dependence numerator.

The second step is to eliminate loop momentum dependence in latter type. Assume that after momentum redefinition, we get an integral with propagators $D_0 = \ell^2 - M_0^2$ and $D_i = (\ell - P_i)^2 - M_i^2, i \leq 3$, where $D_i, i = 0,1,2,3$ have been renewed and not the same as in previous step. The loop momentum dependence in numerator is $\ell^2, \ell \cdot P_i$ as well as tensor structures $\ell^\mu, \ell^\mu\ell^\nu, \cdots$. It is a little tedious to get rid of tensor structures, especially when the rank is high. The idea to eliminate tensor structures is that, loop momentum ℓ^μ should be constructed from external momenta $p_1, \ldots, p_{n-1}$, so integral could be expanded as series of external momenta with same tensor structures. For example, integral with ℓ^μ dependence should be expanded as

$$I_m[\ell^\mu] = \int \frac{d^d\ell}{(2\pi)^d} \frac{\ell^\mu}{(\ell^2 - M_0^2)\cdots((\ell - P_{m-1})^2 - M_{m-1}^2)} = \sum_{i=1}^{m-1} C_i p_i^\mu \ , \tag{3.24}$$

where external momentum $p_i = P_i - P_{i-1}$, and expansion coefficients C_i could be linear combination of scalar integrals. By contracting both sides with $p_{j,\mu}, j = 1, \ldots, m-1$, we get an equation for each j as

$$\int \frac{d^d\ell}{(2\pi)^d} \frac{\ell \cdot p_j}{(\ell^2 - M_0^2)\cdots((\ell - P_{m-1})^2 - M_{m-1}^2)} = \sum_{i=1}^{m-1} \frac{1}{2} C_i \Delta^{ij} \ . \tag{3.25}$$

The left hand side can be reduced to scalar integrals by (3.23), so we get an algebraic linear system of $(m-1)$ equations. By solving these equations we get $(m-1)$ coefficients C_i represented as linear combinations of scalar integrals. So integrals with tensor structures ℓ^μ are reduced to scalar integrals. Similarly, for tensor structures $\ell^\mu\ell^\nu$, we can expand them to $C_{00}g^{\mu\nu} + \sum_{ij} C_{ij} p_i^\mu p_j^\nu$, and by contracting with $g_{\mu\nu}, p_{i,\mu}p_{j,\nu}$ we can get sufficient linear equations to solve coefficients C_{ij}. Although computation will become very tedious for integrals with higher rank tensor structures, the reduction procedure is still the same, and we will end up with all scalar integrals.

The last step is to reduce any n-point scalar integrals $I_n[1]$ to finite number of scalar integrals. For scalar integrals with $n \geq 6$, we can always find non-trivial solution for following 5 equations

$$\sum_{i=1}^{n} \beta_i = 0 \ , \ \sum_{i=1}^{n} \beta_i P_i^\mu = 0 \ , \ \mu = 0, 1, 2, 3 \ . \tag{3.26}$$

With this non-trivial solution, we have an identity

$$\sum_{i=1}^{n} \beta_i D_i = \sum_{i=1}^{n} (\beta_i \ell^2 - 2\ell_\mu \cdot (\beta_i P_i^\mu) + \beta_i P_i^2 - \beta_i M_i^2) = \sum_i \beta_i (P_i^2 - M_i^2) \ . \tag{3.27}$$

Thus we can add an unity $(\sum_i \beta_i D_i)/(\sum_i \beta_i (P_i^2 - M^2))$ to integrand. The factor D_i cancels corresponding propagator while P_i^2, M^2 can be absorbed into scalar part. One thing we need to pay attention to is the scalar pentagon integral $I_5[1]$. In dimensional regularization using $d = 4 - 2\epsilon$, if keeping all expansion orders of ϵ, scalar pentagon integral is an independent master integral. While restricted to $\mathcal{O}(\epsilon^0)$ order, scalar pentagon can be further reduced to four scalar boxes.

3.2.2 One-loop integral reduction and integral basis

From above reduction procedure, we can reduce arbitrary 1-loop integral to master integrals[107, 108], and all kinematic factors are packed into rational coefficients. Formally, the integral reduction can be expressed as

$$A^{1-loop} = \sum_{k=1}^{n} c_{k,i}(\epsilon) I_k^{d,(i)}[1] \ , \tag{3.28}$$

where $n = 4$ for 4-dimensional theory and $n = 5$ for $d = (4 - 2\epsilon)$-dimensional theory. The superscript (i) specifies external momenta configuration, which could be massive or massless leading to different IR behaviors. For 4-dimensional theory, independent master integrals of box integral $I_4[1]$ are

$$\{I_4^{4m}, I_4^{3m}, I_4^{2m,e}, I_4^{2m,h}, I_4^{m}, I_4^{0m}\} \ , \tag{3.29}$$

where the number of m denotes the number of massive external momenta. The two-mass-easy integral $I_4^{2m,e}$ has massive momenta diagonally opposite and two-mass-hard integral $I_4^{2m,h}$ has massive momenta adjacent. Similarly, for triangle integral $I_3[1]$, the independent master integrals are

$$\{I_3^{3m}, I_3^{2m}, I_3^{m}\} \ . \tag{3.30}$$

Zero-mass triangle integral is not allowed since kinematics of three massless momenta do not have real solution. For scalar bubble and tadpole, external momenta are required to be massive, so we only have master integrals I_2, I_1.

The coefficients $c_{k,i}$ in (3.28) are rational functions of external momenta and polarization vectors as well as dimensional regularization parameter ϵ. In practical computation, it is better to use another equivalent expression

$$A^{1-loop} = \sum_{k=1}^{n} c_{k,i}(\epsilon = 0) I_k^{d,(i)}[1] + (\text{rational part}) + \mathcal{O}(\epsilon) \ . \tag{3.31}$$

The coefficients do not have ϵ dependence any more, while extra rational part appears in compensation. The part expanded by master integrals is cut-constructible, since it can be reconstructed by unitarity cut method. Theoretically, if we start reduction procedure directly for integral expression from Feynman diagrams and collect all scalar kinematic factors in every step during the reduction, it is possible to keep all information of rational coefficients $c_{n,i}$ of master integrals. But the reduction procedure is so involved that it is not suggested to do so. Since master integrals are well understood, and coefficients of master integrals can be accessed by unitarity cut method, it is much easer to recover coefficients $c_{n,i}$ by studying unitarity cuts on both sides of (3.31), as far as for theories which are cut-constructible. The unitarity cut method will be introduced in next section.

3.2.3 Discussion on multi-loop integral reduction

One would expect that similar reduction should be valid for higher loop amplitudes, but it is not exactly true. Schematically, multi-loop amplitude still can be expanded into master integrals as

$$A^{L-loop} = \sum_{k,i,j} c_{k,i} I_k^{(i)}[N_j] \ , \tag{3.32}$$

where k is the number of propagators of master integrals, i specifies external momenta configuration and j specifies numerator of integrand. The master integrals are no longer scalar integrals, so it becomes a problem to determine independent numerators appearing in master integrals.

For 4-dimensional 2-loop amplitude, it is possible to reduce the number of propagators to 8, but the numerator can not be reduced to only scalars. This is because not all loop momentum dependence in numerator can be written as (3.23). Thus after reduction, we still get integrals with non-trivial numerators. These integrals should further be reduced by other methods, such as IBP method. For example[39], after reduction, 4-point 2-loop double-box integral takes the form

$$I_4^{2-loop}[(\ell_1\cdot p_4)^a(\ell_2\cdot p_1)^b] = \int \frac{d^4\ell_1 d^4\ell_2}{(2\pi)^8}\frac{(\ell_1\cdot p_4)^a(\ell_2\cdot p_1)^b}{D_0D_1D_2\widetilde{D}_0\widetilde{D}_1\widetilde{D}_2\widehat{D}_0} \ , \tag{3.33}$$

where external momenta are $p_i, i=1,2,3,4$. D_i are propagators containing only ℓ_1, $\widetilde{D}_i$ are propagators containing only ℓ_2, $\widehat{D}_0$ is propagator containing both ℓ_1,ℓ_2. There are 22 choices of (a,b) such that integrals can not be reduced any further. However, by using non-trivial IBP relations, these 22 integrals can be further reduced to master integrals depending on external kinematics. For kinematics of zero-mass, one-mass, two-mass with massive momenta adjacent along the long side, or two-mass with massive momenta diagonal opposite, two master integrals $I_4^{2-loop}[1]$ and $I_4^{2-loop}[\ell_2\cdot p_1]$ are enough to expand the amplitude. For kinematics of two-mass with massive momenta adjacent along the short side or three-mass, we need another one $I_4^{2-loop}[\ell_1\cdot p_4]$ besides previous two master integrals. For four-mass case, we need even one more master integral $I_4^{2-loop}[(\ell_1\cdot p_4)(\ell_2\cdot p_1)]$. In fact, generating these IBP relations is highly non-trivial and time consuming, even though there are a lot of computer packages to do so. Especially for diagrams without apparent symmetry on Feynman graphs, it is almost impossible to perform any practical computation. Another weakness of higher loop integral reduction is that, in (3.31), we assume the explicit results of master integrals $I_k[1]$ are known, so that we can compute coefficients of master integrals by unitarity cut method. The computation of 1-loop master integrals is relatively simple, but computation of general multi-loop master integrals is not trivial.

The integral reduction of 1-loop amplitude is very successful, but not of multi-loop amplitude. In order to simplify multi-loop amplitude computation, we can reduce the integrand before doing integration. Instead of master integrals, we get a set of integrand basis. Then further manipulation can be done to get master integrals from these integrand basis. The computational algebraic geometry method can be introduced to multi-loop amplitude computation, and systematically determine integrand basis. We will describe this method after a brief introduction of algebraic geometry.

3.3 Unitarity cut and generalized unitarity cut

3.3.1 Unitarity cut in 4-dimension and d-dimension

Direct computation of loop amplitude is always very difficult, and this motives us to find indirect methods. The unitarity cut method[101, 109] has been proven to be very efficient when applying to 1-loop amplitude computation. Standard unitarity cut method uses double-cut, which cuts two propagators of 1-loop amplitude to divide it into two tree amplitudes. The double-cut of 1-loop amplitude has very clear physical meaning. When expanding S-matrix as $S = 1 + iT$ with trivial scattering part 1 and interaction matrix T, unitarity condition of S-matrix $S^\dagger S = 1$ implies that $2\mathrm{Im}T = T^\dagger T$. This means the imaginary part of 1-loop amplitude is related to product of two tree-amplitudes. In fact, unitarity cut computes the discontinuity across branch cut singularity of loop amplitude. Effectively, two propagators become on-shell. If loop momenta are 4-dimension, double-cut of two propagators can be expressed mathematically as

$$\frac{1}{\ell_1^2 \ell_2^2} \sim \delta(\ell_1^2)\delta(\ell_2^2) \ , \tag{3.34}$$

where ℓ_1, ℓ_2 are momenta of propagators. For 1-loop amplitude, the discontinuity is given by

$$\Delta A^{1-loop} \equiv \int d^4\ell_1 d^4\ell_2 \delta^{(4)}(\ell_2 - \ell_1 - P)\delta^{(+)}(\ell_1^2)\delta^{(+)}(\ell_2^2) A_L^{tree} \times A_R^{tree} \ , \tag{3.35}$$

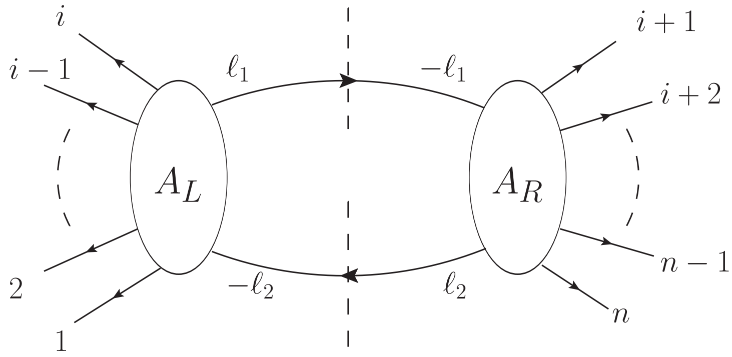

FIGURE 3.1: Standard unitarity cut of one-loop amplitude. The double-cut cuts two propagators, and divide one-loop amplitude to two tree amplitudes.

where two propagators ℓ_1, ℓ_2 are cut, and P is the total momenta in left hand side of double-cut as shown in Figure (3.1). The (+) superscript in delta function denotes the choice of a positive energy solution of $\ell_i^2 = 0$. The delta function of momentum conservation makes one integration over ℓ_1 or ℓ_2 trivial, so it is really 4-dimensional integration. A_L, A_R are tree amplitudes in both sides of double-cut, with two additional legs from on-shell propagators,

$$A_L^{tree} = A_{i+2}(-\ell_2, 1, \ldots, i, \ell_1) \ , \ A_R^{tree} = A_{n-i+2}(-\ell_1, i+1, \ldots, n, \ell_2) \ . \tag{3.36}$$

Of course we should sum over all helicity states of ℓ_1, ℓ_2. The loop momentum ℓ is taken to be on-shell solution of $\ell_1^2 = 0, \ell_2^2 = 0$. Since all momenta are on-shell in unitarity cut, we still have well-defined on-shell tree-amplitudes. Loop momentum has four degrees of freedom, two delta functions can freeze two degrees of freedom, thus there are still two degrees of freedom to be integrated out.

If loop momentum is $d = (4 - 2\epsilon)$-dimension, we should use d-dimensional unitarity cut[110, 111]. The loop momentum ℓ can be decomposed as

$$\ell^{(d)} = \ell^{(4)} + \mu \ ,$$

where μ is a vector in (-2ϵ)-dimension, and $\ell^{(4)}$ is normal 4-dimensional massive vector with $(\ell^{(d)})^2 = (\ell^{(4)})^2 - \mu^2 = 0$. The massive 4-dimensional loop momentum $\ell^{(4)}$ can further be decomposed to massless four vector as

$$\ell^{(4)} = \ell + zP \ ,$$

where $\ell^2 = 0$, z is a free parameter and P is the cut momentum. In this way, the integration measure changes to

$$\int d^{4-2\epsilon}\ell^{(d)} = \int d^{-2\epsilon}\mu \int d^4\ell^{(4)} = \int dz \int d^4\ell\delta(\ell^2)(2\ell\cdot P)\ , \tag{3.37}$$

It separates integration to integral over mass parameter μ and integral over massive scalar. The latter can further be separated to integral over massless scalar and integral over free parameter z. The discontinuity of d-dimensional 1-loop amplitude in d-dimensional unitarity cut is then given by

$$\Delta A^{d,1-loop} \equiv \int d^{-2\epsilon}\mu \int dz\ d^4\ell(2\ell\cdot P)\delta(\ell^2)\delta^{(+)}((\ell_1^{(d)})^2)\delta^{(+)}((\ell_2^{(d)})^2)A_L^{tree}\times A_R^{tree}\ , \tag{3.38}$$

where $(\ell_i^{(d)})^2 = (\ell^{(4)} - P_i)^2 - \mu^2$. Integration over z can be firstly performed by one delta function, and remaining integrations usually can be transferred to contour integration in complex plane.

In spinor-helicity formalism, massless loop momentum can be expressed as spinor variables $\ell = t|\ell\rangle|\ell]$, where t is an auxiliary free parameter. So integration measure expressed with spinor variables has the form

$$\int d^4\ell\delta^+(\ell^2) = \oint_{\widetilde{\lambda}_\ell=\bar{\lambda}_\ell} \langle\ell\ d\ell\rangle\,[\ell\ d\ell] \int t\ dt\ . \tag{3.39}$$

The contour of spinor variable integration is the line along real loop momentum in complex plane, and integration over t is a trivial integration over delta function of propagators[112]. Then using tree-level amplitudes in spinor-helicity formalism, the contour integration in fact is the computation of residues in complex plane.

3.3.2 Generalized unitarity cut

Unitarity of S-matrix ensures that loop amplitude can be constructed from summation of products of sub-loop and tree amplitudes satisfying cut constraints. Although standard unitarity cut of 1-loop amplitude has clear physical meaning as discontinuity crossing branch cut, this physical explanation has no significant importance in practical computation. We can generalize standard unitarity cut to generalized unitarity cut[113, 114], where more than two propagators are cut. Though losing its physical explanation, it still provides constraints on loop amplitudes. With these constraints, part of the information of loop amplitude can be explored. Mathematically, n-ple unitarity cut will set n propagators on-shell, thus provide n delta functions for integral. Loop amplitude is then divided into many sub-amplitudes, which could be lower-loop amplitudes and tree amplitudes. Especially, the maximal unitarity cut will cut all internal propagators, and express loop amplitude as products of only tree amplitudes. This idea can be applied to any n-point L-loop amplitudes.

Suppose we have a 4-dimensional n-point L-loop integral with m propagators

$$A_n^{(L)} = \int \frac{\prod_{i=1}^{L} d^4\ell_i}{(2\pi)^{4L}} \frac{N}{D_0 D_1 \cdots D_{m-1}} \ . \tag{3.40}$$

Then maximal unitarity cut of this integral provides m equations

$$D_i = 0 \ , \ i = 0, 1, \ldots, m-1 \ . \tag{3.41}$$

Loop momenta are constrained by these equations. We can also have near-maximal unitarity cut, which is defined by cutting $(m-1)$ propagators. This gives a constraint of $(m-1)$ equations for loop momenta, which is more relax than constraint of maximal unitarity cut. The fewer propagators being cut, the more information of loop amplitude we get. But it is harder to separate contributions from other graphs when fewer propagators are being cut. The maximal unitarity cut, though can only access fewest information of loop amplitude, is the simplest. It can be served as a guidance for determining multi-loop amplitude. It becomes even more powerful in the computation of 4-dimensional 1-loop $\mathcal{N} = 4$ super-Yang-Mills amplitude, since only box contribution exists for this theory, and maximal unitarity cut can access all information. It gives constraints of four equations, and loop momentum is totally determined by the solution of four equations. So such amplitude is trivially expressed as summation over products of four tree-amplitudes and all possible internal states.

3.3.3 One-loop amplitude computation with unitarity cut

For 1-loop amplitude, what we want to compute is the expansion coefficients $c_{k,i}$ in (3.31). By applying standard unitarity cut (3.35, 3.38) or generalized unitarity cut on both sides of (3.31) and comparing results on both sides, we can separate contributions for coefficients from different master integrals(For a review see [38]). It is already sufficient to extract all information of cut-constructible part by standard unitarity cut, but it is more convenient to start from maximal unitarity cut. Explicitly, the (generalized) unitarity cut on n-point 1-loop amplitude gives

$$\Delta A^{1-loop} = \sum_{k=2}^{4} c_{k,i}(\epsilon = 0) \Delta I_k^{(i)}[1] \ . \tag{3.42}$$

Here we take 4-dimensional theory as example, and assume no internal mass. So pentagon and tadpole master integrals do not contribute. If we use maximal unitarity cut,

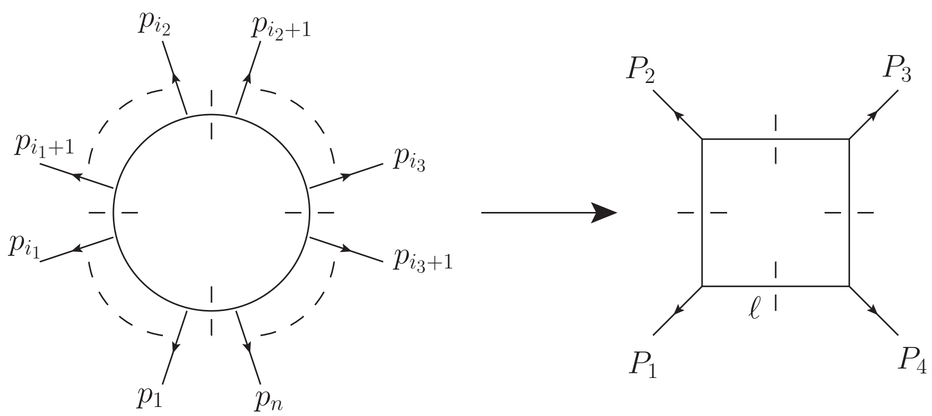

FIGURE 3.2: Quadruple-cut of one-loop amplitude. A specific quadruple-cut of any one-loop integral selects contribution of a specific box integral.

which is quadruple-cut, then only box integrals have non-vanishing results in the right hand side of (3.42). Triangle and bubble integrals do not have corresponding quadruple-cut channels, so they do not contribute in maximal unitarity cut. Integral in left hand side of (3.42) contains $n-1$ propagators which directly generated from Feynman diagram. When cutting four propagators, n external momenta are split to four parts, which we define as $P_1 = p_1 + \cdots + p_{i_1}$, $P_2 = p_{i_1+1} + \cdots + p_{i_2}$, $P_3 = p_{i_2+1} + \cdots + p_{i_3}$, $P_4 = p_{i_3+1} + \cdots + p_n$. This is equivalent to box integral with four external momenta P_1, P_2, P_3, P_4, as shown in Figure (3.2). So one quadruple-cut selects one specific box integral $I_4^{(i)}[1]$,

$$\Delta_4 A^{1-loop} = c_{4,i}(P_1,P_2,P_3,P_4)\Delta_4 I_4^{(i)}[1](P_1,P_2,P_3,P_4) \ . \tag{3.43}$$

Then coefficient of this master integral is simply given by

$$\begin{aligned} c_{4,i}(P_1,P_2,P_3,P_4) \quad = \quad & \frac{1}{2}\sum_{h_i,h'_i}\sum_{\ell\in\mathcal{S}} A_1^{tree}(-\ell_1^{h_1},P_1,\ell_2^{h'_2})A_2^{tree}(-\ell_2^{h_2},P_2,\ell_3^{h'_3}) \\ & \times A_3^{tree}(-\ell_3^{h_3},P_3,\ell_4^{h'_4})A_4^{tree}(-\ell_4^{h_4},P_4,\ell_1^{h'_1}) \ , \end{aligned} \tag{3.44}$$

where $\mathcal{S}$ is the solution of equations

$$\ell_1^2 = \ell^2 = 0 \ \ , \ \ \ell_2^2 = (\ell - P_1)^2 = 0 \ \ , \ \ \ell_3^2 = (\ell - P_1 - P_2)^2 = 0 \ \ , \ \ \ell_4^2 = (\ell + P_4)^2 = 0 \ \ .$$

There are exactly two solutions, and they fix loop momentum at two points in complex plane. By this way, we can get coefficients for all box master integrals by applying all possible quadruple-cut.

We can further get coefficients of triangle integrals with triple-cut. There are two difference of triple-cut from quadruple-cut, which makes triple-cut not as simple as quadruple-cut. The first difference is that triple-cut does not only receive contributions from triangle integrals, but also from box integrals which have the same cut propagators as triangle integrals. For example, if a triple-cut specifies a triangle integral $I_3(P_1, P_2, P_3)$, then box integrals $I_4(P_{11}, P_{12}, P_2, P_3)$, $I_4(P_1, P_{21}, P_{22}, P_3)$ and $I_4(P_1, P_2, P_{31}, P_{32})$, where $P_{i1} + P_{i2} = P_i$, also contribute to the coefficients. We should extract box contributions in order to get correct triangle coefficients. The second difference is that constraints of three equations can only freeze three degrees of freedom of loop momentum. So there is an one-dimensional integration left. Fortunately, we can use this degree of freedom to identify contributions from box and triangle integrals. This can be done with Forde's parametrization[51] of loop momentum for massless propagators. Explicitly, using two massive external momenta P_1, P_2, we can construct

$$(P_1 - xP_2)^2 = 0 \quad , \quad (P_2 - x'P_1)^2 = 0 \ , \tag{3.45}$$

with solutions

$$x_\pm = \frac{(P_1 \cdot P_2) \pm \sqrt{(P_1 \cdot P_2)^2 - P_1^2 P_2^2}}{P_2^2} \quad , \quad x'_\pm = \frac{(P_1 \cdot P_2) \pm \sqrt{(P_1 \cdot P_2)^2 - P_1^2 P_2^2}}{P_1^2} \ . \tag{3.46}$$

So we can define two null vectors, normalized as

$$P_1^\flat = \frac{P_1 - (P_1^2/\gamma)P_2}{1 - (P_1^2 P_2^2/\gamma^2)} \quad , \quad P_2^\flat = \frac{P_2 - (P_2^2/\gamma)P_1}{1 - (P_1^2 P_2^2/\gamma^2)} \ , \tag{3.47}$$

with

$$\gamma_\pm = x_\pm P_2^2 = x'_\pm P_1^2 = (P_1 \cdot P_2) \pm \sqrt{(P_1 \cdot P_2)^2 - P_1^2 P_2^2} \ . \tag{3.48}$$

This defines the flat basis $P_1^\flat, P_2^\flat$. Note that if one of P_1, P_2 is massless, we can still construct two null vectors, but with only one solution x or x'. With flat basis $P_1^\flat, P_2^\flat$, loop momentum can be parameterized as

$$\ell = \alpha_1 |P_1^\flat\rangle |P_1^\flat] + \alpha_2 |P_2^\flat\rangle |P_2^\flat] + \frac{t}{2} |P_1^\flat\rangle |P_2^\flat] + \frac{\alpha_1 \alpha_2}{2t} |P_2^\flat\rangle |P_1^\flat] \ , \tag{3.49}$$

where

$$\alpha_1 = \frac{P_2^2(\gamma - P_1^2)}{\gamma^2 - P_1^2 P_2^2} \quad , \quad \alpha_2 = \frac{P_1^2(\gamma - P_2^2)}{\gamma^2 - P_1^2 P_2^2} \ . \tag{3.50}$$

This parametrization automatically satisfies constraints of three equations

$$\ell^2 = 0 \quad , \quad (\ell - P_1)^2 = 0 \quad , \quad (\ell + P_2)^2 = 0 \ , \tag{3.51}$$

and t is the free parameter characterizing remaining degree of freedom. Box integral behaves differently from triangle integral after substituting this parametrization back to products of tree amplitudes from triple-cut. Since it contains an additional propagator, there are two poles in t. These poles can be removed by expanding the result around point $t=\infty$, and such expansion gives a polynomial in t as

$$[\mathrm{Inf}_t A_1^{tree}A_2^{tree}A_3^{tree}](t)=\sum_{i=0}^{m} f_i t^i\ . \tag{3.52}$$

The triangle coefficient is given by the first term as

$$-[\mathrm{Inf}_t A_1^{tree}A_2^{tree}A_3^{tree}](t)|_{t\to 0}\ . \tag{3.53}$$

Since γ has up to two solutions, the result is actually averaged over solutions of γ.

Remaining coefficients are then bubble coefficients, which are not accessed by quadruple-cut and triple-cut. Similarly, we can get correct bubble coefficients by double-cut after subtracting box and triangle contributions. The loop momentum is parameterized as

$$\ell=y|P_1^{\flat}\rangle|P_1^{\flat}]+\frac{P_1^2}{\gamma}(1-y)|\chi\rangle|\chi]+\frac{t}{2}|P_1^{\flat}\rangle|\chi]+\frac{P_1^2}{2\gamma}\frac{y}{t}(1-y)|\chi\rangle|P_1^{\flat}]\ , \tag{3.54}$$

which automatically satisfies constraints of two equations. Note that there is only one $P_i=P_1$, we should choose another arbitrary external momentum to construct massless momentum basis $P_1^{\flat},\chi$. The bubble coefficient is then given by

$$-i[\mathrm{Inf}_t[\mathrm{Inf}_y A_1^{tree}A_2^{tree}](y)](t)|_{t\to 0,y^m\to\frac{1}{m+1}}-\frac{1}{2}\sum_{\mathcal{S}_{tri}}[\mathrm{Inf}_t A_1^{tree}A_2^{tree}A_3^{tree}](t)|_{t^j\to T(j)}\ , \tag{3.55}$$

where $\mathcal{S}_{tri}$ is set of all triple-cuts by cutting one more propagator besides double-cut, and $T(j)$ is some defining equations[51].

3.3.4 Discussion on multi-loop amplitude computation

For general multi-loop amplitude, there is no systematic way of extracting coefficients of different master integrals as for 1-loop amplitude. One reason is that, master integrals of general multi-loop amplitude are in fact unknown. So we do not even have a practical expansion formula as (3.31). Also the algebraic system of cut equations for multi-loop amplitude is far more complicated than equations of one-loop amplitude. So we could not expect a successful application of unitarity cut method on multi-loop amplitude as 1-loop amplitude.

In order to access as much information as possible of multi-loop amplitude, we can (1) compute all possible maximal unitarity cuts of multi-loop amplitude, and collect all information, including residue dependence if maximal cut does not totally freeze loop momenta, (2) use information of maximal cut to propose an ansatz, (3) compute near-maximal unitarity cut, and compare result with the ansatz. If there is difference, correct the ansatz to incorporate the difference, (4) continue computation of k-ple cut until there is no difference between the ansatz and $(k+1)$-ple cut. In the worst case, this procedure will stop at the fewest number of cuts, where most information of loop amplitude are extracted.

While it is too difficult to study master integrals of multi-loop amplitude, we can instead study integrand basis as first step. The integrand basis can be systematically studied by computational algebraic geometry method. We will describe the method, shortly after an introduction of basic algebraic geometry.

3.4 The algebraic geometry

3.4.1 Variety and ideal

Algebraic geometry is the study of algebraic varieties[115–118]. The *variety* is defined to be the zero locus of a polynomial or many polynomials. In other words, it is the solution space of polynomial equations. There are two basic categories of algebraic variety, the affine variety and projective variety.

The affine variety can be defined through a family of polynomials $F = (f_1, \ldots, f_r)$. Suppose we have r polynomials $f_i, i = 1, \ldots, r$ in polynomial ring $k[X_1, \ldots, X_n]$, where *polynomial ring* is the set of polynomials of n variables $(X_1, \ldots, X_n)$ with coefficients in the field k, which can be taken as real numbers $\mathbb{R}$, complex numbers $\mathbb{C}$, integers $\mathbb{Z}$, etc. For example, polynomial ring of one variable $k[X]$ is the set of polynomials P of the form

$$P = c_0 + c_1 X + c_2 X^2 + \cdots + c_m X^m \ , \tag{3.56}$$

where coefficients c_i are elements of k. The polynomial ring in n variables $(X_1, \ldots, X_n)$ is more complicated, and we should use monomial instead of one variable. The *monomial* is defined as product of n variable in the form

$$X^\alpha = \prod_{i=1}^{n} X_i^{\alpha_i} \ , \tag{3.57}$$

where $\alpha = (\alpha_1, \alpha_2, \ldots, \alpha_n)$ with non-negative integers α_i is the *multi-degree* of monomial. The *degree of monomial* is $|\alpha| = \sum_{i=1}^{n} \alpha_i$. Polynomial ring $k[X_1, X_2, \ldots, X_n]$ is then defined as the set of polynomials

$$P = \sum_{\alpha} c_\alpha X^\alpha \ , \tag{3.58}$$

where $c_\alpha \equiv c_{\alpha_1 \cdots \alpha_n} \in k$. Then polynomial equations

$$\begin{aligned} &f_1(X_1, X_2, \ldots, X_n) = 0 \ , \\ &f_2(X_1, X_2, \ldots, X_n) = 0 \ , \\ &\ldots \\ &f_r(X_1, X_2, \ldots, X_n) = 0 \end{aligned}$$

define an algebraic subset of affine space k^n. If this algebraic subset is irreducible, it defines the *affine algebraic variety* $V(F)$. The variety is associated with geometric objects such as curve, hypersurface, etc. For example, $f(X_1, X_2) = X_1 + X_2 = 0$ defines a line in $\mathbb{R}^2$-plane if $k = \mathbb{R}$.

More generally, if degrees of all polynomials $f_i, i = 1, \ldots, r$ are one, we get the linear affine variety, i.e., lines, planes, etc. We can also get affine variety of plane curve if degrees of polynomials are two. For example,

$$f(X_1, X_2) = a_1 X_1^2 + a_2 X_2^2 + a_3 X_1 X_2 + a_4 X_1 + a_5 X_2 + a_6 = 0 \ ,$$

when $k = \mathbb{R}$, defines a conics. Of course, curves of any degree exist, and the complexity of studying variety increases a lot as increasing of degree. There is a kind of curve called *rational curve*, which can be rational parameterized. For example, if plane curve C defined by $f(X, Y) = 0$ is rational curve, then we can always find two rational functions $\alpha(T), \beta(T)$ to parameterize the curve with identity $f(\alpha(T), \beta(T)) = 0$ holds. It is important to know the curve is rational or not, in order to determine if we could find some rational parametrization for it.

The *projective variety* is defined in projective space. In projective space, polynomial has homogeneous coordinates. For polynomial $P \in k[X_1, \ldots, X_n]$, the homogeneous polynomial can be defined as

$$P'(X'_0, X'_1, \ldots, X'_n) \equiv (X'_0)^{degree\ of\ P} P(\frac{X'_1}{X'_0}, \ldots, \frac{X'_n}{X'_0}) \ , \tag{3.59}$$

with homogeneous coordinates $(X'_0, X'_1, \ldots, X'_n)$ defined through $X_i = X'_i / X'_0$. For example, consider a polynomial $P \in \mathbb{C}[X_1, X_2]$ with the form $P = X_1 X_2 + X_1 + 1$. This is a complex curve in $\mathbb{C}^2$-plane, and the degree of P is two. In projective space $\mathbb{CP}^2$, we introduce new coordinates X'_0, X'_1, X'_2, and define $X_1 = X'_1/X'_0, X_2 = X'_2/X'_0$. Then homogeneous polynomial of P is given by

$$P'(X'_0, X'_1, X'_2) = (X'_0)^2(\frac{X'_1}{X'_0}\frac{X'_2}{X'_0} + \frac{X'_1}{X'_0} + 1) = X'_1X'_2 + X'_1X'_0 + X'_0X'_0 \ ,$$

with each monomial of homogeneous degree two.

The projective variety is defined through a family of homogeneous polynomials $F' = (f'_1, \ldots, f'_r)$ in polynomial ring $k[X'_0, X'_1, \ldots, X'_n]$. It is a subset of projective n-space $\mathbb{P}^n$ over k, defined through the zero locus of homogeneous polynomial equations

$$\begin{aligned} &f'_1(X'_0, X'_1, \ldots, X'_n) = 0 \ , \\ &f'_2(X'_0, X'_1, \ldots, X'_n) = 0 \ , \\ &\ldots \\ &f'_r(X'_0, X'_1, \ldots, X'_n) = 0 \ . \end{aligned}$$

If the projective algebraic set is irreducible, then it is called projective variety.

The *irreducibility* is an important property of variety. The algebraic set is not always irreducible. For example, algebraic set defined by $f = X_1X_2 = 0$ where $f \in \mathbb{R}[X_1, X_2]$ is the union of two irreducible varieties, i.e, the coordinate axes $X = 0$ and $Y = 0$. We can study the irreducibility of a variety with *ideal*. Let A be a polynomial ring $k[X_1, \ldots, X_n]$, and $F = (f_1, \ldots, f_r)$ a subset of A, then the ideal $I(F)$ generated by F is defined as

$$I(F) = \{a_1f_1 + \cdots + a_rf_r | \forall a_i \in A\} \ . \tag{3.60}$$

The definition for projective algebraic set is similar, and homogeneous polynomials F' generate a homogeneous ideal $I'(F')$. Polynomial equations $F = 0$ imply that every element in $I(F)$ is also zero. Solving equations $F = 0$ is equivalent to solving all polynomial equations from ideal $I(F)$. The algebraic set defined by $F = 0$ is then equivalent to the algebraic set $Z(I)$ from solving all polynomial equations in $I(F)$. Note that intersection of finite ideals is also an ideal. Denote the intersection of two ideals as $I_1 \bigcap I_2$, then the algebraic set

$$Z(I_1 \bigcap I_2) = Z(I_1) \bigcup Z(I_2) \ . \tag{3.61}$$

The union of two ideals $I_1 \bigcup I_2$ is not necessary an ideal. The algebraic set

$$Z(I_1 \bigcup I_2) = Z(I_1) \bigcap Z(I_2) \tag{3.62}$$

could be empty if there is no solution for polynomial equations $a_i = 0$, $b_i = 0$, $a_i \in I_1$, $b_i \in I_2$. It is more convenient to study ideal $I(F)$ and algebraic set $Z(I)$ than original equations. If the algebraic set $Z(I)$ is irreducible, it defines a variety, and the ideal is *prime ideal*, which means that the ideal can not be non-trivially written as $I = I_1 \bigcap I_2$. If ideal is not prime ideal, there is a method *primary decomposition of an ideal*, which can decompose the ideal into intersection of many prime ideals. Especially, if the polynomial ring is Noetherian ring, Lasker-Noether theorem states that primary decomposition of ideal I uniquely exists

$$I = \bigcap_{a=1}^{s} I_a \ , \tag{3.63}$$

where s is a finite integer, and each I_a is prime ideal. Then the algebraic set

$$Z(I) = \bigcup_{a=1}^{s} Z(I_a) \tag{3.64}$$

with each $Z(I_a)$ a variety. So in order to determine if an algebraic set defined by $F = 0$ is irreducible or not, we can generate the ideal $I(F)$, and apply primary decomposition method on $I(F)$. If there are more than one prime ideals $I_i(F_i), i > 1$ produced by primary decomposition, then the algebraic set is reducible. The number of prime ideals by primary decomposition is the number of irreducible varieties of algebraic set. The variety $Z(F_i)$ of $F_i = 0$ obtained by primary decomposition is equivalent to the i-th irreducible variety of original algebraic set.

To determine if a polynomial $P \in k[X_1, \ldots, X_n]$ is in the ideal $I(F), F \subset k[X_1, \ldots, X_n]$ or not, we need to do the *polynomial division*. For multivariate polynomial division, naively we would expect that after defining the monomial order, we can get a result by recursively performing $P/f_1, \cdots, P/f_r$ as

$$P = a_1 f_1 + \cdots + a_r f_r + R \ , \tag{3.65}$$

where $a_i \in k[X_1, \ldots, X_n]$, and R is the remainder. If $R = 0$, then $P \in I(F)$. But above procedure is not true for arbitrary $F = (f_1, \ldots, f_r)$. In fact, polynomial division can be applied only when F is *Gröbner basis*. The Gröbner basis $G(F) = (g_1, \ldots, g_{r'})$ can be generated from F by algebraic geometry method, and it is a subset of polynomial ring $k[X_1, \ldots, X_n]$ equivalent to F. Recursively performing the division $P/g_1, \cdots, P/g_{r'}$, we get a result

$$P = a_1 g_1 + \cdots + a_r g_{r'} + R \ , \tag{3.66}$$

where $a_i \in k[X_1, \ldots, X_n]$. The coefficients a_i is not uniquely determined but the remainder R is unique. So if $R = 0$, polynomial P is an element of ideal $I(F)$.

Special attention should be paid to the *monomial order*. For single variable polynomial $f \in k[X]$, it is natural to define ordering $1 \prec X \prec X^2 \prec \cdots$ without any ambiguities. But for multivariate polynomial, there is more than one way of defining monomial order. The monomial order will change explicit results of Gröbner basis and polynomial division. In (3.66), we mentioned that R is uniquely determined. But this is true only for one chosen Gröbner basis. Since explicit result of $G(F)$ depends on the monomial order, if $G(F)$ changes, then remainder R also changes, although different remainders are linearly related. In order to make consistent computation, we should choose a monomial order and use it through the whole computation.

3.4.2 The curve

Polynomials equations $F = (f_1, \ldots, f_r) = 0$, where $F \subset \mathbb{C}[X_1, \ldots, X_n]$, define algebraic set of complex objects. Geometrically, this algebraic set could be complex curve, hypersurface, or even more complicated complex manifold. For the special case where $r = n - 1$, there is only one free complex parameter, and the algebraic set is complex curve. Complex curve is intensively studied by mathematicians. Properties of complex curve are characterized by its topology, and the topology is described by *genus* of the curve. For irreducible algebraic set, i.e., variety, there are two kinds of genus, the *arithmetic genus* and *geometric genus*. The geometric genus, which geometrically illustrated as the handles of complex curve, is topological invariant. It characterizes the topology of curve. This invariance is *birational* invariance, which means that geometric genus is invariant under rational re-parametrization. The arithmetic genus however is not topological invariant, and it depends on the parametrization of complex curve.

The *arithmetic genus* of a complex curve C can be computed by Riemann-Roch theorem. Let C be a projective curve in projective space $\mathbb{P}^n$. Define polynomial ring $S = k[X_0, \ldots, X_n]$ and quotient ring $A = S/I(C)$, where $I(C)$ is ideal of C. Then the Euler characteristic is defined as $\chi(\mathcal{O}_C(n)) = h^0\mathcal{O}_C(n) - h^1\mathcal{O}_C(n)$ for all integer n. The $\mathcal{O}_C$ is the *sheaf* of quotient ring A, and the number h^i are zero for all $i \geq 2$ since C is dimension one of field k. The Riemann-Roch theorem states that for projective curve C of degree d and arithmetic genus g, we have

$$h^0\mathcal{O}_C(n) - h^1\mathcal{O}_C(n) = nd + 1 - g \ . \tag{3.67}$$

Moreover, for large n, we have $h^0\mathcal{O}_C(n) = nd + 1 - g$.

Especially, there is the *algebraic plane curve*, which is the set of zero locus of a polynomial with two variables. The *affine plane curve* can be defined by variety of polynomial equation $f = 0$, where $f \in k[X_1, X_2]$. Similarly, the *projective plane curve* defined in $\mathbb{P}^2$ projective space is the variety $V(f')$ of homogeneous polynomial $f' = 0$, where $f \in k[X'_0, X'_1, X'_2]$. There is a simple expression for arithmetic genus g_A of projective plane curve with homogeneous degree d, given by

$$g_A = \frac{(d-1)(d-2)}{2} \ . \tag{3.68}$$

Of course it is valid for $k = \mathbb{C}$, where we have complex affine plane curve in $\mathbb{C}^2$ and complex projective plane curve in $\mathbb{CP}^2$.

The arithmetic genus g_A not only counts the handles but also the singular points of a curve. A *singular point* of projective curve C is a point $(a_0, a_1, \ldots, a_n)$ such that the rank of Jacobian matrix

$$\left\|\frac{\partial f_i}{\partial X_j}\right\| \ , \quad 1 \le i \le r \ \ , \ \ 0 \le j \le n \tag{3.69}$$

at this point is less than $n-1$. A singular point is *normal* if all tangent lines at the singular point are distinct.

The *geometric genus* g_G can be defined through arithmetic genus g_A and singular points. For a *smooth* curve, i.e., an irreducible projective curve without any singular points, the geometric genus g_G equals to arithmetic genus g_A. There are many algebraic geometry methods to deal with non-smooth projective curve. If all singular points of C are normal singular points, there exists an irreducible projective curve $\widetilde{C}$ from the *normalization* of C, and the geometric genus g_G of C is equal to the arithmetic genus g_A of $\widetilde{C}$. Explicitly, we have

$$g_G \ \ = \ \ g_A - \sum_{p \in \mathrm{Sing}(C)} \frac{1}{2}\mu_p(\mu_p - 1) \ , \tag{3.70}$$

where $Sing(C)$ is the set of all normal singular points p on curve C. μ_p is the *multiplicity* of p, i.e., the number of distinct tangent lines at singular point p. If some singular points are non-normal, there is *blow-up* method that blows up them into normal singular points. Then (3.70) can be modified to compute geometric genus of projective curve.

Curves with geometric genus $g_G = 0$ are rational curves, and curves with geometric genus $g_G = 1$ are elliptic curves. Higher g_G represents more complicated geometric structures. If $k = \mathbb{C}$, the genus has simple topological interpretation. A smooth projective curve is a differentiable variety of dimension one over $\mathbb{C}$ and dimension two over $\mathbb{R}$, thus it is a compact orientable surface. So $g_G = 0$ curve is homeomorphic to a Riemann sphere, and $g_G = 1$ curve to a torus, as well as g_G curve to torus with g_G holes.

The geometric genus g_G is birational invariant, which means that after re-parameterizing curve C_1 to another curve C_2, the geometric genus of C_2 equals to geometric genus of C_1. Re-parametrization of a curve is realized through *birational map*. A *rational map* from variety V_1 to another variety V_2 is defined as a morphism from non-empty open subset U of V_1 to V_2. Concretely, a rational map can be expressed in coordinates using rational functions. A *birational map* from variety V_1 to V_2 is a rational map f from V_1 to V_2 such that there also exists a rational map g from V_2 to V_1 which is inverse to f. gf is an identity map on open set V_1, and fg is an identity map on open set V_2. A birational map induces an isomorphism from a non-empty open subset of V_1 to a non-empty open subset of V_2, and V_1, V_2 are *birational equivalent*.

For complex curves C_1, C_2, if they are birational equivalent, then $g_G(C_1) = g_G(C_2)$. Reversely, if $g_G(C_1) \neq g_G(C_2)$, there is no birational map between C_1 and C_2. Especially, since curve of genus $g_G = 0$ is rational curve and any curves with $g_G > 0$ are not birational equivalent to curve of $g_G = 0$, so there is no rational parametrization for curves of $g_G > 0$.

3.4.3 Examples

Let us consider two polynomials

$$f_1 = yz \quad , \quad f_2 = x^3 + y^3 - xy - z \; , \tag{3.71}$$

defined in polynomial ring $\mathbb{R}[x, y, z]$. f_1 has degree two, and f_2 has degree three. Equation $f_1 = 0$ or $f_2 = 0$ describes a two-dimensional surface in $\mathbb{R}^3$-space. The polynomial equations

$$f_1 = yz = 0 \quad , \quad f_2 = x^3 + y^3 - xy - z = 0 \tag{3.72}$$

define an algebraic subset of affine space $\mathbb{R}^3$. In fact, since they are two equations of three variables, the algebraic subset would describe curve of real dimension one or point of real dimension zero. Geometrically, it is the intersection of two surfaces $f_1 = 0$ and $f_2 = 0$ in $\mathbb{R}^3$.

Let the ideal $I(f_1, f_2)$ be generated from f_1, f_2. Polynomial of the form $a_1 f_1 + a_2 f_2$, where $a_1, a_2 \in \mathbb{R}[x, y, z]$, is an element of $I(f_1, f_2)$. For algebraic system $(f_1 = 0, f_2 = 0)$, each element in $I(f_1, f_2)$ is also zero. So the ideal $I(f_1, f_2)$ is equivalent to algebraic system $(f_1 = 0, f_2 = 0)$.

We can also compute Gröbner basis of ideal I. The result is not unique and depends on monomial order as well as variable ordering when computing by Mathematica. If we choose variable ordering as $\{z, y, x\}$, and also monomial order as *DegreeLexicographic*, then we have

$$G(yz, x^3 - xy + y^3 - z, x^3z - z^2) \equiv G_1(g_1, g_2, g_3) \ . \tag{3.73}$$

If monomial order is *Lexicographic*, we have

$$G(x^3y - xy^2 + y^4, -x^3 + xy - y^3 + z) \equiv G_2(g'_1, g'_2) \ . \tag{3.74}$$

It is clear that they are different.

We can divide any polynomial with Gröbner basis by multivariate polynomial division, or *Polynomial reduce* in Mathematica. For example, dividing $P = x^3y^2 + z^3$ with G_1 in variable ordering $\{x, y, z\}$ and monomial order *Lexicographic*, we get

$$P/G_1 = yg_1 + y^2g_2 + (xy^3 - y^5 + z^3) \ .$$

The remainder $(xy^3 - y^5 + z^3)$ can not be further divided by G_1.

The ideal $I(f_1, f_2)$ is reducible. After *primary decomposition* of ideal I, we get two prime ideals

$$I = I_1 \bigcap I_2 \ \ , \ \ I_1(z, x^3 + y^3 - xy) \ \ , \ \ I_2(y, x^3 - z) \ . \tag{3.75}$$

The algebraic set $Z(I_1)$ or $Z(I_2)$ defines an affine variety $V(I_1)$ or $V(I_2)$. We have

$$Z(I_1 \bigcap I_2) = V(I_1) \bigcup V(I_2) \ . \tag{3.76}$$

For I_1, $Z(I_1)$ is given by solution of

$$z = 0 \ \ , \ \ x^3 + y^3 - xy = 0 \ , \tag{3.77}$$

which is an irreducible plane curve $C_1(x, y)$ in z-plane. For I_2, $Z(I_2)$ is given by solution of

$$y = 0 \ \ , \ \ x^3 - z = 0 \ , \tag{3.78}$$

which is also an irreducible plane curve $C_2(x,z)$ in y-plane. The intersection of two varieties $V(I_1)$, $V(I_2)$ is given by algebraic set $Z(I_1 \bigcup I_2)$

$$Z(I_1 \bigcup I_2) = V(I_1) \bigcap V(I_2) \ , \tag{3.79}$$

by solving equations

$$z = 0 \ \ , \ \ x^3 + y^3 - xy = 0 \ \ , \ \ y = 0 \ \ , \ \ x^3 - z = 0 \ . \tag{3.80}$$

It has a solution $x^3 = 0, y = 0, z = 0$, which is the origin point. This means that two curves C_1, C_2 intersect at origin. Degree of x denotes the multiplicity of solution.

Let us consider affine plane curve $C_1(x,y)$ defined by polynomial function $P(x,y) = x^3 + y^3 - xy = 0$. We can introduce another variable w, and define projective plane curve as

$$P'(x', y', w) = w^3 P(\frac{x'}{w}, \frac{y'}{w}) = (x')^3 + (y')^3 - x'y'w \ . \tag{3.81}$$

It has homogeneous degree three, so arithmetic genus of this plane curve is

$$g_A = (3-1)(3-2)/2 = 1 \ .$$

We can also compute the zero locus of singular points from equations

$$\frac{\partial P'}{\partial x'} = 3(x')^2 - y'w = 0 \ \ , \ \ \frac{\partial P'}{\partial y'} = 3(y')^2 - x'w = 0 \ \ , \ \ \frac{\partial P'}{\partial w} = -x'y' = 0 \ . \tag{3.82}$$

It only has one solution $x' = 0, y' = 0$. By setting $w = 1$, $x = x'$, $y = y'$, and expanding the function at $(x,y) = (0,0)$, we get

$$f(x,y) = x^3 + y^3 - xy \ . \tag{3.83}$$

Tangent line at this singular point is defined by $T(x,y) = -xy = 0$. It has two distinct solutions, the x axis and y axis. So the singular point is normal, and has multiplicity $\mu = 2$. The geometric genus is then $g_G = g_A - 2(2-1)/2 = 0$. It is topologically equivalent to conics, and can be rationally parameterized. One rational parametrization is given by

$$x = \frac{t}{1+t^3} \ \ , \ \ y = \frac{t^2}{1+t^3} \ . \tag{3.84}$$

3.5 Integrand reduction of loop amplitude

Finally we arrive at the section of integrand reduction, especially beyond one-loop amplitude, by computational algebraic geometry method[48, 49]. The 4-dimensional L-loop n-point integral with m propagators is given by

$$I_n^{(L)} = \int \frac{\prod_{i=1}^{L} d^4\ell_i}{(2\pi)^{4L}} \frac{N}{D_0 D_1 \cdots D_{m-1}} \ . \tag{3.85}$$

The number of propagators is constrained by total degrees of freedom of loop momenta. Since each loop momentum is 4-dimensional, L-loop integral has $4L$ degrees of freedom, so the maximal number of propagators should be no larger than $4L$. Otherwise some loop momenta will be over-constrained when applying maximal unitarity cut. Degree of polynomial N is constrained by power counting in order to get UV finite result. Ranks of loop momenta in each monomial of polynomial N should be no larger than ranks of corresponding loop momenta in denominator. This constraint produces a finite but still large set of monomials M_i. We want to get a minimal set of independent monomials from them. The idea is quite simple. Since the denominator is also a polynomial of loop momenta $D(\ell) = D_0 D_1 \cdots D_{m-1}$, we can divide each monomial M_i with denominator. The result is expected to be

$$M_i/D = f_0 D_0 + f_1 D_1 + \cdots + f_{m-1} D_{m-1} + R_i \ , \tag{3.86}$$

where f_i are functions of loop momenta. R_i is the remainder, which is also polynomial of loop momenta. However, we know that the polynomial division can be applied only when polynomial system $(D_0, D_1, \ldots, D_{m-1})$ is Gröbner basis. So we should firstly generate Gröbner basis $G(D) = (g_1, \ldots, g_{m'})$ from polynomials $(D_0, \ldots, D_{m-1})$. The polynomial equations $D_i = 0, i = 1, \ldots, m-1$ can be interpreted as equations of maximal unitarity cut. By dividing monomial M_i with Gröbner basis $G(D)$, we get

$$\frac{M_i}{G(D)} = f'_1 g_1 + \cdots + f'_{m'} g_{m'} + R'_i \ . \tag{3.87}$$

If R'_i is zero, monomial M_i can be expressed as functions of propagators, and it is not independent. If R'_i is non-zero, monomials in remainder R'_i can not be further divided by $G(D)$, so they are independent monomials. These monomials in R'_i define integrand basis. For different Gröbner basis defined from different monomial order and variable ordering, we get different set of integrand basis. But they are equivalent class, and all related by linear transformation.

Above discussion does not rely on the number of external momenta and number of independent loops, so it is quite general and can be applied to integrand induction of any multi-loop amplitudes.

3.5.1 Parametrization of loop momenta

The simple idea above should be implemented systematically in mathematical algorithm by computational algebraic geometry method. The algebraic system is defined by m equations of maximal unitarity cut, where m propagators are polynomials D_i, $i = 0, \ldots, m-1$ defined in polynomial ring $k[X_1, \ldots, X_n]$. Since momenta are taken to be complex, the field $k = \mathbb{C}$. Then the first problem is how to define variables $(X_1, \ldots, X_n)$. These variables come from degrees of freedom of loop momenta. For 4-dimensional L-loop diagram, we have $n = 4L$ variables. A systematic way of defining variables $(X_1, \ldots, X_n)$ is through similar Van Neerven-Vermaseren basis[119]. Expansion of loop momenta with this basis has advantages that the result does not depend on spinor-helicity formalism, and equations of maximal unitarity cut take particular simple form. The momentum basis (e_1, e_2, e_3, e_4) is chosen to be external momenta or ω_j, which are auxiliary momenta perpendicular to all external momenta in momentum basis. If number of external momenta is lager than five, then we can choose arbitrary four external momenta as momentum basis. If number of external momenta is four, then there are only three independent momenta because of momentum conservation. We construct the additional auxiliary momentum ω as $\omega^\mu = \epsilon^{\mu\nu\rho\sigma} P_{1,\nu} P_{2,\rho} P_{3,\sigma}$, where $\epsilon^{\mu\nu\rho\sigma}$ is total anti-symmetric tensor. Then momentum basis is (P_1, P_2, P_3, ω). For three external momenta case, only two independent external momenta P_1, P_2 can be chosen, so we should construct two additional momenta ω_1, ω_2 as

$$\omega_1^\mu = \frac{1}{2}\Big(\Big\langle P_1^\flat | \gamma^\mu | P_2^\flat \Big] + \Big\langle P_2^\flat | \gamma^\mu | P_1^\flat \Big] \Big) \;, \tag{3.88}$$

$$\omega_2^\mu = \frac{i}{2}\Big(\Big\langle P_1^\flat | \gamma^\mu | P_2^\flat \Big] - \Big\langle P_2^\flat | \gamma^\mu | P_1^\flat \Big] \Big) \;, \tag{3.89}$$

with help of flat basis. Then momentum basis can be taken as $(P_1, P_2, \omega_1, \omega_2)$. However, if there are two external momenta, we can only choose one P_1. Then three auxiliary momenta $\omega_1, \omega_2, \omega_3$ should be constructed following conditions $P_1 \cdot \omega_i = 0$, $i = 1, 2, 3$.

Loop momentum ℓ_i can be expanded as

$$\ell_i = (e_1, e_2, e_3, e_4) G_4^{-1} \begin{pmatrix} \ell_i \cdot e_1 \\ \ell_i \cdot e_2 \\ \ell_i \cdot e_3 \\ \ell_i \cdot e_4 \end{pmatrix} \;, \tag{3.90}$$

where $G_4 \equiv G(e_1, e_2, e_3, e_4)$(do not confused with Gröbner basis) is Gram determinant defined in (3.21). When considering $d = 4-2\epsilon$ theory, we can decompose loop momenta $\ell_i^{(d)}$ into 4-dimensional component ℓ_i and mass component $\ell_i^{(-2\epsilon)}$

$$\ell_i^{(d)} = \ell_i + \ell_i^{(-2\epsilon)} , \tag{3.91}$$

and define $\mu_{ij} = -\ell_i^{(-2\epsilon)}\ell_j^{(-2\epsilon)}$. Then we get a set of fundamental scalar products(SPs) as

$$\begin{aligned} \mathcal{SP} &= \{\ell_i \cdot e_j | 1 \le i \le L, 1 \le j \le 4\} \cup \{\mu_{ij} | 1 \le i \le j \le L\} \ , \ d = 4-2\epsilon \ , \\ \mathcal{SP} &= \{\ell_i \cdot e_j | 1 \le i \le L, 1 \le j \le 4\} \ , \ d = 4 \ . \end{aligned} \tag{3.92}$$

These scalar products can be served as variables of algebraic system. Scalar products $\ell_i^2, \ell_i \cdot \ell_j, \ell_i \cdot P_j$ can be expanded as polynomial functions of fundamental scalar products through

$$\begin{aligned} \ell_i \cdot \ell_j &= (\ell_i \cdot e_1, \ell_i \cdot e_2, \ell_i \cdot e_3, \ell_i \cdot e_4) G_4^{-1} \begin{pmatrix} \ell_j \cdot e_1 \\ \ell_j \cdot e_2 \\ \ell_j \cdot e_3 \\ \ell_j \cdot e_4 \end{pmatrix} - \mu_{ij} \ , \\ \ell_i \cdot P_j &= (\ell_i \cdot e_1, \ell_i \cdot e_2, \ell_i \cdot e_3, \ell_i \cdot e_4) G_4^{-1} \begin{pmatrix} P_j \cdot e_1 \\ P_j \cdot e_2 \\ P_j \cdot e_3 \\ P_j \cdot e_4 \end{pmatrix} \ . \end{aligned} \tag{3.93}$$

Then ideal of algebraic system is defined by m equations of maximal unitarity cut $D_i(\mathcal{SP}) = 0$, $i = 1, \ldots, m-1$ in polynomial ring $\mathbb{C}[\mathcal{SP}]$.

A lazy way of defining variables uniformly for all situations is realized by picking two external momenta to construct momentum basis (e_1, e_2, e_3, e_4). It is a direct application of above discussion by always picking two external momenta, no matter how many external legs it has. We can pick two independent momenta P_1, P_2 with $(P_1 + P_2)^2 \neq 0$, and define two null vectors as

$$P_1^{\flat\ \mu} = P_1^\mu - x P_{12}^\mu \equiv \frac{1}{2} \left\langle P_1^\flat | \gamma^\mu | P_1^\flat \right] \ \ , \ \ P_2^{\flat\ \mu} = P_2^\mu - x' P_{12}^\mu \equiv \frac{1}{2} \left\langle P_2^\flat | \gamma^\mu | P_2^\flat \right] \ , \tag{3.94}$$

where x, x' are solutions of $(P_1 - xP_{12})^2 = 0$ and $(P_2 - x'P_{12})^2 = 0$. Then momentum basis can be taken as

$$e_1^\mu = \frac{\langle P_1^\flat | \gamma^\mu | P_1^\flat]}{2\gamma_{12}} \ \ , \ \ e_2^\mu = \frac{\langle P_2^\flat | \gamma^\mu | P_2^\flat]}{2\gamma_{12}} \ \ , \ \ e_3^\mu = \frac{\langle e_1 | \gamma^\mu | e_2]}{2i} \ \ , \ \ e_4^\mu = \frac{\langle e_2 | \gamma^\mu | e_1]}{2i} \ , \tag{3.95}$$

where

$$\gamma_{12}^2 = 2\frac{(P_1P_2)^2 - P_1^2P_2^2}{P_{12}^2} \ . \tag{3.96}$$

The momentum basis satisfies properties that the only non-zero products among them are $e_1e_2 = e_3e_4 = 1$. Definition (3.95) also makes massless limit smoothly, and e_1, e_2 go back to P_1, P_2 respectively when $P_1^2 \to 0$ or $P_2^2 \to 0$.

Loop momenta and external momenta can be expanded into this momentum basis as

$$\ell_i = x_1^i e_1 + x_2^i e_2 + x_3^i e_3 + x_4^i e_3 \ , \tag{3.97}$$

$$P_i = (P_i \cdot e_2)e_1 + (P_i \cdot e_1)e_2 + (P_i \cdot e_4)e_3 + (P_i \cdot e_3)e_4 \ , \tag{3.98}$$

where expansion coefficients x_j^i are variables of algebraic system. The Lorentz invariant scalar products are given by

$$\ell_i \cdot \ell_j = x_1^i x_2^j + x_2^i x_1^j + x_4^i x_3^j + x_3^i x_4^j \ , \tag{3.99}$$

$$\ell_i \cdot P_j = (P_j \cdot e_1)x_1 + (P_j \cdot e_2)x_2 + (P_j \cdot e_3)x_3 + (P_j \cdot e_4)x_4 \ . \tag{3.100}$$

With them we can translate equations of loop momenta to equations of variables x_j^i, $i = 1, \ldots, L$, $j = 1, 2, 3, 4$. The affine ideal is generated by m quadratic polynomials

$$D_i(x_1^1, x_2^1, x_3^1, x_4^1, \ldots, x_1^L, x_2^L, x_3^L, x_4^L) \quad , \quad i = 0, 1, \ldots, m-1 \ ,$$

in polynomial ring

$$\mathbb{C}[x_1^1, x_2^1, x_3^1, x_4^1, \ldots, x_1^L, x_2^L, x_3^L, x_4^L] \ . \tag{3.101}$$

This ideal can be further simplified, since fundamental scalar products are constrained by cut equations. We can systematically define a minimal set of scalar products by Gröbner basis method. Firstly, we generate ideal $I(D)$ from $D = (D_0, \ldots, D_{m-1}) = 0$ in terms of fundamental scalar products $\mathcal{SP}$. Then compute Gröbner basis $G(I)$ of ideal $I(D)$. Remind that we should decide the monomial order and variable ordering, and use them through whole computation. In practical computation with Mathematica, we can set monomial order as *deglex*, since the computation is fast with it. By taking all leading terms $L(G(I))$ in Gröbner basis according to the monomial order, the linear terms in $L(G(I))$ determine a subset of $\mathcal{SP}$ that can be reduced to the complementary of this subset in $\mathcal{SP}$. The scalar products reduced by linear terms in $L(G(I))$ are defined to be reducible scalar products(RSPs), and the remaining scalar products are defined to be irreducible scalar products(ISPs).

This algorithm indeed generates the minimal set of ISPs. To prove this[48], suppose the set of fundamental scalar products is $\mathcal{SP} = (x_1, x_2, \ldots, x_n)$, and the set of RSPs is $(y_1, y_2, \ldots, y_r)$, which is a subset of $\mathcal{SP}$. The remaining scalar products define the set of ISPs $(x'_1, x'_2, \ldots, x'_{r'})$, with $r' + r = n$. The Gröbner basis $G(I)$ must contain a linear polynomial

$$\alpha y_r + \sum_{i=1}^{r'} \beta_i x'_i + \gamma \in I \ , \tag{3.102}$$

where α, β_i, γ are constants and $\alpha \neq 0$. This linear polynomial cannot contain any other y_j, since for given monomial order, y_j is always before y_r when $j < r$. So y_r is a linear function of ISPs on maximal unitarity cut. Consider another linear polynomial

$$\alpha y_{r-1} + \alpha' y_r \sum_{i=1}^{r'} \beta_i x'_i + \gamma \in I \ , \tag{3.103}$$

where α' could be non-zero. y_{r-1} is before y_r in given monomial order since $r - 1 < r$, while no other y_j are contained in this polynomial. We already show that y_r is a linear equation of ISPs, then y_{r-1} is also a linear equation of ISPs. By induction, all y_j are linear equations of ISPs. Furthermore, we can consider x'_j in ISPs. If it can be expressed as linear function of ISPs on maximal unitarity cut, then

$$x'_j - \sum_{i \neq j}^{r'} \beta_i x'_i + \gamma \in I \ . \tag{3.104}$$

In this polynomial, the leading term x'_k is also an ISP. Properties of Gröbner basis ensure that $I(L(I)) = I(L(G(I)))$. So if $x'_k \in L(I)$, then $x'_k \in I(L(G(I)))$. Because $(y_1, y_2, \ldots, y_r)$ are all linear terms in $L(G(I))$, the degree-one scalar product x'_k then should be generated by degree-one monomials of $L(G(I))$ as

$$x'_k = \sum_{i=1}^{r} \beta'_i y_i \ , \tag{3.105}$$

which contradicts the assumption of ring structure. So the set of ISPs is minimal, and we can not write any elements in ISPs as linear functions of remaining ISPs.

Since all RSPs can be expressed as functions of ISPs, we can eliminate them in cut equations. The ideal of algebraic system is then defined by independent quadratic polynomials in polynomial ring $\mathbb{C}[x'_1, x'_2, \ldots, x'_{r'}]$. This simplifies original algebraic system.

3.5.2 The integrand basis

In summary, the algebraic system of maximal unitarity cut is defined by ideal $I(D(\text{ISPs})) \in \mathbb{C}[\text{ISPs}]$, where $\text{ISP} = (X_1, X_2, \ldots, X_{r'})$ is a subset of

$$(x_1^1, x_2^1, x_3^1, x_4^1, \ldots, x_1^L, x_2^L, x_3^L, x_4^L).$$

In order to get integrand basis, we should divide numerator N by Gröbner basis

$$\frac{N}{G(I)} = \frac{N}{g_1 g_2 \cdots g_r} \ . \tag{3.106}$$

The numerator is a polynomial of ISPs, and can be formally written as

$$N = \sum_{\alpha_1, \alpha_2, \ldots, \alpha_{r'}} c_{\alpha_1 \alpha_2 \cdots \alpha_{r'}} X_1^{\alpha_1} X_2^{\alpha_2} \cdots X_{r'}^{\alpha_{r'}} \ . \tag{3.107}$$

Without imposing any constraints, degree of each ISP $\alpha_i = d(X_i)$ can be any non-negative integer, and there is no up-bound for degree $\alpha = \sum_{i=1}^{r'} \alpha_i$ of each monomial. This brings practical difficulty when doing polynomial division. We need to get a finite set of monomials, and this set should be large enough so that no irreducible monomials are missing in the remainder of polynomial division. A natural constraint of monomials is the renormalization conditions for ISPs. For an UV finite theory, degree of each loop momentum in numerator should not be larger than degree of corresponding loop momentum in denominator, and degree of all loop momenta in a monomial should be less than the highest degree of total loop momenta in denominator. Expressed in variables of ISPs, the renormalization conditions impose constraints on degrees α_i of each ISPs directly. For L-loop amplitude with m propagators, they are given by

$$\begin{aligned} &\sum_{j \in \text{all ISPs of } \ell_i} d(x_j^{(i)}) \leq (\text{Number of propagators containing } \ell_i) \ , \ i = 1, \ldots, L \ , \\ &\sum_{i=1}^{L} \sum_{j \in \text{all ISPs of } \ell_i} d(x_j^{(i)}) \leq m - 1 \quad , \quad d(x_j^i) \geq 0 \ . \end{aligned} \tag{3.108}$$

After solving above inequalities, we obtain a finite set M of monomials. Integrand basis is the set of linearly independent monomials in M with respect to denominator of integrand, i.e., the propagators. In order to get integrand basis, we can use following algorithm based on multivariate synthetic division. Firstly, decide a monomial order in polynomial ring $\mathbb{C}[X_1, X_2, \ldots, X_{r'}]$, and compute corresponding Gröbner basis $G(I)$ of $I(D)$. Secondly, generate a finite set M of monomials from renormalization conditions.

Third, for each monomial M_i in M, do the multivariate synthetic division by $G(I)$,

$$M_i/G(I) = f_1 g_1 + \cdots + f_r g_r + R_i \ . \tag{3.109}$$

For given Gröbner basis, the remainder R_i is uniquely determined. Finally, collect all monomials $M(R_i)$ in R_i, and integrand basis B is given by union of all monomials

$$B = \bigcup_i M(R_i) \ . \tag{3.110}$$

If ideal $I(D)$ is irreducible, then there is only one variety $V(D)$. All elements in integrand basis are associated with this variety. However, in most cases ideal $I(D)$ is reducible and can be decomposed to many prime ideals by primary decomposition method as

$$I(D) = \bigcap_{a=1}^{s} I_a(D_a) \ . \tag{3.111}$$

Each prime ideal $I_a(D_a)$ defines a variety $V(D_a)$, and

$$V(D) = \bigcup_{a=1}^{s} V(D_a) \ . \tag{3.112}$$

For s prime ideals, there are s independent solutions for cut equations.

The algebraic system of I_a is usually much simpler than I. So for complicated system, it is better to study each I_a separately, and recover the result of I from these partial results. Following the same algorithm, we can generate Gröbner basis $G(I_a)$ and obtain integrand basis B_{I_a}. This integrand basis is smaller than B. Integrand basis of I can be recovered by

$$B = \bigcup_{a=1}^{s} B_{I_a} \ . \tag{3.113}$$

Of course this union can not be taken by simply adding all monomials in each B_{I_a} together. Given two prime ideals $I_a(D_a), I_b(D_b)$, if the union of ideals $I_{a\cup b}(D_a, D_b)$ is non-trivial, then the intersection of varieties $V(D_a)$ and $V(D_b)$ is also a variety $V(D_a, D_b)$. The integrand basis of $I = I_a \bigcap I_b$ obtained by Gröbner basis $G(I_a \bigcap I_b)$, denoted as union of B_{I_a} and B_{I_b}, is given by

$$B_{I_a \bigcap I_b} \equiv B_{I_a} \bigcup B_{I_b} = B_{I_a} + B_{I_b} - B_{I_a \bigcup I_b} \ , \tag{3.114}$$

where $B_{I_a \bigcup I_b}$ is integrand basis obtained by Gröbner basis of the union $I_a \cup I_b$. This relation can be generalized to any number of prime ideals from primary decomposition of reducible ideal. For example

$$B_{I_a}\bigcup B_{I_b}\bigcup B_{I_c}=B_{I_a}+B_{I_b}+B_{I_c}-B_{I_a\bigcup I_b}-B_{I_a\bigcup I_c}-B_{I_b\bigcup I_c}+B_{I_a\bigcup I_b\bigcup I_c}\ .$$

In practical calculation, we are also interested in the dimension of ideal. For 4-dimensional theory, since there are $4L$ variables and m polynomial equations, the dimension of $I(D)$ is then $\dim(I)=4L-m$. However, if the ideal is reducible, dimension of each prime ideal $\dim(I_a)$ may not equal to $\dim(I)$. Variety $V(D_a)$ could have fewer polynomial equations, thus dimension of $I_a(D_a)$ could be larger than $I(D)$. When considering ideal $I_{a\cup b}(D_a,D_b)$, we get more constraints of polynomial equations than $I(D)$. So dimension $\dim(I_{a\cup b})$ is usually smaller than $\dim(I_a)$ and $\dim(I_b)$. This is easy to understand from geometric picture, since dimension of intersection of two (hyper)surfaces cannot be larger than original (hyper)-surfaces. For example, intersection of two-dimensional surface and one-dimensional curve can at most be one-dimensional curve, and sometimes it is only zero-dimensional point. Dimension of ideal can be computed by algebraic geometry method with many algebraic geometry programs.

3.5.3 Polynomial fitting of expansion coefficients

Advantage of studying prime ideals $I_a, a=1,\ldots,s$ instead of reducible ideal I becomes obvious for polynomial fitting of expansion coefficients. The integrand basis of multi-loop amplitude is usually very large, so a great number of coefficients of integrand basis need to be fitted. Suppose there are n_b monomials in integrand basis. The numerator can be reduced to polynomial of these n_b monomials in the form

$$N=\sum_{\alpha_1,\alpha_2,\ldots,\alpha_{r'}\in B}c_{\alpha_1\alpha_2\cdots\alpha_{r'}}X_1^{\alpha_1}X_2^{\alpha_2}\cdots X_{r'}^{\alpha_{r'}}\ . \tag{3.115}$$

We define

$$\mathbf{c}=(c_1,c_2,\ldots,c_{n_b})\ , \tag{3.116}$$

where c_i denotes a configuration of coefficient $c_{\alpha_1\alpha_2\cdots\alpha_{r'}}$. We want to work out the map from products of tree-level amplitudes to coefficients c_i in solution space of cut equations. In order to do so, we need explicit parametrization of loop momenta using solutions of cut equations. If ideal $I(D)$ has dimension d_I, then ISPs can be expressed as functions of d_I free parameters $(\tau_1,\tau_2,\ldots,\tau_{d_I})$. A rational parametrization is not always possible for reducible ideal I, but could be possible for prime ideals I_a. This is one of motivations that we should work on prime ideals obtained by primary decomposition of original ideal. The loop moneta, as functions of scalar products, are also functions of $(\tau_1, \ldots, \tau_{d_I})$. With suitable choice of momentum basis, free parameters, etc., the parametrization of loop momenta could be simple. After imposing maximal unitarity cut, L-loop n-point integrand becomes

$$\Delta_{cut} = \sum_{h_i, h'_i} A_{n_1}(\ell_{\alpha_1}^{h_1}, P_1, \ell_{\alpha'_1}^{h'_1}) A_{n_2}(\ell_{\alpha_2}^{h_2}, P_2, \ell_{\alpha'_2}^{h'_2}) \cdots A_{n_t}(\ell_{\alpha_t}^{h_t}, P_t, \ell_{\alpha'_t}^{h'_t}) \ , \tag{3.117}$$

where $\ell_{\alpha_i}, \ell_{\alpha'_i}$ are corresponding loop momenta $\ell_i, i = 1, \ldots, L$ being cut. After substituting the parametrization of loop momenta, we get

$$\Delta_{cut} = \sum_{\alpha_1, \alpha_2, \ldots, \alpha_{d_I}} d_{a, \alpha_1 \alpha_2 \cdots \alpha_{d_I}} \tau_1^{\alpha_1} \tau_2^{\alpha_2} \cdots \tau_{d_I}^{\alpha_{d_I}} \ , \tag{3.118}$$

where indices $a = 1, 2, \ldots, s$ denote a given solution of cut equations. We use α to denote configurations $\alpha_1 \alpha_2 \cdots \alpha_{d_I}$, where each α_i is an integer. Suppose for each solution a we get n_a terms with coefficients $d_{a,\alpha}, \alpha = 1, \ldots, n_a$. We can define

$$\mathbf{d} = (d_{1,1}, \ldots, d_{1,n_1}, \ldots, d_{s,1}, \ldots, d_{s,n_s}) \ , \tag{3.119}$$

which has $n_d = \sum_{a=1}^{s} n_a$ elements.

The numerator (3.115) also becomes a series of $(\tau_1, \ldots, \tau_{d_I})$. Since monomials of integrand basis are algebraic linearly independent, we also get n_b terms in $(\tau_1, \ldots, \tau_{d_I})$ expansion. In the maximal unitarity cut, denominator of integrand is transferred to delta functions that lead to cut equations, thus we have $\Delta_{cut} = N$. Equating coefficients of $\tau_1^{\alpha_1} \cdots \tau_{d_I}^{\alpha_{d_I}}$ terms in both sides, we get an equation

$$\sum_{i=1}^{n_d} a'_{k,i} \mathbf{d}_i = \sum_{i=1}^{n_b} b'_{k,i} \mathbf{c}_i \tag{3.120}$$

for each term denoted by $k, k = 1, \ldots, n_b$. Coefficients $a'_{k,i}, b'_{k,i}$ are obtained directly from products of tree amplitudes and monomials of integrand basis after substituting ISPs with parameters $(\tau_1, \ldots, \tau_{d_I})$. In total, we get n_b equations. So we can construct a $n_b \times n_d$ matrix $\mathbf{M}$ relating $\mathbf{d}$ and $\mathbf{c}$ as

$$\mathbf{A}_{n_b \times n_d} \cdot \mathbf{d}^T_{n_d \times 1} = \mathbf{B}_{n_b \times n_b} \cdot \mathbf{c}^T_{n_b \times 1} \to \mathbf{M}_{n_b \times n_d} \cdot \mathbf{d}^T_{n_d \times 1} = \mathbf{c}^T_{n_b \times 1} \ , \tag{3.121}$$

where

$$\mathbf{M}_{n_b \times n_d} = \mathbf{B}^{-1}_{n_b \times n_b} \cdot \mathbf{A}_{n_b \times n_d} \ . \tag{3.122}$$

The matrix $\mathbf{M}$ has rank n_b and invertible. So we can solve coefficients $\mathbf{c}_i$ as functions of known coefficients $\mathbf{d}_i$ from products of tree amplitudes.

For general multi-loop amplitude, integrand basis could contain hundreds of terms, thus matrix $\mathbf{M}$ is very difficult to compute. However, for reducible ideal $I(D)$ that has s prime ideals $I_a(D_a), a = 1, \ldots, s$ obtained by primary decomposition, we can perform polynomial fitting for each ideal $I_a(D_a)$ instead of $I(D)$. Integrand basis of $I_a(D_a)$ contains much smaller number of monomials. Suppose it contains $n_{b'}$ monomials, then we can define

$$\mathbf{c} = (c_1, c_2, \ldots, c_{n_{b'}}) \ . \tag{3.123}$$

From multi-loop integrand we can also define coefficients

$$\mathbf{d} = (d_{a,1}, d_{a,2}, \ldots, d_{a,n_a}) \ , \tag{3.124}$$

for the a-th prime ideal. This is similar to $I(D)$, but now we are only taking coefficients in a given cut solution a, not all independent cut solutions. Then from $n_a \times n_{b'}$ matrix $\mathbf{M}$, we can solve $\mathbf{c}$ as

$$\mathbf{M}_{n_{b'} \times n_a} \cdot \mathbf{b}_{n_a \times 1} = \mathbf{c}_{n_{b'} \times 1} \ . \tag{3.125}$$

Matrix $\mathbf{M}_{n_{b'} \times n_a}$ is much simpler than $\mathbf{M}_{n_b \times n_d}$, which simplifies practical computations. The full set of expansion coefficients can be easily recovered from results of all prime ideals.

Chapter 4

Integrand basis for 4-dimensional two-loop amplitude

Using the basic setup of computational algebraic geometry methods, we are possible to translate the study of integrand reduction as mathematical problems. Generally, algebraic system of multi-loop amplitude is complicated, due to the large number of cut equations as well as too many variables. However, systematic analysis of all 4-dimensional 2-loop amplitudes is possible, because of their relatively simple topologies.

The strategy for integrand reduction of 2-loop amplitudes is as follows,

1. Parameterize loop momenta ℓ_1, ℓ_2 with variables (x_1, x_2, x_3, x_4) and (y_1, y_2, y_3, y_4) by using suitable momentum basis (e_1, e_2, e_3, e_4). Get algebraic system of equations from maximal unitarity cut. If there are m propagators $D_i, i = 0, \ldots, m-1$, then algebraic system is defined by m equations with eight variable $x_i, y_i, i = 1, 2, 3, 4$.

2. Compute ISPs from Gröbner basis. Since the algebraic system is relatively simple, we can also compute ISPs by hand. From m quadratic equations, we should find all possible combinations among them to construct linear equations. By solving these linear equations, we get a set of ISPs. The remaining quadratic equations with variables of ISPs defines an equivalent algebraic system, which is simpler.

3. Compute ideal $I(D)$. Apply primary decomposition for the ideal. If it is reducible, get all prime ideals $I_a(D_a)$. The number of prime ideals equals to the number of non-equivalent cut solutions. We can either study reducible ideal $I(D)$ or prime ideals $I_a(D_a)$.

4. Compute Gröbner basis of reducible ideal $I(D)$ or prime ideals $I_a(D_a)$ for a given monomial order. Get all possible monomials of ISPs that satisfying renormalization

conditions. Divide these monomials with Gröbner basis, and collect all monomials in remainder. They define integrand basis.

5. If $I(D)$ is reducible, study the intersection pattern among varieties $V(I_a)$ of prime ideals $I_a(D_a)$.

6. With knowledge of integrand basis and intersection pattern of varieties $V(I_a)$, we can continue the study such as polynomial fitting of expansion coefficients, and even compute integral basis by IBP relations from integrand basis.

In following sections, firstly topologies of 2-loop amplitude are discussed. Then we focus on 4-dimensional 2-loop amplitudes and provide a general discussion on algebraic system of them. As illustration of the methods, we present detailed analysis for two diagrams. Results of other diagrams can be found in [61].

4.1 Topologies of two-loop amplitude

General diagrams of two-loop amplitudes can be drawn as Figure (4.1) and Figure (4.2). They are constructed from one-loop diagrams by sewing two external legs. Diagrams in Figure (4.1) have two sub-one-loop diagrams connected at a single point. Diagrams in Figure (4.2.B) have two sub-one-loop diagrams connected by one common propagator and diagrams in Figure (4.2.C) have two sub-one-loop diagrams connected by two common propagators.

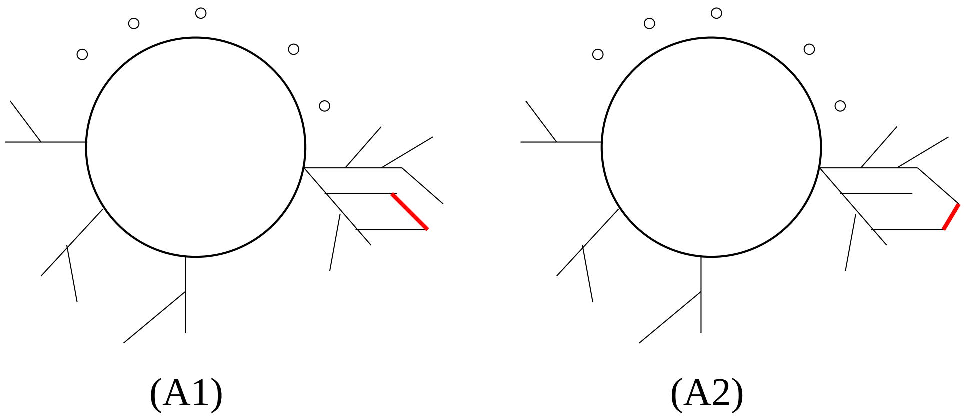

FIGURE 4.1: Illustration of two-loop topology generated from one-loop topology by sewing two external legs that attached to the same tree structure. In sewing (A1), two sub-one-loop topologies do not share the same vertex while in sewing (A2), they do share a common vertex.

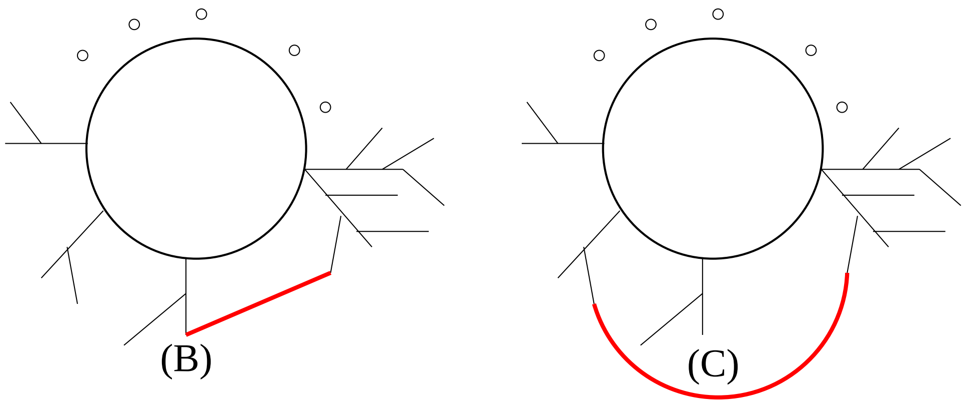

FIGURE 4.2: Illustration of two-loop topology generated from one-loop topology by sewing two external legs that attached to different tree structures. For case (B), two tree structures are adjacent, while for case (C), they are not adjacent.

These diagrams can be distinguished by their propagators. The propagators for each diagram can be separated to three parts

$$\mathcal{D} = D\widetilde{D}\widehat{D} \ , \tag{4.1}$$

where D contains propagators with only ℓ_1, $\widetilde{D}$ contains propagators with only ℓ_2, and $\widehat{D}$ contains propagators with both ℓ_1, ℓ_2. Assume n_1, n_2, n_3 are the numbers of propagators in $D, \widetilde{D}, \widehat{D}$, then topologies of two-loop amplitude can be distinguished by (n_1, n_2, n_3).

We can restrict n_i with condition

$$n_1 \geq n_2 \geq n_3 \tag{4.2}$$

for the freedom of relabeling ℓ_1, ℓ_2. In order to define a solvable algebraic system for renormalizable theory, we can impose inequalities for $d = (4-2\epsilon)$-dimensional theory as

$$n_1, \ n_2, \ n_3 \leq 5 \ , \quad n_1 + n_2 + n_3 \leq 11 \ . \tag{4.3}$$

Solutions of above inequalities can be sorted into four groups according to n_3, denoted by (n_1, n_2) as

$$\begin{aligned}
n_3 = 3: &\ (5,3), (4,4), (4,3), (3,3) \ ; \\
n_3 = 2: &\ (5,4), (5,3), (4,4), (5,2), (4,3), (4,2), (3,3), (3,2), (2,2) \ ; \\
n_3 = 1: &\ (5,5), (5,4), (5,3), (4,4), (5,2), (4,3), (5,1), (4,2), \\
&\ (3,3), (4,1), (3,2), (3,1), (2,2), (2,1), (1,1) \ ; \\
n_3 = 0: &\ (5,5), (5,4), (5,3), (4,4), (5,2), (4,3), (5,1), (4,2), (3,3), \\
&\ (4,1), (3,2), (3,1), (2,2), (2,1), (1,1) \ .
\end{aligned}$$

However, if we focus on 4-dimensional theory, constraints become

$$n_1,\ n_2,\ n_3\ \leq 4\ ,\quad n_1+n_2+n_3 \leq 8\ . \tag{4.4}$$

Then the number of solutions is greatly reduced. We get following solutions

$$\begin{aligned}
n_3 = 2: &\ (4,2),(3,3),(3,2),(2,2)\ ;\\
n_3 = 1: &\ (4,3),(4,2),(3,3),(4,1),(3,2),(3,1),(2,2),(2,1),(1,1)\ ;\\
n_3 = 0: &\ (4,4),(4,3),(4,2),(3,3),(4,1),(3,2),(3,1),(2,2),(2,1),(1,1)\ .
\end{aligned}$$

If $n_3 = 0$, no propagators contain both ℓ_1, ℓ_2, thus solutions with $n_3 = 0$ denote two-loop diagrams with two sub-one-loop structures connected at a single point as shown in Figure (4.3). Integration of ℓ_1, ℓ_2 can be separated, so algebraic system defined by maximal unitarity cut will be combination of two corresponding one-loop topologies. The integrand basis should be slightly modified from two one-loop topologies to two-loop topology. This modification comes from renormalization conditions of monomials. Taking topology (A33) as example, for the left sub-one-loop topology, we denote ISPs as (x_1, x_2), and for the right sub-one-loop topology, we denote ISPs as (y_1, y_2). Then integrand basis can be given by monomials $x_1^{n_1} x_2^{n_2} y_1^{m_1} y_2^{m_2}$ after polynomial division. The renormalization conditions for the left sub-one-loop is $n_1 + n_2 \leq 3$, and for the right sub-one-loop $m_1 + m_2 \leq 3$. However, since two sub-one-loop topologies are connected at one point, we have five vertices in two-loop topology, so $n_1 + n_2 + m_1 + m_2 \leq 5$. Solutions of this additional constraint is smaller than naive combination of solutions of two inequalities from sub-one-loop topologies. Consequently, number of monomials in integrand basis is also smaller than naive product of those in sub-one-loop topologies. Explicitly, representative elements of left and right sub-one-loop triangle topologies can be taken as

$$\{1, x_1, x_2, x_1^2, x_2^2, x_1^3, x_2^3\}\ ,\ \{1, y_1, y_2, y_1^2, y_2^2, y_1^3, y_2^3\}\ ,$$

and the naive product of these two sets gives $7 \times 7 = 49$ monomials of (x_1, x_2, y_1, y_2). However, terms of the form $x_1^3 y_1^3, x_1^3 y_2^3, x_2^3 y_1^3, x_2^3 y_2^3$ should be excluded from integrand basis of (A33), since degree of monomial is larger than five. After subtracting these four terms, we get $7 \times 7 - 4 = 45$ monomials in integrand basis of (A33), which are exactly those by computing with maximal unitarity cut of two-loop topology. Information of other topologies in type (A) can be similarly computed from sub-one-loop topologies with minor modification.

Solutions with $n_3 = 1$ denote all planar two-loop diagrams as shown in Figure (4.4). Solutions with $n_3 = 2$ denote all non-planar two-loop diagrams as shown in Figure (4.5).

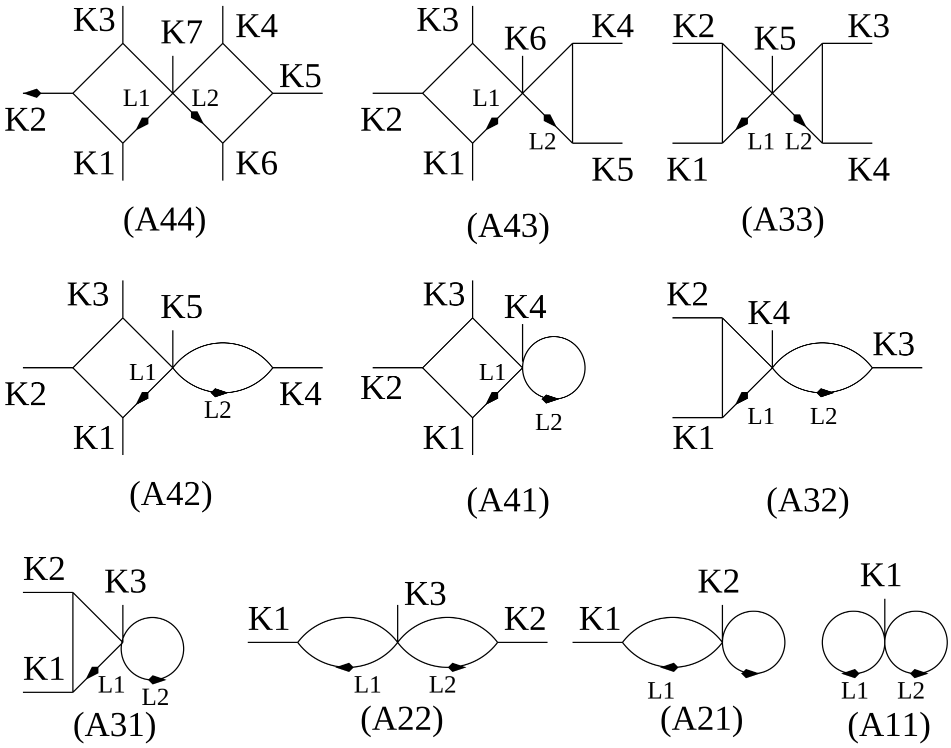

FIGURE 4.3: All 10 topologies of type (A) diagram. Each topology is denoted by (Anm) where n, m are numbers of propagators of the left and right sub-one-loop topologies. All external momenta are out-going.

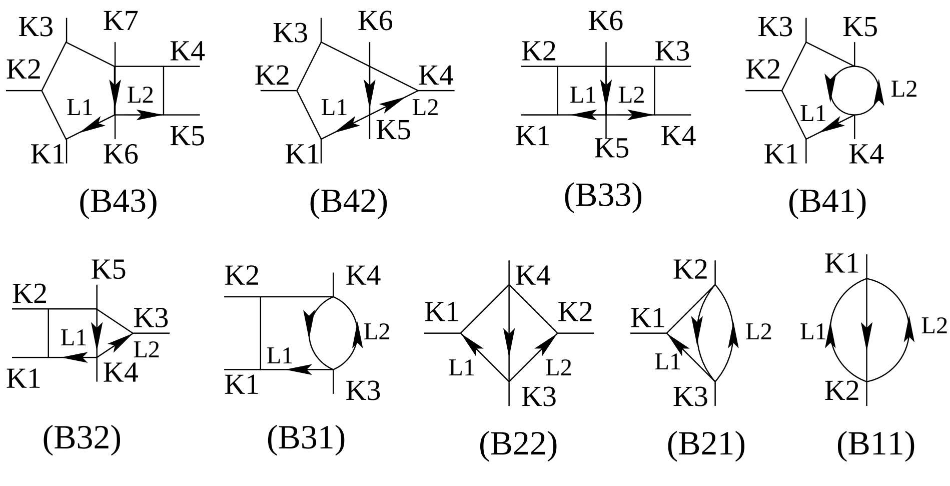

FIGURE 4.4: All 9 topologies of type (B) diagram. Each topology is denoted by (Bnm) where n, m are numbers of propagators containing only ℓ_1 or ℓ_2. All external momenta are out-going.

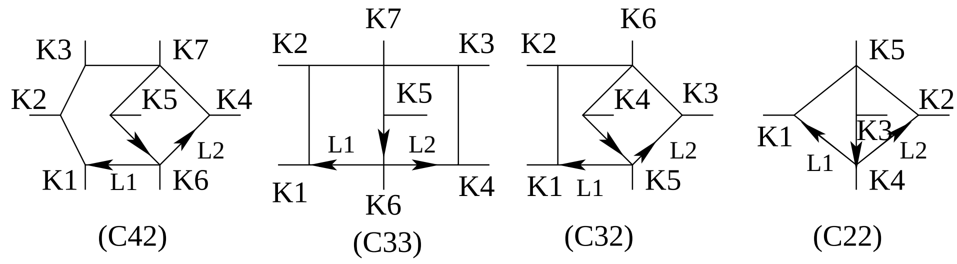

FIGURE 4.5: All 4 topologies of type (C) diagram. Each topology is denoted by (Cnm) where n, m are numbers of propagators containing only ℓ_1 or ℓ_2 respectively. All external momenta are out-going.

4.2 General discussion on equations of maximal unitarity cut

When $n_3 = 1$ or 2, we can explicitly write m propagators $D, \widetilde{D}, \widehat{D}$ as

$$\begin{aligned}
&D_0 = \ell_1^2 \ , \ D_1 = (\ell_1 - K_{a,1})^2 \ , \ \ldots \ , \ D_{n_1-1} = (\ell_1 - K_{a,n_1-1})^2 \ , \\
&\widetilde{D}_0 = \ell_2^2 \ , \ \widetilde{D}_1 = (\ell_2 - K_{b,1})^2 \ , \ \ldots \ , \ \widetilde{D}_{n_2-1} = (\ell_2 - K_{b,n_2-1})^2 \ , \\
&\widehat{D}_0 = (\ell_1 + \ell_2 + K_{c,1})^2 \ , \ \ldots \ , \ \widehat{D}_{n_3-1} = (\ell_1 + \ell_2 + K_{c,n_3})^2 \ ,
\end{aligned} \tag{4.5}$$

where $n_1 + n_2 + n_3 = m$. For 4-dimensional theory, we have $m \leq 8$.

Equations of maximal unitarity cut

$$\begin{aligned}
&D_i = 0 \ , \ i = 0, 1, \ldots, n_1 - 1 \ , \\
&\widetilde{D}_i = 0 \ , \ i = 0, 1, \ldots, n_2 - 1 \ , \\
&\widehat{D}_i = 0 \ , \ i = 0, 1, \ldots, n_3 - 1
\end{aligned} \tag{4.6}$$

define an algebraic set. From above m equations, we can always get $(m-3)$ linear equations by

$$\begin{aligned}
&D_i - D_0 = -2\ell_1 \cdot K_{a,i} + K_{a,i}^2 = 0 \ , \ i = 1, \ldots, n_1 - 1 \ , \qquad (4.7) \\
&\widetilde{D}_i - \widetilde{D}_0 = -2\ell_2 \cdot K_{b,i} + K_{b,i}^2 = 0 \ , \ i = 1, \ldots, n_2 - 1 \ , \\
&\widehat{D}_i - \widehat{D}_0 = 2(\ell_1 + \ell_2) \cdot (K_{c,i+1} - K_{c,1}) + K_{c,i+1}^2 - K_{c,1}^2 = 0 \ , \ i = 1, \ldots, n_3 - 1 \ .
\end{aligned}$$

Remaining three equations

$$D_0 = \ell_1^2 = 0 \ , \ \widetilde{D}_0 = \ell_2^2 = 0 \ , \ \widehat{D}_0 = (\ell_1 + \ell_2 + K_{c,1})^2 = 0 \tag{4.8}$$

are quadratic equations that can not be used to further construct linear equations. Solving $(m-3)$ linear equations, we can write $(m-3)$ variables as functions of remaining

$8-(m-3)=(11-m)$ ISPs. So finally we get an equivalent algebraic system defined by three quadratic equations with $(11-m)$ variables.

If $m=8$, we have three quadratic equations with three variables. By solving these equations we can completely fix solution to points. So geometric picture of this solution is simple. It is isolated points in complex plain. Each point is an inequivalent cut solution, so the number of integrand basis equals to the number of points. Computation of these topologies is trivial.

If $m=7$, we have three quadratic equations with four variables. So solution is described by one complex variable, which is a complex curve. Topologically, it is equivalent to a Riemann sphere. There is an unique topological invariant, the geometric genus g_G, to characterize it. Parametrization of solutions is still simple, and different inequivalent solutions usually intersect at single points.

If $m<7$, solutions of cut equations are described by more than one variables, which describes hyper-surface or complex manifold. Analysis of these solutions is difficult even as mathematical problems. However, it is still possible to study integrand basis by Gröbner basis method, and analyze intersection of inequivalent solutions.

Having algebraic system defined by equations (4.8) and $(11-m)$ ISPs, we can compute Gröbner basis after deciding proper monomial order. Before determining integrand basis, we need to construct a finite set of monomials in numerator satisfying renormalization conditions. Suppose there are m_1 variables x_i and m_2 variables y_i with $m_1+m_2=11-m$ in set of ISPs, then monomials of the form $x_{i_1}^{d(x_{i_1})}\cdots x_{i_{m_1}}^{d(x_{i_{m_1}})}y_{j_1}^{d(y_{j_1})}\cdots y_{j_{m_2}}^{d(y_{j_{m_2}})}$, where $d(x)$ is the degree of variable x, should satisfying following renormalization conditions

$$\sum_{\text{all ISPs of x}} d(x_i)\leq n_1+n_3 \quad , \quad \sum_{\text{all ISPs of y}} d(y_i)\leq n_2+n_3 \ ,$$
$$\sum_{\text{all ISPs of x}} d(x_i)+\sum_{\text{all ISPs of y}} d(y_i)\leq m-1 \quad , \quad d(x_i)\geq 0 \quad , \quad d(y_i)\geq 0 \ . \tag{4.9}$$

It is possible to get hundreds of terms from solving these inequalities. By dividing them with Gröbner basis, we get a set of integrand basis from collecting monomials in remainders.

A complete study of cut equations also includes the study of inequivalent solutions and their relations. Primary decomposition of ideal $I(D,\widetilde{D},\widehat{D})$ gives all prime ideals $I_a(D_a)$. All inequivalent solutions are described by varieties $V(I_a)$. Intersection of two inequivalent solutions $V(I_a)\cap V(I_b)$ is directly given by solving equations $D_a=D_b=0$, i.e., $V(I_1\cup I_2)$. If it has no solution, then there is no intersection. We can study the intersection pattern of all varieties $V(I_a)$ by solving all possible combinations among them. Since the three equations in (4.8) are all quadratic, each of them can at most be factorized to two factors. So at most we can get eight prime ideals. Although intersection pattern becomes complicated as the number of prime ideals increases, algebraic system of each prime ideal becomes simpler. So we can still carry out the computation with help of computer.

The irreducibility of cut equations depends heavily on configuration of external momenta, which can be judged from three-vertex of diagram. Every time when there is massless three-vertex, cut equations will be reducible. In maximal unitarity cut, all internal momenta are massless, so the masslessness of three-vertex is totally determined by external momenta. However, different configurations of external momenta might give the same factorization of cut equations, thus the same prime ideals after primary decomposition. So it is important to survey irreducibility of cut equations under all possible configurations of external momenta.

4.3 Planar penta-triangle topology

In this section, we present result of planar two-loop penta-triangle topology (B42) as shown in Figure (4.4). This topology has 7 propagators, so finally we get three equations with four variables. The solution is one-dimensional complex curve. In fact, four propagators contain only ℓ_1, so cut equations of these four propagators will completely fix (x_1, x_2, x_3, x_4). It gives two solutions, so ideal of cut equation can be at least decomposed to two prime ideals even for most general external momentum configuration.

4.3.1 The integrand basis

In order to get simple expressions for cut equations, we choose two external momenta K_1, K_4, as shown in Figure (4.4), to generate momentum basis (e_1, e_2, e_3, e_4) defined by (3.95). All loop momenta and external momenta can be expanded as

$$\begin{aligned}
&\ell_1 = x_1 e_1 + x_2 e_2 + x_3 e_3 + x_4 e_4 \ , \quad \ell_2 = y_1 e_1 + y_2 e_2 + y_3 e_3 + y_4 e_4 \ , \\
&K_1 = \alpha_{12} e_1 + \alpha_{11} e_2 \ , \quad K_1 + K_2 = \alpha_{22} e_1 + \alpha_{21} e_2 + \alpha_{24} e_3 + \alpha_{23} e_4 \ , \\
&K_1 + K_2 + K_3 = \alpha_{32} e_1 + \alpha_{31} e_2 + \alpha_{34} e_3 + \alpha_{33} e_4 \ , \\
&K_4 = \beta_{12} e_1 + \beta_{11} e_2 \ , \quad K_5 = \gamma_{12} e_1 + \gamma_{11} e_2 + \gamma_{14} e_3 + \gamma_{13} e_4 \ , \\
&K_6 = -(K_1 + K_2 + K_3 + K_4 + K_5) \ .
\end{aligned} \tag{4.10}$$

Coefficients α, β and γ are known for given external momenta. These coefficients are all independent for general external momenta, but would have non-trivial relation for special kinematics. For example, since K_5 or K_6 could be zero without changing penta-triangle topology, momentum conservation will impose constraint on these coefficients if K_5, K_6 are zero. When $K_6 = 0$, we have

$$\gamma_{11} = -\beta_{11} - \alpha_{31} \;,\; \gamma_{12} = -\beta_{12} - \alpha_{32} \;,\; \gamma_{13} = -\alpha_{33} \;,\; \gamma_{14} = -\alpha_{34} \;, \tag{4.11}$$

and when $K_5 = K_6 = 0$, we have

$$\gamma_{1i} = 0 \;,\; \alpha_{31} = -\beta_{11} \;,\; \alpha_{32} = -\beta_{12} \;,\; \alpha_{33} = 0 \;,\; \alpha_{34} = 0 \;. \tag{4.12}$$

These constraints affect the irreducibility of ideal $I(D)$, which we will show later.

Four linear equations

$$\begin{aligned}
D_1 - D_0 &= -2(\alpha_{11}x_1 + \alpha_{12}x_2) + 2\alpha_{11}\alpha_{12} = 0 \;, \\
D_2 - D_0 &= -2(\alpha_{21}x_1 + \alpha_{22}x_2 + \alpha_{23}x_3 + \alpha_{24}x_4) + 2(\alpha_{21}\alpha_{22} + \alpha_{23}\alpha_{24}) = 0 \;, \\
D_3 - D_0 &= -2(\alpha_{31}x_1 + \alpha_{32}x_2 + \alpha_{33}x_3 + \alpha_{34}x_4) + 2(\alpha_{31}\alpha_{32} + \alpha_{33}\alpha_{34}) = 0 \;, \\
\widetilde{D}_1 - \widetilde{D}_0 &= -2(\beta_{11}y_1 + \beta_{12}y_2) + 2\beta_{11}\beta_{12} = 0
\end{aligned} \tag{4.13}$$

can be solved, and four variables (x_1, x_2, x_3, y_2) are expressed as linear functions of four ISPs (x_4, y_1, y_3, y_4). The results are given by

$$\begin{aligned}
x_1 &= \frac{\alpha_{12}(\alpha_{24}\alpha_{33} - \alpha_{23}\alpha_{34})}{\alpha_{12}(\alpha_{23}\alpha_{31} - \alpha_{21}\alpha_{33}) + \alpha_{11}(\alpha_{22}\alpha_{33} - \alpha_{23}\alpha_{32})} x_4 \\
&\quad + \frac{\alpha_{12}(-\alpha_{21}\alpha_{22}\alpha_{33} + \alpha_{11}(\alpha_{22}\alpha_{33} - \alpha_{23}\alpha_{32}) + \alpha_{23}(\alpha_{31}\alpha_{32} + \alpha_{33}\alpha_{34} - \alpha_{33}\alpha_{24}))}{\alpha_{12}(\alpha_{23}\alpha_{31} - \alpha_{21}\alpha_{33}) + \alpha_{11}(\alpha_{22}\alpha_{33} - \alpha_{23}\alpha_{32})} \;,
\end{aligned} \tag{4.14}$$

$$\begin{aligned}
x_2 &= \frac{\alpha_{11}(\alpha_{23}\alpha_{34} - \alpha_{24}\alpha_{33})}{\alpha_{12}(\alpha_{23}\alpha_{31} - \alpha_{21}\alpha_{33}) + \alpha_{11}(\alpha_{22}\alpha_{33} - \alpha_{23}\alpha_{32})} x_4 \\
&\quad + \frac{\alpha_{11}(\alpha_{21}\alpha_{22}\alpha_{33} + \alpha_{12}(\alpha_{23}\alpha_{31} - \alpha_{21}\alpha_{33}) - \alpha_{23}(\alpha_{31}\alpha_{32} + \alpha_{33}\alpha_{34} - \alpha_{33}\alpha_{24}))}{\alpha_{12}(\alpha_{23}\alpha_{31} - \alpha_{21}\alpha_{33}) + \alpha_{11}(\alpha_{22}\alpha_{33} - \alpha_{23}\alpha_{32})} \;,
\end{aligned} \tag{4.15}$$

$$\begin{aligned}
x_3 &= \frac{\alpha_{12}(\alpha_{21}\alpha_{34} - \alpha_{24}\alpha_{31}) + \alpha_{11}(\alpha_{24}\alpha_{32} - \alpha_{22}\alpha_{34})}{\alpha_{12}(\alpha_{23}\alpha_{31} - \alpha_{21}\alpha_{33}) + \alpha_{11}(\alpha_{22}\alpha_{33} - \alpha_{23}\alpha_{32})} x_4 \\
&\quad + \frac{\alpha_{11}((-\alpha_{23}\alpha_{24} - \alpha_{22}\alpha_{21} + \alpha_{22}\alpha_{31})\alpha_{32} + \alpha_{12}(\alpha_{21}\alpha_{32} - \alpha_{22}\alpha_{31}) + \alpha_{22}\alpha_{33}\alpha_{34})}{\alpha_{12}(\alpha_{23}\alpha_{31} - \alpha_{21}\alpha_{33}) + \alpha_{11}(\alpha_{22}\alpha_{33} - \alpha_{23}\alpha_{32})} \\
&\quad + \frac{\alpha_{12}(\alpha_{23}\alpha_{24}\alpha_{31} + \alpha_{21}(\alpha_{31}\alpha_{22} - \alpha_{31}\alpha_{32} - \alpha_{33}\alpha_{34}))}{\alpha_{12}(\alpha_{23}\alpha_{31} - \alpha_{21}\alpha_{33}) + \alpha_{11}(\alpha_{22}\alpha_{33} - \alpha_{23}\alpha_{32})} \;,
\end{aligned} \tag{4.16}$$

and

$$y_2 = \beta_{11}(1 - \frac{y_1}{\beta_{12}}) \;. \tag{4.17}$$

The analytic expression of (x_1, x_2, x_3) seems to be complicated. For purpose of analysis, we can just treat them as linear functions of x_4. For practical computation, we can use computer.

The quadratic equation $D_0 = x_1x_2 + x_3x_4 = 0$ becomes quadratic equation of x_4

$$x_4^2 + a_1x_4 + a_2 = 0 \ , \tag{4.18}$$

where a_1, a_2 are functions of α. Since $x_4 \in \mathbb{C}$, we can get two solutions $x_4^{\Gamma_1}, x_4^{\Gamma_2}$. One would wonder if in some cases $x_4^{\Gamma_1} = x_4^{\Gamma_2}$. This might be true for very special choice of α. But for external momentum configurations considered here, we always get two distinct solutions. So there is no intersection between them. The ideal $I(D_0, \widetilde{D}_0, \widehat{D}_0)$ can be decomposed to two ideals $I_1(x_4 - x_4^{\Gamma_1}, \widetilde{D}_0, \widehat{D}_0)$ and $I_2(x_4 - x_4^{\Gamma_2}, \widetilde{D}_0, \widehat{D}_0)$. They could still be reducible ideals. The other two quadratic equations are

$$\widetilde{D}_0 = \beta_{11}(1 - \frac{y_1}{\beta_{12}})y_1 + y_3y_4 = 0 \ , \tag{4.19}$$

and(for convenience we re-define $\widehat{D}_0 = \widehat{D}_0 - D_0 - \widetilde{D}_0$)

$$\begin{aligned} \widehat{D}_0 = 0 \quad = \quad & \Big(x_2 + \gamma_{11} - (x_1 + \gamma_{12})\frac{\beta_{11}}{\beta_{12}}\Big)y_1 + (x_4 + \gamma_{13})y_3 + (x_3 + \gamma_{14})y_4 \\ & +(x_1 + \gamma_{12})\beta_{11} + \gamma_{11}x_1 + \gamma_{12}x_2 + \gamma_{13}x_3 + \gamma_{14}x_4 + \gamma_{11}\gamma_{12} + \gamma_{13}\gamma_{14} \ , \end{aligned} \tag{4.20}$$

where (x_1, x_2, x_3) should be replaced by linear functions of x_4.

It is not difficult to compute integrand basis directly from Gröbner basis $G(I)$ of ideal $I(D_0, \widetilde{D}_0, \widehat{D}_0)$. Monomials in numerator are terms of the form $x_4^{d(x_4)}y_1^{d(y_1)}y_3^{d(y_3)}y_4^{d(y4)}$ that satisfying renormalization conditions

$$d(x_4) \le 5 \ \ , \ \ d(y_1) + d(y_3) + d(y_4) \le 3 \ \ , \ \ d(x_4) + d(y_1) + d(y_3) + d(y_4) \le 6 \ .$$

There are 94 solutions for these inequalities. Computing Gröbner basis $G(I)$ of ideal $I(D_0, \widetilde{D}_0, \widehat{D}_0)$ with *Degree Lexicographic* monomial order in Mathematica, and dividing 94 monomials with $G(I)$ by multivariate synthetic division, we obtain integrand basis. Representative elements of integrand basis depend on kinematic configurations. In these example, we get 3 types of integrand basis,

1. Kinematic configurations with K_4 massive, there are 14 elements

$$\mathcal{B}_{B42}^{I} = \{1, x_4, y_1, y_3, x_4y_3, y_1y_3, y_3^2, y_3^3, y_4, y_3y_4, y_3^2y_4, y_4^2, y_3y_4^2, y_4^3\} \ . \tag{4.21}$$

2. Kinematic configurations with K_4 massless while at most one of K_5, K_6 is zero, there are 14 elements

$$\mathcal{B}^{II}_{B42} = \{1, x_4, y_1, y_3, x_4y_3, y_1y_3, y_3^2, y_1y_3^2, y_3^3, y_4, y_1y_4, y_4^2, y_1y_4^2, y_4^3\} \ . \tag{4.22}$$

3. Kinematic configurations with K_4 massless while both $K_5 = K_6 = 0$, there are 20 elements

$$\begin{aligned}\mathcal{B}^{III}_{B42} \ = \ & \{1, x_4, y_1, x_4y_1, y_1^2, x_4y_1^2, y_1^3, x_4y_1^3, y_3, y_1y_3, \\ & y_1^2y_3, y_3^2, y_1y_3^2, y_3^3, y_4, y_1y_4, y_1^2y_4, y_4^2, y_1y_4^2, y_4^3\} \ .\end{aligned} \tag{4.23}$$

For practical computation in Mathematica, we should take care of monomial order as well as variable ordering of ISPs. For example, to determine monomial order for x^3y, x^2y^2, xy^3, since they are all degree 4, we cannot list them according to total degree of monomial. If we set variable ordering of ISPs to be $\{x, y\}$, then x should firstly be considered, and we have $x^3y \succ x^2y^2 \succ xy^3$. Otherwise if we set variable ordering to be $\{y, x\}$, y should be considered firstly, and we have $xy^3 \succ x^2y^2 \succ x^3y$. In practical computation, we should not only define monomial order but also variable ordering of ISPs.

4.3.2 Expansion coefficients of integrand basis

Let us briefly describe polynomial fitting of expansion coefficients. For algebraic geometry method, we can translate the integrand $\mathcal{F}(\ell_1, \ell_2)$ computed directly from Feynman diagrams or from generalized unitarity cut method to polynomial function of ISPs $\mathcal{F}(x_4, y_1, y_3, y_4)$. Then divide $\mathcal{F}(x_4, y_1, y_3, y_4)$ with Gröbner basis $G(I)$ of ideal $I(D_0, \widetilde{D}_0, \widehat{D}_0)$. The remainder is a polynomial function. By expanding it as series of integrand basis, we directly get the expansion coefficients.

We do not necessary to use ideal I if it is reducible. Instead, prime ideals of reducible ideal I via primary decomposition can also be used to get a smaller set of equations. Explicitly, we know that ideal $I(D_0, \widetilde{D}_0, \widehat{D}_0)$ can be decomposed to two prime ideals $I_1(x_4 - x_4^{\Gamma_1}, \widetilde{D}_0, \widehat{D}_0)$ and $I_2(x_4 - x_4^{\Gamma_2}, \widetilde{D}_0, \widehat{D}_0)$ for general kinematics. Polynomial division $\mathcal{F}(x_4, y_1, y_3, y_4)/G(I_1)$ gives a remainder

$$\mathcal{R}(\mathcal{F}(x_4, y_1, y_3, y_4)/G(I_1)) = f_1 + f_2y_3 + f_3y_3^2 + f_4y_3^3 + f_5y_4 + f_6y_3y_4 + f_7y_3^2y_4 \ , \tag{4.24}$$

with seven known coefficients f_i.

We can also divide each monomial in integrand basis by Gröbner basis $G(I_1)$, and remainders of these polynomial division are

$$\begin{aligned}
&(1)/G(I_1) \to 1 \ , \ (x_4)/G(I_1) \to d_2 \ , \ (y_1)/G(I_1) \to d_{31}y_4 + d_{32}y_3 + d_{33} \ , \\
&(y_3)/G(I_1) \to y_3 \ , \ (x_4y_3)/G(I_1) \to d_5y_3 \ , \ (y_1y_3)/G(I_1) \to d_{61}y_3y_4 + d_{62}y_3^2 + d_{63}y_3 \ , \\
&(y_3^2)/G(I_1) \to y_3^2 \ , \ (y_3^3)/G(I_1) \to y_3^3 \ , \ (y_4)/G(I_1) \to y_4 \ , \ (y_3y_4)/G(I_1) \to y_3y_4 \ , \\
&(y_3^2y_4)/G(I_1) \to y_3^2y_4 \ , \ (y_4^2)/G(I_1) \to d_{12,1}y_3y_4 + d_{12,2}y_4 + d_{12,3}y_3^2 + d_{12,4}y_3 + d_{12,5} \ , \\
&(y_3y_4^2)/G(I_1) \to d_{13,1}y_3^2y_4 + d_{13,2}y_3y_4 + d_{13,3}y_3^3 + d_{13,4}y_3^2 + d_{13,5}y_3 \ , \\
&(y_4^3)/G(I_1) \to d_{14,1}y_3^2y_4 + d_{14,2}y_3y_4 + d_{14,3}y_4 + d_{14,4}y_3^3 + d_{14,5}y_3^2 + d_{14,6}y_3 + d_{14,7} \ , \qquad (4.25)
\end{aligned}$$

with known coefficients d.

Remainder $\mathcal{R}(\mathcal{F}(x_4, y_1, y_3, y_4)/G(I_1))$ should equal to the expansion of integrand basis with coefficients c_i. So equating the same monomial in both sides, we get 7 equations for 14 unknown coefficients c_i

$$\begin{aligned}
f_1 &= c_1 + c_2d_2 + c_3d_{33} + c_{12}d_{12,5} + c_{14}d_{14,7} \ , \\
f_2 &= c_3d_{32} + c_4 + c_5d_5 + c_6d_{63} + c_{12}d_{12,4} + c_{13}d_{13,5} + c_{14}d_{14,6} \ , \\
f_3 &= c_6d_{62} + c_7 + c_{12}d_{12,3} + c_{13}d_{13,4} + c_{14}d_{14,5} \ , \\
f_4 &= c_8 + c_{13}d_{13,3} + c_{14}d_{14,4} \ , \\
f_5 &= c_3d_{51} + c_9 + c_{12}d_{12,2} + c_{14}d_{14,3} \ , \\
f_6 &= c_6d_{61} + c_{10} + c_{12}d_{12,1} + c_{13}d_{13,2} + c_{14}d_{14,2} \ , \\
f_7 &= c_{11} + c_{13}d_{13,1} + c_{14}d_{14,1} \ . \qquad (4.26)
\end{aligned}$$

Similarly, using Gröbner basis $G(I_2)$ we also get another 7 equations relating $\widetilde{f}_i$ and 14 unknown coefficients c_i. These 14 equations for 14 coefficients c_i can be solved to get all 14 expansion coefficients of integrand basis

Another method, the parametrization method, has already been described in chapter 3. It is closely related to prime ideals of a reducible ideal via primary decomposition. Each prime ideal is an inequivalent cut solution. For example, two prime ideals I_1, I_2 of reducible ideal $I(D_0, \widetilde{D}_0, \widehat{D}_0)$ represent two inequivalent cut solutions, distinguished by $x_4^{\Gamma_1}, x_4^{\Gamma_2}$. For each solution, we can parameterize variables with one parameter $y_1(\tau), y_3(\tau), y_4(\tau)$. Then we have

$$\mathcal{F}(x_4^{\Gamma_i}, y_1(\tau), y_3(\tau), y_4(\tau)) = \sum_{k=1}^{14} c_k \mathcal{B}_{B42,k}(\tau) \ . \qquad (4.27)$$

Coefficients c_i can be fitted by comparing terms that having the same degrees of τ in both sides. This fitting is simple both analytically or numerically.

4.3.3 Irreducibility of cut equations

Ideal $I(D_0, \widetilde{D}_0, \widehat{D}_0)$ can be decomposed to two ideals $I_1(x_4 - x_4^{\Gamma_1}, \widetilde{D}_0, \widehat{D}_0)$, $I_2(x_4 - x_4^{\Gamma_2}, \widetilde{D}_0, \widehat{D}_0)$. For general kinematics, each ideal is irreducible. But they are reducible for kinematic configurations where massless three-vertex appear in diagram. In order to study the irreducibility, let us focus on one ideal $I_i(x_4 - x_4^{\Gamma_i}, \widetilde{D}_0, \widehat{D}_0)$.

After setting $x_4 = x_4^{\Gamma_i}$, $\widehat{D}_0 = 0$ becomes a linear equation in (y_1, y_3, y_4) and $\widetilde{D}_0 = 0$ is still quadratic. In our convention, we have $\beta_{11} \neq 0$ When K_4 is massive. So $\widetilde{D}_0 = 0$ can not naively be factorized. To see when it is factorized, we can parameterize cut solution with $y_1 = \tau$, then

$$\widetilde{D}_0 = 0 \ \rightarrow \ y_3 y_4 + F(\tau) = 0 \ , \quad \widehat{D}_0 = 0 \ \rightarrow \ a y_3 + b y_4 + c(\tau) = 0 \ , \tag{4.28}$$

where a, b are functions of α, β, γ and $x_4^{\Gamma_i}$. $F(\tau)$ is quadratic function of τ and $c(\tau)$ is linear function of τ. From above two equations we can solve

$$y_4 = \frac{ac(\tau) \pm \sqrt{a^2[c(\tau)^2 + 4abF(\tau)]}}{-2ab} \ . \tag{4.29}$$

We are interested in rational parametrization of cut solutions. Only when $c(\tau)^2 + 4abF(\tau)$ inside the square root is a perfect square we can get rational parametrization for y_4. Since $c(\tau)^2 + 4abF(\tau)$ is quadratic function of τ, in order for it to be a perfect square, the discriminant should be zero. Using explicit expressions of $F(\tau)$, $c(\tau)$ and a, b, the discriminant is given by

$$\begin{aligned} &(x_1^{\Gamma_i} x_2^{\Gamma_i} + x_3^{\Gamma_i} x_4^{\Gamma_i})(\beta_{11} - \frac{\Xi}{\beta_{12}}) \\ &+ \frac{(x_2^{\Gamma_i} + \gamma_{11} + \beta_{11})(x_1^{\Gamma_i} + \gamma_{12} + \beta_{12}) + (x_4^{\Gamma_i} + \gamma_{13})(x_3^{\Gamma_i} + \gamma_{14})}{\beta_{12}} \Xi \ , \end{aligned} \tag{4.30}$$

where

$$\Xi = \gamma_{11} x_1^{\Gamma_i} + \gamma_{12} x_2^{\Gamma_i} + \gamma_{13} x_3^{\Gamma_i} + \gamma_{14} x_4^{\Gamma_i} + \gamma_{11}\gamma_{12} + \gamma_{13}\gamma_{14} \ . \tag{4.31}$$

The first term in (4.30) vanishes since $D_0 = x_1^{\Gamma_i} x_2^{\Gamma_i} + x_3^{\Gamma_i} x_4^{\Gamma_i} = 0$. The second term will vanish if at least one K_5 or K_6 is zero. If K_5 is zero, all $\gamma_{1i} = 0$, thus $\Xi = 0$. $K_6 = 0$, we have

$$\gamma_{11} = -\beta_{11} - \alpha_{31} \ \ , \ \ \gamma_{12} = -\beta_{12} - \alpha_{32} \ \ , \ \ \gamma_{13} = -\alpha_{33} \ \ , \ \ \gamma_{14} = -\alpha_{34} \ . \tag{4.32}$$

So the second term becomes

$$\frac{-x_1^{\Gamma_i}\alpha_{31} - x_2^{\Gamma_i}\alpha_{32} - x_3^{\Gamma_i}\alpha_{33} - x_4^{\Gamma_i}\alpha_{34} + \alpha_{31}\alpha_{32} + \alpha_{33}\alpha_{34}}{\beta_{12}}\Xi = \frac{D_3 - D_0}{2\beta_{12}}\Xi \ . \tag{4.33}$$

It vanishes since $D_3 - D_0 = 0$. The reducible ideal $I_i(x_4 - x_4^{\Gamma_i}, \widetilde{D}_0, \widehat{D}_0)$ can be decomposed to two prime ideals via primary decomposition, and in total we get four prime ideals.

We can compute Gröbner basis for each prime ideal, and use them to compute integrand basis. For each prime ideal, we get 4 representative elements in integrand basis. Naively counting the total number of elements, we have $4 \times 4 = 16 > 14$, which is larger than the number of representative elements for $I(D_0, \widetilde{D}_0, \widehat{D}_0)$. The over counting comes from intersections of varieties. Both $V(I_{11} \cup I_{12})$ and $V(I_{21} \cup I_{22})$ are non-empty, and they are single points. So we get integrand basis

$$\begin{aligned} B_{I_{11}} \cup B_{I_{12}} &= B_{I_{11}} + B_{I_{12}} - B_{I_{11} \cup I_{12}} = 4 + 4 - 1 = 7 \ , \\ B_{I_{21}} \cup B_{I_{22}} &= B_{I_{21}} + B_{I_{22}} - B_{I_{21} \cup I_{22}} = 4 + 4 - 1 = 7 \ , \\ B_{I_{11}} \cup B_{I_{12}} \cup B_{I_{21}} \cup B_{I_{22}} &= 7 + 7 = 14 \ , \end{aligned} \tag{4.34}$$

which is exactly the integrand basis given in $\mathcal{B}^I_{B42}$.

If K_4 is massless and at most one of K_5, K_6 is zero, we have $\beta_{11} = 0$. Equation $\widetilde{D}_0 = y_3 y_4 = 0$ is automatically factorized. The other equation $\widehat{D}_0 = 0$ is still a linear equation of (y_1, y_3, y_4), let us assume it to be

$$a y_3 + b y_4 + y_1 + c = 0 \ . \tag{4.35}$$

We get two prime ideals for each $x_4^{\Gamma_i}$ as

$$I_{i1}(x_4 - x_4^{\Gamma_i}, y_3, a y_3 + b y_4 + y_1 + c) \ \ , \ \ I_{i2}(x_4 - x_4^{\Gamma_i}, y_4, a y_3 + b y_4 + y_1 + c) \ . \tag{4.36}$$

So in total we have four prime ideals, and the four inequivalent cut solutions are parameterized by τ as

$$\text{solution 1:} \quad x_4 = x_4^{\Gamma_1} \ , \ y_3 = 0 \ , \ y_4 = \tau \ , \ y_1 = -b\tau - c \ , \tag{4.37}$$

$$\text{solution 2:} \quad x_4 = x_4^{\Gamma_1} \ , \ y_3 = \tau \ , \ y_4 = 0 \ , \ y_1 = -a\tau - c \ , \tag{4.38}$$

$$\text{solution 3:} \quad x_4 = x_4^{\Gamma_2} \ , \ y_3 = 0 \ , \ y_4 = \tau \ , \ y_1 = -b\tau - c \ , \tag{4.39}$$

$$\text{solution 4:} \quad x_4 = x_4^{\Gamma_2} \ , \ y_3 = \tau \ , \ y_4 = 0 \ , \ y_1 = -a\tau - c \ . \tag{4.40}$$

It is easy to see that varieties of I_{11}, I_{12} have an intersecting point at

$$x_4 = x_4^{\Gamma_1} \ , \ y_3 = 0 \ , \ y_4 = 0 \ , \ y_1 = -c \ .$$

Similarly, varieties of I_{21}, I_{22} have an intersecting point at

$$x_4 = x_4^{\Gamma_2} \quad , \quad y_3 = 0 \quad , \quad y_4 = 0 \quad , \quad y_1 = -c \ .$$

Discussion on integrand basis of this kinematic configuration is the same as kinematic configuration where K_4 is massive and at least one of K_5, K_6 is zero. However, representative elements should be modified. The reason is that, when K_4 is massless, we have $\widetilde{D}_0 = y_3 y_4$. Thus monomials with a factor $y_3 y_4$ should be reducible by $\widetilde{D}_0$ and they should be excluded. So we get a different integrand basis $\mathcal{B}^{II}_{B42}$ instead of $\mathcal{B}^{I}_{B42}$.

There is a special kinematic configuration where K_4 is massless and $K_5 = K_6 = 0$. Equations of maximal unitarity cut become

$$\begin{aligned} D_0 &= \Big(-\frac{\alpha_{24}}{\alpha_{23}} x_4 + \frac{\alpha_{23}\alpha_{24} - \alpha_{12}\alpha_{21} + \alpha_{21}\alpha_{22}}{\alpha_{23}} \Big) x_4 = 0 \quad , \quad \widetilde{D}_0 = y_3 y_4 = 0 \ , \\ \widehat{D}_0 &= x_4 y_3 + \Big(-\frac{\alpha_{24}}{\alpha_{23}} x_4 + \frac{\alpha_{21}\alpha_{22} - \alpha_{21}\alpha_{12} + \alpha_{23}\alpha_{24}}{\alpha_{23}} \Big) y_4 = 0 \ . \end{aligned} \tag{4.41}$$

Surprisingly, y_1 disappears in cut equations. So it is not constrained, and should be taken as a free parameter τ_1. We have three cut equations for three variables (x_4, y_3, y_4), but these cut equations are not all independent. There are two non-trivial solutions. The first one is $x_4 = 0, y_4 = 0$. This is a solution of $D_0 = 0, \widetilde{D}_0 = 0$, while the third equation $\widehat{D}_0 = 0$ automatically satisfies. So y_3 in the third equation is not constrained and should be taken as a free parameter τ_2. Similarly, we have another non-trivial solution $x_4 = (\alpha_{21}\alpha_{22} - \alpha_{12}\alpha_{21} + \alpha_{23}\alpha_{24})/\alpha_{24}$, $y_3 = 0$. y_4 should be taken as a free parameter τ_2. In this kinematic configuration, there are two prime ideals, and each ideal is two dimensional. Using Gröbner basis of each prime ideal, we get 10 representative elements in integrand basis. Since there is no intersection between varieties of two prime ideals, we get 20 elements in integrand basis as shown in $\mathcal{B}^{III}_{B42}$.

4.4 Non-planar crossed double-triangle topology

In this section, we present result of another more complicated example, the non-planar two-loop crossed double-triangle topology (C22) as shown in Figure (4.5). This topology has six propagators, so finally we get three quadratic equations with five variables. The cut solutions will be 2-dimensional. Then intersection of varieties of prime ideals could be 1-dimensional curve or points. The number of prime ideals could be as high as eight in some kinematic configurations, which makes discussion more involved.

4.4.1 The integrand basis

For simplicity, we use K_1, K_2 to construct momentum basis (e_1, e_2, e_3, e_4). Loop momenta and external momenta are expanded as

$$\begin{aligned}
&\ell_1 = x_1 e_1 + x_2 e_2 + x_3 e_3 + x_4 e_4 \ \ , \ \ \ell_2 = y_1 e_1 + y_2 e_2 + y_3 e_3 + y_4 e_4 \ , \\
&K_1 = \alpha_{12} e_1 + \alpha_{11} e_2 \ \ , \ \ K_2 = \beta_{12} e_1 + \beta_{11} e_2 \ , \\
&K_4 = \gamma_{12} e_1 + \gamma_{11} e_2 + \gamma_{14} e_3 + \gamma_{13} e_4 \ \ , \ \ K_3 + K_4 = \gamma_{22} e_1 + \gamma_{21} e_2 + \gamma_{24} e_3 + \gamma_{23} e_4 \ , \\
&K_5 = (-K_1 + K_2 + K_3 + K_4) \ .
\end{aligned} \tag{4.42}$$

Three linear equations

$$\begin{aligned}
0 &= D_1 - D_0 = -2(\alpha_{11} x_1 + \alpha_{12} x_2) + 2\alpha_{11}\alpha_{12} \ , \\
0 &= \widetilde{D}_1 - \widetilde{D}_0 = -2(\beta_{11} y_1 + \beta_{12} y_2) + 2\beta_{11}\beta_{12} \ , \\
0 &= \widehat{D}_1 - \widehat{D}_0 = \sum_{i=1}^{4} 2(x_i + y_i)(\gamma_{2i} - \gamma_{1i}) + 2(\gamma_{21}\gamma_{22} + \gamma_{23}\gamma_{24} - \gamma_{11}\gamma_{12} - \gamma_{13}\gamma_{14})
\end{aligned}$$

can be used to solve (x_1, y_2, x_2) as functions of five ISPs $(x_3, x_4, y_1, y_3, y_4)$. Remaining three quadratic equations $D_0 = 0, \widetilde{D}_0 = 0$ and $\widehat{D}_0$(After re-definition of $\widehat{D}_0 = \widehat{D}_0 - D_0 - \widetilde{D}_0$) could be equations with very complicated coefficients. Ideal $I(D_0, \widetilde{D}_0, \widehat{D}_0)$ of algebraic system is defined by

$$D_0(x_3, x_4) = 0 \ \ , \ \ \widetilde{D}_0(y_1, y_3, y_4) = 0 \ \ , \ \ \widehat{D}_0(x_3, x_4, y_1, y_3, y_4) = 0 \tag{4.43}$$

with five ISPs $(x_3, x_4, y_1, y_3, y_4)$.

We can compute Gröbner basis $G(I)$ with *Degree Lexicographic* monomial order and variable ordering $\{x_3, y_3, x_4, y_4, y_1\}$ in Mathematica. To determine integrand basis, we take all possible monomials $x_3^{d(x_3)} x_4^{d(x_4)} y_1^{d(y_1)} y_3^{d(y_3)} y_4^{d(y_4)}$ under renormalization conditions

$$\begin{aligned}
&d(x_3) + d(x_4) \leq 4 \ \ , \ \ d(y_1) + d(y_3) + d(y_4) \leq 4 \ , \\
&d(x_3) + d(x_4) + d(y_1) + d(y_3) + d(y_4) \leq 5 \ .
\end{aligned} \tag{4.44}$$

There are 225 solutions. Dividing these 225 monomials with Gröbner basis, and monomials in remainder of multivariate synthetic division define integrand basis. Depending on kinematic configurations, there are in total 6 types of integrand basis,

1. Kinematic configurations where at least one of K_4, K_5 is non-zero and K_1, K_2 are massive, there are 100 representative elements

$$\mathcal{B}^{I}_{C22} = \{1, x_3, x_4, x_3x_4, x_4^2, x_3x_4^2, x_4^3, x_3x_4^3, x_4^4, y_1, x_3y_1, x_4y_1, x_3x_4y_1, x_4^2y_1, x_3x_4^2y_1, x_4^3y_1, x_3x_4^3y_1, x_4^4y_1, y_1^2, x_3y_1^2, x_4y_1^2, x_4^2y_1^2, x_4^3y_1^2, y_1^3, x_3y_1^3, x_4y_1^3, x_4^2y_1^3, y_1^4, x_3y_1^4, x_4y_1^4, y_1^5, y_3, x_3y_3, x_4y_3, x_4^2y_3, x_4^3y_3, x_4^4y_3, y_1y_3, x_4y_1y_3, x_4^2y_1y_3, x_4^3y_1y_3, y_1^2y_3, x_4y_1^2y_3, y_1^3y_3, x_4y_1^3y_3, y_1^4y_3, y_3^2, x_3y_3^2, x_4y_3^2, y_1y_3^2, x_4y_1y_3^2, y_1^2y_3^2, x_4y_1^2y_3^2, y_1^3y_3^2, y_3^3, x_3y_3^3, x_4y_3^3, y_1y_3^3, x_4y_1y_3^3, y_1^2y_3^3, y_3^4, x_3y_3^4, x_4y_3^4, y_1y_3^4, y_3^5, y_4, x_4y_4, x_4^2y_4, x_4^3y_4, x_4^4y_4, y_1y_4, x_4y_1y_4, x_4^2y_1y_4, x_4^3y_1y_4, y_1^2y_4, x_4y_1^2y_4, x_4^2y_1^2y_4, y_1^3y_4, x_4y_1^3y_4, y_1^4y_4, y_4^2, x_4y_4^2, x_4^2y_4^2, x_4^3y_4^2, y_1y_4^2, x_4y_1y_4^2, x_4^2y_1y_4^2, y_1^2y_4^2, x_4y_1^2y_4^2, y_1^3y_4^2, y_4^3, x_4y_4^3, x_4^2y_4^3, y_1y_4^3, x_4y_1y_4^3, y_1^2y_4^3, y_4^4, x_4y_4^4, y_1y_4^4, y_4^5\} \ . \tag{4.45}$$

2. Kinematic configurations where at least one of K_4, K_5 is non-zero and K_1 is massive, K_2 is massless, there are 100 representative elements. The integrand basis is given by replacing one element from (4.45)

$$\mathcal{B}^{II}_{C22} = \mathcal{B}^{I}_{C22} - \{x_4^2y_4^3\} + \{x_4^2y_1^2y_3\} \ . \tag{4.46}$$

3. Kinematic configurations where at least one of K_4, K_5 is non-zero and K_1 is massless, there are 98 representative elements. The integrand basis is given by removing 17 elements from (4.45) while adding another 15 elements

$$\mathcal{B}^{III}_{C22} = \mathcal{B}^{I}_{C22} - \{x_3x_4, x_3x_4^2, x_3x_4^3, x_3x_4y_1, x_3x_4^2y_1, x_3x_4^3y_1, x_4^2y_3, x_4^3y_3, x_4^4y_3, x_4^2y_1y_3, x_4^3y_1y_3, y_3^5, x_4^2y_1y_4, x_4^3y_1y_4, x_4^2y_1^2y_4, x_4^2y_1y_4^2, y_4^5\} + \{x_3^2, x_3^3, x_3^4, x_3^2y_1, x_3^3y_1, x_3^4y_1, x_3^2y_1^2, x_3^3y_1^2, x_3^2y_1^3, x_3^2y_3, x_3^3y_3, x_3^4y_3, x_3^2y_3^2, x_3^3y_3^2, x_3^2y_3^3\} \ . \tag{4.47}$$

4. Kinematic configurations where both $K_4 = K_5 = 0$ and K_2 is massive, there are 96 representative elements. The integrand basis is given by removing 22 elements in (4.45) while adding another 18 elements

$$\mathcal{B}^{IV}_{C22} = \mathcal{B}^{I}_{C22} - \{x_3x_4, x_3x_4^2, x_3x_4^3, x_3x_4y_1, x_3x_4^2y_1, x_3x_4^3y_1, x_3y_1^2, x_4^2y_1^2, x_4^3y_1^2, x_3y_1^3, x_4^2y_1^3, x_3y_1^4, x_4^2y_3, x_4^3y_3, x_4^4y_3, x_4^2y_1y_3, x_4^3y_1y_3, y_1y_3^4, y_3^5, x_4^2y_1^2y_4, y_1y_4^4, y_4^5\} + \{x_3^2, x_3^3, x_3^4, x_3^2y_1, x_3^3y_1, x_3^4y_1, x_3^2y_3, x_3^3y_3, x_3^4y_3, x_3y_1y_3, x_3^2y_1y_3, x_3^3y_1y_3, x_3^2y_3^2, x_3^3y_3^2, x_3y_1y_3^2, x_3^2y_1y_3^2, x_3^2y_3^3, x_3y_1y_3^3\} \ . \tag{4.48}$$

5. Kinematic configurations where both $K_4 = K_5 = 0$ and K_2 is massless while at least one of K_1, K_3 is massive, there are 96 representative elements. The integrand

basis is given by replacing 9 elements in (4.48)

$$\mathcal{B}^{V}_{C22} = \mathcal{B}^{IV}_{C22} - \{x_4y_3^2, x_4y_1y_3^2, x_4y_1^2y_3^2, x_4y_3^3, x_4y_1y_3^3, x_4y_3^4, x_4y_1^2y_4, x_4y_1^3y_4, x_4y_1^2y_4^2\} + \{x_3y_1^2, x_3^2y_1^2, x_3^3y_1^2, x_4^2y_1^2, x_4^3y_1^2, x_3y_1^3, x_3^2y_1^3, x_4^2y_1^3, x_3y_1^4\} \ . \tag{4.49}$$

6. Kinematic configurations where both $K_4 = K_5 = 0$ and all K_1, K_2, K_3 are massless, there are 144 representative elements

$$\begin{aligned}\mathcal{B}^{VI}_{C22} = \{&1, x_1, x_1^2, x_1^3, x_1^4, x_2, x_1x_2, x_1^2x_2, x_1^3x_2, x_2^2, x_1x_2^2, x_1^2x_2^2, x_2^3, x_1x_2^3, x_2^4, y_1,\\
&x_1y_1, x_1^2y_1, x_1^3y_1, x_1^4y_1, x_2y_1, x_1x_2y_1, x_1^2x_2y_1, x_1^3x_2y_1, x_2^2y_1, x_1x_2^2y_1, x_1^2x_2^2y_1, x_2^3y_1,\\
&x_1x_2^3y_1, x_2^4y_1, y_1^2, x_1y_1^2, x_1^2y_1^2, x_1^3y_1^2, x_2y_1^2, x_1x_2y_1^2, x_1^2x_2y_1^2, x_2^2y_1^2, x_1x_2^2y_1^2, x_2^3y_1^2,\\
&y_1^3, x_1y_1^3, x_1^2y_1^3, x_2y_1^3, x_1x_2y_1^3, x_2^2y_1^3, y_1^4, x_1y_1^4, x_2y_1^4, y_2, x_1y_2, x_1^2y_2, x_1^3y_2, x_1^4y_2,\\
&x_2y_2, x_1x_2y_2, x_1^2x_2y_2, x_1^3x_2y_2, x_2^2y_2, x_1x_2^2y_2, x_1^2x_2^2y_2, x_2^3y_2, x_1x_2^3y_2, x_2^4y_2, y_1y_2,\\
&x_1y_1y_2, x_1^2y_1y_2, x_1^3y_1y_2, x_2y_1y_2, x_1x_2y_1y_2, x_1^2x_2y_1y_2, x_2^2y_1y_2, x_1x_2^2y_1y_2, x_2^3y_1y_2,\\
&y_1^2y_2, x_1y_1^2y_2, x_1^2y_1^2y_2, x_2y_1^2y_2, x_1x_2y_1^2y_2, x_2^2y_1^2y_2, y_1^3y_2, x_1y_1^3y_2, x_2y_1^3y_2, y_2^2, x_1y_2^2,\\
&x_1^2y_2^2, x_1^3y_2^2, x_2y_2^2, x_1x_2y_2^2, x_1^2x_2y_2^2, x_2^2y_2^2, x_1x_2^2y_2^2, x_2^3y_2^2, y_1y_2^2, x_1y_1y_2^2, x_1^2y_1y_2^2,\\
&x_2y_1y_2^2, x_1x_2y_1y_2^2, x_2^2y_1y_2^2, y_1^2y_2^2, x_1y_1^2y_2^2, x_2y_1^2y_2^2, y_2^3, x_1y_2^3, x_1^2y_2^3, x_2y_2^3, x_1x_2y_2^3,\\
&x_2^2y_2^3, y_1y_2^3, x_1y_1y_2^3, x_2y_1y_2^3, y_2^4, x_1y_2^4, x_2y_2^4, y_3, x_1y_3, x_1^2y_3, x_1^3y_3, x_1^4y_3, y_1y_3,\\
&x_1y_1y_3, x_1^2y_1y_3, x_1^3y_1y_3, y_1^2y_3, x_1y_1^2y_3, x_1^2y_1^2y_3, y_1^3y_3, x_1y_1^3y_3, y_3^2, x_1y_3^2, x_1^2y_3^2, x_1^3y_3^2,\\
&y_1y_3^2, x_1y_1y_3^2, x_1^2y_1y_3^2, y_1^2y_3^2, x_1y_1^2y_3^2, y_3^3, x_1y_3^3, x_1^2y_3^3, y_1y_3^3, x_1y_1y_3^3, y_3^4, x_1y_3^4\} \ .\end{aligned} \tag{4.50}$$

The number of representative elements for this topology is already very large, so primary decomposition of reducible ideal will play an important role in simplifying computation. Thus it is important to study irreducibility of ideal before carrying out computation.

4.4.2 Irreducibility of cut equations

For a transparent presentation of results, we use notation $\mathrm{C22}^{(L,N,R)}_{(U,P)}$ to denote various kinematic configurations. Each L, N, R can be either M or m, representing massive or massless momentum of K_1, K_3, K_2 respectively. U, P can be either K_4, K_5 or $\oslash$ if the corresponding one is zero. For example, $\mathrm{C22}^{(M,M,m)}_{(K_4,\oslash)}$ denotes kinematic configuration where K_1, K_3 are massive, K_2 is massless and K_5 is zero.

Depending on kinematic configurations, we can get 1, 2, 4 or 8 prime ideals after primary decomposition of ideal $I(D_0, \widetilde{D}_0, \widehat{D}_0)$. Detailed analysis is given below.

Kinematic configurations $\mathrm{C22}^{(L,N,R)}_{(K_4,K_5)}$

When K_4, K_5 are non-zero, we have 8 different kinematic configurations since each L, N, R has two possibilities M, m. For most general case $\mathrm{C22}^{(M,M,M)}_{(K_4,K_5)}$, ideal $I(D_0, \widetilde{D}_0, \widehat{D}_0)$ is irreducible. We can not further simplify this algebraic system. There is only one prime ideal with dimension two. Coefficients of 100 elements in integrand basis (4.45) should be computed at the same time using Gröbner basis method or parametrization method.

The ideal is reducible when some of K_1, K_2, K_3 are massless. For kinematic configurations

$$\mathrm{C22}^{(M,M,m)}_{(K_4,K_5)} \quad , \quad \mathrm{C22}^{(M,m,M)}_{(K_4,K_5)} \quad , \quad \mathrm{C22}^{(m,M,M)}_{(K_4,K_5)} \; , \tag{4.51}$$

there are two prime ideals after primary decomposition. For $K_1^2 = 0$, D_0 factorizes as $D_0 = x_3 x_4$. Similarly for $K_2^2 = 0$, $\widetilde{D}_0$ factorizes as $\widetilde{D}_0 = y_3 y_4$. For $K_3^2 = 0$, we can solve γ_{24} from

$$K_3^2 = (\gamma_{21} - \gamma_{11})(\gamma_{22} - \gamma_{12}) + (\gamma_{23} - \gamma_{13})(\gamma_{24} - \gamma_{14}) = 0 \; ,$$

After substituting the solution back to $\widetilde{D}_0, \widehat{D}_0$, we can further solve y_3, x_4. Then numerator of equation D_0 is factorized to two factors, which contributes to two inequivalent cut solutions. Let us take $\mathrm{C22}^{(M,M,m)}_{(K_4,K_5)}$ as example to analyze the intersection of prime ideals $I_1(D_0, y_3, \widehat{D}_0)$ and $I_2(D_0, y_4, \widehat{D}_0)$. Using Gröbner basis $G(I_1)$, we get 59 representative elements in integrand basis. Similarly, there are also 59 representative elements in integrand basis when using Gröbner basis $G(I_2)$. To study intersection of varieties $V(I_1)$ and $V(I_2)$, we compute Gröbner basis $G(I_1 \cup I_2)$. The ideal $I' = I_1 \cup I_2$ is one-dimensional, and 18 elements can be obtained by $G(I')$. So using both two prime ideals, we get $59 + 59 - 18 = 100$ representative elements in integrand basis of $I(D_0, \widetilde{D}_0, \widehat{D}_0)$, which agrees with the known result.

For kinematic configurations

$$\mathrm{C22}^{(M,m,m)}_{(K_4,K_5)} \quad , \quad \mathrm{C22}^{(m,m,M)}_{(K_4,K_5)} \quad , \quad \mathrm{C22}^{(m,M,m)}_{(K_4,K_5)} \; , \tag{4.52}$$

there are four prime ideals after primary decomposition of $I(D_0, \widetilde{D}_0, \widehat{D}_0)$. To see this, let us take $\mathrm{C22}^{(m,M,m)}_{(K_4,K_5)}$ for example. The massless conditions of K_1, K_2 reduce two cut equations to $D_0 = x_3 x_4$ and $\widetilde{D}_0 = y_3 y_4$. So we get four prime ideals $I_{11}(x_3, y_3, \widehat{D}_0)$, $I_{12}(x_4, y_3, \widehat{D}_0)$, $I_{21}(x_3, y_4, \widehat{D}_0)$ and $I_{22}(x_4, y_4, \widehat{D}_0)$. Using Gröbner basis of each prime ideal, we get 34 representative elements in integrand basis. Solutions for $(I_{11} \cup I_{12} \cup I_{21} \cup I_{22})$ are two points. We get the same two-point solution for

$$I_{11} \cup I_{12} \cup I_{21} \quad , \quad I_{11} \cup I_{12} \cup I_{22} \quad , \quad I_{11} \cup I_{21} \cup I_{22} \quad , \quad I_{12} \cup I_{21} \cup I_{22} \; .$$

Solutions of $I_{11} \cup I_{22}$ and $I_{12} \cup I_{21}$ are still the same two-point solution. However, solutions of $I_{11} \cup I_{12}$, $I_{11} \cup I_{21}$, $I_{21} \cup I_{22}$ and $I_{12} \cup I_{22}$ are four different one-dimensional curves. Using Gröbner basis of them, we get 10 representative elements in integrand basis for each one. So in total we get

$$\begin{aligned} B_I &= B_{I_{11}} + B_{I_{12}} + B_{I_{21}} + B_{I_{22}} - B_{I_{11}\cup I_{12}} - B_{I_{11}\cup I_{21}} - B_{I_{11}\cup I_{22}} - B_{I_{12}\cup I_{21}} \\ &\quad - B_{I_{12}\cup I_{22}} - B_{I_{21}\cup I_{22}} + B_{I_{11}\cup I_{12}\cup I_{21}} + B_{I_{11}\cup I_{12}\cup I_{22}} + B_{I_{11}\cup I_{21}\cup I_{22}} \\ &\quad + B_{I_{12}\cup I_{21}\cup I_{22}} - B_{I_{11}\cup I_{12}\cup I_{21}\cup I_{22}} \\ &= 34 \times 4 - 10 \times 4 - 2 \times 2 + 2 \times 4 - 2 = 98 \ , \end{aligned} \tag{4.53}$$

as it should be. The geometric picture for this intersection is quite hard to sketch. Briefly, four surfaces intersect at four curves adjacently, and these four curves share two common points.

For $\mathrm{C22}^{(m,m,m)}_{(K_4,K_5)}$, there are eight prime ideals after primary decomposition. Two cut equations can be factorized as $D_0 = x_3x_4$, $\widetilde{D}_0 = y_3y_4$, while the last cut equation $\widehat{D}_0$ can also be factorized as $\widehat{D}_0 = f_1f_2$, where f_i is linear function of $(x_3, x_4, y_1, y_3, y_4)$. 19 and 21 representative elements can be obtained by Gröbner basis of $I_1(x_3, y_3, f_1)$, $I_2(x_3, y_3, f_2)$ respectively(Similarly for $I_7(x_4, y_4, f_1)$ and $I_8(x_4, y_4, f_2)$). For remaining prime ideals $I_3(x_3, y_4, f_1)$, $I_4(x_3, y_4, f_2)$, $I_5(x_4, y_3, f_1)$, $I_6(x_4, y_3, f_2)$, using Gröbner basis of each one we can obtain 20 representative elements in integrand basis. We should further clarify intersection of eight varieties $V(I_i)$. No solution can be found for union of more than four ideals. Considering solution of four ideals, for the following six situations $I_1\cup I_2\cup I_3\cup I_4$, $I_5\cup I_6\cup I_7\cup I_8$, $I_1\cup I_2\cup I_5\cup I_6$, $I_3\cup I_4\cup I_7\cup I_8$, $I_1\cup I_3\cup I_6\cup I_8$ and $I_2\cup I_4\cup I_5\cup I_7$, solutions do exist, which are six points respectively. Solutions of equations from union of three prime ideals exist only when these three prime ideals coming from corresponding situation of four ideals. For example, single point solution exists for $I_1 \cup I_2 \cup I_3 \cup I_4$, and the same single point solution exists for $I_1 \cup I_2 \cup I_3$, $I_1 \cup I_2 \cup I_4$, $I_1 \cup I_3 \cup I_4$ or $I_2 \cup I_3 \cup I_4$. There are possibly $\binom{8}{2} = 28$ situations to be considered for solutions of every two prime ideals. The solutions could be one-dimension curves or points. In order to express results and also the number of representative elements computed by Gröbner basis, we use notation $V_i \cap V_j = (d|m)$ to denote intersection of two varieties, where $V_i = V(I_i)$ is the variety of prime ideal I_i. d is the dimension of prime ideal and m is the number of representative elements that can be obtained by Gröbner basis $G(I_i)$. All possible non-trivial solutions are given by

$$
\begin{aligned}
(1|6) &= V_1 \cap V_2 = V_2 \cap V_4 = V_2 \cap V_6 = V_3 \cap V_4 = V_3 \cap V_8 = V_5 \cap V_6 = V_6 \cap V_8 = V_7 \cap V_8 \ , \\
(1|5) &= V_1 \cap V_3 = V_1 \cap V_6 = V_4 \cap V_7 = V_5 \cap V_7 \ , \\
(0|1) &= V_1 \cap V_4 = V_1 \cap V_5 = V_1 \cap V_8 = V_2 \cap V_3 = V_2 \cap V_7 = V_3 \cap V_6 = V_3 \cap V_7 = V_4 \cap V_5 \\
&= V_4 \cap V_8 = V_5 \cap V_8 = V_6 \cap V_7 \ .
\end{aligned}
$$

Note that the one-dimensional curve solutions are all different.

Kinematic configurations $\mathbf{C22}^{(L,N,R)}_{K_4,\emptyset}$ or $\mathbf{C22}^{(L,N,R)}_{K_5,\emptyset}$

If K_4 or K_5 is zero, there is massless three-vertex even when other external momenta are massive. The ideal $I(D_0, \widetilde{D}_0, \widehat{D}_0)$ is reducible. For kinematic configuration of massive external momenta, we can get two prime ideals I_1, I_2 from primary decomposition. Using Gröbner basis of each prime ideal, we obtain 64 representative elements in integrand basis. Variety of $I_1 \cup I_2$ is one-dimensional curve, and using Gröbner basis $G(I_1 \cup I_2)$, we obtain 28 elements. So the total number of representative elements in integrand basis is $64 + 64 - 28 = 100$.

For kinematic configurations

$$
\text{C22}^{m,M,M}_{K_4/K_5,\emptyset} \ , \quad \text{C22}^{M,m,M}_{K_4/K_5,\emptyset} \ , \quad \text{C22}^{M,M,m}_{K_4/K_5,\emptyset} \ ,
$$

massless condition of K_1, K_2 or K_3 will further factorize cut equations. There are four prime ideals after primary decomposition. Let us take $\text{C22}^{M,M,m}_{K_4/K_5,\emptyset}$ as an example. The four prime ideals I_1, I_2, I_3, I_4 are 2-dimensional, and using Gröbner basis of each one, we can obtain 21 elements in integrand basis from $G(I_1)$ or $G(I_3)$, and 49 elements from $G(I_2)$ or $G(I_4)$. Variety of $I_1 \cup I_2 \cup I_3 \cup I_4$ is a single point. Variety of $I_1 \cup I_2 \cup I_4$ or $I_2 \cup I_3 \cup I_4$ is two points, while variety of $I_1 \cup I_2 \cup I_3$ or $I_1 \cup I_3 \cup I_4$ is single point. Geometrically, we can think that three surfaces $(V(I_1), V(I_2), V(I_4))$ or $(V(I_3), V(I_2), V(I_4))$ intersect at two points t_1, t_2 or t_1, t_3 respectively, with a common point t_1. This point is the solution of $I_1 \cup I_2 \cup I_3 \cup I_4$, as well as solutions of $I_1 \cup I_2 \cup I_3$ and $I_1 \cup I_3 \cup I_4$. There are 6 possible combination of two prime ideals. Among them, $I_1 \cup I_3$ has a single point solution, which is just t_1. Solutions of other combinations are one-dimensional. Using Gröbner basis $G(I_1 \cup I_2)$ or $G(I_3 \cup I_4)$ we can obtain 11 elements. Using Gröbner basis $G(I_1 \cup I_4)$ or $G(I_2 \cup I_3)$ we can obtain 6 elements, while using $G(I_2 \cup I_4)$ we can obtain 10 elements. We can make the counting that

$$
21 \times 2 + 49 \times 2 - 1 - 10 - 11 - 11 - 6 - 6 + 2 + 2 + 1 + 1 - 1 = 100 \ .
$$

For kinematic configurations

$$\mathrm{C22}^{m,m,M}_{K_4/K_5,\emptyset}\ ,\quad \mathrm{C22}^{m,M,m}_{K_4/K_5,\emptyset}\ ,\quad \mathrm{C22}^{M,m,m}_{K_4/K_5,\emptyset}\ ,$$

there are six prime ideals after primary decomposition. Taking $\mathrm{C22}^{m,M,m}_{K_4/K_5,\emptyset}$ as example. We can denote six prime ideals as $I_1(x_3,y_3,f_1)$, $I_2(x_3,y_3,f_2)$, $I_3(x_3,y_4,g_1)$, $I_4(x_4,y_3,g_2)$, $I_5(x_4,y_4,f_3)$ and $I_6(x_4,y_4,f_4)$, where f_i are linear functions and g_i are quadratic functions. Using $G(I_1)$ or $G(I_5)$ we can obtain 19 elements, using $G(I_2)$ or $G(I_6)$ we can obtain 21 elements, while using $G(I_3)$ or $G(I_4)$ we can obtain 34 elements. These six prime ideals are in fact decomposed from the four ideals of $\mathrm{C22}^{m,M,m}_{K_4,K_5}$, in the way that when K_4 or K_5 is zero, two of the four ideals become reducible. Prime ideals I_1,I_2 or I_5,I_6 are originated from these two reducible ideals. No solution exists for union of six prime ideals or of five prime ideals. A single point solution t_1 or t_2 exists for $I_1\cup I_3\cup I_4\cup I_5$ or $I_2\cup I_3\cup I_4\cup I_6$ respectively. The same single point solution also exists for union of three prime ideals that coming from above corresponding four prime ideals. Besides, different single point solution exists for $I_1\cup I_2\cup I_3$, $I_4\cup I_5\cup I_6$, $I_1\cup I_2\cup I_4$ and $I_3\cup I_5\cup I_6$. Solutions of two prime ideals could be points or one-dimensional curves. There is single point solution for $I_1\cup I_5$, $I_2\cup I_6$, and two points solution for $I_3\cup I_4$. Solutions of $I_3\cup I_2$, $I_3\cup I_6$, $I_4\cup I_2$, $I_4\cup I_6$, $I_1\cup I_2$ and $I_5\cup I_6$ are one-dimensional, and using Gröbner basis of them, we can obtain 6 elements for each one. While $I_3\cup I_1$, $I_3\cup I_5$, $I_4\cup I_1$ and $I_4\cup I_5$ are also one-dimensional, and using Gröbner basis we can obtain 5 elements for each one.

For kinematic configuration $\mathrm{C22}^{m,m,m}_{K_4/K_5,\emptyset}$, quadratic functions g_1,g_2 in previous section will further be factorized. So there are eight prime ideals after primary decomposition. More explicitly, besides the four prime ideals $I_1(x_3,y_3,f_1)$, $I_2(x_3,y_3,f_2)$, $I_7(x_4,y_4,f_3)$ and $I_8(x_4,y_4,f_4)$(which are the same as I_1,I_2,I_5,I_6 in previous section), we have another four prime ideals $I_3(x_3,y_4,g'_{11})$, $I_4(x_3,y_4,g'_{12})$, $I_5(x_4,y_3,g'_{21})$ and $I_6(x_4,y_3,g'_{22})$, where g' are linear functions. Using Gröbner basis of them, we can obtain 20 elements for each one. While $I_3\cup I_4$ or $I_5\cup I_6$ is one-dimensional, and using $G(I_3\cup I_4)$ or $G(I_5\cup I_6)$ we can obtain 6 elements. So we have $20+20-6=34$ elements, which agrees with the number of $I(x_3,y_4,g_1)$ or $I(x_3,y_4,g_2)$. There is a single point solution for union of eight prime ideals. The same single point solution exists for union of every seven, six, five, four or three prime ideals. For solutions of two prime ideals, we have

$$\begin{aligned}(1|6) &= V_1\cap V_2 = V_2\cap V_4 = V_2\cap V_5 = V_3\cap V_8 = V_6\cap V_8 = V_7\cap V_8 = V_3\cap V_4 = V_5\cap V_6\ ,\\ (1|5) &= V_1\cap V_3 = V_1\cap V_6 = V_4\cap V_7 = V_5\cap V_7\ ,\end{aligned}$$

and the same single point solution exists for other combinations of two prime ideals.

Kinematic configurations $\mathrm{C22}^{(L,N,R)}_{\emptyset,\emptyset}$

For this type of kinematic configurations, there are three external momenta. Because of momentum conservation, only two of them are independent. So we can still choose K_1, K_2 to generate momentum basis (e_1, e_2, e_3, e_4). Equations of maximal unitarity cut can be explicitly written as

$$\begin{aligned} D_0 &= x_3x_4 + \frac{\alpha_{11}\alpha_{12}}{\beta_{12}}(1-\frac{y_1}{\beta_{12}})y_1 = 0 \ , \\ \widetilde{D}_0 &= y_3y_4 + \beta_{11}(1-\frac{y_1}{\beta_{12}})y_1 = 0 \ , \\ \widehat{D}_0 &= x_4y_3 + x_3y_4 + \frac{\alpha_{12}\beta_{11}+\alpha_{11}\beta_{12}}{\beta_{12}}(1-\frac{y_1}{\beta_{12}})y_1 = 0 \ . \end{aligned} \tag{4.54}$$

For massive K_1, K_2, K_3, there are six prime ideals after primary decomposition, given by

$$\begin{aligned} &I_1^{C22^{(M,M,M)}_{(\emptyset,\emptyset)}}(y_3, x_3, y_1) \ , \quad I_2^{C22^{(M,M,M)}_{(\emptyset,\emptyset)}}(y_3, x_3, y_1-\beta_{12}) \ , \\ &I_3^{C22^{(M,M,M)}_{(\emptyset,\emptyset)}}(y_4, y_1, x_4) \ , \quad I_4^{C22^{(M,M,M)}_{(\emptyset,\emptyset)}}(y_4, y_1-\beta_{12}, x_4) \ , \\ &I_5^{C22^{(M,M,M)}_{(\emptyset,\emptyset)}}(y_3y_4+\beta_{11}(1-y_1/\beta_{12})y_1, y_3\alpha_{12}-x_3\beta_{12}, y_4\alpha_{11}-x_4\beta_{11}) \ , \\ &I_6^{C22^{(M,M,M)}_{(\emptyset,\emptyset)}}(y_3y_4+\beta_{11}(1-y_1/\beta_{12})y_1, -y_3\alpha_{11}+x_3\beta_{11}, y_4\alpha_{12}-x_4\beta_{12}) \ . \end{aligned} \tag{4.55}$$

Using Gröbner basis $G(I_i), i = 1,2,3,4$ we can obtain 19 representative elements in integrand basis, while using $G(I_i), i = 5,6$ we can obtain 36 elements. There is no solution for union of six or five prime ideals. A single point solution can be found for $I_2 \cup I_4 \cup I_5 \cup I_6$ or $I_1 \cup I_3 \cup I_5 \cup I_6$ respectively. The same single point solution can be found for unions of three prime ideals that coming from above corresponding four prime ideals. No solution exists for other combinations of three prime ideals. Considering union of two prime ideals, no solution can be found for $I_1 \cup I_2$, $I_1 \cup I_4$, $I_2 \cup I_3$ and $I_3 \cup I_4$, and a single point solution can be found for $I_1 \cup I_3$, double point solution can be found for $I_5 \cup I_6$. Solutions of remaining combinations of two prime ideals are one-dimensional curve.

For kinematic configurations

$$\begin{aligned} &\mathrm{C22}^{(m,M,M)}_{(\emptyset,\emptyset)} \ , \quad \mathrm{C22}^{(M,m,M)}_{(\emptyset,\emptyset)} \ , \quad \mathrm{C22}^{(M,M,m)}_{(\emptyset,\emptyset)} \ , \\ &\mathrm{C22}^{(m,m,M)}_{(\emptyset,\emptyset)} \ , \quad \mathrm{C22}^{(m,M,m)}_{(\emptyset,\emptyset)} \ , \quad \mathrm{C22}^{(M,m,n)}_{(\emptyset,\emptyset)} \ , \end{aligned}$$

there are still six prime ideals after primary decomposition. These ideals are the same as (4.55) for $\mathrm{C22}^{(m,M,M)}_{(\emptyset,\emptyset)}$, $\mathrm{C22}^{(M,m,M)}_{(\emptyset,\emptyset)}$, $\mathrm{C22}^{(m,m,M)}_{(\emptyset,\emptyset)}$. But for kinematic configurations $\mathrm{C22}^{(M,M,m)}_{(\emptyset,\emptyset)}$, $\mathrm{C22}^{(m,M,m)}_{(\emptyset,\emptyset)}$ and $\mathrm{C22}^{(M,m,m)}_{(\emptyset,\emptyset)}$, the first four prime ideals are still the same,

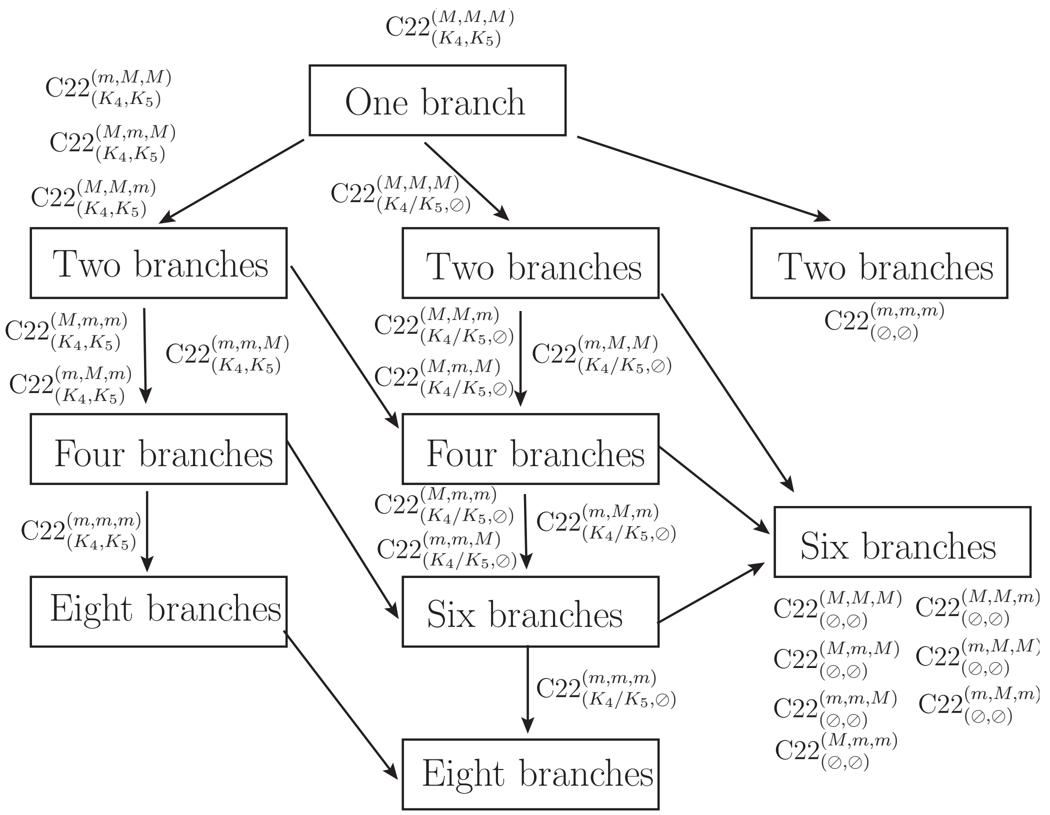

FIGURE 4.6: Irreducibility of ideal $I(D_0, \widetilde{D}_0, \widehat{D}_0)$ under different kinematic configurations. Branch denotes the prime ideal obtained by primary decomposition. The arrows indicate how reducible ideals are decomposed to prime ideals.

while the last two prime ideals are given by

$$
\begin{aligned}
I_5^{C22^{(M,M,m),(m,M,m),(M,m,m)}_{(\emptyset,\emptyset)}} & (y_3, -y_4\alpha_{12} + x_4\beta_{12}, x_3y_4 + \alpha_{11}(1 - y_1/\beta_{12})y_1) \ , \\
V_6^{C22^{(M,M,m),(m,M,m),(M,m,m)}_{(\emptyset,\emptyset)}} & (y_4, x_4y_3 + \alpha_{11}(1 - y_1/\beta_{12})y_1, -y_3\alpha_{12} + x_3\beta_{12}) \ .
\end{aligned} \tag{4.56}
$$

However, it dose not change the intersection among varieties of six prime ideals.

For the last kinematic configuration $C22^{(m,m,m)}_{(\emptyset,\emptyset)}$, we only have non-trivial solutions $|1\rangle \sim |2\rangle \sim |3\rangle$ or $|1] \sim |2] \sim |3]$ when momenta are complex. This means that K_1, K_2 can not used to define four momenta in the momentum basis. However, we can choose momentum basis as momenta K_1, K_2 and two arbitrary e_3, e_4 that satisfying

$$
K_1 \cdot K_2 = K_1 \cdot e_3 = K_2 \cdot e_4 = e_3 \cdot e_4 = 0 \ , \ K_1 \cdot e_4 = K_2 \cdot e_3 = 1 \ . \tag{4.57}
$$

With this momentum basis, the three linear equations are given by

$$
\begin{aligned}
& D_1 - D_0 = -2x_4 = 0 \ \ , \ \ \widetilde{D}_1 - \widetilde{D}_0 = -2y_4 = 0 \ , \\
& \widehat{D}_1 - \widehat{D}_0 = -2(x_4 + y_4) - 2(x_3 + y_3) = 0 \ ,
\end{aligned} \tag{4.58}
$$

with solution

$$x_4 = 0\ ,\ y_4 = 0\ ,\ x_3 = -y_3\ . \tag{4.59}$$

Remaining three quadratic equations are

$$\begin{aligned} D_0 &= 2(x_1x_4 + x_2x_3) = 0 \quad , \quad \widetilde{D}_0 = 2(y_1y_4 + y_2y_3) = 0\ , \\ \widehat{D}_0 &= 2(x_1 + y_1)(x_4 + y_4) + 2(x_2 + y_2)(x_3 + y_3) = 0\ . \end{aligned} \tag{4.60}$$

In the solution (4.59), $\widehat{D}_0 = 0$ automatically vanishes. So in fact there are only two independent quadratic equations

$$D_0 = x_2y_3 = 0 \quad , \quad \widetilde{D}_0 = y_2y_3 = 0\ . \tag{4.61}$$

Then algebraic system is defined by two quadratic equations of five ISPs $(x_1, x_2, y_1, y_2, y_3)$. The solution is no longer 2-dimensional. This is why we have 144 representative elements in integrand basis, which is much larger than those of other kinematic configurations. After primary decomposition of $I(x_2y_3, y_2y_3)$, we get two prime ideals $I_1(y_3)$ and $I_2(x_2, y_2)$. I_1 is 4-dimensional, and using Gröbner basis $G(I_1)$ we can obtain 114 elements. I_2 is 3-dimensional, and using $G(I_2)$ we can obtain 49 elements. $I_1 \cup I_2$ is 2-dimensional and we can obtain 19 elements. So using these two prime ideals, we obtain $114 + 49 - 19 = 144$ elements.

The numbers of prime ideals after primary decomposition for various kinematic configurations are summarized in Figure (4.6).

Chapter 5

Genus of curve from multi-loop amplitude

Maximal unitarity cut of a given diagram generates an algebraic system of polynomial equations. Solutions of these equations could describe point, curve or (hyper-)surface in complex plane. Solution of point is trivial to analyze, while solution of (hyper-)surface is too difficult to study. However, for complex curve, fruitful mathematics can be used to study its properties. In this chapter, we will focus on Feynman diagrams where solution of equations of maximal unitarity cut defines complex curve, and study the topological invariant genus of such curve using computational algebraic geometry.

5.1 From non-plane curve to plane curve

5.1.1 Birational map of non-plane curve to plane curve

In 4-dimensional theory, a L-loop diagram with $(4L-1)$ propagators generates equations of curve using maximal unitarity cut. This complex curve is defined by more than one quadratic equations, which is not favorable for genus computation. However, since geometric genus is birational invariant, we can birationally project the non-plane curve onto a plane, and compute the genus of plane curve, which is given by (3.70). If the curve is non-singular, i.e., it is smooth and has no singular points, then $g_G = g_A$, which is simply given by (3.68). Otherwise we should identify all singular points and their multiplicities, and also apply *blow up* process if singular points are not normal.

The way of mapping a non-plane curve defined by m quadratic equations with $(m+1)$ variables to plane curve defined by one polynomial equation with two variables is not unique. Any birational maps of variables leads to equivalent plane curves, and geometric genus keeps the same for all birational equivalent curves. An automatic way is to use elimination process with Gröbner basis method. To realize this process in Mathematica, let us assume that we have m quadratic equations $Q_i, i = 1, \ldots, m$ with $(m+1)$ variables $(X_1, X_2, \ldots, X_{m+1})$. The motivation is to get an equivalent plane curve $f(X_1', X_2') = 0$, where X_1', X_2' are arbitrary two variables from X_i, and the remaining variables are denoted as $X_3', \ldots, X_{m+1}'$. Then

1. Compute Gröbner basis $G(I)$ of ideal $I(Q_1, Q_2, \ldots, Q_m)$ with given monomial order, for example *Lexicographic*, and the ISP ordering $\{X_3', \ldots, X_{m+1}', X_1', X_2'\}$. This ordering is important, and we should put X_1', X_2' in the last two positions.

2. After getting a Gröbner basis with r polynomials $(g_1, g_2, \ldots, g_r)$, where g_i are polynomials of all or some variables from $(X_1, \ldots, X_{m+1})$, select the g_i whose variables have no common intersection with $(X_3', X_4', \ldots, X_{m+1}')$.

3. By this construction, usually there is only one g_i that can be selected from above step. We can define plane curve $f(X_1', X_2') = g_i$. Of course plane curve equations are different depending on the choice of X_1', X_2'. For some choices there could be no results, which means that we can not project non-plane curve onto plane curve with those two variables X_1', X_2'. Also for some choices we get a result, but the degree of plane curve is smaller than those from other choices of X_1', X_2'. In order to get a realistic result, it is suggested to repeat step 2 for all possible choices of X_1', X_2' from $(X_1, \ldots, X_{m+1})$, and use one of the plane curves $f(X_1', X_2')$ that has highest degree.

This elimination process using Gröbner basis method is systematic, but it is not explicit. We do not know the details of birational map that leads to birational equivalent plane curve. Another explicit but not quite systematic way of getting an equivalent plane curve can be taken as follows. If some of quadratic equations are conics, i.e., quadratic equation with two variables of the form

$$a_1 x^2 + a_2 xy + a_3 y^2 + a_4 x + a_5 y + a_6 = 0 \ , \tag{5.1}$$

with a_1, a_2, a_3 not all zero, we can take coordinate transformation $x \to X + b_1 Y$, $y \to Y + b_2 X$. In the coordinate (X, Y), we have

$$\begin{aligned}&(a_3 b_2^2 + a_2 b_2 + a_1) X^2 + (a_1 b_1^2 + a_2 b_1 + a_3) Y^2 + (a_2 + 2a_1 b_1 + 2a_3 b_2 + a_2 b_1 b_2) XY \\ &+ (a_4 + a_5 b_2) X + (a_5 + a_4 b_1) Y + a_6 = 0 \ .\end{aligned} \tag{5.2}$$

We can take b_1, b_2 as solutions of $a_3 b_2^2 + a_2 b_2 + a_1 = 0$ and $a_1 b_1^2 + a_2 b_1 + a_3 = 0$. So X^2, Y^2 terms disappear in the equation. Then it is trivial to write equation of conics as $Q' = x'y' - c = 0$ after linear coordinate transformations $x' \to x'(X)$, $y' \to y'(Y)$. In this case, one variable can be expressed as rational function of the other as $x' = c/y'$. Step by step, hopefully we can get meromorphic equations after using all equations of conics. If only one meromorphic equation is left, then the numerator of meromorphic equation defines an equivalent plane curve. Otherwise the curve is still defined by more than one polynomial equations, and we should further eliminate them by other methods.

5.1.2 Compute singular points and genus

Suppose finally we project non-plane curve onto a birational equivalent plane curve from above discussions as

$$F(X, Y) = 0 \;, \tag{5.3}$$

where the highest degree of monomials in $F(X, Y)$ is d. We assume ideal $I(F)$ is irreducible. If not, we should study the genus of each irreducible ideal after primary decomposition of $I(F)$. Primary decomposition is easy for ideal defined by one equation. We just factorize $F(X, Y)$, and each factor defines a prime ideal. For irreducible ideal $I(F)$, we can compute singular points of a curve $F(X, Y) = 0$ by definition (3.69). Practically, it is better to use projective plane curve. Introducing a third coordinate Z', we get a homogenous polynomial $P(X', Y', Z')$ of degree d that defines a projective plane curve

$$P(X', Y', Z') = (Z')^d F\left(\frac{X'}{Z'}, \frac{Y'}{Z'}\right) = 0 \;, \tag{5.4}$$

where $X = X'/Z', Y = Y'/Z'$. Let $Z' = 1$, we return to affine plane curve $F(X, Y) = P(X, Y, 1)$. Singular points are solutions of equations

$$P(X', Y', Z') = \frac{\partial P(X', Y', Z')}{\partial X'} = \frac{\partial P(X', Y', Z')}{\partial Y'} = \frac{\partial P(X', Y', Z')}{\partial Z'} = 0 \;. \tag{5.5}$$

If there is no solution, then plane curve is *smooth* and we can safely use $g_G = g_A$. If there are solutions, in order to apply formula (3.70) we should analyze the properties of singular points. The location of singular points could be at affine plane $Z' = 1$, given by solutions of

$$P(X', Y', 1) = \frac{\partial P(X', Y', 1)}{\partial X'} = \frac{\partial P(X', Y', 1)}{\partial Y'} = 0 \;. \tag{5.6}$$

Or it could be at the infinite $Z' = 0$, given by non-trivial solutions of

$$P(X', Y', 0) = \frac{\partial P(X', Y', 0)}{\partial X'} = \frac{\partial P(X', Y', 0)}{\partial Y'} = \frac{\partial P(X', Y', Z')}{\partial Z'}\Big|_{Z'=0} = 0 \ . \tag{5.7}$$

Since each monomial in homogeneous polynomial has degree d, the partial derivative of P has degree $(d-1)$. After setting $Z' = 0$, the non-zero terms of polynomial P are monomials $X^a Y^{d-a}$, and non-zero terms of $\partial P/\partial X', \partial P/\partial Y', \partial P/\partial Z'$ are monomials $X^a Y^{d-1-a}$. So above equations have a trivial solution $X' = 0, Y' = 0, Z' = 0$. The non-trivial solutions are given by $X' = X'_0, Z' = 0$ or $Y' = Y'_0, Z' = 0$. We have the freedom to define $Y' = 1$ or $X' = 1$ to get an affine plane curve.

In order to study properties of a singular point, we should compute tangent lines at the singular point. They are given by non-zero homogeneous part of lowest degree in Taylor series of polynomial at the singular point. Explicitly, for singular point at affine plane $(X', Y') = (X, Y) = (X_0, Y_0)$, we can expand the function of plane curve as

$$F(X + X_0, Y + Y_0) \ , \tag{5.8}$$

and tangent lines are defined by terms of lowest degree $T(X, Y)$ in above expansion. For singular point at infinite, for example $(X', Z') = (X'_0, 0)$, we can define $Y' = 1$ in projective plane curve $P(X', Y', Z')$, and expand it as

$$P(X' + X'_0, 1, Z') \ . \tag{5.9}$$

Tangent lines are defined by terms of lowest degree $T(X', Z')$ in above expansion. Equivalently, we can go back to affine plane curve by coordinate re-definition $X' = XY', Z' = ZY'$, and

$$F(X, Z) = \frac{1}{(Y')^d} P(XY', Y', ZY') \ . \tag{5.10}$$

The factor $1/(Y')^d$ cancels Y' in $P(XY', Y', ZY')$ and we get an affine plane curve $F(X, Z) = 0$ in coordinate (X, Z). So at coordinate $(X, Z) = (X'_0/Y', 0)$, the function of plane curve is expanded as

$$F(X + \frac{X'_0}{Y'}, Z) \ . \tag{5.11}$$

If singular point is normal, the multiplicity μ_p of singular point p equals to the degree of tangent line T, which is also the number of distinct solutions of tangent line equation $T = 0$. For polynomial T of degree d_T, there would be d_T solutions for $T = 0$. However, number of distinct solutions of $T = 0$ could be smaller than degree of T. For example, if $T(X, Z) = (X + Z)^2 = 0$, degree of T is two, but the two solutions $X + Z = 0$ and

$-(X+Z)=0$ are the same. So there is only one distinct solution, and two tangent lines are not distinct. A singular point is normal if all tangent lines at the singular point are distinct. A singular point is non-normal if there are non-distinct tangent lines, which means that the number of distinct solutions of $T=0$ is smaller than the degree of T. For non-normal singular points, the multiplicity μ_p is no longer given by degree of tangent line T or the number of distinct solutions of tangent line equation $T=0$.

To study properties of non-normal singular point, we need to perform *blow up* process. Suppose we have a non-normal singular point at $(X',Y',Z')=(X'_0,Y'_0,1)$(discussion of singular point at infinite is the same), and plane curve is expanded as

$$F(X,Y)=P(X'=X,Y'=Y,1)|_{X\to X+X'_0,Y\to Y+Y'_0}=P(X+X'_0,Y+Y'_0,1)\ . \quad (5.12)$$

So singular point $(X',Y')=(X'_0,Y'_0)$ has been transferred to $(X,Y)=(0,0)$. There is no constant term in above expansion, since by definition $F(X,Y)=0$ at singular point $(X,Y)=(0,0)$. So we can assume

$$F(X,Y)=\sum_{d'=d_T}^{d}\sum_{a=0}^{d'}c_{d',a}X^aY^{d'-a}\ , \quad (5.13)$$

where d is degree of $F(X,Y)$, and d_T is the lowest degree of monomials. The function of tangent line is defined as

$$T(X,Y)=\sum_{a=0}^{d_T}c_{d_T,a}X^aY^{d_T-a}\ . \quad (5.14)$$

Assume $T(X,Y)=0$ has s distinct solutions, where $s<d_T$ since it is a non-normal singular point. We can blow up the singular point by defining a new variable t through $Y=Xt$. Then

$$F(X,Xt)=\sum_{d'=d_T}^{d}\sum_{a=0}^{d'}c_{d',a}X^{d'}t^{d'-a}=X^{d_T}\sum_{d'=d_T}^{d}\sum_{a=0}^{d'}c_{d',a}X^{d'-d_T}t^{d'-a}\ . \quad (5.15)$$

We can always take out a factor X^{d_T}, and define a new plane curve $F'(X,t)$ as

$$F'(X,t)=X^{-d_T}F(X,Xt)=\sum_{d'=d_T}^{d}\sum_{a=0}^{d'}c_{d',a}X^{d'-d_T}t^{d'-a}\ . \quad (5.16)$$

The new curve $F'(X,t)=0$ is birational equivalent to original curve $F(X,Y)=0$. To get singular points for $F'(X,t)=0$, we can set $X'=X'_0$, or equivalently $X=0$, and solve equation

$$F'(X,t)|_{X=0} = 0 \ . \tag{5.17}$$

The non-zero terms of $F'(0,t)$ is given by $d' = d_T$. So we have

$$F'(0,t) = \sum_{a=0}^{d_T} c_{d_T,a} t^{d_T-a} \ . \tag{5.18}$$

It is a polynomial of degree d_T. Equation $F'(0,t) = 0$ still has s distinct solutions $t_i, i = 1, \ldots, s$, since coordinate transformation does not change properties of solutions. However, singular point of $P(X',Y',Z') = 0$ at $(X',Y',Z') = (X'_0, Y'_0, 1)$ which has s distinct tangent lines, has blown up to s singular points of $F'(X,t) = 0$ at $(X,t) = (0,t_i)$, $i = 1, \ldots, s$. We can compute tangent lines at these singular points if all of them are normal. If certain singular points are still non-normal, we can blow up them again until all singular points are normal. In the genus computation, we should count all normal singular points and non-normal singular points of the original plane curve, and also the non-normal singular points and normal singular points of plane curves after blowing up certain non-normal singular points. More explicitly, for a non-normal singular point with tangent line of degree d_T which is blown up to s normal singular points p_i^{non}, we should minus

$$\frac{1}{2} d_T(d_T - 1) + \sum_{i=1}^{s} \frac{1}{2} \mu_{p_i^{non}} (\mu_{p_i^{non}} - 1) \tag{5.19}$$

in the genus computation formula (3.70), in order to get the correct geometric genus.

5.2 Genus of curve from two-loop diagrams

In this section, we present results of 4-dimensional two-loop diagrams. All 4-dimensional two-loop topologies have been given in Chapter 4. The topologies that having seven propagators will generate equations of complex curve in maximal unitarity cut. They are box-triangle topology (A43) in Figure (4.3), planar penta-triangle topology (B42), planar double-box topology (B33) in Figure (4.4), and non-planar crossed-box topology (C32) in Figure (4.5). Topology (A43) is trivial. Cut equations of sub-one-loop box topology completely fix solution of loop momenta ℓ_1. With this solution, the remaining equations are equivalent to cut equations of one-loop triangle topology. So we get three quadratic equations, and from which we can construct two linear equations. After solving two linear equations, we get an equivalent plane curve, which is an equation of conics. The conics is birational equivalent to genus-0 Riemann sphere. Topology (B42) is also trivial. Cut equations of four propagators that containing only ℓ_1 will complete fix solution of ℓ_1. With this solution, the remaining three equations are again equivalent to cut equations of one-loop triangle topology. So it has genus-0 for each solution of ℓ_1. Topologies (B42) and (C32) are not trivially genus 0, and we will present the results below.

5.2.1 Genus of planar double-box diagram

The algebraic system of maximal unitarity cut under general kinematic configuration can be reduced to an equivalent algebraic system with three quadratic equations

$$Q_1(x_1, x_2) = 0 \quad , \quad Q_2(y_1, y_2) = 0 \quad , \quad Q_3(x_1, x_2, y_1, y_2) = 0 \; , \tag{5.20}$$

as we have intensively discussed in Chapter 4. Further eliminating two equations and two variables via Gröbner basis method, we get a birational equivalent plane curve. This plane curve has degree 8, so the arithmetic genus is

$$g_A = \frac{(d-1)(d-2)}{2} = 21 \; . \tag{5.21}$$

Computing singular points and tangent lines at these singular points, we find 8 singular points of multiplicity $\mu_p = 2$ and 2 singular points of multiplicity $\mu_p = 4$. So the geometric genus is

$$g_G = g_A - \sum_{p \in Sing(C)} \frac{1}{2}\mu_p(\mu_p - 1) = 21 - 8 \times 1 - 2 \times 6 = 1 \; . \tag{5.22}$$

This result is consistent with that in [42].

Notice that $Q_1 = 0, Q_2 = 0$ are conics, we can explicitly birational map non-plane curve to plane curve without using Gröbner basis. Through linear coordinate transformation, it is easy to write $Q_1 \to Q'_1 = x'_1 x'_2 - c_1$ and $Q_2 \to Q'_2 = y'_1 y'_2 - c_2$. So we can do the following substitutions $x'_1 = c_1/x'_2, y'_1 = c_2/y'_2$ in Q_3. The quadratic terms in Q_3 are transferred by

$$x'_1 y'_1 \to \frac{c_1 c_2}{x'_2 y'_2} \quad , \quad x'_1 y'_2 \to \frac{c_1 y'_2}{x'_2} \quad , \quad x'_2 y'_1 \to \frac{c_2 x'_2}{y'_2} \quad , \quad x'_2 y'_2 \to x'_2 y'_2 \; , \tag{5.23}$$

after substitution. The resulting Q'_3 is a meromorphic function

$$Q'_3 = \frac{n(x'_2, y'_2)}{d(x'_2, y'_2)} \; , \tag{5.24}$$

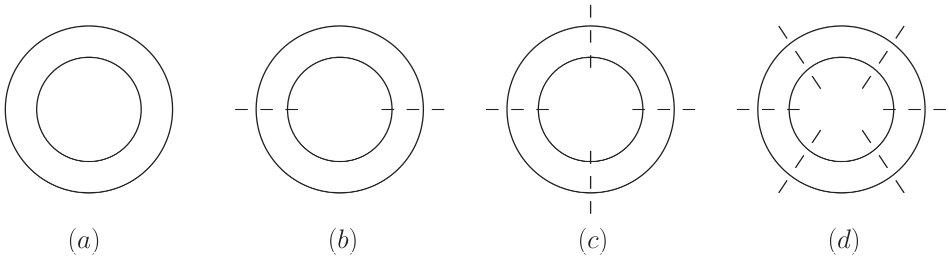

FIGURE 5.1: Degenerate topological pictures of cut equations for two-loop double-box diagram. Tubes of torus is shrunk to points along the dashed line, for given kinematic configurations.

where $n(x'_2, y'_2)$ has degree 4 and $d(x'_2, y'_2)$ has degree 2. The numerator $n(x'_2, y'_2) = 0$ defines a birational equivalent plane curve. We have arithmetic genus $g_A = 3(3-1)/2 = 3$. There are 2 singular points of multiplicity $\mu_p = 2$. Thus we again get geometric genus $g_G = 3 - 2 = 1$.

Topological picture of genus

The ideal of cut equations is usually reducible under many specific kinematic configurations. Genus computation is only for irreducible ideal. If the ideal is reducible, we should compute genus of prime ideals after primary decomposition. Then connection of genus among different prime ideals should also be studied. Complex curve of genus-1 is topological equivalent to a torus, so topological picture of genus for reducible ideal should be deduced from shrinking tube of torus to points. These points separate torus to many parts, which correspond to prime ideals. For torus with one hole, the topological picture is simple. The shrinking of tubes will break the hole, and we should get genus-0 Riemann spheres connected at points. Above argument is indeed true. After computing genus of each prime ideal after primary decomposition, we find that they all have genus-0. The three types of shrinking are shown in Figure (5.1). The dashed lines are shrunk to points and the Riemann spheres separated by these points have no possibility of forming holes. So they could only be genus-0. There are two, four and six Riemann spheres connected by points and linked adjacently into a chain, corresponding to the number of prime ideals under specific kinematic configurations. This topological picture is exactly the same as described in [42].

5.2.2 Genus of non-planar crossed-box diagram

Let us consider (C32) in Figure (4.5). Using K_1, K_3 to generate momentum basis (e_1, e_2, e_3, e_4), we write equations of maximal unitarity cut as four linear equations

$$\begin{aligned}
L_1 &= 2(\alpha_{11}x_1 + \alpha_{12}x_2 - \alpha_{11}\alpha_{12}) = 0 \ , \\
L_2 &= 2(\alpha_{21}x_1 + \alpha_{22}x_2 + \alpha_{23}x_3 + \alpha_{24}x_4 - \alpha_{21}\alpha_{22} - \alpha_{23}\alpha_{24}) = 0 \ , \\
L_3 &= 2(\beta_{11}y_1 + \beta_{12}y_2 - \beta_{11}\beta_{12}) = 0 \ , \\
L_4 &= -2\sum_{i=1}^{4}(x_i + y_i)(\gamma_{2i} - \gamma_{1i}) - 2(\gamma_{21}\gamma_{22} + \gamma_{23}\gamma_{24} - \gamma_{11}\gamma_{12} - \gamma_{13}\gamma_{14}) = 0 \ ,
\end{aligned}$$

and three quadratic equations

$$\begin{aligned}
&Q_1 = 2(x_1x_2 + x_3x_4) = 0 \quad , \quad Q_2 = 2(y_1y_2 + y_3y_4) = 0 \ , \\
&Q_3 = 2(x_1y_2 + x_2y_1 + x_3y_4 + x_4y_3) + 2\sum_{i=1}^{4}(x_i + y_i)\gamma_{1i} + 2(\gamma_{11}\gamma_{12} + \gamma_{13}\gamma_{14}) = 0 \ .
\end{aligned}$$

Four linear equations can be solved to express four variables as functions of remaining four variables. The choice of remaining four variables is not unique, and we can get different curves from different ways of solving linear equations. However, they are all birational equivalent. So we can choose the most convenient way to solve four linear equations.

Suppose we have solved four linear equations, and remaining three quadratic equations of four variables (x_1, x_2, y_1, y_2)

$$Q_1(x_1, x_2) = 0 \quad , \quad Q_2(x_1, x_2, y_1, y_2) = 0 \quad , \quad Q_3(x_1, x_2, y_1, y_2) = 0 \tag{5.25}$$

define a complex curve. Since only one equation $Q_1 = 0$ is conics, it is not explicit to project it to plane curve by trivial coordinate transformation as described for planar double-box diagram. We can still take coordinate transformation for Q_1 and express $x'_2 = c_1/x'_1$. Then Q_2, Q_3 become meromorphic functions $Q'_2(x'_1, y_1, y_2)$, $Q'_3(x'_1, y_1, y_2)$, and numerators of them have degree four. Numerators of $Q'_2 = 0, Q'_3 = 0$ define an equivalent curve, and we can project this non-plane curve onto plane curve by elimination process via Gröbner basis method. We can also get a plane curve by computing the *resultant*. Numerators of $Q'_2 = 0, Q'_3 = 0$ can be written as

$$\begin{aligned}
a_2(x'_1, y_1)y_2^2 + a_1(x'_1, y_1)y_2 + a_0(x'_1, y_1) = 0 \ , \\
b_2(x'_1, y_1)y_2^2 + b_1(x'_1, y_1)y_2 + b_0(x'_1, y_1) = 0 \ ,
\end{aligned} \tag{5.26}$$

where a_i, b_i are quadratic functions. Then we can eliminate y_2 by computing *resultant* of above two equations, and get a plane curve equation $F(x_1', y_1) = 0$. This plane curve is birational equivalent to (5.26) via the inverse map

$$y_2 = \frac{-a_2(x_1', y_1)b_0(x_1', y_1) + a_0(x_1', y_1)b_2(x_1', y_1)}{a_2(x_1', y_1)b_1(x_1', y_1) - a_1(x_1', y_1)b_2(x_1', y_1)} \ . \tag{5.27}$$

So they have the same geometric genus. The resulting plane curve $F(x_1', y_1) = 0$ has degree $d = 8$, so the arithmetic genus is

$$g_A = \frac{1}{2}(d-1)(d-2) = 21 \ . \tag{5.28}$$

There are 18 normal singular points of multiplicity $\mu_p = 2$, so the geometric genus is

$$g_G = g_A - \sum_{p \in Sing(C)} \frac{1}{2}\mu_p(\mu_p - 1) = 21 - 18 \times 1 = 3 \ . \tag{5.29}$$

So the curve is associated to a genus-3 Riemann surface, which is topologically equivalent to a torus with three holes.

Topological picture of genus

For general kinematics, ideal of cut equations is irreducible. So the genus of curve is 3, and the topological picture is sketched in Figure (5.2.a). Under specific kinematic configurations, the ideal is reducible. So we should study each prime ideal via primary decomposition and also the degenerate topological pictures.

We begin analysis with kinematic configuration where reducible ideal can be decomposed to two prime ideals. There are two types of kinematic configurations we need to consider, and each type gives different degenerate topological pictures.

1. Kinematic configurations where at least one momentum of K_1, K_2 is massless while others are general. For $K_1^2 = 0$, Q_1 factorizes as $Q_1 = x_3x_4$, and for $K_2^2 = 0$, Q_1 factorizes as $Q_1 = f_1(x_3, x_4)f_2(x_3, x_4)$, where f_1, f_2 are linear polynomials of (x_3, x_4). So we get two prime ideals $I_1(f_1, Q_2, Q_3)$, $I_2(f_2, Q_2, Q_3)$ via primary decomposition. We can project the curve of each ideal to plane curve either by coordinate transformation or by Gröbner basis method. The plane curve has degree 4 and two normal singular points of multiplicity $\mu_p = 2$, so

$$g_G = 3 - 2 \times 1 = 1 \ .$$

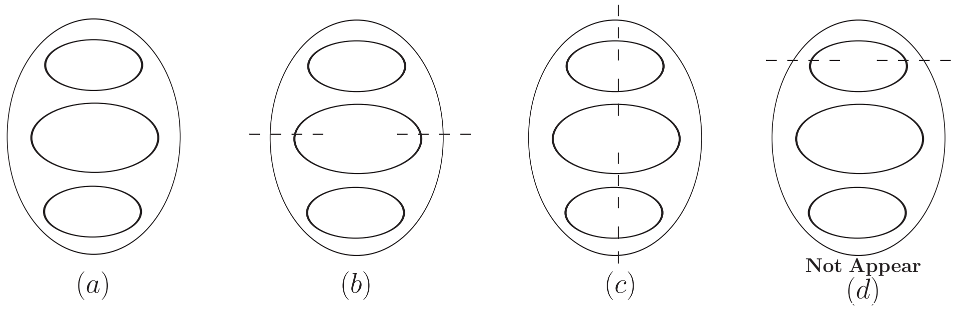

FIGURE 5.2: Degenerate topological pictures of cut equations for non-planar two-loop crossing-box diagram.

Varieties $V(I_1)$ and $V(I_2)$ intersect at two points. So the topological picture is given by shrinking two tubes to points along the dashed lines as shown in Figure (5.2.b).

2. Kinematic configurations where only one of K_3, K_4 is massless or only one of K_5, K_6 is zero, while others are general. Ideal of cut equations are reducible, and can be decomposed to two prime ideals. It is easy to see that, for $K_3^2 = 0$, since $Q_2 = y_3y_4$, we get two prime ideals directly from $Q_2 = 0$. For other kinematic configurations, factorization of $I(Q_1, Q_2, Q_3)$ is not obvious. We can decompose it via primary decomposition by Macaulay2[120]. Anyway, we get two prime ideals I_1, I_2. Using equations of each ideal, we can project the curve onto plane curve. Each plane curve has degree 4, and there are three normal singular points of multiplicity $\mu_p = 2$. So the geometric genus is

$$g_G = 3 - 3 \times 1 = 0 \ .$$

Solution of $I = I_1 \cup I_2$ is four points, so the topological picture is given by shrinking 4 tubes to points along dashed lines as shown in Figure (5.2.c).

Note that from topological picture of genus-3 torus, naively there is another degenerate topological picture as shown in Figure (5.2.d). It is associated to reducible ideal where two prime ideals via primary decomposition define genus-2 and genus-0 complex curves. However, no kinematic configuration leads to this degenerate topological picture. We can explain this as consequence of symmetry between two prime ideals by parity symmetry, so they should have the same genus.

The ideal $I(Q_1, Q_2, Q_3)$ could be decomposed to four, six and eight prime ideals via primary decomposition under other specific kinematic configurations. The topological picture of them can be explained as consequence of overlapping Figure (5.2.b) and (5.2.c). We again denote kinematic configurations as $\text{C32}^{(L,N,R)}_{(U,P)}$, where

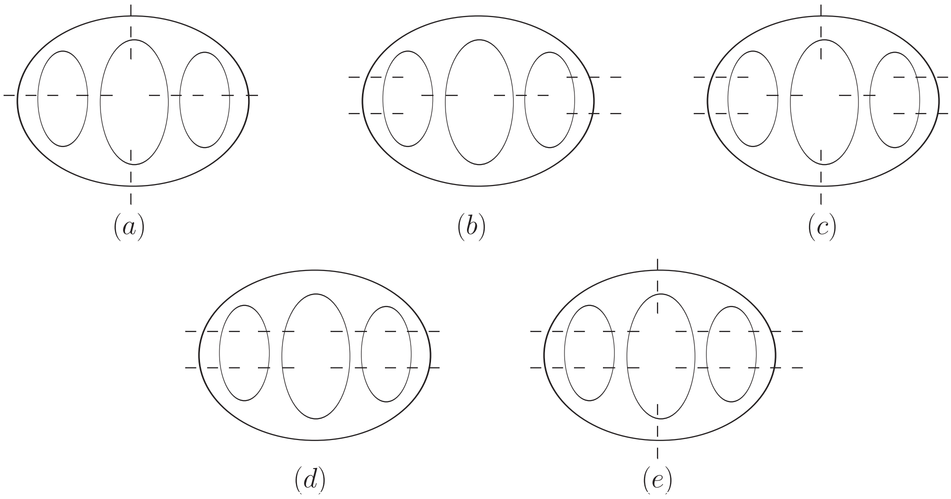

FIGURE 5.3: More degenerate topological pictures of cut equations for non-planar two-loop crossing-box diagram.

- $L = m$ if at least one of K_1, K_2 is massless, otherwise $L = M$,
- $R = m$ if K_3 is massless, otherwise $R = M$,
- $N = m$ if K_4 is massless, otherwise $N = M$,
- $U = \oslash$ if $K_5 = 0$, otherwise $U = K_5$,
- $P = \oslash$ if $K_6 = 0$, otherwise $P = K_6$.

For $L = m$, i.e., $\mathrm{C32}^{(m,M,M)}_{(K_5,K_6)}$, the topological picture is degenerated in the way as shown in Figure (5.2.b), and for other cases $\mathrm{C32}^{(M,m,M)}_{(K_5,K_6)}$, $\mathrm{C32}^{(M,M,m)}_{(K_5,K_6)}$, $\mathrm{C32}^{(M,M,M)}_{(K_5,\oslash)}$ or $\mathrm{C32}^{(M,M,M)}_{(\oslash,K_6)}$, the topological picture is degenerated in the way as shown in Figure (5.2.c). The degenerate topological picture for more than two prime ideals can be determined by combining above conditions.

Explicitly, if we combine massless condition $L = m$ with another condition of $N = m$, $R = m$, $U = \oslash$ or $P = \oslash$, i.e., for kinematic configurations

$$\mathrm{C32}^{(m,M,m)}_{(K_5,K_6)} \quad , \quad \mathrm{C32}^{(m,m,M)}_{(K_5,K_6)} \quad , \quad \mathrm{C32}^{(m,M,M)}_{(K_5,\oslash)} \quad , \quad \mathrm{C32}^{(m,M,M)}_{(\oslash,K_6)} \quad ,$$

the topological picture is given by overlapping of (5.2.b) and (5.2.c), as shown in (5.3.a). This gives four genus-0 Riemann spheres, which indicates that in these kinematic configurations, the ideal can be decomposed to four prime ideals. Each prime ideal defines a genus-0 curve. If we combine one condition $N = m$ or $R = m$ with another condition $U = \oslash$ or $P = \oslash$, i.e., for kinematic configurations

$$\mathrm{C32}^{(M,M,m)}_{(K_5,\oslash)} \quad , \quad \mathrm{C32}^{(M,M,m)}_{(\oslash,K_6)} \quad , \quad \mathrm{C32}^{(M,m,M)}_{(K_5,\oslash)} \quad , \quad \mathrm{C32}^{(M,m,M)}_{(\oslash,K_6)} \quad ,$$

the topological picture is given by overlapping two copies of Figure (5.2.c). There are four dashed lines as shown in Figure (5.2.c). When overlapping two copies of (5.2.c) in these kinematic configurations, the middle two dashed lines coincide with each other. So the resulting topological picture is as shown in (5.3.b). Again this gives four genus-0 Riemann spheres.

It is not hard to conclude that Figure (5.3.c) is the overlapping of Figure (5.2.b) and (5.3.b). So this degenerate topological picture should be given by kinematic configurations

$$\mathrm{C32}^{(m,M,m)}_{(K_5,\oslash)}\ ,\ \mathrm{C32}^{(m,M,m)}_{(\oslash,K_6)}\ ,\ \mathrm{C32}^{(m,m,M)}_{(K_5,\oslash)}\ ,\ \mathrm{C32}^{(m,m,M)}_{(\oslash,K_6)}\ .$$

It has six genus-0 Riemann spheres, which means that ideal of cut equations can be decomposed to six prime ideals. For kinematic configurations with both $N = R = m$ or $U = P = \oslash$, i.e., $\mathrm{C32}^{(M,m,m)}_{(K_5,K_6)}$ or $\mathrm{C32}^{(M,M,M)}_{(\oslash,\oslash)}$, the topological picture is then directly given by overlapping two copies of (5.2.c) without any coinciding lines, as shown in Figure (5.3.d). It also gives six genus-0 Riemann spheres. In fact, even if imposing more conditions of N, R, U or P, the extra dashed lines will coincide with these eight dashed lines as shown in Figure (5.3.d). So the following kinematic configurations

$$\mathrm{C32}^{(M,m,m)}_{(K_5,\oslash)}\ ,\ \mathrm{C32}^{(M,m,m)}_{(\oslash,K_6)}\ ,\ \mathrm{C32}^{(M,M,m)}_{(\oslash,\oslash)}\ ,\ \mathrm{C32}^{(M,m,M)}_{(\oslash,\oslash)}\ ,\ \mathrm{C32}^{(M,m,m)}_{(\oslash,\oslash)}$$

give the same topological picture (5.3.d).

Finally, we can overlap Figure (5.2.b) and (5.3.d). This corresponds to setting $L = m$ in the kinematic configurations of Figure (5.3.d). So for

$$\begin{array}{l}\mathrm{C32}^{(m,m,m)}_{(K_5,K_6)}\ ,\ \mathrm{C32}^{(m,M,M)}_{(\oslash,\oslash)}\ ,\ \mathrm{C32}^{(m,m,m)}_{(K_5,\oslash)}\ ,\ \mathrm{C32}^{(m,m,m)}_{(\oslash,K_6)}\ ,\\ \mathrm{C32}^{(m,M,m)}_{(\oslash,\oslash)}\ ,\ \mathrm{C32}^{(m,m,M)}_{(\oslash,\oslash)}\ ,\ \mathrm{C32}^{(m,m,m)}_{(\oslash,\oslash)}\ ,\end{array}$$

the topological picture is given by Figure (5.3.e). There are eight genus-0 Riemann spheres. The primary decomposition of ideal $I(Q_1, Q_2, Q_3)$ indeed gives eight prime ideals. From explicit computation, we get geometric genus-0 for all curves defined by prime ideals. The computation agrees with above analysis.

5.3 Genus of curve from three-loop diagrams

The algebraic system of cut equations from three-loop diagrams is more complicated than that of two-loop diagrams. However, the computation process is similar. For 4-dimensional theory, we should consider diagrams with 11 propagators. Equations of

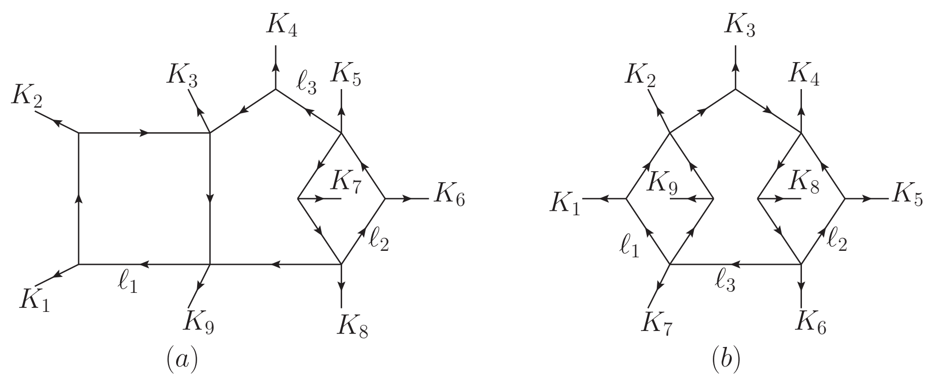

FIGURE 5.4: (a) Non-planar three-loop box-crossed-pentagon diagram, (b) Non-planar three-loop crossed-crossed-pentagon diagram. All external momenta are out-going and massive. Loop momenta are denoted by ℓ_1, ℓ_2, ℓ_3.

maximal unitarity cut then define a complex curve. We will birational project the curve onto plane curve, and compute the geometric genus from arithmetic genus and knowledge of singular points. A complete analysis of three-loop diagrams involves too many topologies, and here we present results of some selected diagrams to illustrate the computation and analysis.

5.3.1 Genus of non-planar box-crossed-pentagon diagram

We discuss three-loop box-crossed-pentagon diagram as shown in Figure (5.4.a) in this section. Maximal unitarity cut gives 11 cut equations of 12 variables, and they define a complex curve. As usual, we can choose two external momenta to construct momentum basis (e_1, e_2, e_3, e_4), and expand cut equations with variables defined by expansion coefficients of three loop momenta. The 11 propagators are given by

$$\begin{aligned}
&\text{Only } \ell_1 \ : \ D_0 = \ell_1^2 \ , \ D_1 = (\ell_1 - K_1)^2 \ , \ D_2 = (\ell_1 - K_1 - K_2)^2 \ , \\
&\text{Only } \ell_2 \ : \ \widetilde{D}_0 = \ell_2^2 \ , \ \widetilde{D}_1 = (\ell_2 - K_6)^2 \ , \\
&\text{Only } \ell_3 \ : \ \bar{D}_0 = \ell_3^2 \ , \ \bar{D}_1 = (\ell_3 - K_4)^2 \ , \ \bar{D}_2 = (\ell_3 - K_1 - K_2 - K_3 - K_4 - K_9)^2 \ , \\
&\text{Mixed } \ell_2, \ell_3 \ : \ \widehat{D}_0 = (\ell_2 - \ell_3 - K_5 - K_6)^2 \ , \ \widehat{D}_1 = (\ell_2 - \ell_3 - K_5 - K_6 - K_7)^2 \ , \\
&\text{Mixed } \ell_1, \ell_3 \ : \ \widehat{D}_2 = (\ell_1 + \ell_3 - K_1 - K_2 - K_3 - K_4)^2 \ .
\end{aligned}$$

It is easy to see that from them we can construct six linear equations. Then six variables can be solved as functions of remaining six variables. The remaining five quadratic equations of six variables define an equivalent complex curve. Using elimination process via Gröbner basis method, we can project the curve onto an equivalent plane curve, and compute its singular points.

We can also analyze the birational map step by step. Since equation of conics can always be rational parameterized, so from three cut equations $D_0 = D_1 = D_2 = 0$, we can rationally parameterize ℓ_1 by one free parameter x. From three cut equations $\bar{D}_0 = \bar{D}_1 = \bar{D}_2 = 0$, we can also rationally parameterize ℓ_3 by one free parameter w. However, there are only two propagators containing ℓ_2. So using $\widetilde{D}_0 = \widetilde{D}_1 = 0$, we rationally parameterize ℓ_2 by two free parameters y, z. By substituting $\ell_1(x), \ell_2(y,z), \ell_3(w)$ back to the remaining three mixed loop momenta propagators, they become meromorphic functions. The numerators f_1, f_2, f_3 of three meromorphic functions are polynomials of (x, y, z, w). Explicitly, the three equations

$$f_1(y,z,w) = 0 \quad , \quad f_2(y,z,w) = 0 \quad , \quad f_3(x,w) = 0 \tag{5.30}$$

define a birational equivalent complex curve. The degree of them are higher than two.

To project the non-plane curve defined by (f_1, f_2, f_3) to plane curve, we can eliminate y and w from these equations by computing *resultant*. Firstly, notice that if we ignore four propagators $D_0, D_1, D_2, \widehat{D}_2$ that containing ℓ_1, and treat $K_1 + K_2 + K_3 + K_9$ as one external momentum, then the remaining propagators describe non-planar two-loop crossed-box diagram of ℓ_2, ℓ_3. So $f_1(y,z,w) = 0$, $f_2(y,z,w) = 0$ define a genus-3 complex curve. From previous section we know that each f_1, f_2 has degree 4, and can be written as

$$\begin{aligned} &a_2(z,w)y^2 + a_1(z,w)y + a_0(z,w) = 0 \ , \\ &b_2(z,w)y^2 + b_1(z,w)y + b_0(z,w) = 0 \ . \end{aligned} \tag{5.31}$$

Thus we can eliminate y just like the case (5.26) to get a plane curve. The birational equivalence is guaranteed by inverse map like (5.27). The resulting equation $F(z,w) = 0$ has degree 8. Then the original algebraic system is birational equivalent to following two equations

$$\begin{aligned} &a'_8 w^8 + a'_7(z)w^7 + a'_6(z)w^6 + a'_5(z)w^5 + a'_4(z)w^4 \\ &\qquad\qquad + a'_3(z)w^3 + a'_2(z)w^2 + a'_1(z)w + a'_0(z) = 0 \ , \\ &b'_2(x)w^2 + b'_1(x)w + b'_0(x) = 0 \ , \end{aligned} \tag{5.32}$$

where a'_i, $i = 0, \ldots, 6$ and b'_i, $i = 0, 1, 2$ are quadratic polynomials, while $a_7(z)$ is linear and a_8 is constant. We can further eliminate w by computing *resultant* of above two equations and get a plane curve $F'(x,z) = 0$. This step is also birational with an inverse map

$$w = \frac{p(x,z)}{q(x,z)} \ , \tag{5.33}$$

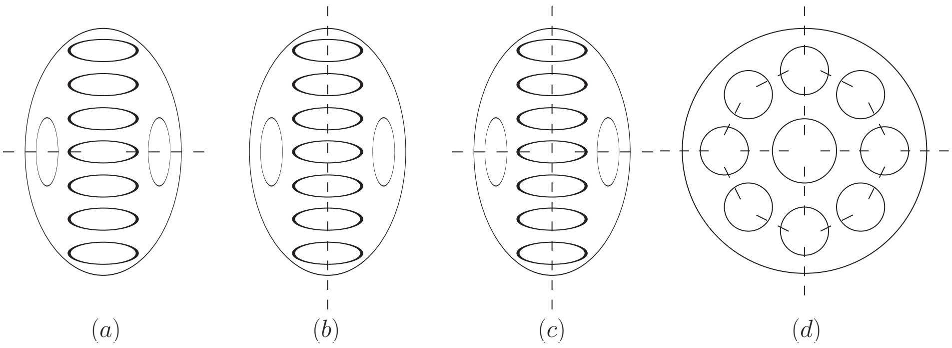

FIGURE 5.5: Degenerate topological pictures of cut equations for non-planar three-loop box-crossed-pentagon diagram.

where $p(x, z)$ and $q(x, z)$ can be computed by Gröbner basis method.

Plane curve $F'(x, z) = 0$ has degree 20. By computing singular points of this curve, we find that there are 32 normal singular points of multiplicity $\mu_p = 2$, one normal singular point of multiplicity $\mu_p = 4$, and also a non-normal singular point. The tangent line $T(x, z)$ of non-normal singular point has degree $d_T = 16$, but there are only 12 distinct solutions for $T(x, z) = 0$. After blowing up the non-normal singular point, we get 8 normal singular points of multiplicity $\mu_p = 1$ and 4 normal singular points of multiplicity $\mu_p = 2$. So the genus is finally given by

$$\begin{aligned} g_G &= g_A - \Big[32 \times \frac{2(2-1)}{2} + 1 \times \frac{4(4-1)}{2}\Big] \\ &\quad - \Big[1 \times \frac{16(16-1)}{2} + 8 \times \frac{1(1-1)}{2} + 4 \times \frac{2(2-1)}{2}\Big] = 9 \ . \end{aligned} \tag{5.34}$$

Topological picture of genus

After solving six linear equations, we get five quadratic equations

$$\begin{aligned} &Q_1(x_1, x_2) = 0 \ , \ Q_2(y_1, y_2, z_1, z_2) = 0 \ , \ Q_3(z_1, z_2) = 0 \ , \\ &Q_4(x_1, x_2, z_1, z_2) = 0 \ , \ Q_5(y_1, y_2, z_1, z_2) = 0 \ . \end{aligned} \tag{5.35}$$

If all external momenta are general, it is an irreducible curve. Under some specific kinematic configurations, the ideal $I(Q_1, Q_2, Q_3, Q_4, Q_5)$ is reducible. Thus it is important to study the degenerate topological picture of genus for this reducible ideal. There are a lot of kinematic configurations to be considered, but most of them could be constructed from combinations of other two or more kinematic configurations, as we have illustrated in two-loop non-planar crossed-box diagram. Here as examples, we will present results for some simple reducible ideals.

The simplest example comes from kinematic configurations where quadratic polynomials $Q_1(x_1, x_2)$ or $Q_3(z_1, z_2)$ factorizes, since they are conics. If at least one of K_1, K_2 is massless, then Q_1 can be simply factorized to two factors. If K_4 is massless, then Q_3 can be factorized to two factors. In any cases, the ideal $I(Q_1, Q_2, Q_3, Q_4, Q_5)$ is reducible, and can be decomposed to two prime ideals via primary decomposition. As usual, we can project each prime ideal onto plane curve. The resulting plane curve has degree 12. So the arithmetic genus is $g_A = 55$. There are 16 normal singular points of multiplicity $\mu_p = 2$, 1 normal singular point of multiplicity $\mu_p = 4$ and one non-normal singular point. The tangent line at this non-normal singular point has degree $d_T = 8$, but it only has six distinct solutions. After blowing up, we get six normal singular points. Among them four singular points have multiplicity $\mu_p = 1$ and two singular points have multiplicity $\mu_p = 2$. So finally we get

$$g_G = 55 - 16 \times 1 - 1 \times \frac{4(4-1)}{2} - 1 \times \frac{8(8-1)}{2} - 2 \times 1 = 3 \ . \tag{5.36}$$

Varieties of two prime ideals intersect at four points. So the degenerate topological picture is given by shrinking four tubes of genus-9 torus to points along dashed lines as shown in Figure (5.5.a).

If K_6 or K_7 is massless, it is possible to factorize $Q_2 = f_1 f_2$, where $f_1(y_1, y_2, z_1, z_2)$ and $f_2(y_1, y_2, z_1, z_2)$ are linear functions. So we have two prime ideals $I_1(Q_1, f_1, Q_3, Q_4, Q_5)$ and $I_2(Q_1, f_2, Q_3, Q_4, Q_5)$. Similarly, we can birational project each one onto a plane curve. The resulting plane curve has degree 12, and 20 normal singular points of multiplicity $\mu_p = 2$, one normal singular point of multiplicity $\mu_p = 4$ and one normal singular point of multiplicity $\mu_p = 8$. So we get

$$g_G = 55 - 20 \times 1 - 1 \times \frac{4(4-1)}{2} - 1 \times \frac{8(8-1)}{2} = 1 \ . \tag{5.37}$$

The degenerate topological picture is not hard to conclude, since there are two genus-1 tori. The only possible way of shrinking tubes of genus-9 torus to points is shown in Figure (5.5.b), along dashed lines. We can see that there are 8 intersecting points between two genus-1 tori. This observation agrees with the result of explicit computation from union of two prime ideals.

If K_1 and K_6 are massless, each Q_1, Q_2 can be factorized to two factors. Thus the reducible ideal can be decomposed to four prime ideals. After projecting each ideal onto plane curve, we find that it has degree 4 and 3 normal singular points of multiplicity $\mu_p = 2$. So the genus is simply $g_G = 0$. The degenerate topological picture is given by overlapping of Figure (5.5.a) and (5.5.b), which is shown in (5.5.c). Intersection of four varieties of prime ideals then can be easily read from this picture.

If K_1, K_4, K_6 are massless, then each Q_1, Q_2, Q_3 can be factorized to two factors. There are eight prime ideals via primary decomposition. It is easy to compute the birational equivalent plane curve associated to each prime ideal. Each one has degree 3, with only one normal singular point of multiplicity $\mu_p = 2$. So again they are all genus $g_G = 0$ Riemann spheres. However, the degenerate topological picture is not trivially given by overlapping two copies of (5.5.a) and (5.5.b) in this kinematic configuration, since cut equations are somehow entangled. By studying intersections among varieties of eight prime ideals, we can produce the degenerate topological picture as shown in Figure (5.5.d).

5.3.2 Genus of non-planar crossed-crossed-pentagon diagram

We discuss three-loop non-planar crossed-crossed-pentagon diagram as shown in Figure (5.4.b) in this section. The algebraic system of cut equations becomes even more complicated than previous example. The complexity of curve can be inferred by the degree of curve. The higher the degree is, the more complicated the curve will be. Naively, the up-bound of degree can be obtained from cut equations. For example, for two-loop diagrams, the curve is defined by three quadratic equations. So the highest degree of plane curve by projecting the non-plane curve is $2^3 = 8$. Sometimes the three quadratic equations are not completely independent, and degree of corresponding plane curve is smaller than 8. Similarly, for three-loop diagrams, the curve is defined by five quadratic equations. So the highest degree of plane curve is $2^5 = 32$. Such a curve is of course very complicated. In the previous three-loop non-planar box-crossed-pentagon diagram, the degree of plane curve is 20.

For diagram considered in this section, the 11 propagators are given by

$$\begin{aligned}
&\text{Only } \ell_1 \ : \ D_0 = \ell_1^2 \ , \quad D_1 = (\ell_1 - K_1)^2 \ , \\
&\text{Only } \ell_2 \ : \ \widetilde{D}_0 = \ell_2^2 \ , \quad \widetilde{D}_1 = (\ell_2 - K_5)^2 \ , \\
&\text{Only } \ell_3 \ : \ \bar{D}_0 = \ell_3^2 \ , \quad \bar{D}_1 = (\ell_3 - K_1 - K_2 - K_7 - K_9)^2 \ , \\
&\qquad\qquad \bar{D}_2 = (\ell_3 + K_4 + K_5 + K_6 + K_8)^2 \ , \\
&\text{Mixed } \ell_1, \ell_3 \ : \ \widehat{D}_0 = (\ell_3 - \ell_1 - K_7)^2 \ , \quad \widehat{D}_1 = (\ell_3 - \ell_1 - K_7 - K_9)^2 \ , \\
&\text{Mixed } \ell_2, \ell_3 \ : \ \widehat{D}_2 = (\ell_2 + \ell_3 + K_6)^2 \ , \quad \widehat{D}_3 = (\ell_2 + \ell_3 + K_6 + K_8) \ .
\end{aligned}$$

Explicitly, we can construct six linear equations to solve six variables. The remaining five quadratic equations define a complex curve. This curve can be birational projected onto plane curve by elimination process via Gröbner basis method. For purpose of analysis, notice that we can rationally parameterize ℓ_1 by two parameters (x, y) and

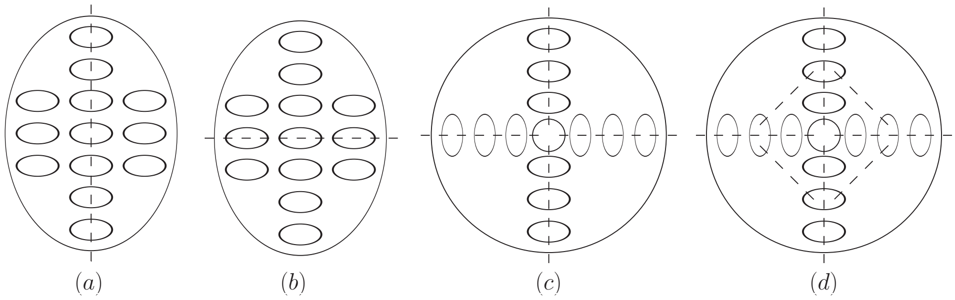

FIGURE 5.6: Degenerate topological pictures of cut equations for non-planar three-loop crossed-crossed-pentagon diagram.

ℓ_2 by two parameters (z, w) from corresponding two equations $D_0 = 0, D_1 = 0$ and $\widetilde{D}_0 = 0, \widetilde{D}_1 = 0$, and also rationally parameterize ℓ_3 by one free parameter τ from three cut equations $\bar{D}_0 = \bar{D}_1 = \bar{D}_2 = 0$. Substituting $\ell_1(x, y)$, $\ell_2(z, w)$ and $\ell_3(\tau)$ back to remaining four quadratic equations with mixed loop momenta, they become

$$f_1(x, y, \tau) = 0 \quad , \quad f_2(x, y, \tau) = 0 \quad , \quad f_3(z, w, \tau) = 0 \quad , \quad f_4(z, w, \tau) = 0 \ . \tag{5.38}$$

We can observe that this diagram in fact contains two copies of two-loop non-planar crossed-box diagrams defined by $(f_1 = 0, f_2 = 0)$ and $(f_3 = 0, f_4 = 0)$. So using the discussion of two-loop non-planar crossed-box diagram, we can similarly eliminate y from (f_1, f_2) and w from (f_3, f_4) by computing *resultant*. Then we get two equations

$$g_1(x, \tau) = 0 \quad , \quad g_2(z, \tau) = 0 \ . \tag{5.39}$$

This elimination is birational, and g_1, g_2 have degree 8. g_1 is quadratic in x and g_2 is quadratic in z. By computing *resultant* of g_1, g_2, we can further eliminate τ, and birationally project non-plane curve to plane curve. So by computing genus of this plane curve, we get genus of original curve.

The plane curve has degree 24. There are 184 normal singular points of multiplicity $\mu_p = 2$, two normal singular points of multiplicity $\mu_p = 8$. The geometric genus is given by

$$g_G = 253 - 184 \times 1 - 2 \times \frac{8(8-1)}{2} = 13 \ . \tag{5.40}$$

Topological picture of genus

After solving six linear equations, we get five quadratic equations

$$\begin{aligned} &Q_1(x_1, x_2, z_1, z_2) = 0 \quad , \quad Q_2(y_1, y_2, z_1, z_2) = 0 \quad , \quad Q_3(z_1, z_2) = 0 \ , \\ &Q_4(x_1, x_2, z_1, z_2) = 0 \quad , \quad Q_5(y_1, y_2, z_1, z_2) = 0 \ . \end{aligned} \tag{5.41}$$

For general kinematics, ideal $I(Q_1, Q_2, Q_3, Q_4, Q_5)$ is irreducible.

If K_1 is massless, Q_1 can be factorized to two factors. Thus the reducible ideal can be decomposed to two prime ideals I_1, I_2. Solution of $I_1 \cup I_2$ is eight points. The degenerate topological picture of genus is given by Figure (5.6.a). From Figure (5.6.a), we know that plane curve of each prime ideal should be genus-3. After projecting curve of each prime ideal onto a plane curve using elimination process via Gröbner basis method, we find that it has degree 12. There are 40 normal singular points of multiplicity $\mu_p = 2$, two normal singular points of multiplicity $\mu_p = 4$. So the genus is given by

$$g_G = \frac{1}{2}(12-1)(12-2) - 40 \times 1 - 2 \times \frac{4(4-1)}{2} = 3 \,, \tag{5.42}$$

as expected. If K_3 is massless, we also get two prime ideals from factorization of Q_3. The plane curve of each prime ideal has degree 12. There are 38 normal singular points of multiplicity $\mu_p = 2$, two normal singular points of multiplicity $\mu_p = 4$. So we have

$$g_G = \frac{1}{2}(12-1)(12-2) - 38 \times 1 - 2 \times \frac{4(4-1)}{2} = 5 \,. \tag{5.43}$$

The only possible degenerate topological picture of genus-13 torus which has two genus-5 tori is shown in Figure (5.6.b). So intersection of varieties of two prime ideals is four points. By computing $V(I_1 \cup I_2)$, we find that it is indeed four points.

It is not difficult to conclude that if both K_1, K_3 are massless, the degenerate topological picture should be given by overlapping of Figure (5.6.a) and (5.6.b). The resulting picture is four genus-1 tori linked in a chain, with intersecting points indicated by dashed lines of both Figures. Explicit computation of plane curve for each prime ideal agrees with this degenerate topological picture. The plane curve has degree 6, and 9 normal singular points of multiplicity $m_p = 2$. So the genus is given by

$$g_G = \frac{1}{2}(6-1)(6-1) - 9 \times 1 = 1 \,, \tag{5.44}$$

as expected.

Since K_1, K_5 are symmetric in the diagram (5.4.b), the condition of $K_5^2 = 0$ gives the same degenerate topological picture as Figure (5.6.a). So when combining $K_1^2 = 0$, $K_5^2 = 0$ together, the degenerate topological picture should be given by overlapping two copies of Figure (5.6.a), as shown in Figure (5.6.c). Then we get four genus-0 Riemann spheres linked in a chain, with four intersecting points between adjacent spheres. By explicit computation, we find that there are indeed four prime ideals after primary decomposition, which can be easily seen from factorized functions Q_1, Q_2. The plane

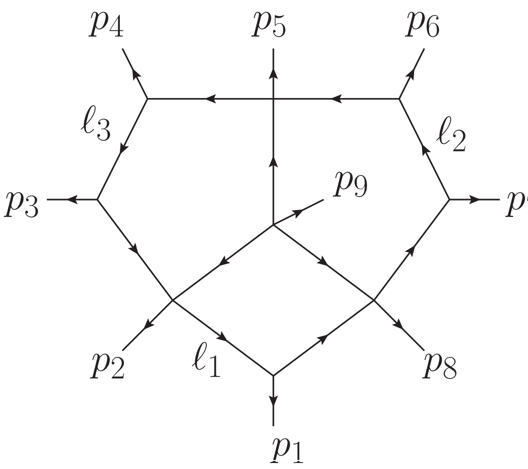

FIGURE 5.7: Non-planar three-loop "Mercedes" logo diagram. All external momenta are out-going and massive. Loop momenta are denoted by ℓ_1, ℓ_2, ℓ_3.

curve of each prime ideal has degree 6, and there are 10 normal singular points of multiplicity $\mu_p = 2$. So the genus is $g_G = 10 - 10 \times 1 = 0$, as indicated in Figure (5.6.c).

If K_1, K_3, K_5 are massless, each Q_1, Q_2, Q_3 can be factorized to two factors. The equations are not totally independent, so the degenerate topological picture is no longer given by overlapping of Figure (5.6.b) and (5.6.c). After primary decomposition, we get eight prime ideals. The plane curve of each prime ideal has degree 3, and only one normal singular point of multiplicity $\mu_p = 2$. So $g_G = 0$. The degenerate topological picture is given in (5.6.d), after computing intersections among varieties of eight prime ideals.

5.3.3 Genus of Mercedes-logo diagram

In this section, we present result of three-loop "Mercedes-logo" diagram, as shown in Figure (5.7). Although algebraic system of maximal unitarity cut for this diagram becomes more complicated, the mathematical method of computing genus still keeps the same. The 11 propagators are given by

$$
\begin{aligned}
&\text{Only } \ell_1 \ : \ D_0 = \ell_1^2 \ , \ D_1 = (\ell_1 - K_1)^2 \ , \\
&\text{Only } \ell_2 \ : \ \widetilde{D}_0 = \ell_2^2 \ , \ \widetilde{D}_1 = (\ell_2 - K_6)^2 \ , \ \widetilde{D}_2 = (\ell_2 + K_7)^2 \ , \\
&\text{Only } \ell_3 \ : \ \bar{D}_0 = \ell_3^2 \ , \ \bar{D}_1 = (\ell_3 - K_3)^2 \ , \ \bar{D}_2 = (\ell_3 + K_4)^2 \ , \\
&\text{Mixed } \ell_1, \ell_2 \ : \ \widehat{D}_0 = (\ell_2 - \ell_1 + K_7 + K_1 + K_8)^2 \ , \\
&\text{Mixed } \ell_2, \ell_3 \ : \ \widehat{D}_1 = (\ell_3 - \ell_2 + K_4 + K_5 + K_6)^2 \ , \\
&\text{Mixed } \ell_1, \ell_3 \ : \ \widehat{D}_2 = (\ell_1 - \ell_3 + K_2 + K_3)^2 \ .
\end{aligned}
$$

No linear equations can be constructed from propagators of mixed loop momenta, so we can only get five linear equations. The complex curve is then defined by six quadratic equations of seven variables. Notice that we can rationally parameterize ℓ_1 by two variables x, y, ℓ_2 by one variable z, and ℓ_3 by one variables w. After substituting $\ell_1(x, y)$, $\ell_2(z)$, $\ell_3(w)$, the remaining three propagators of mixed loop momenta become meromorphic functions. The numerators of three meromorphic functions

$$f(x, y, z) = 0 \quad , \quad g(w, z) = 0 \quad , \quad h(x, y, w) = 0 \ . \tag{5.45}$$

define a birational equivalent curve. We can further birational project it onto plane curve $F(y, w) = 0$ by computing the *resultant*, as described in previous sections. This plane curve has degree 20. There are 36 normal singular points of multiplicity $\mu_p = 2$, one normal singular point of multiplicity $\mu_p = 16$, and one normal singular point of multiplicity $\mu_p = 4$. So the genus is given by

$$g_G = \frac{(20-1)(20-2)}{2} - 36 \times 1 - 1 \times \frac{16(16-1)}{2} - 1 \times \frac{4(4-1)}{2} = 9 \ . \tag{5.46}$$

Coincidentally, genus of Mercedes-logo diagram equals to genus of box-crossed-pentagon diagrams. When considering the kinematic configurations presented in box-crossed-pentagon diagram, the degenerate topological pictures of genus are also the same. More explicitly, if K_4 is massless, we get two prime ideals, and the degenerate topological picture is given by Figure (5.5.a). If K_1 is massless, there are also two prime ideals, and the degenerate topological picture is given by Figure (5.5.b). If both K_1, K_4 are massless, the picture is given by Figure (5.5.c). Furthermore, when K_1, K_4, K_6 are massless, there are eight prime ideals, and the degenerate picture is given by Figure (5.5.d).

Chapter 6

Conclusion

It is always difficult to give a final conclusion, since there are always new possibilities and results proposed for well-studied problems. Especially for amplitude computation, where new ideas always shape the power of old methods. The simple formulation of MHV amplitude has already been provided in 1986 by Parke and Taylor[87]. But only after almost twenty years the simplicity of tree amplitudes is being explored, with the discovery of BCFW recursion relation[5, 6]. The BCJ relation[17] can also find its hints back to 1981 where similar kinematic identity at four points is used to explain certain zeros in cross sections[121, 122]. But it is only formulated and proved very recently. The same situation happens for gravity amplitude. The KLT relation is discovered in 1985 for string amplitudes, but it has little progress in field theory gravity amplitude computation for many years except some results of MHV gravity amplitude. However, it is again studied three years ago[94], and a family of equivalent KLT relations are proposed. Some interesting vanishing identities of Yang-Mills amplitudes also appear as a byproduct of this study[93]. After a complete survey of super-KLT relation with any number of supersymmetry[70], it seems that all possible studies are already done. However, within around one year, new simple formulation of MHV gravity amplitude is provided by Hodges[123], which is equivalent to KLT formula when kinematic invariants are allowed to be off-shell in a novel way. A series of researches are then done on these tree gravity amplitude formulations[124].

The traditional notations, ideas and methods, which are somehow forgotten for many years, also contribute actively with a modern interpretation. Especially for the idea of S-matrix program[7–9], where only general assumptions as locality, unitarity are used to analyze scattering amplitudes. Only after the discovery of BCFW recursion relation, these general assumptions are then well formulated in analytic function of single complex variable for amplitudes. The spinor-helicity formalism plays tremendous role in the computation of amplitude using BCFW recursion relation. The unitarity cut and generalized unitarity cut combined with spinor-helicity formalism and BCFW recursion relation then are served as powerful tool of computing loop amplitudes, though they are also already used almost twenty years ago.

For multi-loop gravity amplitude computation, the only practical method by now seems to be the BCJ conjecture[27, 28] that constructing such amplitude from double copies of multi-loop Yang-Mills amplitudes. But it also suffers from the computation complexity, and a better understanding of this conjecture is still required. For multi-loop Yang-Mills amplitude computation, the algebraic geometry methods are introduced. Application of these methods to loop amplitude computation is still preliminary, especially for diagrams where generalized unitarity cut defines very complicated complex manifold. We still need to work hard in order to get a practical computation method for any point any loop amplitude.

So we are going to give a final conclusion about this thesis. It contains discussions of works that have been done during my PhD, distributed in three papers. In the KLT paper[70], we present the complete map of any products of super-Yang-Mills theories to super-gravity theories by super-KLT relations in four dimension. Linear symmetry groups of super-gravity theories and explanation of vanishing identities of Yang-Mills amplitudes due to violation of symmetry groups are derived. A graphical method is introduced which simplifies the counting of states, and helps to identify relevant symmetries. In the integrand paper[61], we attempts to classify integrand basis of all 4-dimensional two-loop topologies. The classification is taken by firstly determine all topologies from structures of propagators, then determine the independent monomials in numerator of integrand by Gröbner basis. The branch structures of reducible ideal defined by equations of maximal unitarity cut under specific kinematic configuration are discussed. In the genus paper[71], a special type of loop topologies where cut equations define the complex curve is studied. The genus of complex curve is computed by algebraic geometry method, with knowledge of the degree and singular points of the curve. The degenerate topological picture of genus for reducible curve is also discussed.

This is the end of this thesis, but not the end of research. We are waiting to know more.

Bibliography

[1] Nima Arkani-Hamed, Freddy Cachazo, and Jared Kaplan. What is the Simplest Quantum Field Theory? *JHEP*, 1009:016, 2010. doi: 10.1007/JHEP09(2010)016.

[2] Edward Witten. Perturbative gauge theory as a string theory in twistor space. *Commun.Math.Phys.*, 252:189–258, 2004. doi: 10.1007/s00220-004-1187-3.

[3] Freddy Cachazo, Peter Svrcek, and Edward Witten. MHV vertices and tree amplitudes in gauge theory. *JHEP*, 0409:006, 2004. doi: 10.1088/1126-6708/2004/09/006.

[4] Kasper Risager. A Direct proof of the CSW rules. *JHEP*, 0512:003, 2005. doi: 10.1088/1126-6708/2005/12/003.

[5] Ruth Britto, Freddy Cachazo, and Bo Feng. New recursion relations for tree amplitudes of gluons. *Nucl.Phys.*, B715:499–522, 2005. doi: 10.1016/j.nuclphysb.2005.02.030.

[6] Ruth Britto, Freddy Cachazo, Bo Feng, and Edward Witten. Direct proof of tree-level recursion relation in Yang-Mills theory. *Phys.Rev.Lett.*, 94:181602, 2005. doi: 10.1103/PhysRevLett.94.181602.

[7] David I. Olive. Exploration of s-matrix theory. *Phys. Rev.*, 135:B745–B760, Aug 1964. doi: 10.1103/PhysRev.135.B745.

[8] G.F. Chew. *The Analytic S-Matrix: A Basis for Nuclear Democracy.* W.A.Benjamin, Inc., 1966.

[9] R.J. Eden, P.V. Landshoff, D.I. Olive, and J.C. Polkinghorne. *The Analytic S-Matrix.* Cambridge University Press, 1966.

[10] Ming-xing Luo and Cong-kao Wen. Recursion relations for tree amplitudes in super gauge theories. *JHEP*, 0503:004, 2005. doi: 10.1088/1126-6708/2005/03/004.

[11] Ruth Britto, Bo Feng, Radu Roiban, Marcus Spradlin, and Anastasia Volovich. All split helicity tree-level gluon amplitudes. *Phys.Rev.*, D71:105017, 2005. doi: 10.1103/PhysRevD.71.105017.

[12] J.M. Drummond and J.M. Henn. All tree-level amplitudes in N=4 SYM. *JHEP*, 0904:018, 2009. doi: 10.1088/1126-6708/2009/04/018.

[13] Michelangelo L. Mangano, Stephen J. Parke, and Zhan Xu. Duality and Multi - Gluon Scattering. *Nucl.Phys.*, B298:653, 1988. doi: 10.1016/0550-3213(88)90001-6.

[14] Zvi Bern and David A. Kosower. Color decomposition of one loop amplitudes in gauge theories. *Nucl.Phys.*, B362:389–448, 1991. doi: 10.1016/0550-3213(91)90567-H.

[15] Michelangelo L. Mangano and Stephen J. Parke. Multiparton amplitudes in gauge theories. *Phys.Rept.*, 200:301–367, 1991. doi: 10.1016/0370-1573(91)90091-Y.

[16] Ronald Kleiss and Hans Kuijf. Multi - Gluon Cross-sections and Five Jet Production at Hadron Colliders. *Nucl.Phys.*, B312:616, 1989. doi: 10.1016/0550-3213(89)90574-9.

[17] Z. Bern, J.J.M. Carrasco, and Henrik Johansson. New Relations for Gauge-Theory Amplitudes. *Phys.Rev.*, D78:085011, 2008. doi: 10.1103/PhysRevD.78.085011.

[18] N.E.J. Bjerrum-Bohr, Poul H. Damgaard, and Pierre Vanhove. Minimal Basis for Gauge Theory Amplitudes. *Phys.Rev.Lett.*, 103:161602, 2009. doi: 10.1103/PhysRevLett.103.161602.

[19] S. Stieberger. Open and Closed vs. Pure Open String Disk Amplitudes. 2009.

[20] Vittorio Del Duca, Lance J. Dixon, and Fabio Maltoni. New color decompositions for gauge amplitudes at tree and loop level. *Nucl.Phys.*, B571:51–70, 2000. doi: 10.1016/S0550-3213(99)00809-3.

[21] Bo Feng, Rijun Huang, and Yin Jia. Gauge Amplitude Identities by On-shell Recursion Relation in S-matrix Program. *Phys.Lett.*, B695:350–353, 2011. doi: 10.1016/j.physletb.2010.11.011.

[22] Yin Jia, Rijun Huang, and Chang-Yong Liu. $U(1)$-decoupling, KK and BCJ relations in $\mathcal{N} = 4$ SYM. *Phys.Rev.*, D82:065001, 2010. doi: 10.1103/PhysRevD.82.065001.

[23] Jia-Hui Huang, Rijun Huang, and Yin Jia. Tree amplitudes of noncommutative U(N) Yang-Mills Theory. *J.Phys.*, A44:425401, 2011. doi: 10.1088/1751-8113/44/42/425401.

[24] Yi-Xin Chen, Yi-Jian Du, and Bo Feng. A Proof of the Explicit Minimal-basis Expansion of Tree Amplitudes in Gauge Field Theory. *JHEP*, 1102:112, 2011. doi: 10.1007/JHEP02(2011)112.

[25] Hong-bao Zhang. Note on the non-adjacent BCFW deformations. 2010.

[26] H. Kawai, D.C. Lewellen, and S.H.H. Tye. A Relation Between Tree Amplitudes of Closed and Open Strings. *Nucl.Phys.*, B269:1, 1986. doi: 10.1016/0550-3213(86)90362-7.

[27] Zvi Bern, John Joseph M. Carrasco, and Henrik Johansson. Perturbative Quantum Gravity as a Double Copy of Gauge Theory. *Phys.Rev.Lett.*, 105:061602, 2010. doi: 10.1103/PhysRevLett.105.061602.

[28] Z. Bern, J.J.M. Carrasco, and H. Johansson. The Structure of Multiloop Amplitudes in Gauge and Gravity Theories. *Nucl.Phys.Proc.Suppl.*, 205-206:54–60, 2010. doi: 10.1016/j.nuclphysbps.2010.08.019.

[29] Z. Bern, J.J.M. Carrasco, Lance J. Dixon, H. Johansson, and R. Roiban. The Complete Four-Loop Four-Point Amplitude in N=4 Super-Yang-Mills Theory. *Phys.Rev.*, D82:125040, 2010. doi: 10.1103/PhysRevD.82.125040.

[30] Zvi Bern, John Joseph Carrasco, Lance J. Dixon, Henrik Johansson, and Radu Roiban. Amplitudes and Ultraviolet Behavior of N = 8 Supergravity. *Fortsch.Phys.*, 59:561–578, 2011. doi: 10.1002/prop.201100037.

[31] Z. Bern, C. Boucher-Veronneau, and H. Johansson. N ¿= 4 Supergravity Amplitudes from Gauge Theory at One Loop. *Phys.Rev.*, D84:105035, 2011. doi: 10.1103/PhysRevD.84.105035.

[32] Z. Bern, J.J.M. Carrasco, L.J. Dixon, H. Johansson, and R. Roiban. Simplifying Multiloop Integrands and Ultraviolet Divergences of Gauge Theory and Gravity Amplitudes. *Phys.Rev.*, D85:105014, 2012. doi: 10.1103/PhysRevD.85.105014.

[33] Z. Bern, J.J.M. Carrasco, H. Johansson, and R. Roiban. The Five-Loop Four-Point Amplitude of N=4 super-Yang-Mills Theory. *Phys.Rev.Lett.*, 109:241602, 2012. doi: 10.1103/PhysRevLett.109.241602.

[34] Zvi Bern, Scott Davies, Tristan Dennen, Alexander V. Smirnov, and Vladimir A. Smirnov. The Ultraviolet Properties of N=4 Supergravity at Four Loops. 2013.

[35] Zvi Bern, Scott Davies, and Tristan Dennen. The Ultraviolet Structure of Half-Maximal Supergravity with Matter Multiplets at Two and Three Loops. *Phys.Rev.*, D88:065007, 2013. doi: 10.1103/PhysRevD.88.065007.

[36] Zvi Bern, Scott Davies, Tristan Dennen, and Yu-tin Huang. Ultraviolet Cancellations in Half-Maximal Supergravity as a Consequence of the Double-Copy Structure. *Phys.Rev.*, D86:105014, 2012. doi: 10.1103/PhysRevD.86.105014.

[37] Zvi Bern, Scott Davies, Tristan Dennen, and Yu-tin Huang. Absence of Three-Loop Four-Point Divergences in N=4 Supergravity. *Phys.Rev.Lett.*, 108:201301, 2012. doi: 10.1103/PhysRevLett.108.201301.

[38] Ruth Britto. Loop Amplitudes in Gauge Theories: Modern Analytic Approaches. *J.Phys.*, A44:454006, 2011. doi: 10.1088/1751-8113/44/45/454006.

[39] Janusz Gluza, Krzysztof Kajda, and David A. Kosower. Towards a Basis for Planar Two-Loop Integrals. *Phys.Rev.*, D83:045012, 2011. doi: 10.1103/PhysRevD.83.045012.

[40] David A. Kosower and Kasper J. Larsen. Maximal Unitarity at Two Loops. *Phys.Rev.*, D85:045017, 2012. doi: 10.1103/PhysRevD.85.045017.

[41] Kasper J. Larsen. Global Poles of the Two-Loop Six-Point N=4 SYM integrand. *Phys.Rev.*, D86:085032, 2012. doi: 10.1103/PhysRevD.86.085032.

[42] Simon Caron-Huot and Kasper J. Larsen. Uniqueness of two-loop master contours. *JHEP*, 1210:026, 2012. doi: 10.1007/JHEP10(2012)026.

[43] Henrik Johansson, David A. Kosower, and Kasper J. Larsen. Two-Loop Maximal Unitarity with External Masses. *Phys.Rev.*, D87:025030, 2013. doi: 10.1103/PhysRevD.87.025030.

[44] Henrik Johansson, David A. Kosower, and Kasper J. Larsen. An Overview of Maximal Unitarity at Two Loops. *PoS*, LL2012:066, 2012.

[45] Henrik Johansson, David A. Kosower, and Kasper J. Larsen. Maximal Unitarity for the Four-Mass Double Box. 2013.

[46] Mads Sogaard. Global Residues and Two-Loop Hepta-Cuts. *JHEP*, 1309:116, 2013. doi: 10.1007/JHEP09(2013)116.

[47] Mads Sogaard and Yang Zhang. Multivariate Residues and Maximal Unitarity. 2013.

[48] Yang Zhang. Integrand-Level Reduction of Loop Amplitudes by Computational Algebraic Geometry Methods. *JHEP*, 1209:042, 2012. doi: 10.1007/JHEP09(2012)042.

[49] Pierpaolo Mastrolia, Edoardo Mirabella, Giovanni Ossola, and Tiziano Peraro. Scattering Amplitudes from Multivariate Polynomial Division. *Phys.Lett.*, B718:173–177, 2012. doi: 10.1016/j.physletb.2012.09.053.

[50] Giovanni Ossola, Costas G. Papadopoulos, and Roberto Pittau. Reducing full one-loop amplitudes to scalar integrals at the integrand level. *Nucl.Phys.*, B763: 147–169, 2007. doi: 10.1016/j.nuclphysb.2006.11.012.

[51] Darren Forde. Direct extraction of one-loop integral coefficients. *Phys.Rev.*, D75: 125019, 2007. doi: 10.1103/PhysRevD.75.125019.

[52] R. Keith Ellis, W.T. Giele, and Z. Kunszt. A Numerical Unitarity Formalism for Evaluating One-Loop Amplitudes. *JHEP*, 0803:003, 2008. doi: 10.1088/1126-6708/2008/03/003.

[53] Walter T. Giele, Zoltan Kunszt, and Kirill Melnikov. Full one-loop amplitudes from tree amplitudes. *JHEP*, 0804:049, 2008. doi: 10.1088/1126-6708/2008/04/049.

[54] Giovanni Ossola, Costas G. Papadopoulos, and Roberto Pittau. On the Rational Terms of the one-loop amplitudes. *JHEP*, 0805:004, 2008. doi: 10.1088/1126-6708/2008/05/004.

[55] S.D. Badger. Direct Extraction Of One Loop Rational Terms. *JHEP*, 0901:049, 2009. doi: 10.1088/1126-6708/2009/01/049.

[56] Ronald H.P. Kleiss, Ioannis Malamos, Costas G. Papadopoulos, and Rob Verheyen. Counting to One: Reducibility of One- and Two-Loop Amplitudes at the Integrand Level. *JHEP*, 1212:038, 2012. doi: 10.1007/JHEP12(2012)038.

[57] Pierpaolo Mastrolia, Edoardo Mirabella, Giovanni Ossola, and Tiziano Peraro. Integrand-Reduction for Two-Loop Scattering Amplitudes through Multivariate Polynomial Division. *Phys.Rev.*, D87:085026, 2013. doi: 10.1103/PhysRevD.87.085026.

[58] Pierpaolo Mastrolia, Edoardo Mirabella, Giovanni Ossola, Tiziano Peraro, and Hans van Deurzen. The Integrand Reduction of One- and Two-Loop Scattering Amplitudes. *PoS*, LL2012:028, 2012.

[59] Simon Badger, Hjalte Frellesvig, and Yang Zhang. Hepta-Cuts of Two-Loop Scattering Amplitudes. *JHEP*, 1204:055, 2012. doi: 10.1007/JHEP04(2012)055.

[60] Simon Badger, Hjalte Frellesvig, and Yang Zhang. An Integrand Reconstruction Method for Three-Loop Amplitudes. *JHEP*, 1208:065, 2012. doi: 10.1007/JHEP08(2012)065.

[61] Bo Feng and Rijun Huang. The classification of two-loop integrand basis in pure four-dimension. *JHEP*, 1302:117, 2013. doi: 10.1007/JHEP02(2013)117.

[62] P. Mastrolia, E. Mirabella, G. Ossola, and T. Peraro. Multiloop Integrand Reduction for Dimensionally Regulated Amplitudes. 2013.

[63] C.G. Papadopoulos, R.H.P. Kleiss, and I. Malamos. Reduction at the integrand level beyond NLO. *PoS*, Corfu2012:019, 2013.

[64] Giovanni Ossola. Automated computation of scattering amplitudes. 2013.

[65] Simon Badger, Hjalte Frellesvig, and Yang Zhang. Multi-loop Integrand Reduction with Computational Algebraic Geometry. 2013.

[66] F.V. Tkachov. A Theorem on Analytical Calculability of Four Loop Renormalization Group Functions. *Phys.Lett.*, B100:65–68, 1981. doi: 10.1016/0370-2693(81)90288-4.

[67] K.G. Chetyrkin and F.V. Tkachov. Integration by Parts: The Algorithm to Calculate beta Functions in 4 Loops. *Nucl.Phys.*, B192:159–204, 1981. doi: 10.1016/0550-3213(81)90199-1.

[68] S. Laporta. Calculation of master integrals by difference equations. *Phys.Lett.*, B504:188–194, 2001. doi: 10.1016/S0370-2693(01)00256-8.

[69] S. Laporta. High precision calculation of multiloop Feynman integrals by difference equations. *Int.J.Mod.Phys.*, A15:5087–5159, 2000. doi: 10.1016/S0217-751X(00)00215-7.

[70] Poul H. Damgaard, Rijun Huang, Thomas Sondergaard, and Yang Zhang. The Complete KLT-Map Between Gravity and Gauge Theories. *JHEP*, 1208:101, 2012. doi: 10.1007/JHEP08(2012)101.

[71] Rijun Huang and Yang Zhang. On Genera of Curves from High-loop Generalized Unitarity Cuts. *JHEP*, 1304:080, 2013. doi: 10.1007/JHEP04(2013)080.

[72] Lance J. Dixon. Calculating scattering amplitudes efficiently. 1996.

[73] Lance J. Dixon. A brief introduction to modern amplitude methods. 2013.

[74] Paolo Benincasa and Freddy Cachazo. Consistency Conditions on the S-Matrix of Massless Particles. 2007.

[75] Song He and Hong-bao Zhang. Consistency Conditions on S-Matrix of Spin 1 Massless Particles. *JHEP*, 1007:015, 2010. doi: 10.1007/JHEP07(2010)015.

[76] Bo Feng, Junqi Wang, Yihong Wang, and Zhibai Zhang. BCFW Recursion Relation with Nonzero Boundary Contribution. *JHEP*, 1001:019, 2010. doi: 10.1007/JHEP01(2010)019.

[77] Bo Feng and Chang-Yong Liu. A Note on the boundary contribution with bad deformation in gauge theory. *JHEP*, 1007:093, 2010. doi: 10.1007/JHEP07(2010)093.

[78] Bo Feng and Zhibai Zhang. Boundary Contributions Using Fermion Pair Deformation. *JHEP*, 1112:057, 2011. doi: 10.1007/JHEP12(2011)057.

[79] Stephen J. Parke and T. R. Taylor. Amplitude for n-gluon scattering. *Phys. Rev. Lett.*, 56:2459–2460, Jun 1986. doi: 10.1103/PhysRevLett.56.2459.

[80] Frits A. Berends, W.T. Giele, and H. Kuijf. On relations between multi - gluon and multigraviton scattering. *Phys.Lett.*, B211:91, 1988. doi: 10.1016/0370-2693(88)90813-1.

[81] V.P. Nair. A Note on MHV amplitudes for gravitons. *Phys.Rev.*, D71:121701, 2005. doi: 10.1103/PhysRevD.71.121701.

[82] James Bedford, Andreas Brandhuber, Bill J. Spence, and Gabriele Travaglini. A Recursion relation for gravity amplitudes. *Nucl.Phys.*, B721:98–110, 2005. doi: 10.1016/j.nuclphysb.2005.016.

[83] Henriette Elvang and Daniel Z. Freedman. Note on graviton MHV amplitudes. *JHEP*, 0805:096, 2008. doi: 10.1088/1126-6708/2008/05/096.

[84] L.J. Mason and David Skinner. Gravity, Twistors and the MHV Formalism. *Commun.Math.Phys.*, 294:827–862, 2010. doi: 10.1007/s00220-009-0972-4.

[85] Dung Nguyen, Marcus Spradlin, Anastasia Volovich, and Congkao Wen. The Tree Formula for MHV Graviton Amplitudes. *JHEP*, 1007:045, 2010. doi: 10.1007/JHEP07(2010)045.

[86] Z. Kunszt. Combined Use of the Calkul Method and N=1 Supersymmetry to Calculate QCD Six Parton Processes. *Nucl.Phys.*, B271:333, 1986.

[87] Stephen J. Parke and T.R. Taylor. Perturbative QCD Utilizing Extended Supersymmetry. *Phys.Lett.*, B157:81, 1985. doi: 10.1016/0370-2693(85)91216-X.

[88] Massimo Bianchi, Henriette Elvang, and Daniel Z. Freedman. Generating Tree Amplitudes in N=4 SYM and N = 8 SG. *JHEP*, 0809:063, 2008. doi: 10.1088/1126-6708/2008/09/063.

[89] N.E.J. Bjerrum-Bohr, Poul H. Damgaard, Bo Feng, and Thomas Sondergaard. Proof of Gravity and Yang-Mills Amplitude Relations. *JHEP*, 1009:067, 2010. doi: 10.1007/JHEP09(2010)067.

[90] Bo Feng and Song He. KLT and New Relations for N=8 SUGRA and N=4 SYM. *JHEP*, 1009:043, 2010. doi: 10.1007/JHEP09(2010)043.

[91] J.M. Drummond, M. Spradlin, A. Volovich, and C. Wen. Tree-Level Amplitudes in N=8 Supergravity. *Phys.Rev.*, D79:105018, 2009. doi: 10.1103/PhysRevD.79.105018.

[92] N.E.J. Bjerrum-Bohr, Poul H. Damgaard, Bo Feng, and Thomas Sondergaard. Unusual identities for QCD at tree-level. *J.Phys.Conf.Ser.*, 287:012030, 2011. doi: 10.1088/1742-6596/287/1/012030.

[93] N.E.J. Bjerrum-Bohr, Poul H. Damgaard, Bo Feng, and Thomas Sondergaard. New Identities among Gauge Theory Amplitudes. *Phys.Lett.*, B691:268–273, 2010. doi: 10.1016/j.physletb.2010.07.002.

[94] N.E.J. Bjerrum-Bohr, Poul H. Damgaard, Bo Feng, and Thomas Sondergaard. Gravity and Yang-Mills Amplitude Relations. *Phys.Rev.*, D82:107702, 2010. doi: 10.1103/PhysRevD.82.107702.

[95] Z. Bern, Lance J. Dixon, M. Perelstein, and J.S. Rozowsky. Multileg one loop gravity amplitudes from gauge theory. *Nucl.Phys.*, B546:423–479, 1999. doi: 10.1016/S0550-3213(99)00029-2.

[96] Bo Feng, Song He, Rijun Huang, and Yin Jia. Note on New KLT relations. *JHEP*, 1010:109, 2010. doi: 10.1007/JHEP10(2010)109.

[97] Henriette Elvang, Yu-tin Huang, and Cheng Peng. On-shell superamplitudes in N=4 SYM. *JHEP*, 1109:031, 2011. doi: 10.1007/JHEP09(2011)031.

[98] E. Cremmer and B. Julia. The SO(8) supergravity. *Nuclear Physics B*, 159:141–212, November 1979. doi: 10.1016/0550-3213(79)90331-6.

[99] Frits A. Berends and W. Giele. The Six Gluon Process as an Example of Weyl-Van Der Waerden Spinor Calculus. *Nucl.Phys.*, B294:700, 1987. doi: 10.1016/0550-3213(87)90604-3.

[100] Michelangelo L. Mangano. The Color Structure of Gluon Emission. *Nucl.Phys.*, B309:461, 1988. doi: 10.1016/0550-3213(88)90453-1.

[101] Zvi Bern, Lance J. Dixon, David C. Dunbar, and David A. Kosower. One loop n point gauge theory amplitudes, unitarity and collinear limits. *Nucl.Phys.*, B425:217–260, 1994. doi: 10.1016/0550-3213(94)90179-1.

[102] Bo Feng, Yin Jia, and Rijun Huang. Relations of loop partial amplitudes in gauge theory by Unitarity cut method. *Nucl.Phys.*, B854:243–275, 2012. doi: 10.1016/j.nuclphysb.2011.08.024.

[103] Stephen G. Naculich. All-loop group-theory constraints for color-ordered SU(N) gauge-theory amplitudes. *Phys.Lett.*, B707:191–197, 2012. doi: 10.1016/j.physletb.2011.12.010.

[104] Alexander C. Edison and Stephen G. Naculich. SU(N) group-theory constraints on color-ordered five-point amplitudes at all loop orders. *Nucl.Phys.*, B858:488–501, 2012. doi: 10.1016/j.nuclphysb.2012.01.019.

[105] Alexander C. Edison and Stephen G. Naculich. Symmetric-group decomposition of SU(N) group-theory constraints on four-, five-, and six-point color-ordered amplitudes. *JHEP*, 1209:069, 2012. doi: 10.1007/JHEP09(2012)069.

[106] G. Passarino and M. Veltman. One-loop corrections for e+e- annihilation into mu+ mu- in the Weinberg model. *Nucl. Phys. B*, 160:151.

[107] Zvi Bern, Lance J. Dixon, and David A. Kosower. Dimensionally regulated one loop integrals. *Phys.Lett.*, B302:299–308, 1993. doi: 10.1016/0370-2693(93)90400-C.

[108] Zvi Bern, Lance J. Dixon, and David A. Kosower. Dimensionally regulated pentagon integrals. *Nucl.Phys.*, B412:751–816, 1994. doi: 10.1016/0550-3213(94)90398-0.

[109] Zvi Bern, Lance J. Dixon, David C. Dunbar, and David A. Kosower. Fusing gauge theory tree amplitudes into loop amplitudes. *Nucl.Phys.*, B435:59–101, 1995. doi: 10.1016/0550-3213(94)00488-Z.

[110] Charalampos Anastasiou, Ruth Britto, Bo Feng, Zoltan Kunszt, and Pierpaolo Mastrolia. D-dimensional unitarity cut method. *Phys.Lett.*, B645:213–216, 2007. doi: 10.1016/j.physletb.2006.12.022.

[111] Charalampos Anastasiou, Ruth Britto, Bo Feng, Zoltan Kunszt, and Pierpaolo Mastrolia. Unitarity cuts and Reduction to master integrals in d dimensions for one-loop amplitudes. *JHEP*, 0703:111, 2007. doi: 10.1088/1126-6708/2007/03/111.

[112] Freddy Cachazo, Peter Svrcek, and Edward Witten. Gauge theory amplitudes in twistor space and holomorphic anomaly. *JHEP*, 0410:077, 2004. doi: 10.1088/1126-6708/2004/10/077.

[113] Ruth Britto, Freddy Cachazo, and Bo Feng. Generalized unitarity and one-loop amplitudes in N=4 super-Yang-Mills. *Nucl.Phys.*, B725:275–305, 2005. doi: 10.1016/j.nuclphysb.2005.07.014.

[114] Ruth Britto, Evgeny Buchbinder, Freddy Cachazo, and Bo Feng. One-loop amplitudes of gluons in SQCD. *Phys.Rev.*, D72:065012, 2005. doi: 10.1103/PhysRevD.72.065012.

[115] Robin Hartshorne. *Algebraic geometry*. Springer-Verlag, New York, 1977. ISBN 0-387-90244-9. Graduate Texts in Mathematics, No. 52.

[116] Daniel Perrin. *Algebraic geometry*. Universitext. Springer-Verlag London Ltd., London, 2008. ISBN 978-1-84800-055-1; 978-2-7598-0048-3. doi: 10.1007/978-1-84800-056-8. An introduction, Translated from the 1995 French original by Catriona Maclean.

[117] M. F. Atiyah and I. G. Macdonald. *Introduction to commutative algebra*. Addison-Wesley Publishing Co., Reading, Mass.-London-Don Mills, Ont., 1969.

[118] David Cox, John Little, and Donal O'Shea. *Ideals, varieties, and algorithms*. Undergraduate Texts in Mathematics. Springer, New York, third edition, 2007. ISBN 978-0-387-35650-1; 0-387-35650-9. doi: 10.1007/978-0-387-35651-8. An introduction to computational algebraic geometry and commutative algebra.

[119] W.L. van Neerven and J.A.M. Vermaseren. LARGE LOOP INTEGRALS. *Phys.Lett.*, B137:241, 1984. doi: 10.1016/0370-2693(84)90237-5.

[120] Daniel R. Grayson and Michael E. Stillman. Macaulay2, a software system for research in algebraic geometry. Available at http://www.math.uiuc.edu/Macaulay2/.

[121] Dong-pei Zhu. Zeros in Scattering Amplitudes and the Structure of Nonabelian Gauge Theories. *Phys.Rev.*, D22:2266, 1980. doi: 10.1103/PhysRevD.22.2266.

[122] C.J. Goebel, F. Halzen, and J.P. Leveille. Angular zeros of Brown, Mikaelian, Sahdev, and Samuel and the factorization of tree amplitudes in gauge theories. *Phys.Rev.*, D23:2682–2685, 1981. doi: 10.1103/PhysRevD.23.2682.

[123] Andrew Hodges. A simple formula for gravitational MHV amplitudes. 2012.

[124] Freddy Cachazo and David Skinner. Gravity from Rational Curves. *Phys.Rev.Lett.*, 110:161301, 2013. doi: 10.1103/PhysRevLett.110.161301.